THE
PHYSICAL REVIEW
A Journal of Experimental and Theoretical Physics
VOL. 46, No. 8 OCTOBER 15, 1934 SECOND SERIES

Measurement of the Energy of a Beta-Ray of Radium B

F. A. SCOTT, *The Rice Institute*
(Received June 4, 1934)

The energy of the most intense beta-ray line from radium B has been measured and found to be 2.6145×10^5 electron-volts, taking e/m to be 1.760×10^7 e.m.u. per gram. The value of $H\rho$ for this line was found to be 1931.8 gauss cm. The spectrum was obtained by the magnetic focussing method and the magnetic field was measured by the Cotton balance method. All measurements were made to within one part in ten thousand and it is hoped that the error in $H\rho$ is not greater than this. The value for the energy of course depends on the value of e/m and hence may be in error by about one part in one thousand.

INTRODUCTION

IN 1924, Ellis and Skinner[1] determined the energies of the β-rays from radium B and they believed the results accurate to one part in five hundred. Recently further experiments have been done on these rays by Ellis.[2] The results of these experiments show that the 1924 values are too high by about one part in 150. For the most intense β-ray from radium B in 1924 Ellis and Skinner obtained a value of $H\rho$ of 1938 gauss cm. (H is the magnetic field strength, and ρ the radius of curvature of the path of the ray.) The recent results give the value of $H\rho$ for the same line as 1925.5 gauss cm. The present experiments were undertaken with the object of determining the value of $H\rho$ for this line with greater accuracy. All quantities have been measured to within one part in ten thousand and it is hoped that the value of $H\rho$ is not in error by more than this.

APPARATUS

The β-ray spectrum of radium B was obtained by using the magnetic focussing method. The magnetic field was produced by a large permanent cobalt steel magnet. The poles of this magnet were square and 10 cm on each edge. The faces of these poles were ground until they were nearly flat. Pole pieces of mild steel were then placed in contact with the poles of the magnet. These pole pieces were cylindrical in shape, had a diameter of 15 cm and were 7.5 cm long. The surfaces of these pole pieces were flat to about one-thousandth of an inch. The faces of the pole pieces were adjusted parallel and then made vertical by means of a plumb line. The gap between them was 2.4 cm long. With the field used, 1282 gauss, the permeability of the pole pieces was about 1000 so that the field was assumed to be horizontal in the gap.

The strength of the magnetic field was measured by the Cotton balance method.[3] The Cotton balance consists essentially of two parallel

[1] Ellis and Skinner, Proc. Roy. Soc. **A105**, 165 (1924).
[2] Ellis, Proc. Roy. Soc. **A143**, 350 (1934).
[3] Cotton and Dupouy, Congrès International d'Électricité, Vol. III, Sec. 2 E, 208 (1932).

vertical conductors connected at their lower ends by a horizontal conductor. These conductors are hung from a balance so that the horizontal conductor is perpendicular to the horizontal magnetic field to be measured. A measured current is passed through the conductors and the force on the horizontal conductor is measured with the balance. If the parallel conductors are exactly vertical, there is no vertical force on them so that the force measured by the balance is equal to the force on the horizontal conductor. The effective length of the horizontal conductor is equal to the distance between the two parallel vertical conductors. In this experiment these vertical conductors are supported by an optically worked glass plate so that they are very exactly straight and parallel. According to Cotton this method is capable of measuring the magnetic field with an accuracy much greater than one part in twenty thousand. It is therefore superior to the induction methods used by Ellis and others with which it is difficult to get an accuracy of one part in one thousand. The errors in the induction method are probably due to the difficulty of making coils of exactly known areas. In the Cotton balance the distance between the vertical conductors is comparatively easy to measure.

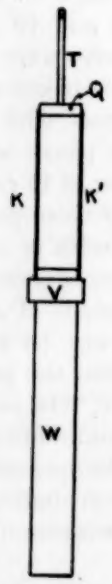

FIG. 1. Conductor support for Cotton balance.

An optically worked Pyrex glass plate 30×3 ×0.45 cm was obtained from the Gaertner Scientific Company. The two long edges were plane and parallel to within one-five hundredth of a millimeter for a distance of 15 cm and then parallel to within one-one hundredth of a millimeter for the remainder of the distance. Thin silver strips of uniform thickness were fastened very closely to the sides of the plate with shellac and joined at the bottom. The strips were held very tightly against the glass in a specially constructed press while the shellac dried so that no appreciable thickness of shellac remained between the silver and the glass. Both sides of each silver strip formed a good plane mirror. At the top of the plate aluminum strips K and K' (Fig. 1) were held tightly against the silver by an ebonite block V. The upper ends of these aluminum strips were fastened to another ebonite block Q. From this second block extended two other aluminum strips T and T' which were attached to one arm of a sensitive balance. These aluminum strips fitted into supports on the balance which, when lowered on the knife edge of the balance, permitted the plate to swing freely both in the plane of the plate and in the plane at right angles to the surface of the plate. Light tin foil strips were attached to the aluminum strips K and K' at the block Q to supply current to the silver strips on the plate. These strips of foil were hung in vertical planes parallel to the horizontal component of the magnetic field (2.5 gauss) and brought out to an ebonite block placed in front of Q and at the same height as Q. The tin foil strips were about 10 cm long. The ends of the strips were at the same level but the middle points were about one centimeter below the ends. It can easily be shown that the very small resultant of the forces on the balance due to the action of the magnetic field on the current in these strips remains unchanged when the current is reversed so that no error is introduced by this force. Permanent connections were made to this third ebonite block by twisted leads coming from a reversing switch. The balance was mounted on a track above the magnet at such a height that the bottom of the glass plate came to the center of the pole pieces. By sliding the balance on the track it was possible to move the glass plate into or out of the field as desired.

The plate was surrounded by a brass box attached to the bottom of the balance case to prevent air currents from disturbing it. A mirror was mounted on the main knife edge of the balance and its deflections were observed by a lamp and scale about two meters from the mirror. The balance had a sensitivity of 19.5 mm per milligram and the scale could be read accurately to 0.2 mm by a hand magnifier. Since the value of the force measured was 200 milligrams, it could easily be measured to less than one part in ten thousand. The balance was so arranged that it could be rotated about a vertical axis through the center of the plate in order to determine the position of the plate for maximum force when the plane of the glass plate is perpendicular to the magnetic field. The plate was made vertical by a plumb line.

The current to the balance was supplied through a reversing switch which moved a lever and placed a 200 milligram weight on top of the glass plate when the current was reversed. The switch was attached to the base of the balance and was made so that the current in it gave no appreciable field. By the use of this arrangement the weight could be put on top of the glass plate and the current reversed without lifting the planes off the knife edges on the balance beam and without seriously disturbing the balance when the current was properly adjusted. The weight was of platinum and was standardized at the Bureau of Standards and had a value of 199.99 ± 0.01 milligrams. It had not been removed from its box since it was received.

The current to the glass plate was supplied by a lead storage battery. This battery consisted of two six volt 160 ampere hour capacity lead storage batteries connected in parallel. The batteries were first fully charged and then allowed to discharge until the voltage was nearly steady. Such a combination gave a very steady current.

The current to the plate was measured by means of a standard resistance and a Leeds and Northrup potentiometer with standard cell. The coils and slidewire of the potentiometer were tested for resistance variations and were found to be of the value designated. As a final check the three standard cells were checked against each other by means of the potentiometer and the potentials of the cells as measured by the instrument agreed with the certified values to less than one part in ten thousand. Two standard resistances furnished by Leeds and Northrup were used. One resistance was checked against the other in order to determine if any damage was done to either resistance during transit. The resistances each had a value of 4.0001 international ohms at 25°C correct to within 0.005 percent. The resistances had very small temperature coefficients which changed sign at about 25°C showing that the resistances had flat minimum values at this temperature. Since all measurements were made between 23°C and 25°C, it was not necessary to correct the resistances for temperature variations. It is scarcely necessary to mention that manganin standard resistances usually have the above characteristics which are in no way exceptional. These resistances were calibrated by the Bureau of Standards in February, 1934. The standard cells were calibrated by the Bureau of Standards in February, 1934, and were accurate to 0.01 percent at 24°C. Three such cells were used whose e.m.f.'s were, respectively, 1.01883, 1.01884, 1.01885 international volts. Since the relative values of these cells agreed with the Bureau's values to within one part in ten thousand it was assumed that the cells had not been damaged appreciably in transit. All measurements of length, current, etc., were done in two rooms whose temperature was maintained between 23°C and 25°C. With the small temperature variation it was unnecessary to correct the values of the resistance, standard cell potentials, or measurements of length for temperature variations to obtain the desired accuracy of one part in ten thousand. The current to the plate was adjusted to 0.25 international ampere in order to give the proper force in the magnetic field for the given weight.

The value of the acceleration of gravity used in determining the force from the standard weight was furnished by Dr. Blau of the Research Department of the Humble Oil and Refining Company, of Houston. This value of g is 979.28 cm/sec.^{2} and is much more accurate than is necessary for the present experiments. It was determined by taking the value of g at a government station near Houston and correcting it for

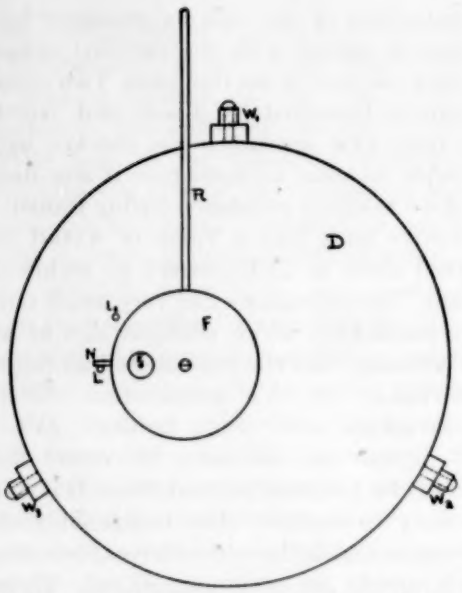

FIG. 2. Apparatus for measuring magnetic field variations.

the difference of position using the experimentally determined gravity gradients over the region in question.

The variations in the magnetic field were determined by means of a small coil of 1000 turns and diameter of 0.90 cm. This coil was attached to a high sensitivity low resistance galvanometer used as a fluxmeter which gave a deflection of 1 mm for a change of 0.094 gauss through the coil. The apparatus shown in Fig. 2 was designed to measure the variations in the field along the actual path of the β-rays. The large brass disk D was 15 cm in diameter and was fitted tightly over one of the pole pieces by screws through the blocks W_1, W_2, W_3. The coil E was fastened onto a smaller disk F which was so placed on the larger disk that if F were rotated 180° clockwise by the handle R the small coil followed the actual path of the β-rays in the magnetic field from M to O (Fig. 7). A small plug N was fastened to the side of F and by the use of a series of properly spaced stops screwed into the larger disk D it was possible to flip the coil through a small angle. Two of these stops, L_1 and L_2, are shown. The stops were so spaced that the coil could be flipped through an angle of 30° at a time and thus determine the difference in the strength of the field at two points on the electron path. The coil was placed initially at M and rotated along the path to O. By rotating the large disk D through 180° the field variations along the path from O to M' could also be mapped. The curve shown in Fig. 3 gives the angular variations of the field along the electron paths. δH represents the variations in the field from point to point in gauss, and θ is the angular distance along the path of the β-rays. The portion of the curve to the left of the axis gives the variations along the curved path OM and that to the right of the δH axis gives the variations in the field along the path OM' (Fig. 7).

The bottom of the glass plate attached to the balance for measuring the field came to O and extended for a distance of 1.5 cm on either side of O. Since the plate measured the average field over this distance and the field at O is desired, it was necessary to measure the variations in the field along the horizontal line through O. This was done by mounting the small coil on a bar which could be slid across the disk D. A plug in the side of the bar moved between stops 1 cm apart screwed into the surface of the disk. The curve of Fig. 4 gives these variations. The coil was placed at A, a distance of 1.5 cm from O and slid over a distance of one centimeter and the variation determined. The stops were then adjusted and the variation for the second centimeter obtained. A similar observation was made for the third centimeter. The average value of δH obtained from this curve is $+0.06$ gauss. The average field $\overline{H}$ measured by the glass plate is equal to the field at A plus the average δH, or $\overline{H}=H_A+0.06$ gauss. Since the field at O is $+0.17$ gauss greater than H_A, we get finally $H_O=\overline{H}+0.11$ gauss.

Hartree[4] has shown that if the magnetic field is not constant over the β-ray path, then the same point of impact would be obtained on the photographic plate by the electrons in a field of strength H given by $H=H_O+\frac{1}{2}\int \sin\theta\delta H\, d\theta$ where the integral extends over the path, H_O is the field at the β-ray source, θ is the angle turned through from the initial direction of propagation, and δH is the variation in the field from the point to point along the path. By plotting $\sin\theta\delta H$ against θ a curve is obtained for

[4] Hartree, Proc. Camb. Phil. Soc. **21**, 746 (1923).

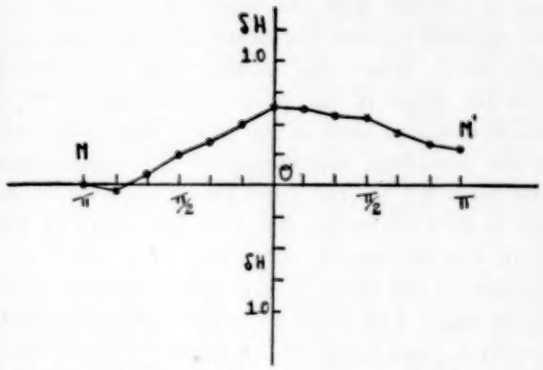

FIG. 3. Angular variations in magnetic field along paths of β-rays.

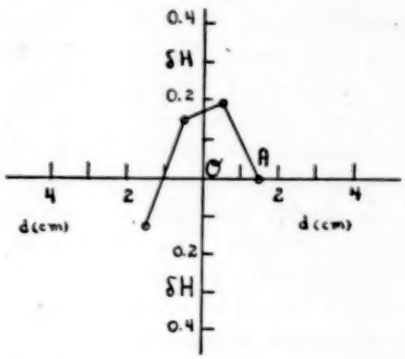

FIG. 4. Variations in magnetic field across center of field.

each path, half the area under which gives the Hartree correction. Such a curve is shown in Fig. 5 and is obtained from the angular variation curve in the following manner. The point where the angular variation curve crossed the δH axis represents the field at O. The variations of δH with respect to O are then computed by taking the difference between the δH at O and that corresponding to some particular point on the path of the β-ray. Knowing the variations with respect to the field at O, the Hartree correction is easily plotted. The correction for the path OM computed from the curve is -0.385 gauss; that for the path OM' is -0.112 gauss. The average correction for the two paths is -0.248 or -0.25 gauss. The equivalent field is obtained from

$$H = H_0 + \tfrac{1}{2}\int \sin\theta \delta H \, d\theta$$

$$= \bar{H} + 0.11 - 0.25$$

$$= \bar{H} - 0.14.$$

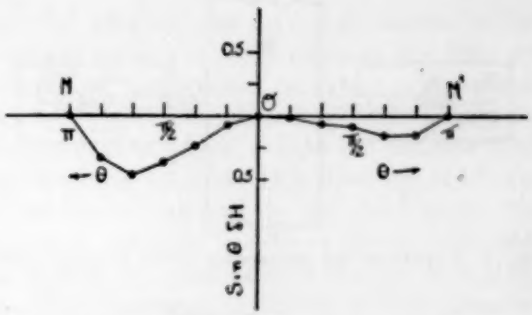

FIG. 5. Hartree correction curve for magnetic field variations.

Thus -0.14 gauss represents the total correction which must be applied to the average field computed from the balance reading to obtain the equivalent field for the β-ray paths.

The equation for the motion of the β-rays along their paths in the magnetic field is

$$Hev = mv^2/\rho$$

whence

$$H\rho = \frac{mv}{e} = \frac{m_0}{e} \cdot \frac{v}{(1-v^2/c^2)^{\frac{1}{2}}}.$$

The energy of such rays is obtained from these relations:

$$E = m_0c^2\{1/(1-v^2/c^2)^{\frac{1}{2}} - 1\} \text{ ergs}$$

$$V = 299.8\{[(H\rho)^2 + (cm_0/e)^2]^{\frac{1}{2}} - (cm_0/e)\} \text{ e. v.}$$

$$= 299.8\{[(H\rho)^2 + (1703.41)^2]^{\frac{1}{2}} - 1703.41\}.$$

The value of $\bar{H}$ is computed from the force and current used by the relation $\bar{H} = F/(i_1+i_2)l$ where i_1 is the value of the current before reversal, i_2 the value of the current after reversal, l the mean distance between the centers of the silver strips on the two sides of the glass plate and F the force measured with the balance. The current through the balance was expressed in absolute electromagnetic units and the value of the force was determined from the standard weight and the acceleration due to gravity. In computing the energy of the β-rays the values $C = 2.9980 \times 10^{10}$ cm/sec. and $e/m = 1.760 \times 10^7$ e.m.u. per g were used.

The radius of curvature ρ was obtained by measuring the spectrum obtained on the photographic plates used in the apparatus (Fig. 7)

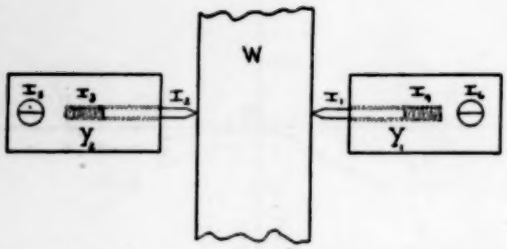

FIG. 6. Apparatus for measuring width of glass plate.

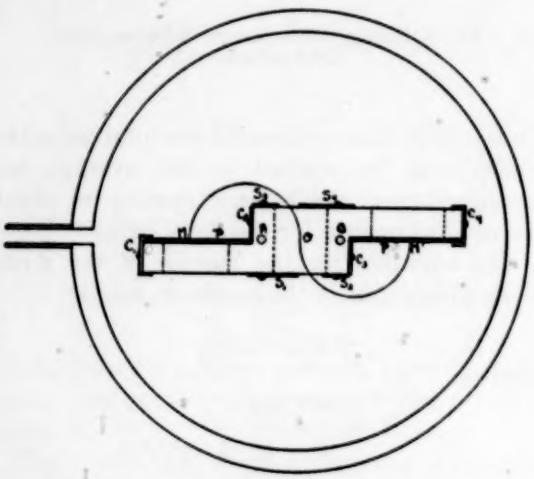

FIG. 7. Magnetic focussing apparatus for obtaining spectrum.

that is subsequently described. All measurements of length were made with a Gaertner comparator on which one scale division on the wheel corresponded to 0.0001 cm. Since only the ratio of lengths is required, it was not necessary to check the comparator against a standard of length. All measurements of length were made near the center of the screw of the comparator. For the desired accuracy of one part in ten thousand it was not necessary to consider possible errors in the screw.

The width of the glass plate without and with the silver was measured on the Gaertner comparator with the device shown in Fig. 6. Y_1 and Y_2 are brass blocks that are fastened to the bed plate of the comparator by blocks, I_5 and I_6. I_1 and I_2 are soft steel rods with rounded points that slide in holes in the blocks. Back of each of these rods in the holes is a light coiled spring I_3 or I_4. The glass plate W was fastened to the bed plate of the comparator and the blocks Y_1 and Y_2 adjusted until the points of the rods were just in contact with the edges of the plate but not pressed against the plate with any appreciable force. When the points were in contact with the edges of the plate, the image of these points could be seen in the plate. The cross hair of the travelling microscope of the comparator was then set on the junction of each of these points with its image and thus the width of the plate was measured. After the silver strip was applied to the plate similar measurements were again made. The silver strip had sufficient polish to give a good image of the points. This method gives the distance between the parallel reflecting planes and no error would be introduced if the points penetrated into the silver but the points were rounded and did not penetrate appreciably. In making these measurements, the plate W and the steel points were illuminated from above. Measurements were made on the width of the plate throughout its entire length, but the average of the measurements over only the first half of the length was used in computing the length of the current. This distance represents a portion of the plate, 7.5 cm of which are within the gap and 7.5 cm of which are outside the gap. Table I gives the measurements for the plate alone and for the plate with the strips for the same 15 cm of length. Each measurement represents an average of four readings. The average length of the current was obtained by taking the average distance between the centers of the silver strips and was 3.08253 cm which is probably accurate to within one part in ten thousand.

TABLE I. *Measurements of plate with and without silver strips.*

Distance from bottom of plate	Width of plate alone	Width of plate with strips
End	3.07105 cm	
1.5 cm	3.07109	3.09310 cm
3	3.07104	3.09434
5	3.07104	3.09424
7	3.07121	3.09416
9	3.07103	3.09453
11	3.07108	3.09312
13	3.07106	3.09445
	Av. 3.07107 cm	Av. 3.09399 cm

The average values of the widths with and without the silver strips are practically equal to the widths at 7 cm from the end of the plate

where the magnetic field changes rapidly. The widths near the lower end of the plate and above 7 cm where the field is weak are not important. It was considered, nevertheless, proper to use the average width because small variations in the width may be due to errors in the measurements rather than to real variations in the width. The average deviation from the mean of the width without the strips is very small and that with the strips is 0.00050 cm so that the average deviation from the mean in the distance between the centers of the strips is 0.00025 cm or about one part in ten thousand.

In Table II is given a sample set of data observed for computing the value of H by means of the balance. E_1 and E_2 are the potentiometer readings across the standard resistance before and after reversing the current through the balance. The quantity δ represents the force that must be added to that of the standard weight to give the proper force. If the current had been of such a value as to give a force on reversal exactly equal to that of the standard weight, then δ would have been zero.

TABLE II. *Sample set of data.*

Reading of balance before reversing current = 24.05 cm
Reading of balance after reversing current = 23.43 cm
$\delta = 0.318$ milligram
$E_1 = 0.99270$ international volt
$E_2 = 0.99290$ international volt
$i_1 = 0.24816$ international ampere $= 0.024813$ abs. e.m.u.
$i_2 = 0.24821$ international ampere $= 0.024818$ abs. e.m.u.

$$\overline{H} = \frac{F}{(i_1+i_2)l} = \frac{(0.19999+0.000318)979.28}{(0.049631)\times 3.08253} = 1282.17 \text{ gauss}$$

Subtracting the correction from this value of H gives $1282.17 - 0.14 = 1282.03$ gauss.

A diagram of the apparatus used in obtaining the spectrum of the β-rays from radium B is shown in Fig. 7. The brass block $C_1 C_4$ has a small hole drilled through it at O in which the source was placed. The source consisted of a platinum wire 0.25 mm in diameter which had been activated by exposing it to the emanation from 20 milligrams of radium. $P P$ are ordinary process plates whose sensitive surfaces are in line with the source at O. These plates are held firmly in place by clamps C_1, C_2, C_3, C_4. S_1, S_2, S_3, S_4 are adjustable slit jaws. Slots were cut in the block as indicated by the dotted lines. By using a frame of this type two lines are obtained, one on each photographic plate. The lines at M and M' are produced by the β-rays which describe semi-circular paths as shown in the diagram. Since the outer edges of the lines are very sharp, the radius of curvature of these lines can be readily determined by subtracting the diameter of the wire at O from the distance MM' and dividing by four. This distance MM' was about six centimeters in the field used. The lines were near the middle of the photographic plates and the possible shift due to drying the film was considered negligible. It was measured with the comparator; one line was seen directly and the other through the photographic plate and the slot in the block. The frame was placed in a brass box on two pegs which came through the frame at A and B.

The box was tested for magnetic impurities. This test was made with a coil of diameter 2.5 cm and 2750 turns connected to a fluxmeter which gave a deflection of 1 mm for a change of field of 0.05 gauss through the coil. This coil was mounted in the center of the air gap of the permanent magnet while the brass box and cover were placed in the gap, one part on either side of the coil, and then withdrawn. The net change in the flux through the coil was zero as shown by the fluxmeter, indicating that the material did not change the field appreciably. The brass box surrounding the glass plate on the balance was also tested in a similar manner by placing the box about the coil and then removing it. It also had no effect on the field.

The box containing the frame was placed between the poles of the large permanent cobalt steel magnet and exhausted by a Hypervac pump. The plates were exposed for three hours, the life of the active deposit, and then developed. This was accomplished by immersing the entire frame in the developer. It was found that the plates gave the best results when developed in process developer for 4 or 5 minutes and fixed and washed in the usual way. After they had dried they were measured with the Gaertner comparator and the value of ρ, the radius of curvature, determined. The average value of ρ obtained in this manner may be used since the field over each path is nearly the same. The following values of ρ were obtained with different plates over a period of two months: 1.50704, 1.50669, 1.50684, 1.50705, 1.50667, 1.50675. It will be seen that they agree very closely. This

indicates that the magnetic field remained very constant, which is no doubt due to the fact that the magnet was kept at nearly constant temperature.

The results listed in Table III give a series of values for ρ and H obtained at nearly the same

TABLE III. *Values of H and ρ.*

H	ρ
1282.03 gauss	1.50668 cm
1282.04	1.50705
1282.08	1.50668
1281.92	1.50701
1282.04	1.50675
1282.00	1.50686
Av. 1282.02 gauss	Av. 1.50684 cm

times. The last figures in these values have little real significance but were retained to avoid errors in the computations. The values of H have had the correction -0.14 gauss applied to them. Using the average values of H and ρ obtained one gets a value for $H\rho = 1931.80$ and an energy $E = 2.6145 \times 10^5$ electron volts for the particular β-ray under consideration taking e/m equal to 1.760×10^7 e.m.u. per gram. The value for the energy found depends on the value of e/m assumed and so may be in error by about one part in one thousand.

The probable error in the value of H computed in the usual way is ± 0.00016 and that in the value of ρ is ± 0.000044 so that $H = 1931.80 \pm 0.12$. This method of measuring H has the advantage of using only that portion of the magnetic field within 3 cm of the center of the pole pieces where the variations in the field were very small. Likewise by using two semicircular paths it was possible to employ twice as strong a magnetic field as if only one semicircular path had been used. Cotton mentions that his balance method seems to give values lower than induction methods for measuring magnetic field strengths by 18 parts in ten thousand. If this is true then the result obtained for $H\rho$ may be lower than that to be expected from induction methods.

The writer wishes to express his indebtedness to Professor H. A. Wilson for suggesting the problem and for his interest and guidance during the progress of the work.

A Very High Altitude Survey of the Effect of Latitude upon Cosmic-Ray Intensities And an Attempt at a General Interpretation of Cosmic-Ray Phenomena

I. S. Bowen, R. A. Millikan and H. Victor Neher, *California Institute of Technology*

(Received July 24, 1934)

The results of a very high altitude geographical survey extending in airplanes from Northern Canada to Peru, to altitudes of 22,000 feet, and, in three stratosphere flights made within the United States, to altitudes of 60,000 feet, are interpreted in the light of (1) the Epstein and the Lemaitre-Vallarta analysis of the effect of the earth's magnetic field, and (2) the Bowen-Millikan proof that the immediate agents responsible for the ionization of the atmosphere are electrons (+ and −), rather than protons or heavier nuclei. The main conclusions reached are: (1) that the resistance of the atmosphere to incoming electrons is 1 billion volts because of extranuclear encounters, 5 billion volts because of nuclear encounters; (2) that nuclear electron encounters produce only very soft secondaries, both photons and electrons; (3) that incoming photons produce most of the ionization found at sea-level or at sub-sea-level depths; (4) that nearly all of the non-field sensitive part of the ionization of the atmosphere above sea-level is due to photons of energy 200 ± 170 million electron volts; (5) that in the equatorial belt a small part of the ionization is due to incoming secondary electrons of energies as high as 10 billion volts; (6) that these are responsible for the east-west effect and the longitude effect found in the equatorial belt; (7) that the field sensitive part of the ionization increases rapidly with increasing latitude in going from Panama to Spokane because incoming secondaries of energies decreasing from 8 billion to 2 billion volts get through the blocking effect of the field in rapidly increasing numbers with increasing latitude and add greatly in northern latitudes to the underlying ionization of the upper-air produced by the incoming photons; (8) that the only source now in sight of the observed cosmic-ray energies is matter-annihilation; (9) that the softest components of the cosmic rays have the energies corresponding to the partial annihilation or atom building hypothesis, while the hardest components have energies corresponding to the complete atom-annihilation hypothesis; (10) that these processes may conceivably be taking place (1) because of the very low temperatures that facilitate the clustering of hydrogen in interstellar space, or (2) because of such extreme temperature conditions of the opposite sort as are found in novae, as suggested by Zwicky.

§I. Introductory

THE following is a detailed report of the results of a very high altitude survey of the effect of latitude upon cosmic-ray intensities planned in the late fall of 1931, a preliminary report upon which was made at the Atlantic City meeting of the A. A. A. S. in December, 1932.[1, 2] As indicated in that report, as well as in a lecture[3] delivered in Paris in November, 1931, such latitude effects were to be anticipated at high altitudes, even if they did not appear at low. For cosmic-ray photons traversing space in all directions must in any case produce secondary electrons wherever they traverse matter, whether that be in interstellar space, in nebulae, or in the atmospheres of suns through which they must sometimes pass in their travel of billions of years through space. So that if cosmic-ray photons exist at all, space must be traversed in all directions to some extent, at least, both by these photons and by their secondary electrons. The only question for experiment to determine is as to the proportions between the two.

It was thought that a suitable high-altitude survey would throw light upon this question. For these electronic secondaries were expected, from the direct cosmic-ray-energy measurements already under way at the Norman Bridge Laboratory and from Epstein's calculations published as early as 1930, to possess insufficient energy to get to the earth's surface at the equator through the blocking effect of the earth's magnetic field, but amply sufficient to penetrate that field in the higher magnetic latitudes. To be specific, Epstein[4] had found that billion volt electrons could only get in north of magnetic latitude 59°. Since, however, such latitude effects had been shown to be non-existent at the earth's surface in the region between Pasadena (mag. lat. 41°) and Churchill, Manitoba[5] (mag. lat.

[1] Robert A. Millikan, Phys. Rev. **43**, 665 (1933).
[2] Bowen, Millikan and Neher, Phys. Rev. **44**, 246 (1933).
[3] Robert A. Millikan, *Annales de Institut H. Poincare*, 1933, p. 452.
[4] Paul S. Epstein, Proc. Nat. Acad. Sci. **16**, 658 (1930).
[5] R. A. Millikan, Phys. Rev. **36**, 1597 (1930). These results were checked in 1932 by Millikan and Neher

70°), it was thought highly important from the standpoint of our planning in 1931 to look for them at high altitudes in northern Canada where electrons of too little energy to penetrate to sea-level might get through the earth's magnetic field and make their presence felt in the upper regions of the atmosphere.

Indeed, Epstein's analysis had shown that electrons of a given energy *should be distributed uniformly over a polar cap* which should of course extend farther and farther south the higher the incoming energy. In this analysis, however, atmospheric absorption had been ignored. But the greater part (about three-fourths) of the electrons the energies of which were being directly measured in the Norman Bridge Laboratory actually had energies under a billion volts, and since no appreciable number of billion-volt electrons could possibly penetrate the atmosphere (see below), even if they could get through the earth's magnetic field, it is obviously only at high altitudes that the effects of such entering electrons could be expected to be observed. Epstein's figures were available to us when we planned this high altitude survey in the late fall of 1931. We therefore arranged at that time, through the kind assistance of the Royal Canadian Air Force, to make our northern-most high altitude airplane flight at Cormorant Lake, Manitoba in magnetic latitude 63° N, where we hoped to get a crucial test of the existence inside this cap of incoming electrons of billion-volt energies or less. The other localities in which we planned and carried out flights in the succeeding summer (1932) were Spokane (54° N), where Captain Breene flew most skilfully for us, March Field, California (41° N), where Colonel Arnold and the other officers of the Field were extraordinarily generous in their assistance, Panama (20° N), where General Foulois gave directions again for Army assistance, and Peru (4° S), where the Pan American Airways pilots flew to high altitudes for us. The success of these airplane observations is largely due to the development of a vibration-free electroscope yielding as good photographic records on a moving and tipping platform, like an airplane, as in a laboratory.

(between Los Angeles and Victoria, B. C.) and by Bennett, Dunham, Bramhall and Allen, Phys. Rev. **42**, 446 (1932).

§II. The Results of the 1932 Airplane Latitude Survey

The whole of the results of the aforementioned survey are given in Fig. 1, in which the readings at different depths, in meters of water, beneath the top of the atmosphere, are given in ions per cc per sec. formed in air at atmospheric pressure. The geomagnetic latitude is determined from the assumption generally made now by geophysicists that the chief component of the earth's magnetic field is a dipole, the northern pole of which emerges at 69° 8′ W, 78° 30′ N.

The main points to be noted in connection with Fig. 1 are (1) that up to the altitude reached, namely, 4.5 m of water beneath the top, no detectable difference is found between the readings at Cormorant Lake (63° N) and those at Spokane (54° N); (2) that at 4.5 m (22,000 ft.) there is a 12 percent larger ionization at Cormorant Lake and Spokane than at March Field, and that this difference decreases smoothly to zero at sea-level; (3) that no measurable difference appears between the curves taken in Panama (20° N) and Peru (4° S); (4) that the Panama reading at 20° N is 29 percent lower

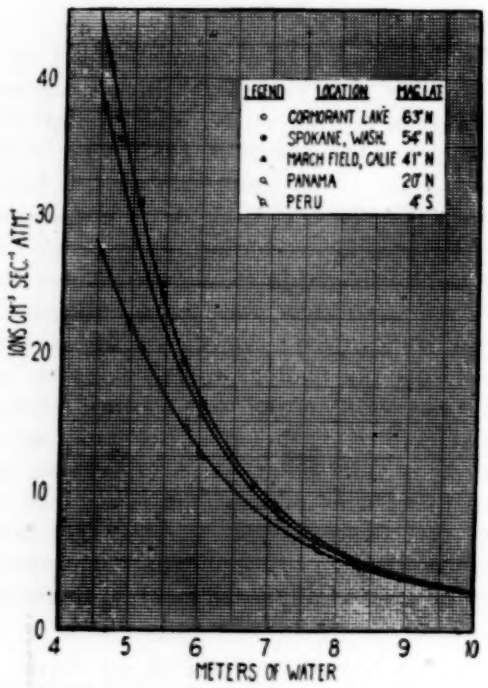

FIG. 1. Summary of results of the 1932 airplane latitude survey.

than the March Field reading and 38 percent lower than the Spokane and Cormorant Lake readings; (5) that the area between the uppermost and the lowermost curves represents that portion of the ionization which is due directly or indirectly to field-sensitive rays, while the area underneath the lower curve is that portion of the ionization which is due to non-field sensitive rays.

§III. Loss of Energy of Incoming Cosmic-Ray Electrons in Reaching Sea-Level about Six Billion Electron Volts

Anderson and Neddermeyer have counted with a great deal of care the average number of ions formed per centimeter by a high speed cosmic-ray electron at normal pressure. This can be done accurately if cloud-chamber tracks are chosen which correspond to the passage of an electron a little before the expansion so that the ions have had say a second to diffuse before the water condenses upon them, for the droplets are then well separated. Their result is 32 ions per cm. According to Kuhlenkampf's measurements, each electron removed from the molecules of air represents an expenditure of 32 electron volts of energy. These figures give 1020 electron volts of energy lost per cm of air-path. This, multiplied by the number of centimeters of air in an atmosphere, namely, $1033/.00117 = 8.83 \times 10^6$, gives 900,000,000 electron volts loss of energy in penetrating the atmosphere. Since the greater part of the electrons that reach the earth's surface have come in within 45° of the normal, we may take the average electron as entering at say 26°, the cosine of which is 0.9, so that a billion electron volts per atmosphere may be taken as the energy dissipated per electron in reaching the surface *on the incorrect assumption that no secondary rays are formed in so doing.*

There are, however, three different ways of determining the *total* resistance of the atmosphere, *including the formation of secondaries.*

(1) According to Epstein's computations, which are in excellent agreement with those made by Lemaitre and Vallarta,[6] 2.4 billion volt rays will just begin to get through the earth's magnetic field at magnetic latitude 49, and be completely through at latitude 57, so that there should be a latitude effect due to these rays, as well as to those of lesser energy, between Spokane (mag. lat. 54°, where 2.4 billion-volt rays should be varying most rapidly) and Cormorant Lake, provided incoming secondary electrons of these energies exist at all. Anderson's direct energy measurements have revealed the existence of such rays, and in addition the high altitude latitude effect found farther south (Fig. 1) shows that even higher energy electron-secondaries are formed. *The reason, then, that we did not find a latitude effect between Spokane and Cormorant Lake must be that rays of this energy cannot penetrate the atmosphere so as to show their effect at the highest altitude at which we made measurements, namely, 4.5 equivalent meters of water beneath the top of the atmosphere.* This means that the total resistance of the atmosphere (equivalent to 10 m of water) to incoming electrons (+ or −) must be more than $10/4.5 \times 2.4$, or 5.3 billion volts. A possible uncertainty in this mode of approach to the problem lies in the fact that we do not know whether locating the effective position of the north magnetic pole for the purposes here under consideration at 78 N, 69 W, is strictly legitimate, though it is the recognized practice of geophysicists, and, in addition, it introduces a larger measure of self-consistency into our own geographical readings than does any other point when used as a magnetic pole.

(2) The second mode of approach is to start with Anderson's and Neddermeyer's direct measurements of the loss in energy of electrons of energy between 40 million and 300 million volts in passing through lead. The mean value of this energy-loss (see accompanying paper by Anderson and Neddermeyer) is now 52 million volts per cm of lead. Since the mass absorption law holds fairly well in the highest energy range in which the loss of energy of electrons in traversing matter has been measured, lead having in fact some 9 times the absorptive power of water[7] per cm^3, we assume that this relation holds for cosmic-ray electrons, and obtain for the resistance of the atmosphere (10 m water) $= 52 \times 10^6 \times 1033/9 = 6$ billion volts. This might

[6] Lemaitre and Vallarta, Phys. Rev. **43**, 91 (1933).

[7] See *Radiations*, etc., Rutherford, *et al.*, p. 427, 1930; also Bethe, Zeits. f. Physik **76**, 293 (1932).

be in error by 20 percent, but probably not more than that.

(3) The third mode of approach is to utilize the fact that there is no sea-level latitude effect between Pasadena (41° N) and Churchill (70° N), while there is a marked latitude effect higher up in the atmosphere (Fig. 1). But according to Epstein it takes just 4 billion-volt electrons to begin to get through the earth's magnetic field at 40° N, and these will produce a latitude effect up to mag. lat. 52. A marked latitude effect is actually shown in the upper air (Fig. 1) in this region, but none at sea-level. Hence, if there are 4 billion-volt incoming secondaries, the resistance of the atmosphere must be at least 4 billion electron volts to prevent them from reaching sea-level. Indeed, a few 6, 7 and even 8 billion-volt electrons are needed to produce the latitude effect shown in Fig. 1 between Panama (20° N) and Pasadena (41° N). Again, according to Epstein and Lemaitre, the latitude effect of 5.5 billion-volt electrons should begin at lat. 34° and be finished at lat. 50°. Its practical absence at sea-level means that the resistance of the atmosphere is at least that much. The effect of the few 7 and 8 billion-volt electrons needed to carry the observed latitude effect both in high altitudes and at sea-level down to 20° would be finished at about 45° and should be very small down to 41°, so that the practical absence of a sea-level effect between 41° and the pole fixes the total resistance of the atmosphere at about 6 billion electron volts. In view of the three modes of approach, especially the last two, this value can scarcely be in error by as much as 20 percent.

The main result of this whole analysis of atmospheric resistance to incoming electrons is found in the conclusion that *about five-sixths, or 83 percent, of all the "field-sensitive" ionization found between the upper and lower curves of Fig. 1 is due to secondaries formed within the atmosphere.*

A second result of nearly equal importance is that since none of these secondaries, either photons or electrons, are sufficiently penetrating to get down to sea-level and reflect there the latitude effects actually existing at higher altitudes they are on the average low energy secondaries, the photons probably having an average energy, estimated from their inability to reach sea-level, of less than say 50 million volts, while the secondary electrons must for the same reason have an energy under say 500 million volts. This checks qualitatively with the results already published, for the energies of these very photons are exhibited in Figs. 7, 8 and 10,[8] and those shown all have energies under 30 million volts and many of them under a million. In fact, the energy of the photons produced by the disappearance of positive-electrons, such as are always formed in high energy nuclear encounters, is known from the experiments of Thibaud[9] and Lauritsen[10] to be about 0.5 million volt, and many such must be formed. On the other hand, the electron secondaries formed by electrons, examples of which are shown in Figs. 13 and 14,[8] are in these particular cases seen to possess energies only up to 50 million volts. Indeed, not only Anderson's and Neddermeyer's photographs, but all beta-ray photographs, show that the transfer of a very large part of the energy of an electron to another electron is a very rare event, while a high energy photon in general transfers a large fraction of its energy to the electron with which it collides.

§IV. Second Proof of the Atmospheric Origin of the Great Bulk of the Observed Ionizing Cosmic-Ray Particles

A preliminary report was made at Atlantic City in December, 1932 upon the results of a second method of testing whether or not a very large fraction of the ionization of the atmosphere is due to secondary electrons formed within our atmosphere. The method consists in taking an unshielded electroscope to a very high altitude and then observing the ionization found inside the same electroscope when it is taken to the same altitude inside a heavy shield of lead.

Fig. 2 shows the results of such tests made at March Field through the cooperation of the Army officers stationed there. If the lead screen, here 10 cm thick, acted simply as a resistance of the type considered in the first paragraph of §III, so that no secondary rays, photons, or

[8] Anderson, Millikan, Neddermeyer and Pickering, Phys. Rev. **45**, 352 (1934).
[9] Thibaud, Phys. Rev. **45**, 781 (1934).
[10] I. R. Crane and C. C. Lauritsen, Phys. Rev. **45**, 430 (1934).

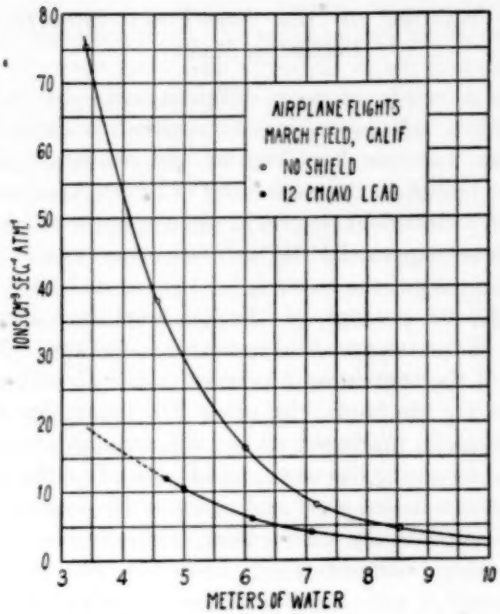

FIG. 2. Measurements in shielded and unshielded ionization chambers at various altitudes.

electrons were stimulated within it, then the ratio between the ionization found within it, first without screen, second with screen, would reveal what fraction of the electrons existing at the given altitude possess sufficient energy to penetrate the given thickness of lead. Since it is known that many new secondaries are actually stimulated within the lead, and since these all increase the actual ionization existing within the shielded electroscope, the foregoing ratio gives merely the lower limit to the number of electrons having energies under the value required to penetrate the lead. Since the shield was here 10 cm thick, the figure shows that at 29,000 feet at least 70 percent and more, probably 90 percent, of all the electron-rays existing at that altitude have energies under 520 million volts, this being, according to the Anderson measurements, the energy required to traverse 10 cm of lead. *Practically none of these electron-rays could have come in from outside, since it requires at this latitude at least 4 billion-volt electrons to get into the atmosphere through the blocking effect of the earth's magnetic field.*

§V. The Fordney-Settle Flight

The recent Fordney-Settle flight was even better adapted to bringing to light the cogency of the foregoing mode of approach to the problem of the origin of the ionization of the atmosphere. We had one of our self-recording instruments on that flight. Fig. 3 gives a section of the film. The electroscope was automatically charged up at five minute intervals and the slope of the line running diagonally across each interval gives the rate of discharge. The balloonists rose to the top very rapidly—in some 20 minutes, as the record shows—and remained there for three and a half hours, then descended rapidly. The result is that the mean readings at the top 62,000 feet are very reliable, but the intervening points are less so on account of the rapidity of the ascent. The results are plotted in Fig. 4, the lower curve giving the results obtained by Dr. A. H. Compton with his electroscope inside of 6.5 cm of lead. Fig. 5 gives the lower limit to the fraction of the electron-rays existing at each altitude, the energies of which must lie under 330 million volts. It is seen, then, that from a depth beneath the top of the atmosphere of

FIG. 3. Section of film from the Neher automatic recording electroscope taken during the ascent to the stratosphere of the balloon in the Fordney-Settle flight of November 20, 1933. Each of the nine panels across which the sloping dark line moves from left to right corresponds to a five-minute time interval. The slope is proportional to the rate of discharge of the electroscope, which in turn is proportional to the intensity of the cosmic rays. In the first panel the balloon was at an elevation of about 20,000 feet, and in the next twenty minutes (four panels) while the balloon was rising to a height of 45,000 feet the slope, or cosmic-ray intensity, rose tenfold. From there on to the highest altitude attained, 62,000 feet, the rate of rise of the balloon was much less rapid. It remained at or near the top for three and a half hours, so that this film yielded accurate measurements of cosmic-ray intensities at the higher and lower altitudes, but not at the intermediate ones.

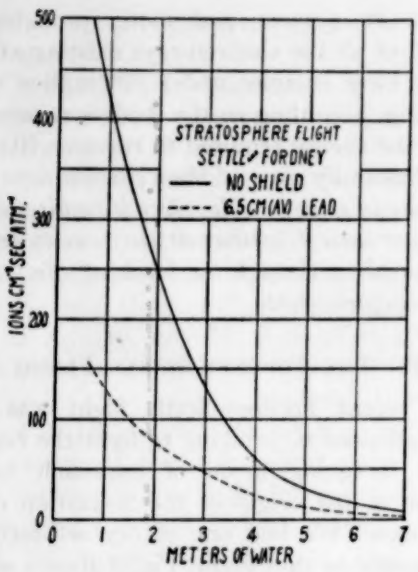

FIG. 4. Measurements made with an unshielded ionization chamber on the Fordney-Settle flight. The dotted curve gives the results obtained by A. H. Compton (Phys. Rev. **45**, 441 1934)) with his shielded electroscope.

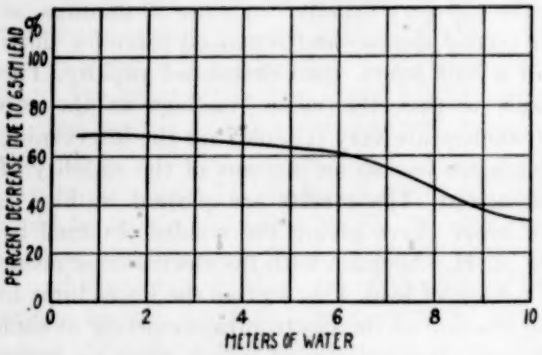

FIG. 5. Effect of a 6.5 cm lead shield on the ionization measurements.

about 6 meters of water, i.e., from Pike's Peak up to a point but 60 cm of water beneath the top, not less than 70 percent and probably more than 90 percent of the electron rays have too small energies to penetrate the 6 cm lead shield, i.e., they have energies under 330 million volts. Since these figures apply to the whole atmosphere, i.e., to both the field-sensitive and the non-field-sensitive parts of the ionization, *we may conclude with certainty that as I stated in the Atlantic City paper in 1932, "all but a very small part of the ionization of the air is due to secondaries produced within the atmosphere."*

§VI. Nature of the Non-Field Sensitive Incoming Rays

As a result of four different trips by our sensitive, self-registering, vibration-free electroscopes, between Los Angeles and Mollendo, or other points on the west coast of South America, all of which yield results in close agreement, the sea-level equatorial dip in cosmic-ray intensity in this part of the world is 7 ± 1 percent. In other words, 93 percent of the sea-level ionization here is due to non-field sensitive rays, and only 1/6 of the remaining 7 percent is due *directly* to incoming electrons, the other 5/6 being due to secondaries produced within the atmosphere by these incoming electrons, all of which in order to get down to sea-level and produce the observed sea-level latitude effect must, according to the preceding computations, have an energy of between 6 and 8 billion electron volts. *There need then be only enough incoming electrons of this energy to produce directly at sea-level about 1 percent of the observed ionization.*

The 93 percent of non-field-sensitive ionization must be due either to photons or else to incoming electrons of energies somewhat above 8 billion, or possibly 10 billion, electron volts so that they can get through the earth's magnetic field into the equatorial belt. We have evidence which will be presented in another paper that there are at least a small number of such incoming electrons that reach sea-level in the equatorial belt—enough to produce directly at sea-level another 1 or $1\frac{1}{2}$ percent of the observed sea-level ionization. *Indeed, it is just these rays, multiplied 6-fold in their effectiveness in exciting counters by their progeny of secondaries, which are responsible for the east-west effect observed in Peru by Johnson*[11] *and Korff.*[12] The incoming electrons here in question may all be assumed to be positives either arbitrarily or better, from our point of view, because the highest energy photons, which may be assumed to have produced them some time in their travel through space, tend to be absorbed primarily by the nuclei of atoms, and in all nuclei positive electrons, of course, predominate, while hydrogen nuclei contain no negatives at all, and hydrogen constitutes,

[11] Thos. H. Johnson, Phys. Rev. **45**, 569 (1934).
[12] S. A. Korff, Phys. Rev. **46**, 75 (1934).

according to Russell, 95 percent of the universe. On the other hand, the lower energy photons will of course tend to be absorbed in all substances more by extra-nuclear electrons, which are all negatives, for it is these extra-nuclear electrons that are responsible for all the ionization described by the Klein-Nishina formula. The earth's magnetic field then separates out the incoming electrons on the basis of energy, the lower energies, primarily negatives, coming in at the poles—the very highest energies, very few in number, and coming mostly perhaps from hydrogen, being alone able to break through at the equator.

The foregoing facts and considerations lead, then, to the presentation of the following reasons for the view that the great bulk of the *sea-level ionization*, more than 85 percent of it, and indeed of all the non-field sensitive effects, must be attributed to photons.

(1) It is precisely the above-mentioned smallness in the required number of incoming positives that is needed to remove the contradiction heretofore existing between the demands of the east-west effect for an excess of positives at sea-level, and Anderson's direct determination[13] of the general equality in the numbers of positives and negatives passing through his cloud chamber at all energies, even up to 3 billion volts. Practically all of these electrons (+ and −) observed by Anderson are secondaries formed within our atmosphere and in the materials surrounding the cloud chamber. These may all be expected to be about equally divided between positives and negatives, while the 1 to 2 percent of ionization that must be attributed to the direct effect of incoming 10 billion-volt positives in order to account for the 6 to 12 percent west excess observed in Johnson's and Korff's Peru work with counters, involves an excess of positives wholly negligible in Anderson's work. This is powerful support for the view that the great bulk of the sea-level ionization must be due to photons. If it were due wholly, or even in any considerable measure, to incoming positives of 10 billion-volt energies and more, why do these not appear in the cloud chamber measurements which are capable of measuring with considerable dependability electron energies up to 4 billion volts, which is what is left of the energy of the 10 billion-volt electron after it has penetrated to sea-level? These 4 billion-volt tracks should be present in large numbers and they should be predominantly positives, quite contrary to the observations of both Anderson and Kunze.

(2) On the other hand, photons of this order of energy are actually and unquestionably found in photographs such as Figs. 9 and 11.[8] Here there are seen to spring directly from the body of the lead showers that can be due only to photons, since no ionizing track enters the top of the lead. Further, the joint energy of these showers is here from one to three billion volts, i.e., much too large to permit them to be accounted for as secondaries produced within the atmosphere by incoming electrons (see §III). There seems to be no escape, then, from regarding these showers as resulting from incoming photons themselves.

(3) If the great bulk of the non-field sensitive part of the ionization of the atmosphere is not due to these incoming photons, but rather to incoming electrons, then these latter, in order to ionize as strongly near the equator as near the poles—this is the definition of non-field-sensitive rays—must possess incoming energies of 10 billion volts or more, and produce directly one-sixth of all the ionization found at sea-level. The other five-sixths of the ionization which these rays produce directly or indirectly at sea-level would be due to the *very low* energy secondaries that incoming electrons were found to create in the atmosphere (see §III). In other words, the distribution of electron energies in a cloud chamber should then be, many energies below 50 million volts, few if any between 50 million and 4 billion, and many above 4 billion. This is a distribution completely at variance with that directly observed by both Anderson and Kunze, who find the great majority of the observed particles having energies between 300 million and 2 billion volts. These are much too energetic to be the secondaries produced by electrons, not energetic enough to be the incoming electrons themselves. Further, though neither Anderson nor Kunze find any large number of electrons of 4 billion volts or more, the one or two percent of such rays necessary to account for the latitude

[13] Carl D. Anderson, Phys. Rev. **44**, 406 (1933).

effect, longitude effect, and east-west effect, are so few in number as to be easily reconcilable with their observations. *The great bulk of the sea-level ionization, then, appears to be due to the effects of incoming photons.* And the energies of these photons must be of the same order of magnitude as those of the observed electrons, three-fourths of which are under a billion volts and half of which under 700 million volts.

(4) The photons of from 1 billion to 3 billion volts of energy *actually observed* in our 20,000 gauss field at the Norman Bridge Laboratory have ample penetrating power (see below) to produce all the effects observed by Millikan and Cameron and by Regener down to depths of from 100 to 300 meters of water, i.e., 10 to 30 atmospheres, whereas since the resistance of the atmosphere to an electron is 6 billion volts, incoming electrons to get down to such depths would have to have from 60 to 180 billion volts of energy. Such energies are out of all relation to those that have been found either in Pasadena or in Rostock; so that the ionization found in lakes by Millikan and Cameron, and checked by others, can scarcely be due to anything but such photons as are actually observed in our cloud chamber. (See 2 above.)

Incidentally, the relative penetrating power of photons and electrons of the same energy is of the order of 100 to 1 up to the highest accurately measured energies, and there is evidence that it remains of this order also for cosmic rays of the highest observed energy. Thus, the total number of ion pairs formed per cm of air path by electrons of energy 1,450,000 volts is given as 46[14] and at 32 volts per pair this gives a maximum range to electrons of this energy of 1.1 cm of water. But photons from Ra C of this energy pass easily through as much as a meter of water before being reduced to say 1 percent of their original intensity. Similarly, in the cosmic-ray field if photons have 100 times the penetrating power of electrons, the foregoing 180 billion volts required to drive electrons through 30 atmospheres of water is replaced by 1.8 billion volts for photons. But photons of 2 billion volts energy are in the range actually and commonly observed in the cloud chamber work at the Bridge Laboratory, so that the foregoing relative penetrating powers of 100 to 1 are at least in keeping with the above-mentioned facts.

(5) As for the characteristics of the ionization of the atmosphere *above* sea-level, they are even more difficult to reconcile with the hypothesis that the non-field sensitive portion is due in any large measure to incoming electrons, for Fig. 1 shows that the ionization, even in the equatorial belt, rises exponentially, or better as a sum of exponential terms,[15] clear up to the highest point reached (4.5 m below the top). This behavior is characteristic of photon absorption, but not at all of electron absorption. Indeed, it was shown by Bowen, and independently by both Epstein and Langer, that any rays coming in uniformly from all directions as the cosmic rays do, and ionizing uniformly along their path, as electrons do, when we neglect their nuclear secondaries, will give rise to a linear variation of ionization with altitude measured from the end of their range, i.e., from the level of the mean depth to which they penetrate.

Now, since the energy of all incoming electrons that can get through the blocking effect of the earth's field into the equatorial belt is 10 billion volts or more, the end of the range is nearly two atmospheres below the top so that a linear rate of increase above this level represents say a 50 percent increase from sea-level up to 22,000 feet (4.5 meters) and a still smaller increase from 4.5 meters up to the top. *The observed increase is, on the other hand, some 1000 percent from sea-level up to 22,000 feet, and much more than that above that point.*

This enormous discrepancy can be somewhat reduced, but not at all eliminated, by taking account of the secondaries produced by the incoming electrons through the mechanism of nuclear encounters, for since we have shown that these are all low energy secondaries, else they would produce a sea-level latitude effect between Pasadena and Churchill, the energy of the incoming electron must be frittered away in quite a large number of relatively small steps, i.e., more or less uniformly, even by these nuclear encounters.

[14] *Radiations*, etc., Rutherford, *et al.*, p. 447, 1930; also Bethe, Zeits. f. Physik **76**, 293 (1932).

[15] Millikan, Bowen and Neher, Phys. Rev. **44**, 250 (1933).

Nuclear photon absorption, on the other hand, whether brought about by photoelectric or by Compton encounters, consists in general—and we can also deduce this from our photographs—in the transfer of a large part of the energy of the photon to the ejected electron or electrons,[16] thus yielding an exponential law of absorption.

The absorption, then, by the atmosphere of incoming electrons of 10 billion volts and more, even though it might follow a law intermediate between that of linear and exponential absorption, must distinctly lean toward the former, and cannot possibly yield an altitude-ionization curve even remotely resembling that found experimentally from sea-level up to 4.5 m in Fig. 1 and up to 0.6 m in Fig. 4. *This constitutes the most general and the most cogent argument against the attempt to explain the non-field-sensitive portion of the cosmic-ray ionization as due primarily to incoming high-energy electrons, low-energy electrons being barred out by the blocking effect of the earth's field.*

If, on the other hand, incoming photons are the main ionizing agents, then, whether the nuclear absorption is of the photoelectric type or the Compton type,—and it is presumably the former—the mean energy of these photons must be of the same order of magnitude as the mean energy of the electrons produced by them, namely, say 200 ± 170 million electron volts. These figures are again consistent with the view that cosmic-ray photons have a penetrating power of the order of 100 times that of electrons of the same energy, for we have earlier shown that the effect of the main component of the cosmic rays—that for which the absorption coefficient is of the order $\mu=0.5$—just about reaches down to sea-level, while it requires six billion-volt incoming electrons to have such a range.

(6) Again, evidence for the view that the ionization found in the atmosphere *above sea-level* cannot be produced wholly or even chiefly by 10 billion-volt incoming electrons is found in the consideration that the penetrating power of such rays, both as to their primary and their secondary constituents, must obviously increase, or at most remain constant with increasing altitude, since the energy of the ionizing agents at the top of the atmosphere is 10 billion volts and at the bottom but 4 billion. On the other hand, *the observed mean penetrating power actually decreases very markedly as shown in Fig. 5 between sea-level (10 m) and 6 m of water beneath the top.* It is difficult to see how this can be interpreted save in terms of photons of decreasing mean hardness with increasing altitude. Above 6 m, Fig. 5 shows that the penetrating power continues to decrease, but now much less rapidly, as though the ionization were now due mainly to a single photon band of coefficient of absorption somewhere near $\mu=0.5$. This part of the curve of Fig. 5 must, however, be attributed to a mixture of causes, as shown in §VII below.

§VII. Effects Due to the Field-Sensitive Portion of the Incoming Rays

All of the field sensitive part of the ionization produced by cosmic rays is, of course, due directly or indirectly to incoming electrons. When we compute from the difference between the ordinates of the upper and lower curves of Fig. 1, the mean *apparent* absorption coefficient of the rays producing this ionization, it comes out roughly $\mu=1.0$ per meter of water. But we are not disposed to attach any physical significance to this *apparent* coefficient, since it is due to the ionization produced at the end of the ranges of electrons of widely varying energies. However, the rapid rise with altitude of the ionization between the upper and lower curves of Fig. 1 may be understood from the following considerations. We have already shown in §IV and §V why we regard the chief component of the non-field-sensitive portion of the upper-air ionization as due to a beam of incoming photons of energy of the order 200 ± 170 million electron volts. Such a beam would get into equilibrium with its secondaries at a depth below the top corresponding to the range of say 300 million-volt electrons which, since it takes 6 billion-volt electrons to penetrate the atmosphere—10 meters of water—would be at a depth beneath the top of $300/6000\times10=0.5$ m. If the earth had no magnetic field and if the cosmic rays were all of this frequency there would be at all latitudes an exponential rise of the ionization with altitude at a rate somewhere near $\mu=0.5$ per meter of

[16] Anderson, Millikan, Neddermeyer and Pickering, Phys. Rev. **45**, 363 (7) (1933).

water clear to the top if the beam were in equilibrium with its secondaries upon entering. On the other hand, if it entered as a *pure* photon beam, unmixed with any of its secondaries, the ionization would start from zero at the outer edge of the atmosphere and rise to a maximum a 0.5 m below the top and then fall off exponentially (with $\mu=0.5$) for increasing depths beneath the top.

The foregoing simple picture does not correspond to reality for at least two important reasons. First, the incoming cosmic rays are distributed over a wide range of energies, the distribution curve at sea level, according to Anderson[17] having a very weak intensity at energies as high as 3 or 4 billion volts, increasing rapidly with decreasing energy and going through a maximum at say 600 million volts. This maximum, according to our own measurements herewith presented, moves rapidly toward lower energies with increasing altitude.

The second big factor of disturbance to the foregoing simple picture is the earth's magnetic field. If the photons of all the preceding energies were in equilibrium with their secondaries before entering the earth's magnetic field, this equilibrium would in any case be entirely destroyed by that field. At Panama, for example, all the electron secondaries below about 8 billion volts are blocked out by that field, while at Spokane all electron secondaries down to say 2 billion volts get through. This accounts for the rapid rise with altitude of the field sensitive ionization represented by the difference between the Panama and the Spokane curves (Fig. 1). For, as Anderson's energy-distribution curves show, the number of incoming secondary electrons increases rapidly as the energy decreases from 8 billion down to 2 billion volts. The result is not at all the linear rise with altitude discussed in §VI 5 due to incoming electrons of a given energy above 10 billion volts, but a very much more rapid rise due to the fact that 2 billion-volt electrons, for example, first let in copiously through the field at magnetic latitude 52°, can only penetrate one-third of the way through the atmosphere and hence must do all their ionizing above that level. The effect here under consideration is very beautifully shown in Fig. 6, in which we present a comparison of the results of all the recent stratosphere flights. In the most northerly of these, the Fordney-Settle one,—measurements by Millikan and Neher, the most accurate yet made—the ionization near the top is seen to be very much larger than in the two Bowen-Millikan flights or the Regener flight all made at about mag. lat. 42°, where no electrons of energies under about 4 billion volts can get through the earth's magnetic field. There is still some experimental uncertainty with respect to these three lower curves of Fig. 6, but not enough to change the main conclusion here drawn.

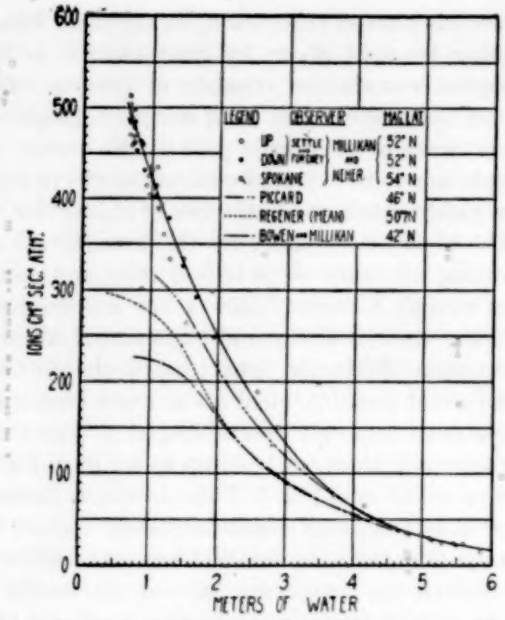

FIG. 6. Comparison of the results of recent high altitude measurements.

We interpret also the *shapes* of the upper part of the curves made by Bowen and Millikan and by Regener at latitude 42° as due to the effect of the incoming electrons of between 4 billion and 8 billion volts. For there are now no longer present the incoming 2 to 4 billion-volt secondaries to add to the ionization of the underlying photons in the upper part of the atmosphere, while the 4 to 8 billion ones are approaching the energies at which they penetrate the entire atmosphere and are therefore nearing the conditions that give rise to the linear ionization law discussed in §VI 5. In a word,

[17] Carl D. Anderson, Phys. Rev. **44**, 406 (1933).

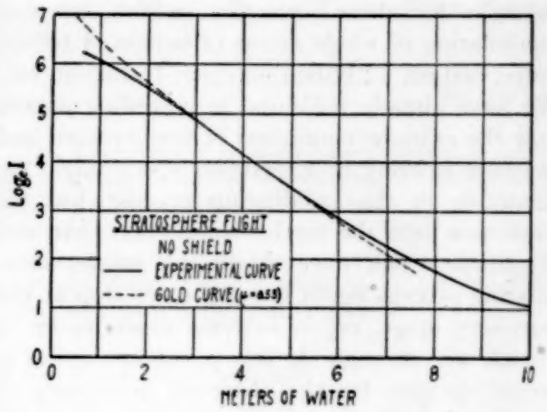

FIG. 7. Logarithmic plot of the ionization measurements made on the Fordney-Settle flight.

then, the altitude-ionization curve shown in Fig. 6 represents a combination of the effects of the incoming photons of energies of the order 200 ± 170 million volts, and such incoming secondary electrons as the earth's magnetic field will let through. These latter should be very strong ionizers in sufficiently northern latitudes and at great altitudes, but should do a relatively small part of the ionizing in the equatorial belt. There they must be responsible for the longitude effect and the east-west effect, both found in the equatorial belt. We are hoping to do some higher altitude flights near the equator to test further these conclusions.

Fig. 7 shows the results of the Fordney-Settle flight plotted on a log scale. This displays nicely (1) how from sea-level (10 m) up to the height of Pikes Peak (6 m) a sum of exponentials is needed to reproduce the observed ionization; (2) how a single absorption coefficient $\mu=0.55$ takes care of the ionization from 6 m to 2.5 m below the top, despite the complex character of the causes at work in this region, i.e., relatively low energy photons plus high energy (8 billion to 2 billion volts) incoming secondary electrons; (3) how at a depth of about 2.5 m below the top the constancy of the exponential rise at $\mu=0.55$ breaks down, presumably because of the effect of the incoming secondary electrons.

VIII. The Origin of the Cosmic Rays

The conclusions of the preceding sections rest upon the two fundamental postulates, namely, (1) the general validity of the analysis of Epstein and Lemaitre-Vallarta as to the effect of the earth's magnetic field on incoming electrons; and (2) the validity of the evidence that in general the immediate ionizing agents in the production of cosmic-ray ionization are free positive and negative electrons, other ionizing agents not being necessarily absent entirely but at any rate exerting a negligible influence. The general qualitative validity of the first postulate will scarcely be questioned, and its quantitative validity is not of vital importance. For example, if the energies necessary to get through the earth's magnetic field were but half those computed by Epstein, the whole scale of electron energies would be reduced one-half without fundamentally modifying the reasoning or the conclusions.

The second postulate that the immediate ionizing agents are electrons (+ and −) rests upon two sorts of evidence. First, we have studied most carefully thousands of cloud-chamber photographs without finding any evidence for the presence in appreciable amount of protons or other heavy particles of any sort. If the Newtonian laws of encounter hold, protons, neutrons, or other heavy particles cannot transfer energies of millions and billions of volts to electrons such as we find in all our photographs. Only electrons and photons can possibly produce the type of effects shown in Figs. 7, 8, 9, 10, 11, 12, 13, 14.[8] The combination of ionization, range and curvature shown in all these tracks fixes the ionizing agent in practically all cases as an electron (+ or −). Even more certain evidence on this point, however, is found in the fact that the multiplying factor due to raising the pressure in an electroscope is the same for gamma-rays and cosmic rays. We have tested this point directly or indirectly clear up practically to the top of the atmosphere. This means, as Bowen and Millikan first showed[18] that the fraction of ions formed that recombine is the same in both cases, and this can be true only if the immediate ionizing agent has in general the same ionizing power per cm of path in the two cases.

Given the correctness of these two postulates,

[18] R. A. Millikan and I. S. Bowen, Nature, Oct. 2, 1931; also R. A. Millikan, Phys. Rev. 39, 397 (1932).

it follows, for the reasons given in §VI, that the whole non-field-sensitive portion of the ionization cannot possibly be due to incoming electrons of an energy of 10 billion volts and more, and yet these are the only electron energies which the earth's magnetic field permits to penetrate into the equatorial belt. The very fact, then, that we need incoming photons at all to interpret cosmic-ray effects eliminates entirely the possibility that the source of the cosmic rays is to be found in cosmic electrical fields which impart these 10 billion-volt energies to electrons that fall through them.

So far, then, as we can now see, the only remaining possible source of these observed energies lies in atomic transformations taking place in accordance with Einstein's equation $E=mc^2$. The building out of hydrogen of the common elements is of course only a special case of this transformation of mass into radiant energy, and since such building of the helium atom releases 30 million electron volts, of oxygen 116 million, of silicon 216 million, of iron 460 million, there is no other origin which we can now see of the great absorption band found by us in the equatorial belt at about $\mu=0.5$ and modified by its mixture in the temperate belt with incoming secondary electrons into something like $\mu=0.55$. This band alone seems to be responsible for about 90 percent of the cosmic-ray ionization in the equatorial belt. Its energy is at least of the right order to fit this hypothesis, and no other source of energies of these magnitudes is yet in sight. It will be recalled that the condensation or clustering of hydrogen atoms into hydrogen "dust" in the intense cold of interstellar space is a necessary antecedent to the building-up act. The conclusions of modern astronomers as to the existence of much interstellar dust is not out of line with this hypothesis.

But since the foregoing analysis requires a small number of cosmic-ray energies as high as 10 billion volts, there seems to be no origin in sight for these save the sudden *complete* annihilation of whole atoms of helium, 4 billion volts; carbon, 12 billion; oxygen, 16 billion, etc. We have already indicated in preceding papers how the extreme conditions of temperature and pressure existing in interstellar space might be favorable to the building-up process, but we must now add the further suggestion that any condition which once starts the matter-annihilating process might in some cases stop at the part-way stage, or, in extreme cases, carry it completely through. If this possibility exists it would account for the observed uniformity of distribution of all the cosmic-ray bands, high energy as well as low, over the celestial dome, the most extraordinary characteristic of these rays. If we discard such suggestions to locate the events giving rise to cosmic rays in interstellar space we then seem to be forced to postulate, as Baade and Zwicky[19] do, some other sort of extraordinary conditions not depending on low temperatures and pressures, such as those existing in novae, to call forth both these partial and complete annihilation processes; or, again, we could take the alternative already suggested by other scientists and associate these annihilation processes with conditions existing at some preceding time when the universe was in a different state from that now existing. *At any rate, in the present state of our knowledge both the partial annihilation of matter, like that exhibited in the building of the common elements out of hydrogen, and the complete annihilation of atoms, seem to be called for to account for the energies actually found in the cosmic rays.*

All of the foregoing work has been made possible through a grant from the Carnegie Corporation of New York, administered by the Carnegie Institution of Washington. We desire to express our deep appreciation for this assistance.

[19] W. Baade and F. Zwicky, Proc. Nat. Acad. Sci. **20**, 259 (1934).

A Coincidence Test of the Corpuscular Hypothesis of Cosmic Rays

DAVID S. HSIUNG, *Ryerson Physical Laboratory, University of Chicago*

(Received August 17, 1934)

Three Geiger-Müller counters were arranged vertically so that double coincidences were recorded by the counters 1 and 2 and triple coincidences by counters 1, 2 and 3 simultaneously. The third counter was permanently shielded by a lead cylinder of 2.5 cm thickness which is sufficient to absorb all the secondaries produced in the absorber. Counts were made under three conditions:

	Double(hr.$^{-1}$)	Triple(hr.$^{-1}$)
(A) Without lead absorber	202.44±1.84	42.43±0.83
(B) With 20 cm of lead between counters 1 and 2	124.48±1.43	30.50±0.50
(C) With 20 cm of lead above counter 1	142.17±1.08	32.55±0.52

The reduction in the number of counts due to the lead was thus slightly greater in position *B* than in position *C*. That this difference can be ascribed to secondaries is shown by the fact that *B*/*C* is less for the double coincidences than for the triple ones. The data can be interpreted by assuming that the coincidences are due chiefly to penetrating ionizing particles, some of which are stopped by the lead (for which *B* should equal *C*), with the addition of a few coincidences in case *C* due to secondaries produced in the lead by a penetrating ray associated with a penetrating particle traversing the shielded tube 3. It does not appear possible to account for these coincidences in terms of corpuscles excited by photons unless the photons either are absorbed in the atmosphere before reaching the apparatus, or are accompanied throughout their path by ionizing particles, which would practically mean treating the photons as ionizing particles. That is, the coincidences seem to be due to penetrating ionizing particles and not to secondary particles produced by photons which traverse the lead. This view is further supported by the close agreement of the absorption coefficients computed from this experiment ($\mu = 2.2\times10^{-3}$ cm^{-1}) with those determined from ionization chamber measurements of the cosmic rays ($\mu = 1.90\times10^{-3}$ cm^{-1}).

IT has been pointed out by Compton,[1] Auger[2] and others[3] that the hypothesis of charged corpuscles is adequate to account for the effect of the earth's magnetic field on the intensity and angular distribution of cosmic rays, for their absorption in the atmosphere and in deep water, and for the various coincidence experiments performed with Geiger-Müller counters. A few investigators, including Millikan[4] and Regener,[5] impressed by the close agreement between the absorption coefficient of the strong softer component of cosmic rays and that calculated for photons resulting from various types of nuclear transformations, have preferred the photon hypothesis.

In 1929 Bothe and Kolhörster[6] developed a coincidence method for counting the penetrating particles. From the fact that the absorption in gold of the particles producing the coincidence was nearly the same as that of the cosmic rays as measured with ionization chambers, they identified these corpuscular rays with the cosmic radiation itself. When Rossi[3, 7] repeated Bothe and Kolhörster's experiments he found that secondaries are produced in lead by cosmic rays, which are also able to produce coincidences. Using three counters, Rossi confirmed Bothe and Kolhörster's results by showing that up to a thickness of 101 cm of lead the absorption of the coincidences follows closely that characteristic of cosmic rays as found by depth-ionization measurements. Yet in this work also the results were somewhat confused by the presence of secondaries. Rossi showed that the mean penetrating power of these secondary particles was about one cm of lead, and argued that since only those secondary particles produced in the lowest layer of the absorber could get out, the coincidences which they produce should be a constant fraction of the total number. More recent studies by Rossi,[7] Swann and Montgomery,[8] Johnson and Street,[9] and others have

[1] A. H. Compton, Nature **131**, 713 (1933); Science **77**, 480 (1933); The Science of Radiology, 398 (1933); Phys. Rev. **45**, 441 (1934).

[2] P. Auger, J. de physique et le radium **5**, 1 (1934).

[3] B. Rossi, Zeits. f. Physik **68**, 64 (1931); Rend. Lincei **15**, 734 (1932); La Ricera Scientifica **3**, No. 7 (1932); A. Corlin, Annals Univ. Lund. No. 4 (1934); J. Clay, Amsterdam Proc. **35**, 1282; **36**, 62 (1933); T. H. Johnson, Phys. Rev. **41**, 545 (1932).

[4] R. A. Millikan, Phys. Rev. **43**, 661 (1933), *et al.*

[5] E. Regener, Phys. Zeits. **34**, 880 (1933), *et al.*

[6] W. Bothe and W. Kolhörster, Zeits. f. Physik **56**, 751 (1929).

[7] B. Rossi, Zeits. f. Physik **82**, 151 (1933); Nature **132**, 173 (1933).

[8] W. F. G. Swann and C. C. Montgomery, Phys. Rev. **44**, 52 (1933).

[9] T. H. Johnson and J. C. Street, Phys. Rev. **40**, 638 (1931); **42**, 142 (1932).

shown also that frequent coincidences result from showers of ionizing particles which originate in the roof of the building and sometimes in the atmosphere itself. The number of such coincidences in Rossi's absorption experiments was presumably nearly independent of the thickness of the lead.

The present paper describes a coincidence experiment performed under such conditions that coincidences due to showers of ionizing particles and of secondaries from the lead absorbers can be distinguished from those due to primary ionizing particles passing directly through the counters. A measurement of the absorption of these primary particles in the lead is also obtained.

In one of Rossi's early experiments, using a double coincidence counter, he placed the absorbing lead alternately above and between the counting tubes. If the coincidences were due entirely to penetrating particles directly traversing both counters, the effect of the lead in stopping these particles and reducing the coincidence rate should be the same in both positions. If, however, photons should produce secondaries in the lead capable of passing through the counters, coincidences might be produced with the lead block above the counters, but not if placed between, since the photon would not itself ionize the gas in the first counter. The experiment showed a lower counting rate with the lead between the two tubes than when placed above them. This could be explained as due to a mixture of primary photons and ionizing particles, or as due to primary ionizing particles which may produce secondaries in the lead.

The present experiment is similar to that of Rossi except that a third counter, shielded with 2.5 cm lead, is placed below the other two. The results obtained with this arrangement are such as to show that if photons produce any ionizing secondaries in the lead blocks, they have a range of less than 2.5 cm in lead, and are thus to be distinguished from the penetrating particles responsible for the triple coincidences. The absorption of the penetrating particles by the lead is in close agreement with the value found by Rossi, when his value is corrected for the effect of spurious coincidences, and supports the view taken by previous experimenters that these penetrating ionizing particles may be identified with the primary cosmic rays.

Apparatus and Procedure

Three Geiger-Müller counters were made in the laboratory according to the technique of Mott-Smith.[10] The sheet copper tube is 4 cm in diameter and 25 cm long. The central wire is of tungsten, 0.025 mm in diameter. The tubes were cleaned, evacuated, baked out and filled to 4.5 cm pressure with cleaned air and a trace of iodine vapor. All tubes were tested for uniformity on the counter circuits before sealing off.

The amplifying circuit shown in Fig. 1, was based on that described by T. H. Johnson.[11] It was, however, so arranged that the circuits 1 and 2 form double, and these together with circuit 3 form triple coincidences. Coincidences are recorded by an electromagnetic device which

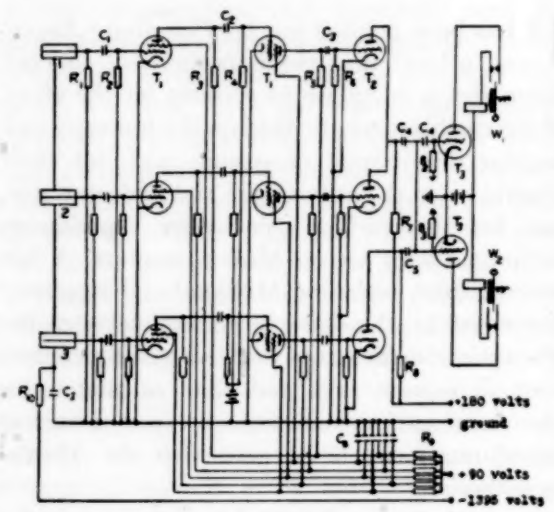

1, 2, 3, G–M counters
R_1, 10^{10} ohms
R_2, 10^7 ohms
R_3, 5×10^4 ohms
R_4, 10^6 ohms
R_5, 2×10^4 ohms
R_6, 10^5 ohms
R_7, 5×10^4 ohms
R_8, 2.5×10^4 ohms
R_9, 2×10^4 ohms
R_{10}, 10^6 ohms
C_1, 10^{-6} mf
C_2, 2×10^{-3} mf
C_3, 2.5×10^{-4} mf
C_4, 6×10^{-3} mf
C_5, 2×10^{-3} mf
C_6, 2 mf
T_1, tube 24A
T_2, tube 27A
T_3, thyratron No, 1 (256A)
T_4, thyratron No. 2 (256A)
W_1, watch recorder for doubles
W_2, watch recorder for triples
B_2, C-bias (−45 v) on thyratron 1
B_4, C-bias (−55 v) on thyratron 2

Fig. 1.

[10] L. M. Mott-Smith, Phys. Rev. **39**, 403 (1932).
[11] T. H. Johnson and J. C. Street, J. Frank. Inst. **215**, 239 (1933).

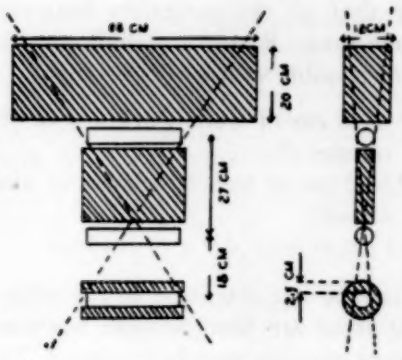

FIG. 2.

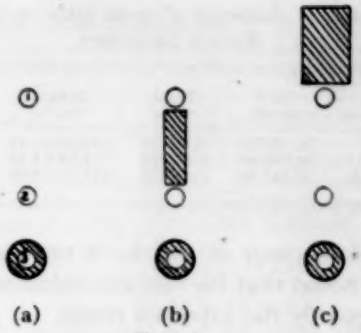

FIG. 3.

operates the escapement of a watch and also serves to break the plate circuit of the thyratron. After proper voltage adjustment, the apparatus was given repeated tests by the application of a negative potential to the grid of the first stage of each circuit separately and jointly. It was found that thyratron No. 1 went off only when the negative potential was applied to the grid of the first stage of circuits 1 and 2 or all the three circuits, and thyratron No. 2 went off only when the negative potential was applied to the grid of the first stage of all three circuits. In order to insure the necessary constant voltages in spite of the considerable current demand, a combination of accumulator batteries and *B* eliminators was used. It was thus possible to prevent the counting rate from varying appreciably throughout the several months required for the experiment.

Referring to Fig. 2, the three counters were arranged vertically so that double coincidences were recorded by counters 1 and 2 and triple ones simultaneously by counters 1, 2 and 3. The distance from center to center was 18 cm between counters 1 and 2, and 27 cm between counters 1 and 3. The lead cylinder permanently surrounding the third counter was of sufficient thickness (2.5 cm) to absorb all the secondaries produced in the lead absorber placed above.* The thickness of the absorbing block for different experimental conditions was always the same, 20 cm; but the area of the horizontal cross section was determined by the geometrical configuration in relation to the separation of the counting tubes. This is shown in Figs. 2(a) and 2(b).

Counts were made under three conditions:

(A) With no absorber ..... (Fig. 3(a))
(B) With absorber between counters 1 and 2 ..... (Fig. 3(b))
(C) With absorber above counter 1. (Fig. 3(c))

From the coincidences so recorded the false coincidences must be subtracted in order to obtain the abundance of the systematic coincidences. Theoretically, the number of the accidental double coincidences may be calculated[11] in terms of the relaxation time and the individual counting rate. Practically it was preferred to count the accidentals directly by placing all the counters in a horizontal plane.

Preliminary readings taken in the basement of Eckhart Hall are tabulated in Table I. Under condition *B* one should expect a decrease both in double and triple coincidences due to the absorption of the primary corpuscles. Under condition *C* the amount of primary rays absorbed should be the same as under condition *B*, but the secondary rays generated in the lowest part of the absorber should increase the double coincidences, without any effect, however, on

TABLE I. *Preliminary counts in basement of Eckhart Hall.*

Case	Coincidences Observed		Accidentals		Systematic	
	Double ($hr.^{-1}$)	Triple ($hr.^{-1}$)	Double ($hr.^{-1}$)	Triple ($hr.^{-1}$)	Double ($hr.^{-1}$)	Triple ($hr.^{-1}$)
A	142.33±3.4	28.13±1.5	29.9	0.9	112.43±3.4	27.23±1.5
B	121.70±3.1	22.98±1.4	29.9	0.9	91.80±3.1	23.08±1.4
C	129.35±3.2	24.00±1.4	29.9	0.9	99.45±3.2	23.10±1.4

* This point was tested by auxiliary experiments in which a shield of 8.0 cm was used. The results were unchanged by this heavier shield.

TABLE II. *Summary of counts taken on roof of Ryerson Laboratory.*

Case	Hours	Total double	Total triple	Double (hr.$^{-1}$)	Triple (hr.$^{-1}$)
A	60	12,146.56	2,546.56	202.44±1.84	42.43±0.83
B	120¼	15,002.09	3,676.40	124.48±1.45	30.50±0.50
C	121⅛	17,261.84	3,953.30	142.17±1.08	32.55±0.52

the triple because of the shield on counter 3. It is to be noted that the last two columns in Table I give exactly the expected result.

In order to reduce the effect of secondaries from the walls of the building the apparatus was finally installed within a thin wooden shelter on the roof of Ryerson Laboratory. The double and triple coincidences were continuously registered as before under each of the three conditions *A*, *B* and *C*, the results being summarized in Table II. The registration duration for the individual readings was 20 hours. During this time readings of the two watch recorders were taken at different intervals and the voltages on different parts of the apparatus were frequently checked. It will be seen that the double coincidences in case *C* are more frequent than in case *B*, in accord with Rossi's finding. The ratio of the counting rate B/C for triple coincidences, 0.94 ± 0.02, is, however, nearer to unity than the corresponding ratio for double coincidences, 0.88 ± 0.01.

INTERPRETATION

This result was to have been expected if most of the coincidences are due to ionizing particles passing directly through all three counters, for they should produce secondaries in case *C* which though capable of penetrating counters 1 and 2 to give double coincidences, would not enter the shielded counter 3 to give a triple coincidence. The small remaining difference between the triple coincidences in cases *B* and *C* may be explained thus: A primary particle on traversing the large lead shield in case *C* ejects from it secondaries which enter counters 1 and 2, while the penetrating primary particle passes on through counter 3. An adequate corpuscular interpretation of the result is thus readily found.

Let us now investigate the possibility of accounting for these results on the view that the coincidences result from secondary beta-particles produced by photons. For simplicity, we shall assume that all the secondary beta-rays have the same range R, and we shall consider three different possible values of this range:

I. $R<2.5$ cm of lead (thickness of shield on counter 3).
II. $R>20$ cm of lead (thickness of absorption screen).
III. 2.5 cm of lead $<R<20$ cm lead.

If we confine our attention to the triple coincidences, there are four possible ways in which coincident impulses may be produced. These are:

1. A single β traverses counters 1, 2 and 3.
2. β_1 traverses 1 and 2, while β_2 traverses 3.
3. β_1 traverses 1, while β_2 traverses 2 and 3.
4. β_1 traverses 1, β_2 traverses 2, and β_3 traverses 3.

Possibility 1 represents a single β-particle of high range setting off all three counters. Coincidences due to pairs, showers and bursts of ions are represented by possibilities 2, 3 and 4.

Table III summarizes, for cases I, II and III and 1, 2, 3, and 4, the predicted values of B/C, where B represents the coincidence rate with the absorbing block between counters 1 and 2 and C the rate with the absorber above the counters. In this table, we assume that 20 cm of lead reduces the number of traversing β's by a factor K. Due to the passage of the photons and the incident β's through the lead, secondaries are emitted from its lower side which are m times the number of β's striking the upper side. The total emergent β's are then $L=K+m$ times as many as the incident β's. Usually $L<1$; but always $L>K$ except when $m=0$, which would mean no secondaries due to photons. Thus for cases I and III, $K=0$ and $L=m$; for the case II, $0<K<L$. In calculating the ratio B/C in case II we note that since the range of the β's is greater than 20 cm, they will probably originate at a distance above the counters about equal to the air equivalent of 20 cm of lead, i.e., about 2 km away. Thus without the lead absorber above the counters it is highly improbable that more than one particle originating at such a distance will strike the counter tubes. The same argument applies with somewhat less weight to case III, but not necessarily to case I.

Examination of Table III will show that of the 12 imagined types of coincidences only those

TABLE III. *Summary of predicted values of B/C under various assumptions.*

Possibilities for triple coincidences	I $R<2.5$ cm Pb	II $R>20$ cm Pb	III $2.5<R<20$ cm Pb
1. β through 1, 2, 3	$B/C=K/(K+m)=0$	$B/C=K/(K+m)<1$	$B/C=K/(K+m)=0$
2. β_1 through 1, 2 β_2 through 3	$(B/C)_1=K/(K+m)=0$ $(B/C)_2\sim 1$ $(B/C)_1(B/C)_2\doteq 0$	$(B/C)_1=K/(K+m)<1$ $(B/C)_2\sim 0$ because β_1 originates far away in exp. B $(B/C)_1(B/C)_2\doteq 0$	$(B/C)_1=K/(K+m)=0$ $(B/C)_2\ll 1$ (Distant origin of β_1) $(B/C)_1(B/C)_2=0$
3. β_1 through 1 β_2 through 2, 3	$(B/C)_1=1/m>1$ $(B/C)_2=0$ (can't penetrate tube 3) $(B/C)_1(B/C)_2=0$	$(B/C)_1=1/L>1$ $(B/C)_2\sim 0$ same reason as above $(B/C)_1(B/C)_2\sim 0$	$(B/C)_1=1/m>1$ $(B/C)_2\ll 1$ same reason as above $(B/C)_1(B/C)_2\ll 1$
4. β_1 through 1 β_2 through 2 β_3 through 3	$(B/C)_1=1/m>1$ $(B/C)_2\sim 1$, if origin of β_1 is from tube 1, otherwise $\ll 1$ $(B/C)_3\sim 1$ same reason as above $(B/C)_1(B/C)_2(B/C)_3\sim 1$	$(B/C)_1=1/L>1$ $(B/C)_2\sim 0$ same reason as above $(B/C)_3\sim 0$ same reason as above $(B/C)_1(B/C)_2(B/C)_3\sim 0$	$(B/C)_1=1/m>1$ $(B/C)_2\ll 1$ same reason as above $(B/C)_3\ll 1$ same reason as above $(B/C)_1(B/C)_2(B/C)_3\ll 1$

characterized as *I 4* and *II 1* are capable of giving the observed result of B/C almost equal to 1. These we now examine in further detail.

In case *I 4* the photon must traverse the lead shield about counter 3, since the β-ray which it emits is incapable of passing through the shield. The photon must, however, have already produced two β's which will have entered counters 1 and 2. If in experiment *B*, with the lead between counters 1 and 2, the probability of a β-ray passing through tube 1 is to be comparable with that for *C* when the lead is directly over counter 1, the probable origin of the first β-particle must be only a very short distance above the first counter. This condition cannot be fulfilled if the range of the β's is much greater than the thickness of the counter tube wall. Case *I 4* is thus satisfactory only if the photon has a high probability of producing a separate β-ray which will ionize the gas in each counter traversed. That is, the photon itself acts as an ionizing particle.

This is identical with the conclusion required by Johnson and Street's[12] experiment, with counters similarly arranged, by comparing the triple coincidences with doubles in counters 1 and 3. His results indicated that if the triple coincidences are due to secondary β-rays produced by photons, there must *always* be a β-ray passing through the counter traversed by the photon. Such an action by a photon is so contrary to our knowledge of the catastrophic nature of β-particle production by photons, either as photo- or recoil-electrons, that it seems justifiable to rule out this possibility.

We have noted above that the observed ratio of $B/C=0.94$ can be accounted for in terms of penetrating ionizing particles traversing all three counters, with an occasional production of secondaries in experiment *C* traversing counters 1 and 2. This interpretation will still hold if, as in case *II 1*, the β-particles are produced by photons in the atmosphere above the apparatus. If, however, any appreciable fraction of these penetrating β-rays are produced by the photons traversing the lead, B/C should be markedly less than 1. If all the coincidences were due to penetrating β-particles produced in the lead, counter 1 would receive no β's in case *B*, so B/C should be 0. From the observed ratio 0.94 we can say that less than six percent, if any, of the coincidences in experiment *C* are due to penetrating secondaries produced by photons in the lead absorber.

For highly penetrating photons passing through the atmosphere, equivalent to about 90 cm of lead, and then through 20 cm of lead directly over the counting tubes, much more than six percent of the β-particles reaching the tubes should originate in the lead absorbers. The small β-ray production in the lead might, however, be interpreted by supposing that

[12] T. H. Johnson and J. C. Street, Phys. Rev. **42**, 144 (1932).

photons had been more than 94 percent absorbed in the atmosphere before reaching the apparatus, whereas, the resulting β-particles were more penetrating than the parent photons. We thus reach what seems to be the only permissible photon interpretation of this experiment, namely, that the photons themselves are almost or completely absorbed in the atmosphere above the apparatus, but produce β-particles more penetrating than the photons which cause the observed coincidences. This experiment cannot distinguish such penetrating secondary β-particles if unaccompanied by their parent photons, from primary β-rays coming from above the atmosphere.

Absorption of Coincidence Particles

Comparison of the absorption of the coincidence-producing particles with that of cosmic rays as measured in ionization chambers shows that these absorptions are nearly the same, thus supporting the conclusion of earlier workers that the radiations measured by the two methods are of fundamentally the same nature.

From the usual absorption coefficient formula,

$$\mu=(1/x)\log(I_0/I), \tag{1}$$

where x is the thickness of the absorbing screen, and I_0/I is the ratio of the counting rate without to that with the screen, and by assuming in each case the absorbing block between tubes 1 and 2, where secondaries are of least importance, we get for the double coincidences,

$$\mu_{Pb2}=24\times10^{-3}\text{ per cm} \tag{2}$$

and for the triple coincidences,

$$\mu_{Pb3}=16\times10^{-3}\text{ per cm.} \tag{3}$$

Kolhörster and Tuwim[13] give the following relation between the absorption coefficients of cosmic rays in different substances:

$$\frac{\mu_{H_2O}}{\mu_{Pb}}=\frac{\rho_{H_2O}(Z/A)_{H_2O}}{\rho_{Pb}(Z/A)_{Pb}}. \tag{4}$$

Here ρ is the density (10.6 g/cc in these experiments) and Z and A are the atomic number and weight, respectively. Thus we find,

$$\mu_{H_2O}=0.142\mu_{Pb}$$
$$=3.2\times10^{-3}\quad\text{(doubles)} \tag{5}$$
or
$$=2.2\times10^{-3}\quad\text{(triples).}$$

To compare the values for the absorption coefficient thus obtained with that from ionization chamber measurements, we calculate first the intensity supposing that the radiation enters normally into the atmosphere. This is given by Gross'[14] transformation,

$$\psi=I-PdI/dP,$$

where ψ is the intensity for rays coming vertically through the atmosphere I is that as observed from all directions, and P is the barometric pressure. The absorption coefficient is then determined graphically from the ψ *vs.* P curve from the relation,

$$\mu=d\psi/\psi dP.$$

From the values of I *vs.* P collected by Eckhart[15] we thus find for the absorption in water at a depth of 11.5 meters, the equivalent of the atmosphere plus half of the 20 cm lead absorber,

$$\mu=1.90\times10^{-3}\text{ cm}^{-1}\quad\text{(ionization).} \tag{6}$$

The agreement between this value for μ and that from the triple counter method where secondaries play a minimum rôle, is as close as can be expected in view of the difference in procedure, and indicates that the rays responsible for the coincidences are the same kind as those measured with ionization chambers. This supports the findings of Bothe and Kolhörster and of Rossi. We have shown, however, that the coincidences here studied are due to ionizing particles of high penetrating power. The close agreement of their absorption coefficients is thus most readily interpreted on the view that the cosmic rays observed with ionization chambers likewise consist of ionizing particles.

It gives me great pleasure to acknowledge my indebtedness to Professor A. H. Compton for the suggestion of the problem and for his constant inspiration and helpful advice throughout the investigation. I wish also to express my thanks to The Rockefeller Foundation for the Fellowship that enabled me to work on this problem.

[13] W. Kolhörster and L. Tuwim, Physikalische Probleme der Hohenstrahlung, 148 (1934).

[14] B. Gross, Zeits. f. Physik **83**, 214 (1933).

[15] C. Eckhart, Phys. Rev. **45**, 851 (1934).

Two-Crystal Study of the Structure and Width of *K* X-Ray Absorption Limits

WALTER H. ZINN, *Columbia University*

(Received June 13, 1934)

The double-crystal spectrometer has been used to examine the *K* absorption limits of the elements Se, Rb, Zr, Mo and compounds of these elements. All of the substances examined show structure either on the short wave-length side of the main absorption limit or in the limit itself. The intensity and location are discussed with reference to the theory of secondary structure given by Kronig. The widths of the absorption limits have been measured and it is shown that the widths are approximately constant for elements of atomic number less than 32 and that from there on they increase as the fourth power of the atomic number.

THE purpose of this investigation is to obtain data on the structure, width and the effect of chemical combination on the structure and width of the *K* absorption limits of elements of atomic number greater than 34. Barnes[1] has used the double-crystal ionization method to examine the fine structure[2] of the *K* limits for the elements manganese to zinc. All other investigations of *K* limits of the elements of atomic number less than 34 have been made with the single crystal spectrograph. Bergen Davis and Harris Purks[3] have demonstrated that the two-crystal spectrometer is suitable for measurements of the widths of limits of elements of higher atomic number, while recently P. A. Ross[4] has used this instrument to measure secondary structure as well.

APPARATUS

The double-crystal x-ray spectrometer has been described by Bergen Davis and Harris Purks.[5] A water-cooled tungsten target x-ray tube with a thin glass window provided the continuous spectrum. The beam was limited by slits 0.4 cm wide and 0.8 cm high. The cylindrical ionization chamber, of length 7 cm and diameter 2.5 cm, was filled with methyl bromide gas. The ionization current was amplified by an FP-54 pliotron and read on a Leeds and Northrup type *R* galvanometer. Rates of deflection of the galvanometer were observed. Sensitivities of 10,000 mm/volt to 30,000 mm/volt were found convenient, the corresponding currents being of the order of 3 to 1×10^{-15} ampere.

The absorbing screens were prepared in various ways. Substances in powder form were ground as fine as possible and then sifted onto cigarette paper coated with a thin layer of castor oil, several sheets being used as the absorbing screen. The selenium compounds were pressed between two very thin sheets of mica by a pair of brass grids. As these compounds appeared to react with the paper and glue this method was necessary. The rubidium was distilled into a small Pyrex tube with very thin glass windows and then a small amount was melted on one of the windows to form the absorbing layer.

The absorbing screens were placed either between the crystals and the x-ray tube, or, between the second crystal and ionization chamber. With the exception of rubidium, the screens were oscillated back and forth several times a second in order that spurious effects due to non-uniformities in the thickness of the screens would be avoided.

To make certain that the transmission curves represented changes in the x-ray intensity due to the absorbing substances and not fluctuations in the primary radiation, the following procedure was adopted. For a particular setting of the second crystal three rates of deflection readings were made with the absorbing screen in position and then three readings with the screen replaced by an aluminum sheet. The rates of deflection with the aluminum in the beam were approximately the same as those for the absorbing substance in the region of secondary structure. A comparison of a plot of the aluminum readings and the transmission curve makes it possible to

[1] Barnes, Phys. Rev. **44**, 141 (1933).
[2] See Hull, Phys. Rev. **40**, 676 (1932) for the distinction between fine and secondary structure.
[3] Bergen Davis and Harris Purks, Phys. Rev. **32**, 336 (1928).
[4] Ross, Phys. Rev. **44**, 977 (1933).
[5] Bergen Davis and Harris Purks, Proc. Nat. Acad. Sci. **13**, 419 (1927).

definitely distinguish structure from errors in measurement. When it was desired to measure the shift in position of the absorption limit due to chemical combination, rates of deflection for each setting of the crystal were recorded for the element, for the compound, and for the unfiltered radiation.

Experimental Results

In Figs. 1 to 4 typical experimental curves are shown. The abscissae are wave-lengths in x-units obtained from the second crystal angle readings. Since no attempt was made to measure the wave-length position of the absorption limit, the center or half maximum of the edge was fixed on the wave-length scale at the best value given in Siegbahn's *Spectroskopie der Roentgenstrahlen.* The ordinates are the I/I_0 values for the free metal (lowest) curve where I is the x-ray energy transmitted through the absorber and I_0 is the incident energy. For comparison the transmission curves of the compounds, plotted to the same scale as the metal, are shown displaced an arbitrary amount above the free metal curve so that their secondary structures do not overlap. The I/I_0 values for the compounds are nearly the same as those for the metal. At the top of the figure is shown a plot of the radiation transmitted by the aluminum sheet and for which the I/I_0 value is the same as the I/I_0 values in the region of secondary absorption. Each curve is the result of a single run and each point is the average of the three rate of deflection readings. Five or more exactly similar curves were obtained for each substance.

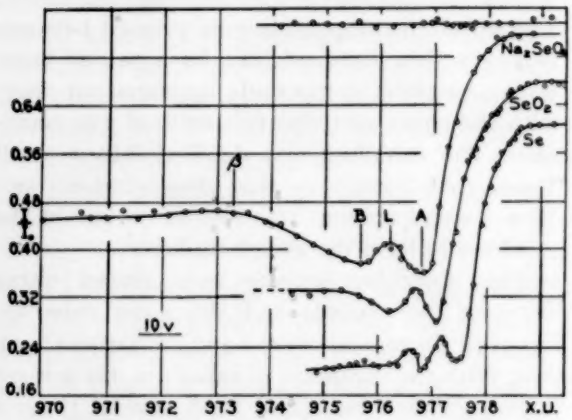

Fig. 1. The absorption limits of Se, SeO_2 and Na_2SeO_4.

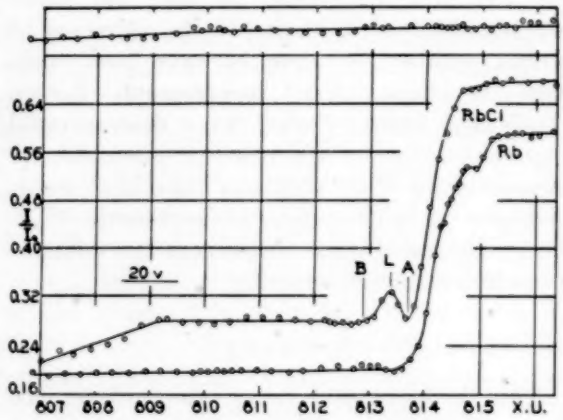

Fig. 2. The absorption limits of Rb and RbCl.

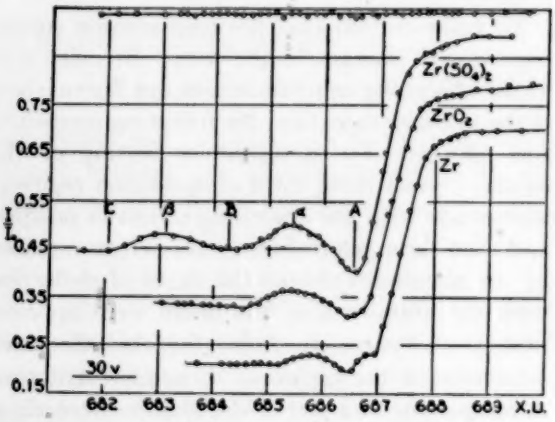

Fig. 3. The absorption limits of Zr, ZrO_2 and $Zr(SO_4)_2$.

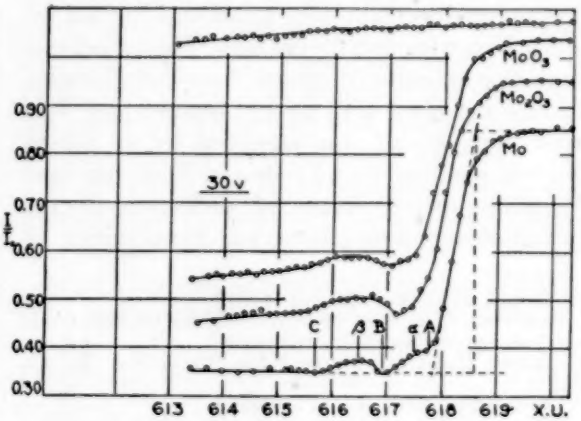

Fig. 4. The absorption limits of Mo, Mo_2O_3 and MoO_3.

Discussion of Results

Table I gives the separation in volts of the secondary structure from the center of the absorption edge. The convention of Coster and Veldkamp[6] of labelling the minima of the transmission curves by A, B, C and the maxima by α, β, γ is followed.

Table I. *Position (in volts) of secondary structure.*

	A	α	B	β	C
Se	4.5	8.3	13.0	15.6	20.5
SeO_2	5.6	10.7	17.5		
Na_2SeO_4	6.2	13.5	20.6	50.0	
Rb					
RbCl	9.3	12.5	23		
Zr	11.5	17.2	23	43	53
ZrO_2	18.5	47	70		
$Zr(SO_4)_2$	13.7	43	72	107	128
Mo	14	24	41	56	79
Mo_2O_3	25	51	80		
MoO_3	28	51	80		

All of the substances show some structure. Rubidium is the only one which shows fine structure of the kind found by Barnes.[1] No structure is found farther from the principal edge than 110 volts. From a comparison of the various curves for the same substance it is concluded that the position of the structure can be specified to within 10 seconds of angle on the second crystal. This is less than 2 volts for selenium and 5 volts for molybdenum.

Hanawalt[7] has examined Se and SeO_2 by the single crystal photographic method. Within the errors of measurement the curves of Fig. 1 are in agreement with his results. Idei[8] photographed Se and Na_2SeO_4 as well. For Se he gives a single absorption line at 102 volts which probably is second order silver absorption. For Na_2SeO_4 he gives a minimum at 16.0 volts, the next maximum at 48 volts and the minimum at 104 volts. This would be similar to the Na_2SeO_4 curve of Fig. 1 if the first small maximum were not resolved. From this comparison it is clear that the two-crystal spectrometer is suitable for secondary structure measurements and that, due to its great resolving power, it should reveal structure which could be detected only with great difficulty by the single crystal spectrograph.

Ross[4] has examined zirconium and molybdenum with the double-crystal spectrometer. For the maxima α and β he obtains 21 and 52 volts for zirconium, 25.9 and 53.5 volts for molybdenum. For molybdenum these values and the ones of Table I are in agreement within the experimental error. The discrepancy of approximately 10 volts in the position of the zirconium structure hardly can be ascribed to experimental error. Perhaps the disagreement may be explained by the fact that Ross employed foils for both elements while in this case the zirconium was in powder form.

According to the theory of the secondary structure given by Kronig,[9] the structure depends on the type of crystal lattice in which the absorbing atom finds itself. It follows from this that elements which crystallize with the same type of lattice should have similar secondary structures. Kronig also has shown that the separation of the structure from some zero level, which can be taken as the main edge, is proportional to $1/a^2$ where a is the crystal lattice constant. Therefore, the structures of two elements of the same lattice type should be identical if one of them is multiplied by the square of the ratio of the lattice constants. Coster and Veldkamp[10] compared the structures of Pt, Cu and Au in this way and found that the theory is verified. Fe and Mo belong to the body-centered cubic system. Although Fe shows a much richer structure than Mo such a comparison can be made for the first few maxima.

The long lines of Fig. 5 represent the distances of the maxima and the short lines the distances of the minima of the transmission curves from the principal edge. The distances for Mo have all been multiplied by $(a_{Mo}/a_{Fe})^2$. The heavy line on the right is the principal edge and it is seen that arbitrarily displacing the Mo edge about 5 volts brings the secondary structures approximately together. A shift of 5 volts is permissible because of the experimental error in measuring the position and because in the photographic work no definite point in the edge is chosen from which to measure the structure.

[6] D. Coster and J. Veldkamp, Zeits. f. Physik **70**, 306 (1931).
[7] J. D. Hanawalt, Phys. Rev. **37**, 718 (1931).
[8] Idei, Sci. Rep. Tokoku Imp. Univ. **19**, 653 (1930).
[9] R. de L. Kronig, Zeits. f. Physik **70**, 317 (1931); **75**, 191 (1932); **75**, 468 (1932).
[10] D. Coster and J. Veldkamp, Zeits. f. Physik **74**, 191 (1932).

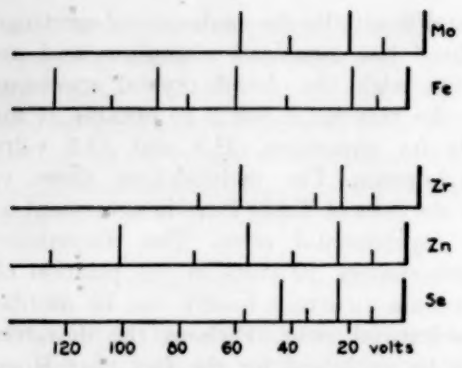

FIG. 5. Comparison of secondary structure for elements of the same crystal type.

Zr, Se and Zn have lattices of the hexagonal type. Fig. 5 also shows the structures of Zr and Se expanded for comparison with the Zn structure. The agreement for Zn and Zr is very good but for Se there is none. The data for Fe and Zn are from Coster and Veldkamp.[10]

Secondary structure is characterized by magnitude as well as by location. The intensity of the structure is defined as the ratio of the largest change in absorption coefficient in going from a maximum to a minimum to the average absorption coefficient. Coster and Veldkamp[10] have proposed the general rule that the higher the melting point of a substance the greater will be the changes in the absorption coefficient in the region of secondary structure. That is, the intensity depends on the melting point. This would be expected from Kronig's theory.

As evidence, Coster and Veldkamp point out that the intensities of 19 percent for Fe, 13 percent for Cu and 7 percent for Zn, measured at room temperature, are in the same relative order as the respective melting points 1550°, 1083° and 419°C. The values of the maximum intensity and the melting points for the elements examined here are shown in Table II.

TABLE II. *Maximum intensity of secondary structure and melting points.*

	Melting Points	Intensity
Se	220°C	13 %
Rb	38	0
Zr	1700	6.5
Mo	2620	5.5

Since rubidium was within 15°C of its melting point it would not be expected to show any secondary structure. Hg[11] and Ga[12] with low melting points also show no structure. The intensities for Zr and Mo, however, are approximately one-third as great as for Fe and yet their melting points are higher. Great care was used in selecting, by trial, screens of thickness which gave most pronounced structure. It is surprising that Se with a relatively low melting point has a greater intensity than either Mo or Zr. These results are not in agreement with the rule stated above.

The small intensity for Mo and Zr perhaps explains why not more structure was found for these elements, although they were examined over a region of 300 volts on the short wavelength side of the main absorption edge. It is estimated that structure with an intensity as small as 4 percent could have been observed with little difficulty.

As would be expected, the secondary structures of an element and its compound are not similar either in position or in intensity. The change in intensity in going from the element to the compound is sometimes considerable. For example, the intensity for Zr is 6.5 percent while for the compound $Zr(SO_4)_2$ it is 13 percent.

TABLE III. *Displacement of the K limits in compounds.*

Compound	Volts	Compound	Volts
SeO_2	4.5±0.4	$Zr(SO_4)_2$	8.0±0.8
Na_2SeO_4	7.0±0.4	Mo_2O_3	5.1±1.0
RbCl	1.5±0.5	MoO_3	5.1±1.0
ZrO_2	4.6±0.8		

Table III gives the displacement of the absorption edges of the compounds with respect to the absorption edges of the elements. The displacements are measured from the center of the element edge to the center of the compound edge. All of the shifts are to the short wavelength side of the absorption limit of the element.

Table IV lists the widths of the absorption edges measured as the base of the triangle shown on the Mo curve of Fig. 4. The values given are uncorrected averages of measurements

[11] Hanawalt, Phys. Rev. **37**, 715 (1931).
[12] Kievit and Lindsay, Phys. Rev. **36**, 648 (1930).

TABLE IV. *Width of K absorption limits.*

	Substance	Seconds	Volts		Substance	Seconds	Volts
34	Se	42±3	7.9±0.6	40	Zr	53±3	20.2±1.2
	SeO_2	40±3	7.5±0.6		ZrO_2	46±3	17.6±1.2
	Na_2SeO_4	43±3	8.1±0.6		$Zr(SO_4)_2$	46±3	17.6±1.2
35	KBr	49±3	10.4±0.6	42	Mo	47±3	22.0±1.4
37	Rb	47±3	12.8±0.8		Mo_2O_3	45±3	21.2±1.4
	RbCl	42±3	11.4±0.8		MoO_3	65±3	30.5±1.4

from curves obtained with the same screen. Richtmyer and Barnes[13] have stated that an unambiguous value of the width is obtained only if it is measured from a plot of μ/ρ against λ rather than from a plot of I/I_0 against λ. Accordingly, $\log(I_0/I)$ was plotted and the widths were again measured. The two sets of values were the same within the errors of measurement.

Various corrections for the "crystal width" have been proposed. The formula calculated by Schwarzschild[14] would give a negligible correction for the crystals used in this work. Ross,[4] however, subtracts twice the half maximum width of the $(1, -1)$ rocking curve from the observed absorption limit width. This would mean a subtraction of 15 seconds from each of the widths of Table IV since the crystals had a half maximum rocking curve width of 7.5 seconds. There is, as yet, no good proof that one correction is better than another.

Chemical combination has practically no effect on the width of the absorption limit. In only one case, molybdenum and its trioxide, is the difference in widths greater than the experimental error. It was, therefore, considered permissible to use the width of the bromine limit measured in the compound KBr for plotting widths and atomic number. The KBr curve is not shown in this paper.

In Fig. 6 the volt widths of the elements which have been measured by Barnes,[1] by Ross,[4] as well as those of this investigation are plotted against the atomic number. The points of the upper curve are the uncorrected values. Those of the lower curve are the upper curve values corrected in the Ross manner. Since it is not probable that a correction greater than the Ross

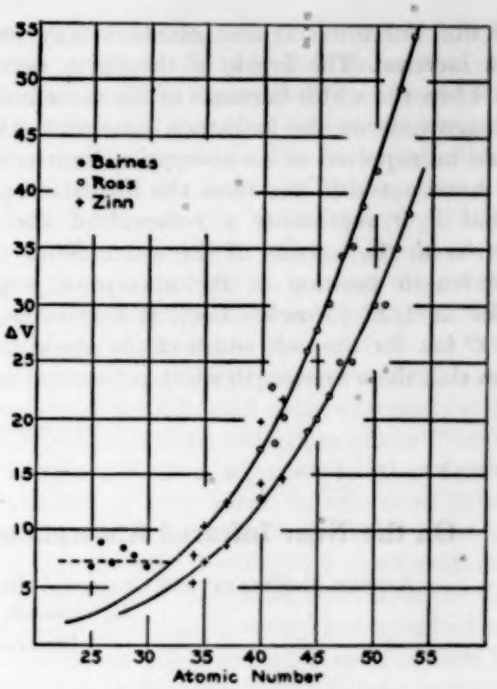

FIG. 6. Plot of the volt widths of the K absorption limits against the atomic number.

correction should be used, the points of Fig. 6 represent the extreme values for the widths. When the absorption limit itself exhibits considerable fine structure there is more than one way of drawing the triangle whose base is used as the width of the limit. For the elements manganese to zinc, studied by Barnes, the construction for measuring the width was made on that part of the curve which would give the smallest value. In this connection it should be noted that the method of determining the width is an artificial and arbitrary one.

The solid lines are plots of the equation $\Delta V = KZ^4$ with two different values for the constant K. For the atomic numbers 34 to 53 the experimental points fit the curves very well. Richtmyer and Barnes[15] have measured the widths of the K limits of W and Au. The upper curve gives values 20 percent too large for the uncorrected widths and the lower curve gives values 50 percent too large for the corrected widths of these elements.

It is clear that in the neighborhood of atomic number 32 the widths reach a constant value,

[13] Richtmyer and Barnes, Phys. Rev. **45**, 754A (1934).
[14] Schwarzschild, Phys. Rev. **32**, 162 (1928).
[15] Richtmyer and Barnes, Science **77**, 459 (1933).

and that for lower atomic numbers they may even increase. The break in the curve occurs just when the width becomes of the same order of magnitude as the ionization potential. This would be expected as an absorption limit could not have a width less than the ionization potential if it represents a removal of the K electron to the outside of the atom. Since the wave-length position of the absorption edges varies as $1/Z^2$ (Moseley law), it follows from the Z^4 law for the volt width of the absorption edges that the wave-length width is constant and independent of Z. This becomes obvious when it is noted that the "seconds" widths of the elements of Table IV are very nearly constant. It would appear then that the diffuseness of the K level is due to something like a classical damping which for lines gives a constant value for $\Delta\lambda$.

In conclusion, the author wishes to express his thanks to Professor Bergen Davis for suggesting this investigation and for his interest and advice throughout the course of the experiment.

OCTOBER 15, 1934 PHYSICAL REVIEW VOLUME 46

On the Near Infrared Absorption Spectrum of Mono-Deutero-Acetylene

ANDREW McKELLAR* AND CHARLES A. BRADLEY, JR.,* *George Eastman Laboratory of Physics, Massachusetts Institute of Technology*

(Received July 30, 1934)

The absorption spectrum of mono-deutero-acetylene has been photographed over the region 6000–10,500A in the first order of a 21-foot grating using absorbing columns up to 20 feet in length at atmospheric pressure. One band was found with origin at 10,302A. It is attributed to the molecule C_2HD. From the rotational constants of the band and similar data from the C_2H_2 bands, the interatomic distances in acetylene are computed as $r_{CC}=(1.247\pm0.008)\times10^{-8}$ cm and $r_{CH}=r_{CD}=(0.940\pm0.036)\times10^{-8}$ cm.

FROM a study of the bands of the "heavy" acetylenes considerable interesting information concerning physical properties of the acetylene molecule can be obtained. This possibility was mentioned by Randall and Barker[1] in their preliminary report of experimental results obtained on the far infrared bands of C_2D_2 and C_2HD. From the expected intensity alternation ratio in the C_2D_2 bands a check can be obtained on the nuclear mechanical moment of the deuterium atom and from the moments of inertia of any two of the acetylene molecules C_2H_2, C_2HD or C_2D_2, the internuclear distances can be directly calculated.

Consideration of previous work[2–9] on the infrared absorption spectrum of acetylene indicates that two of the valence vibrational frequencies of C_2D_2 associated with the C–D motions should have magnitudes of about 2400 and 2500 cm^{-1}. Employing the notation of Sutherland[9] these are the vibrations ν_3 and ν_2, respectively. Therefore the band of C_2D_2 corresponding to the strong λ7887 band of C_2H_2 should lie at about 10,300A. The λ7887 band, from which Childs and Mecke determined the nuclear spin of the proton, is believed assignable to the combination $\nu_3+3\nu_2$. While the present paper was being written there appeared a *Letter to the Editor of Nature* by Herzberg, Patat and Spinks[10] on the near infrared bands of "heavy" acetylene. Reference will be made to this later.

In our work the "heavy" acetylene was prepared by allowing water consisting of certainly more than 95 percent D_2O (sp. gr. 1.1054, indicating >99 percent D_2O) to drop slowly on finely ground calcium carbide. The gas generated

* National Research Fellow.

[1] Randall and Barker, Phys. Rev. **45**, 124 (1934).

[2] Levin and Meyer, J.O.S.A. **16**, 137 (1928).

[3] Hedfeld and Mecke, Zeits. f. Physik **64**, 151 (1930).

[4] Childs and Mecke, Zeits. f. Physik **64**, 162 (1930).

[5] Mecke, Zeits. f. Physik **64**, 173 (1930).

[6] Hedfeld and Lueg, Zeits. f. Physik **77**, 446 (1932).

[7] Lochte-Holtgreven and Eastwood, Zeits. f. Physik **79**, 450 (1932).

[8] Mecke, Zeits. f. physik. Chemie **B17**, 1 (1932).

[9] Sutherland, Phys. Rev. **43**, 883 (1933).

[10] Herzberg, Patat and Spinks, Nature **133**, 951 (1934).

passed through tubes filled with ground CaC_2 and through a trap cooled with solid CO_2 into the absorption cell. As explained below, the spectrum points to the presence of much more than the expected amount of C_2HD, and thus of protium. In photographing the λ10,370 and λ10,166 bands of C_2H_2 we found no evidence of any absorption by possible contaminating substances when the C_2H_2 was made from commercial calcium carbide and distilled water. Thus it was felt unnecessary to make special efforts to purify the acetylene made from D_2O except evacuating and flaming thoroughly the generating apparatus and absorption cell. Apparently the protium must have come from the generating materials. Very recently, Jungers and Taylor[11] in preparing the deutero-ammonias from the reaction of D_2O on magnesium nitride, found that when the magnesium nitride was not strongly heated, 100 percent D_2O produced deutero-ammonia containing only 68 percent deuterium. This they attribute to protium bound in the magnesium nitride as amido- or imido-groups. From very carefully prepared magnesium nitride they were able to obtain ammonia containing 99 percent of the hydrogen in the form of the D isotope. Thus we infer that considerable protium was probably present in our calcium carbide despite the fact that it was subjected to evacuation before being used. An obvious test of the presence of protium in the calcium carbide would be the use of calcium carbide prepared from thoroughly degassed pure carbon and pure CaO.

The absorption chamber consisted of four cells, each five feet long, three of which were arranged in the form of an N. They were filled with "heavy" acetylene to a pressure of 80 cm of mercury. The positive pole of a carbon arc served as a source of light and the spectrum was photographed in the first order of a 21 foot concave grating, higher orders being eliminated by means of a suitable filter. Eastman 1Q plates supersensitized with ammonia were used and third order iron arc lines served as standards.

Under the above conditions in the region 6000–10,500A only one absorption band was observed (except the atmospheric oxygen and water vapor bands). Its origin lies at λ10,302. It has a single R and P branch; the same structure as the ordinary acetylene bands. Its P branch appeared to exhibit alternating intensities though not as pronounced as in the C_2H_2 bands. Despite the evidence of the varying intensities and the fact that this band falls very close to the predicted position for a C_2D_2 band and although, as stated above, we find the presence of enough protium to form sufficient C_2HD surprising, we attribute the band to the latter molecule. The purely chance coincidence of members of the R branch of the extremely strong λ10,370 band of C_2H_2 with lines of the P branch of the present band accounts for the apparent alternation of intensities. In our most intense exposure the P branch of the C_2H_2 band was seen very faintly. To obtain a confirmation of the superposition mentioned here, both the C_2H_2 and the C_2HD bands were photographed side by side on one plate and each more intense line in the P branch of the C_2HD band was seen to occur at a wave-length corresponding to that of one of the stronger lines in the R branch of the C_2H_2 band. This latter band exhibits alternating intensities, the intensity ratio being 3 : 1.

Twenty-two lines in the P branch and twenty-six lines in the R branch of the band have been measured on each of three plates. The wave numbers of the lines, considered accurate to within one-tenth of a wave number, are given

TABLE I. *C_2HD band at λ10,302.*

J	$R(J)$	$P(J)$	$\Delta_2F(J)$ upper state $=R(J)-P(J)$	$\Delta_2F(J)$ normal state $=R(J-1)-P(J+1)$
1		9702.32 cm^{-1}		
2	9710.08 cm^{-1}	00.31	9.77	
3	12.17	9698.32	13.85	13.98
4	14.01	96.10	17.91	18.22
5	15.77	93.95	21.82	22.06
6	17.62	91.95	25.67	26.08
7	19.36	89.69	29.67	30.24
8	21.21	87.38	33.83	34.28
9	22.80	85.08	37.72	38.26
10	24.51	82.95	41.56	42.16
11	26.36	80.64	45.72	46.25
12	27.88	78.26	49.62	50.59
13	29.43	75.77	53.66	54.35
14	31.03	73.53	57.50	58.25
15	32.57	71.17	61.40	62.49
16	34.21	68.54	65.67	66.82
17	35.61	65.75	69.86	71.02
18	37.13	63.19	73.94	74.84
19	38.45	60.77	77.68	78.77
20	39.89	58.36	81.53	82.71
21	41.18	55.74	85.44	86.71
22	42.48	53.18	89.30	
23	43.80			
24	45.06			
25	46.16			
26	47.60			
27	48.69			

$B=0.99398\pm0.00039$
$I=(27.828\pm0.042)\times10^{-40}$ g cm^2
$B_0=1.00905\pm0.00048$
$I_0=(27.412\pm0.043)\times10^{-40}$ g cm^2

[11] Jungers and Taylor, J. Chem. Phys. **2**, 373 (1934).

in Table I. Here also are given the corresponding term differences from which, by the method of least squares, were calculated the rotational constants B for the upper and lower states involved. The relations applicable here are the well-known term difference formulae, $R(J)-P(J)=4B(J+\frac{1}{2})$ and $R(J-1)-P(J+1)=4B_0(J+\frac{1}{2})$ for the upper and lower states, respectively. For the two states the moments of inertia of the C_2HD molecule were obtained directly from the B values, and are also given in the table. The probable errors of the various quantities have been computed on the basis of the internal consistency of the data with the usual expressions derived from the theory of least squares.

Previous calculations of the internuclear distances of the atoms composing the linear acetylene molecule have of necessity been based on the assumption that either r_{CH} or r_{CC} is the same as in some other molecule containing these atoms. To obtain their values $r_{CH}=1.08\times10^{-8}$ cm and $r_{CC}=1.19\times10^{-8}$ cm, Hedfeld and Mecke accepted for acetylene the value of r_{CH} computed for methane from the Raman data on CH_4 obtained by Dickinson, Dillon and Rasetti.[12] These data taken in conjunction with the moment of inertia of C_2H_2 enabled the computation of r_{CC}. Now, however, having available the moments of inertia of both C_2H_2 and C_2HD in their normal states, the internuclear distances can be directly calculated. The only postulate involved is that the distances r_{CH} and r_{CD} in the acetylenes are equal. This is certainly so to a high order of accuracy. From the moments of inertia $I_0=(23.509\pm0.040)\times10^{-40}$ g cm^2 for C_2H_2 and $I_0=(27.412\pm0.043)\times10^{-40}$ g cm^2 for C_2HD, we calculate the internuclear distances to be $r_{CC}=(1.247\pm0.008)\times10^{-8}$ cm and $r_{CH}=r_{CD}=(0.940\pm0.036)\times10^{-8}$ cm. This is seen to be in good agreement with the value $r_{CC}=(1.22\pm0.08)\times10^{-8}$ cm obtained by Wierl[13] from electron diffraction in acetylene.

In the previously mentioned letter by Herzberg, Patat and Spinks[10] four bands were photographed. Despite the fact that they used 93 percent pure D_2O only bands due to C_2HD were found. One of these corresponds to our λ10,302 band and the other three are beyond the region of sensitivity of the Eastman 1Q plates. They obtain for the internuclear distances $r_{CC}=1.205\times10^{-8}$ cm and $r_{CH}=1.062\times10^{-8}$ cm which differ from those given here by several times more than the probable error of the determinations. Herzberg and his collaborators assign their four bands to certain vibrational transitions and take as a basis for their assignments those of Lochte-Holtgreven and Eastwood[7] for C_2H_2. The latter have been shown by Sutherland[9] to lead to flagrant discrepancies. He also has shown that the anharmonic terms for C_2H_2 amount to as much as 150 cm^{-1} in some cases. It would thus seem an almost certainly fruitless task to attempt the assignment of vibrational transitions to the C_2HD bands until all the five fundamental frequencies are found in the far infrared and enough additional bands are located to permit the evaluation of the anharmonic terms. At present only the frequencies ν_4 and ν_5 are known.[1]

[12] Dickinson, Dillon and Rasetti, Phys. Rev. **34**, 582 (1929).

[13] Wierl, Ann. d. Physik **13**, 453 (1932).

Note on the Structure of the Compton Modified Band

G. E. M. JAUNCEY, *Washington University, St. Louis*

(Received August 24, 1934)

The distribution-in-wave-length of the intensity of scattered x-rays about the center of the Compton modified band gives directly the distribution-in-component-velocity of the electrons producing the band. The two distribution functions are of the same form.

IN 1925 de Broglie,[1] Wentzel[2] and Jauncey,[3] applying the principles of conservation of energy and of momentum to the scattering of an x-ray quantum by an initially moving electron, independently arrived at a formula which for an initial electron velocity small compared with that of light may be written in the form

$$L=\lambda(\beta_x \text{ vers } \phi-\beta_y \sin \phi) \qquad (1)$$

and

$$L=\lambda'-\lambda-(h/mc\lambda) \text{ vers } \phi, \qquad (2)$$

where λ and λ' are, respectively, the wave-lengths of the primary and scattered quanta, βc is the initial velocity of the electron, $\beta_x c$ is the component of this initial velocity in the direction of propagation of the primary quantum (the x-axis), $\beta_y c$ is the component in the scattering plane and in a direction (the y-axis) perpendicular to $\beta_x c$, and ϕ is the angle of scattering. The quantity L is the difference between the wave-length scattered by a moving electron and that of a quantum scattered by an electron at rest. Jauncey[3] making use of Eq. (1) showed that, when x-rays are scattered by electrons moving with equal speeds βc but in random directions, the width of the Compton band is

$$\delta\lambda=4\lambda\beta \sin \tfrac{1}{2}\phi \qquad (3)$$

with an almost constant intensity distribution in the band. Proceeding from this Jauncey[4] then considered the case for scattering by electrons which have a speed distribution. The electrons whose speeds are between βc and $(\beta+d\beta)c$ give rise to a band of width given by Eq. (3). By an awkward process of graphical integration the intensity distribution in the Compton band was worked out for scattering by electrons in elliptic Bohr orbits. Later, DuMond[5] and Chandrasekhar[6] applied this method to the scattering of x-rays by electrons which have the Fermi-Dirac speed distribution. They both arrived at a parabolic shape for the curve representing the intensity distribution in the Compton band.

However, it is not necessary to integrate as Jauncey[4] and DuMond[5] have done. There is instead a very simple relation between the component velocity distribution of the electrons and the intensity distribution in the Compton band. DuMond[5] has written Eq. (1) in the form

$$L=2\lambda(u/c) \sin \tfrac{1}{2}\phi, \qquad (4)$$

where u is the component of the initial electron velocity along the bisector of the angle between the direction of propagation of the primary quantum and the reverse of that of the scattered quantum. As a consequence of the linear relation between L and u as shown by Eq. (4), it is immediately seen that, if $f(u)\cdot du$ is the number of electrons with velocity components between u and $u+du$, the number of scattered quanta whose L's are between L and $L+dL$ is proportional to $f(Lc/2\lambda \sin \frac{1}{2}\phi)\cdot dL$. Hence, if the intensity distribution $I(L)$ in the Compton band is found by an instrument such as DuMond's multicrystal spectrograph,[5] the component velocity distribution function of the electrons is obtained by plotting $I(L)$ not against L but against $Lc/2\lambda \sin \frac{1}{2}\phi$. We then have the curve of $f(u)$ plotted against u. *The structure of the Compton band thus gives directly the graph of the component velocity distribution function of the electrons producing the band.* Since the Fermi-Dirac theory as applied by Sommerfeld to the

[1] L. de Broglie, Ann. d. Physique **3**, 102 (1925).
[2] G. Wentzel, Phys. Zeits. **26**, 441 (1925).
[3] G. E. M. Jauncey, Phil. Mag. **49**, 427 (1925); Phys. Rev. **25**, 314 (1925).
[4] G. E. M. Jauncey, Phys. Rev. **25**, 723 (1925).
[5] J. W. M. DuMond, Phys. Rev. **33**, 643 (1929).
[6] S. Chandrasekhar, Proc. Roy. Soc. **A125**, 231 (1929).

conduction electrons in metals demands that the component velocity distribution at ordinary temperatures be parabolic, the structure of the Compton band scattered by these electrons is therefore also parabolic.

In conclusion, the point of this note was implicit in the author's papers[3, 4] of 1925 and in DuMond's paper[5] of 1929 but so far as the author knows has not been stated explicitly before.

OCTOBER 15, 1934 PHYSICAL REVIEW VOLUME 46

Effect of Electron Binding upon the Magnitude of the Compton Shift

P. A. ROSS AND PAUL KIRKPATRICK, *Department of Physics, Stanford University*

(Received July 24, 1934)

Precision measurements of the Compton shift for ninety degree scattering of the wave-lengths 0.435A, 0.496A and 0.631A by carbon and by beryllium have been performed, using the ring-target x-ray tube and a double spectrometer, under the assumption that the mean shift for two mutually supplementary angles of scattering equals the ninety degree shift. In all cases the observed shift is less than h/mc, the value required by the Compton formula, the maximum percentage discrepancy being 2.4 percent, observed in the case of λ0.631A scattered from carbon. These observations fulfill the predictions inherent in Wentzel's theory of scattering by bound electrons, and are consistent with the explicit shift formula previously deduced by the present authors, as regards dependence of the shift upon wave-length and upon ionization energy of the scatterer. They are also in satisfactory quantitative agreement with the theoretical shift formulas of F. Bloch.

INTRODUCTORY

THE announcement of the observation of scattered x-rays of modified wave-length by A. H. Compton[1] in 1923 was accompanied and supported by a theory so concise and acceptable, and so nicely confirmed in a number of laboratories, that less attention has been paid in subsequent years to possible minor inaccuracies in the original description than would have been devoted to the aftermath of a discovery less completely set forth in the first instance. The early shift measurements of Sharp[2] and of Kallmann and Mark,[3] agreeing satisfactorily with the Compton equation $\Delta\lambda=(h/mc)(1-\cos\varphi)$, operated to establish this equation as correct within the limits of possible observation. More recent experiments by Nutting[4] have resulted in values of the 90° shift which are from one to two percent lower than the value h/mc required by Compton's equation. Nutting also remarked that the mean of all determinations available in 1930 was somewhat below h/mc but considered this to be a result of experimental error and concluded that the experiments as a whole were in agreement with the Compton formula.

The incompleteness of the type of treatment employed by Compton had been considered, however, by Wentzel,[5] in whose theory of scattering we may discern the implicit requirement that the wave-length modification occasioned by scattering by bound electrons shall be less than that expected of the practically free electrons of Compton. Wentzel's treatment does not provide an explicit shift formula, comparable in simplicity to the Compton equation given above. Such an equation has been deduced by the present authors[6] from relatively simple energy and momentum considerations, and Bloch[7] has derived a similar and more complete relation upon the broader basis of wave mechanical theory. The present paper offers experimental evidence relevant to this question, in the form of results of precision measurements of the wave-length shifts accompanying the scattering of radiations of three different wave-lengths by carbon and by beryllium.

[1] A. H. Compton, Phys. Rev. **21**, 483 (1923).
[2] H. M. Sharp, Phys. Rev. **26**, 691 (1925).
[3] H. Kallmann and H. Mark, Naturwiss. **14**, 3 (1925).
[4] F. L. Nutting, Phys. Rev. **36**, 1267 (1930).
[5] G. Wentzel, Zeits. f. Physik **43**, 1, 779 (1927).
[6] P. A. Ross and Paul Kirkpatrick, Phys. Rev. **45**, 223 (1934).
[7] F. Bloch, following paper.

Apparatus

It is probably safe to state that the difficulties encountered in the spectrometric study of scattered x-rays all result from the weakness of these radiations. We have found it possible to overcome these difficulties to a large extent by using as a source the ring-target x-ray tube previously described.[8] This source combines a target area of about 10 cm² with good constancy of scattering angle. The principle of this tube and the geometry of its use in shift measurements are illustrated in Fig. 1. The focal ring is the complete locus of

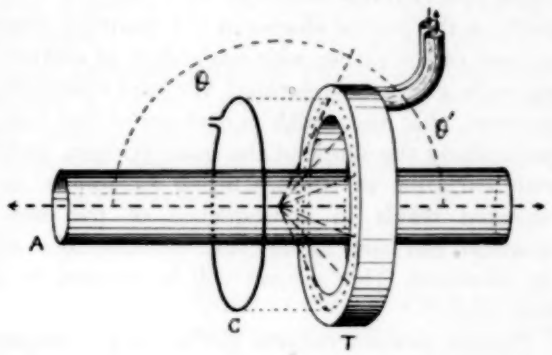

Fig. 1. Schematic representation of the ring-target x-ray tube for the study of scattering. *C* is a tantalum filament (support not shown), and *T* the hollow annular target, supported by its cooling tubes. *A* is a thin-walled and open-ended aluminum tube to enclose the scatterer. External walls of x-ray tube not shown. With the scatterer at the point of convergence of the rays indicated by broken lines from the focal ring, radiation emerges from the aluminum tube after undergoing scattering at the mutually supplementary angles θ and θ'.

x-ray sources consistent with a given angle of scattering from a concentrated scatterer. The scattering angle is controlled by the position of the scattering body in the tube which lies along the target axis. Mutually supplementary angles of scattering are available at all times, since the scatterer sends radiation both ways along the tube axis. This is an important matter since, as shown below, it liberates us from that bugbear of shift measurements: uncertainty of scattering angle. There are no windows in the line of sight of the spectrometer nor any other parts to scatter undesired radiation to the observing apparatus. The thicknesses of the disk-shaped carbon and beryllium scatterers used in this work were, respectively, 2.96 mm and 4.85 mm. The face areas of the scatterers were such that they occupied approximately the full cross section of the one-inch aluminum tube through the target axis.

The double spectrometer employed has been fully described[9] but it will be useful to emphasize again that by no possibility can its scales be in error by an amount comparable to the probable errors attached to the observations which follow, much less to the observed shift defects or differences between the measured shifts and those predicted by the Compton formula. The angular scale of the *B* crystal, a circle by Societe Genevoise, has been checked by intercomparison of its parts, by comparator observation of the linear motion of the end of a two-meter bar fixed to its turn-table, and by the observation of many well-known spectrum lines and limits. In a spectrometer of this type the *A* crystal is never required to rotate and we have made sure by optical lever observations that no rotations approaching a second of arc can, in fact, occur as the crystal is caused to execute its permissible motions.

The spectrometer was equipped with polished calcite crystals characterized by faces ten centimeters long and rocking curves 41 seconds in full width at half maximum. In the spectrometer system sensitivity was sacrificed to stability to such an extent that with the crystals operating at full aperture and the x-ray tube under a load of three to three and a half kw a single scattering observation required an exposure one minute in duration.

Experimental Procedure

Former shift measurements have as a rule been made with the strong $K\alpha$ doublets of the elements. Though the intensity available in this way is of great advantage, it is well known that modified $K\alpha$ spectra show little or no resolution, on account of the Doppler broadening of the lines, and this introduces an uncertainty into the shift determination, inasmuch as it must be measured between a single line and a pair. Though such a measurement could perhaps be successfully carried out, either by graphic resolu-

[8] Paul Kirkpatrick and P. A. Ross, Rev. Sci. Inst. **4**, 645 (1933).

[9] P. A. Ross, Rev. Sci. Inst. **3**, 253 (1932).

tion of the modified line or by location of the centroid of the unmodified, we have had reason to distrust these methods and have chosen to avoid this complication by the use of the much weaker β-line, which is, practically speaking, single and symmetrical.

All of our observations have been directed to the determination of wave-length shifts associated with a scattering angle of 90°. With the scatterer in a given position (not necessarily the precise position for ninety-degree scattering) we observe the magnitude of the shifts first with radiation emerging from one end of the tube, and then from the other (Fig. 1). Since the observing spectrometer is necessarily stationary, this is, of course, done by rotating the x-ray tube through 180° about a vertical axis passing through the scatterer, the exactitude of the angle of rotation being checked by observing a mirror on the x-ray tube through a telescope equipped with a Gauss eyepiece. The mean of these two shifts, after certain small corrections have been applied, is taken to be the shift associated with a scattering angle of 90°.

This conclusion is readily justified under the original Compton shift equation, which at worst is certainly an excellent approximation to the truth. For if $\Delta\lambda$ and $\Delta\lambda'$ are the shifts observed at the (unknown) supplementary angles φ and φ' we have by addition $\Delta\lambda+\Delta\lambda'=2h/mc$.

We recently proposed,[6] amending the Compton equation to read $\Delta\lambda=(h/mc)(1-\cos\varphi)-D\lambda^2$, a proposal to be more fully discussed in a later paragraph. It is readily verified that this expression similarly leads to the conclusion that the mean of the shifts for two supplementary angles is equal to the 90° shift.

The modified lines obtained show a broad base, sloping gradually up to a steeper peak. These observations were not well adapted to a study of the precise shapes of the modified lines because of the rather wide variability of scattering angle which was tolerated. We have observed, however, that the width and shape of the line, particularly the shape of the basal portion, vary with variation of the scattering substance, an expected result in consequence of the non-identical electron momentum distributions of the elements. This subject will be treated in a later paper.

Present interest centers in the upper, steeper portion of the modified line. Our shift measure-

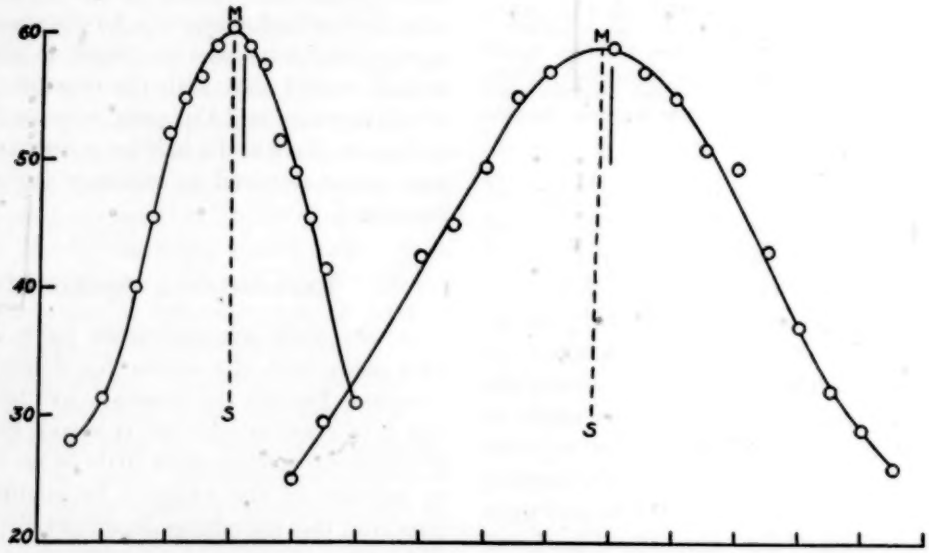

FIG. 2. Modified $K\beta$ of molybdenum, scattered by carbon. Ordinates are electrometer scale divisions per minute. Abscissas are angular settings of B crystal with reference to an arbitrary zero. The divisions marked off on this axis are at intervals of four minutes of arc. Angles of scattering for these two curves are supplementary, that for the left curve being about 64°. On this scale the unmodified Mo $K\beta$ would be about four minutes to the left of the axis of ordinates. Dashed lines are center lines of these curves. The parallel solid lines are the center lines which would be required by the Compton shift formula.

ments are measurements of the wave-length interval from the centroid of the unmodified $K\beta$ line to the *maximum* of the modified line. This maximum was found by locating midpoints at various heights and connecting them by a smooth line such as SM in Fig. 2, terminating in the maximum, M. In a large number of cases the line SM was found to show no measurable systematic inclination to right or left, so that the *maximum* practically means also the centroid of the upper portion of the modified line.

A number of preliminary curves were obtained with the scatterer placed rather accurately in the ninety-degree position, but since this is a position of low scattered intensity all final data were collected with the mean scattering angle equal to 64° or its supplement. No measurable difference between real 90° shifts and the corresponding mean shifts for mutually supplementary angles was observed.

Corrections

The most important correction which must be applied to the shifts as observed is that which compensates for the effect of scatterer thickness upon the mean angle of scattering. Due to absorption of the emergent scattered radiation within the scatterer the side of the scatterer which is away from the spectrometer is in a disadvantageous position as compared to the side toward that instrument, and as a result the *effective position* of the scatterer is not identical for the two supplementary angles of scattering, though the real position of the scatterer relative to the target remains unchanged. This means that the two *effective angles* of scattering are not accurately supplementary and that a correction for this inaccuracy must be calculated. To obtain the 90° shift in the case of a disk scatterer whose thickness is small in comparison to its diameter analysis shows that one must add to the mean of the wave-length shifts pertaining to the two supplementary angles of observation a small length δ given by

$$\delta=\frac{c\sin^2\varphi}{2\mu R}\left\{\frac{1}{\sec\varphi+1}\log\left[\frac{1+e^{-\mu X(\sec\varphi+1)}}{2}\right]-\frac{1}{\sec\varphi-1}\log\left[\frac{1+e^{-\mu X(\sec\varphi-1)}}{2}\right]\right\}.$$

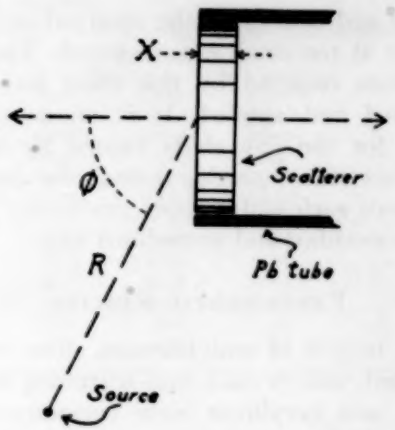

FIG. 3. Arrangement of scattering disk and source (not to scale). Quantities concerned in scattering angle corrections are illustrated.

In these equations c is the (approximate) 90° wave-length shift, and μ the mean absorption coefficient of the modified and unmodified radiation in the scatterer. The other symbols are defined by Fig. 3.

No x-ray spectrometer is uniformly sensitive to different wave-lengths, since crystal reflection and the absorption by windows, air and chamber gas exhibit wave-length variations. This total sensitivity variation distorts any spectral feature under observation, causing apparent shifts in the positions of lines and absorption limits. The shift of a narrow line may be so slight as to be unobservable but for lines having real widths as great as those of modified scattered lines the effect may not be dismissed without investigation.

Accordingly the variation of spectrometer sensitivity with wave-length was investigated by comparing the measured relative intensities of the K lines of certain elements with the real relative intensities given by Williams.[10] The sensitivity was found to increase slightly with wave-length, a result indicating incomplete absorption in the ionization chamber. From the observed sensitivity characteristics shift corrections applicable to the modified lines were computed.

The scattered radiation in emerging from the scatterer undergoes filtration which tends to suppress the long wave-length side of the modi-

[10] J. H. Williams, Phys. Rev. **44**, 146 (1933).

fied line and thus cause the observed maximum to occur at too small a wave-length. The small corrections required by this effect have been calculated and applied. It is unnecessary to correct for the line shifts caused by vertical divergence of rays passing through the spectrometer, since such shifts apply practically identically to modified and unmodified lines.

Experimental Results

Ring targets of molybdenum, silver and tin were used, and in each case scattering disks of carbon and beryllium were successively employed. With each of the six combinations the contour of the modified $K\beta$ line was traced out with the spectrometer five or six times, using a scattering angle of about 64°, and again with the supplement of this angle. Thus for each scatterer and radiation a value of the ninety-degree shift is obtained which derives from ten or more individual shift measurements. All of these data, together with the corrections discussed above, are summarized in Table I.

The superiority of the carbon data over the best obtainable with beryllium was evident throughout the investigation. Though the density of scattering electrons in the two substances was approximately the same the beryllium was contaminated by a small amount of some heavy impurity which was sufficient to give the specimen a measured linear absorption coefficient three times as great as that of the carbon. In spite of this difficulty it was deemed important to collect such beryllium data as could be had, in order to compare the magnitudes of shifts produced by different scattering atoms.

Discussion

The most striking feature of the data in Table I is the fact that all the ninety-degree shifts are less than the Compton value, h/mc, by amounts much too great to be attributable to experimental error. In the case of Mo $K\beta$ scattered by carbon this discrepancy attains the high value of 2.4 percent. This is in agreement with earlier results,[11] announced at the 188th meeting of the American Physical Society. We have made over a hundred measurements of this shift within the past two years, using various wave-lengths and angles, and with scatterers differing in material, size and shape. In all of this work the general conclusion that the ninety-degree shift is measurably less than h/mc has been uniformly confirmed. It should perhaps be recorded that all of these measurements have been performed with the same apparatus.

In our revision[6] of the shift equation of Compton the binding energy E of the scattering electrons was considered and the scattering process was assumed to be of finite duration. According to the revised equation $\Delta\lambda=(h/mc)(1-\cos\varphi)-\lambda^2kE/hc$ where k is a constant of the order of magnitude of unity, whose precise value cannot be calculated by the elementary methods upon which the derivation was based. So long as we are in ignorance of k it is not possible to achieve a complete quantitative comparison of theory with experiment, though general conclusions may be drawn regarding the theoretical and experimental variation of the ninety-degree shift with wave-length and binding energy. At ninety degrees the equation above requires $\Delta\lambda_{90}=h/mc-D\lambda^2$, which means that in Fig. 4 the observed points should fall upon a straight line of negative slope having an intercept at h/mc on the axis representing shifts. It is seen that the beryllium data, though scattered, show a definite wave-length variation of this sort, while the carbon points lie very close indeed to a line of the required type. Furthermore the carbon shifts differ from h/mc in all cases more than do the shifts of beryllium, a fact which may be reasonably interpreted along the lines of the present theory as a result of the greater binding energies characterizing the electrons of carbon.

It is unprofitable to press a classical or semi-classical theory of atomic processes beyond a certain point and it is particularly unnecessary in this case since the matters under discussion are treated from a more fundamental standpoint in the following paper which Professor Felix Bloch, at our suggestion, has been so kind as to prepare. As he shows, it is possible to deduce a shift equation without ambiguity and without any arbitrarily adjustable constants. His results for the shift of the maximum of the modified line

[11] P. A. Ross and Paul Kirkpatrick, Phys. Rev. **45**, 135 (1934).

TABLE I. *Summary of data and corrections.*

Radiation	λ (X.U.)	Scatterer	*B* crystal shift angle	$\Delta\lambda_{90}$ uncorrected (X.U.)	Corrections: Scatterer thickness (additive)	Corrections: Spectrometer sensitivity (subtractive)	Corrections: Scatterer filtering (additive)	$\Delta\lambda_{90}$ corrected (X.U.)
Sn $K\beta$	435.	carbon	27.16′	23.87	0.03	0.02	0.00	23.88±0.03
" "	435.	beryllium	27.29′	23.98	0.16	0.02	0.01	24.13±0.06
Ag $K\beta$	496.	carbon	27.09′	23.78	0.03	0.02	0.00	23.79±0.03
" "	496.	beryllium	27.02′	23.72	0.19	0.02	0.02	23.91±0.06
Mo $K\beta$	631.	carbon	26.87′	23.52	0.05	0.02	0.01	23.56±0.03
" "	631.	beryllium	27.03′	23.66	0.24	0.02	0.02	23.90±0.06

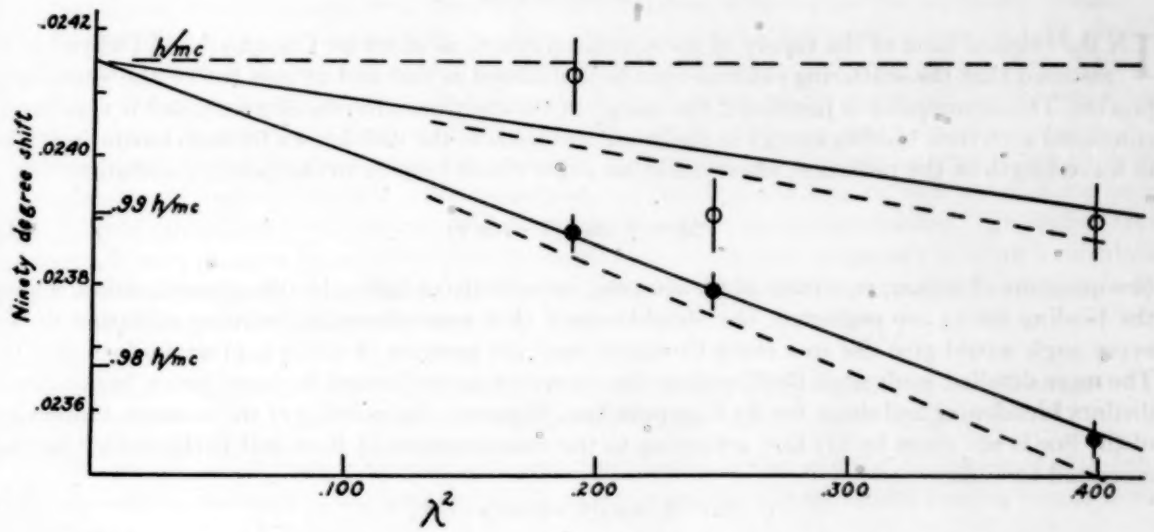

FIG. 4. Wave-length shift in Angstroms for ninety-degree scattering *vs.* square of incident wave-length in Angstroms. Single circles represent observed scattering by beryllium; double circles by carbon. Solid lines are the straight lines which best fit the data and possess the intercept h/mc. Dotted lines indicate the requirements of Bloch's theory.

in ninety-degree scattering are given by the dotted lines in Fig. 4. The agreement between experiment and theory, though not perfect, is most encouraging. Further experiments, with pure beryllium and with many other scatterers, are now in preparation.

In the problem of the determination of fundamental physical constants it has been the practice to accept the measured value of any ninety-degree shift as a determination of h/mc. It is now seen that conclusions so drawn must be erroneous, and that h/mc is to be determined by extrapolating observed shift data to zero wave-length. The carbon data of Fig. 4 when treated in this way yield a value $h/mc=0.02418 \pm 0.00004$. The precision of this determination will be greatly improved by the use of a wider range of wave-lengths.

It remains to acknowledge our appreciation to the National Research Council for a grant-in-aid which made possible the purchase of apparatus essential to this investigation.

Contribution to the Theory of the Compton-Line

F. BLOCH, *Department of Physics, Stanford University*

(Received July 24, 1934)

Starting from Wentzel's theory of the Compton scattering of bound electrons, and assuming that the motion of the electrons in the atom can be described by hydrogenic eigenfunctions, general formulae are developed for the calculation of the intensity distribution in the Compton line. It is shown that the interaction of the electrons with the atomic nucleus gives not only a broadening of the Compton line but makes it also asymmetrical, shifting at the same time the position of the maximum intensity from Compton's value $\Delta\lambda=(h/m_0c)(1-\cos\theta)$. The "defect of the Compton shift" is shown to be quadratic in the wave-length of the incident radiation. This law as well as the value of the constant entering into it are found to agree satisfactorily with experiment.

1. INTRODUCTION

IN the original form of the theory of the Compton effect, as given by Compton[1] and Debye,[2] it is assumed that the scattering electrons can be considered as free and at rest before the scattering process. This assumption is justified if the energy of the electrons after having scattered is very large compared with their binding energy in the atom, and leads to the well-known formula for the increase in wave-length of the radiation, observed at an angle θ with respect to the primary radiation:

$$\Delta\lambda=(h/m_0c)(1-\cos\theta) \tag{1}$$

(h=quantum of action, m_0=mass of the electron, c=velocity of light). In this approximation, where the binding forces are neglected, one should expect that monochromatic primary radiation under every angle would give rise to a *sharp* Compton line,[3] the position of which is given by formula (1). The more detailed analysis of the Compton line, however, as performed in recent years[4] has shown a distinct broadening and shape for the Compton line. Moreover, the position of the maximum intensity of the line is not given by (1) but, according to the measurements of Ross and Kirkpatrick,[5] by the corrected formula

$$\Delta\lambda=(h/m_0c)(1-\cos\theta)-D\lambda^2, \tag{2}$$

D being a constant which depends on the scattering substance, and λ the wave-length of the primary radiation. For the wave-lengths and observation angles used the order of magnitude of the "defect of the Compton shift"

$$\delta\lambda=D\lambda^2 \tag{3}$$

is of the order of magnitude of 1 percent of the total shift $\Delta\lambda$.

It is clear that both the broadening of the line and the defect of the shift are due to the binding forces, acting on the scattering electrons. As DuMond[6] showed, the broadening of the line can easily be understood by ascribing it to the Doppler effect, due to motion of the electrons in the atom and therefore proportional to their velocities. Indeed, the observation of the broadening of the Compton line may be said to give direct information about the velocity distribution of the electrons in the atom. Since the average speed of an electron is essentially proportional to the square root of its binding

---

[1] A. H. Compton, Phys. Rev. **21**, 483 (1923).
[2] P. Debye, Phys. Zeits. **24**, 161 (1923).
[3] The very small broadening of the line, due to the reaction of the scattered radiation on the electron can here be entirely neglected. Compare I. Waller, Zeits. f. Physik **88**, 436 (1934).
[4] G. E. M. Jauncey, Phys. Rev. **25**, 314 (1925); **31**, 723 (1928); H. M. Sharp, ibid. **26**, 691 (1925); Jesse W. M. DuMond, ibid. **33**, 643 (1929); **36**, 146 (1930); F. L. Nutting, ibid. **36**, 1267 (1930).
[5] See the preceding paper of P. A. Ross and Paul Kirkpatrick.
[6] Jesse W. M. DuMond, Rev. Mod. Phys. **5**, 1 (1933).

energy, the broadening of the Compton line is also proportional to this square root. It is obvious that the consideration of the Doppler effect can only explain a *symmetrical* broadening of the line around the position of its center of gravity as given by (1), since the average of the electronic velocities in the atom vanishes.

In order to get an explanation of the defect of the shift $\delta\lambda$, one has to go one step further. By a simple consideration, Ross and Kirkpatrick[7] obtained for the constant D in (2) and (3)

$$D=\kappa E/hc, \tag{4}$$

where E is the binding energy of the electron under consideration and κ a numerical constant of the order of magnitude 1, the exact value of which could not be obtained by their semiclassical method. Nevertheless, formulae (3) and (4) account for the observed order of magnitude of the defect $\delta\lambda$, and for its dependence on λ. Since the broadening of the line is essentially proportional to $\sqrt{E}$ while $\delta\lambda$ is proportional to E, the latter may be said to be a higher order effect, provided the binding energy is considered small compared with the recoil energy of the electron after the scattering process.

A consistent wave-mechanical scheme of the Compton effect of bound electrons has been given by Wentzel.[8] However, he worked out his formulae only for the case of a K-electron, as in the hydrogen atom, and furthermore restricted himself to an approximation which accounted for the broadening but not for the defect of the shift of the Compton line. In order to make possible a quantitative comparison between the theory and the measured data for Be and C[5] we have generalized his results for the case of higher electronic orbits, assuming that the forces acting on each electron can be approximately described by a Coulomb field with properly chosen screening constant. The method represents a series-expansion in powers of the binding energy, which goes far enough to allow a calculation of the defect $\delta\lambda$; in this approximation the law (3) is verified and the constant D is determined in satisfactory agreement with experiment.

2. General Formulae for the Intensity of Radiation, Scattered by an Electron in a Coulomb Field

We consider an electron with principal quantum number n and angular momentum $lh/2\pi$ before the scattering process in a Coulomb field with effective nuclear charge Ze; its binding energy is then given by

$$E=2\pi^2Z^2e^4m_0/n^2h^2. \tag{5}$$

We call the frequencies of the incident and scattered radiations ν and ν', respectively, and the energy of the electron after the scattering process

$$W=h^2k^2/8\pi^2m_0=h\nu-h\nu'-E. \tag{6}$$

It will be assumed that

$$h\nu\ll m_0c^2, \tag{7}$$

so that all relativistic effects can be neglected; furthermore we assume

$$E\ll W. \tag{8}$$

We shall see later that, in order to account for the defect of the Compton shift, it is sufficient to consider in the expression for the scattered intensity only terms of the relative order of magnitude 1 and $(E/W)^{\frac{1}{2}}$. In this approximation, as in Wentzel's paper (G), we still need only to consider Dirac's "true scattering" processes.

Using formulae (10), (12), (12a) of G, and considering that the primary radiation is unpolarized,

---

[7] P. A. Ross and Paul Kirkpatrick, Phys. Rev. **45**, 223 (1934).

[8] G. Wentzel, Zeits. f. Physik **43**, 1, 779 (1927); Zeits. f. Physik **58**, 348 (1929). (We shall refer to this paper from now on as "G".)

we can write the intensity scattered by our electron at an angle θ with the direction of the incident radiation into a frequency range between ν' and $\nu'+d\nu'$ in the form

$$dI_{nla}=I_P\frac{2\pi^2e^4}{m_0c^4r^2}\cdot\frac{1+\cos^2\theta}{hk}d\nu'\int_{-\infty}^{+\infty}|\epsilon_{nla,\,km}(\Delta k)|^2dm, \tag{9}$$

where I_P is the intensity of the primary radiation, r the distance from the scattering atom, k the quantity defined by (6). $\epsilon_{nla,\,km}(\Delta k)$ is the matrix-element, associated with transitions of the electron from the initial state (n, l, a) to the final state (k, m). As in G, we use parabolic coordinates ξ, η, φ to describe the position of the electron; if $\mathfrak{v}$ and $\mathfrak{v}'$ are vectors with an absolute value equal to the frequencies and directed in the direction of propagation of the incident and scattered radiations, respectively, the azimuth φ of our parabolic system of coordinates is measured around an axis in the direction of the vector

$$\Delta\boldsymbol{k}=(2\pi/c)(\mathfrak{v}-\mathfrak{v}'). \tag{10}$$

The quantity a in (9) is the azimuthal quantum number of the initial state with respect to this axis, m is a parabolic quantum number, related to the direction of momentum of the recoil electron, Δk is the absolute value of the vector $\Delta\boldsymbol{k}$, defined by (10). The matrix-element $\epsilon_{nla,\,km}(\Delta k)$ is then given by[9]

$$\epsilon_{nla,\,km}(\Delta k)=\tfrac{1}{4}\int_0^{2\pi}d\varphi\int_0^{\infty}d\xi\int_0^{\infty}d\eta(\xi+\eta)e^{i\Delta k(\xi-\eta)/2}\psi_{kma}(\xi\eta\varphi)\psi^*_{nla}(\xi\eta\varphi). \tag{11}$$

ψ^*_{nla} is the conjugate-complex of the normalized eigenfunction ψ_{nla} of the initial state, ψ_{kma} is the eigenfunction of the final state. We add here the azimuthal quantum number a to the two quantities (k, m), used before to describe the final state in order to remember that the component of the angular momentum in the direction of $\Delta\boldsymbol{k}$ remains unchanged during the scattering process, due to the fact that the perturbation function $e^{i\Delta k(\xi-\eta)/2}$ does not contain the azimuth φ. Writing

$$\psi_{kma}(\xi\eta\varphi)=u_{kma}(\xi\eta)e^{ia\varphi}, \tag{12}$$

$$\psi^*_{nla}(\xi\eta\varphi)=u_{nla}(\xi\eta)e^{-ia\varphi}, \tag{12a}$$

we can perform in (11) the integration over φ, finding

$$\epsilon_{nla,\,km}(\Delta k)=\frac{\pi}{2}\int_0^{\infty}d\xi\int_0^{\infty}d\eta(\xi+\eta)e^{i\Delta k(\xi-\eta)/2}u_{kma}(\xi\eta)u_{nla}(\xi\eta). \tag{11a}$$

According to (8) the final state (kma) has to be assumed to be in the continuous spectrum. Using the well-known methods developed by Schrödinger,[10] the eigenfunction $u_{kma}(\xi\eta)$ can be represented as in G by complex integrals. We write

$$u_{kma}(\xi\eta)=C_{kma}(\xi\eta)^{a/2}(ik)^{-2a}f_{kma}(\xi)g_{kma}(\eta) \tag{13}$$

with

$$\left.\begin{aligned}f_{kma}(\xi)&=(1/2\pi i)\oint e^{t_1\xi}(t_1+ik/2)^{(a-1)/2+i(\beta+m)}(t_1-ik/2)^{(a-1)/2-i(\beta+m)}dt_1\\ g_{kma}(\eta)&=(1/2\pi i)\oint e^{t_2\eta}(t_2+ik/2)^{(a-1)/2+i(\beta-m)}(t_2-ik/2)^{(a-1)/2-i(\beta-m)}dt_2\end{aligned}\right\} \tag{14}$$

and

$$\beta=(1/2k)(4\pi^2Zm_0e^2/h^2). \tag{15}$$

[9] Compare G, formulae (4) and (26).
[10] E. Schrödinger, Ann. d. Physik **4**, 361 (1926); **4**, 437 (1926).

The same considerations which lead to formula (24) in G give the constant of normalization, entering into (13)

$$C_{kmu}=\tfrac{1}{2}\pi^{-1}k^{a+1}e^{\pi\beta}|\Gamma[(1-a)/2+i(\beta+m)]||\Gamma[(1-a)/2+i(\beta-m)]|. \tag{14a}$$

With this normalization and the condition, that

$$\tfrac{1}{4}\int_0^{2\pi}d\varphi\int_0^{\infty}d\xi\int_0^{\infty}d\eta(\xi+\eta)|\psi_{nla}(\xi\eta\varphi)|^2=1 \tag{16}$$

it can be shown, as in G, that under the assumption (8)

$$\int_0^{\infty}dk\int_{-\infty}^{+\infty}dm|\epsilon_{nla,\ km}(\Delta k)|^2=1, \tag{17}$$

which, using (6) and (9) gives for the total intensity scattered at the angle θ

$$I_{nla}=\int dI_{nla}=I_P(e^4/2m_0^2c^4r^2)(1+\cos^2\theta). \tag{18}$$

This is Thomson's formula for the scattering of free electrons. We shall see later, that in our approximation, although the spectral distribution is changed, the total intensity is still given by (18), since (17), in this approximation, remains valid.

In polar coordinates, $r\vartheta$, the function u_{nla} in (12a) is given by[11]

$$u_{nla}=C_{nla}e^{-\alpha r/2}(\alpha r)^l P_l^a(\cos\vartheta)L_{l+n}^{2l+1}(\alpha r) \tag{19}$$

where the constant C_{nla} has to be determined such that (16) is fulfilled and α is given by

$$\alpha=8\pi^2Zm_0e^2/nh^2. \tag{20}$$

In order to get a general expression for the quantity (11a) consider the expression

$$q_{la}(k,m,\Delta k,t)=-\frac{2}{\pi}\sum_{n=1}^{\infty}\frac{\epsilon_{nla,\ km}(\Delta k)}{C_{nla}(n+l)!}t^{n-l-1}. \tag{21}$$

Performing the summation under the integral in (11a) and using the formula[12]

$$\sum_{n=1}^{\infty}L_{n+l}^{2l+1}(\alpha r)\frac{t^{n-l-1}}{(n+l)!}=\frac{(-1)^{2l+1}}{(1-t)^{2l+2}}e^{-\alpha rt/(1-t)}$$

and (19), we find

$$q_{la}(k,m,\Delta k,t)=\frac{(-1)^{2l+1}}{(1-t)^{2l+2}}\int_0^{\infty}d\xi\int_0^{\infty}d\eta(\xi+\eta)e^{i\Delta k(\xi-\eta)/2}u_{kma}(\xi\eta)(\alpha r)^l P_l^a(\cos\vartheta)e^{-(\alpha r/2)(1-t)/(1+t)}. \tag{22}$$

In order to express the variables r and ϑ, entering in (22), by means of the parabolic coordinates ξ and η, we use the expressions

$$r=\xi+\eta/2,\qquad \cos\vartheta=(\xi-\eta)/(\xi+\eta). \tag{23}$$

Writing

$$P_l^a(\cos\vartheta)=(1-\cos^2\vartheta)^{a/2}\sum_{p=0}^{l-a}c_p\cos^p\vartheta, \tag{24}$$

[11] Cf. A. Sommerfeld, *Wave Mechanics*, page 60 ff.
[12] E. Schrödinger, Ann. d. Physik **4**, 437 (1926).

where the quantities c_p are certain numbers defining the spherical harmonics P_l^a, we find, using (13), (14), (22), (23) and (24)

$$q_{la}(k, m, \Delta k, t) = -\frac{(ik)^{-2a}}{4\pi^2}\frac{\alpha^l}{2^{l-a}}C_{kma}\frac{(-1)^{2l+1}}{(1-t)^{2l+2}}\sum_{p=0}^{l-a}c_p\int_0^\infty d\xi\int_0^\infty d\eta(\xi+\eta)^{1+l-a-p}(\xi-\eta)^p(\xi\eta)^a$$

$$\times\exp\left[i\Delta k\frac{\xi-\eta}{2}+\frac{\alpha}{4}\frac{1+t}{1-t}(\xi+\eta)\right]\oint e^{t_1\xi}\left(t_1+\frac{ik}{2}\right)^{(a-1)/2+i(\beta+m)}\left(t_1-\frac{ik}{2}\right)^{(a-1)/2-i(\beta+m)}dt_1$$

$$\times\oint e^{t_2\eta}\left(t_2+\frac{ik}{2}\right)^{(a-1)/2+i(\beta-m)}\left(t_2-\frac{ik}{2}\right)^{(a-1)/2-i(\beta-m)}dt_2$$

$$=-\frac{(ik)^{-2a}}{4\pi^2}\frac{\alpha^l}{2^{l-a}}C_{kma}\frac{(-1)^{2l+1}}{(1-t)^{2l+2}}\lim_{\mu_1,\mu_2\to 0}\sum_{p=0}^{l-a}c_p\left(\frac{\partial}{\partial\mu_1}+\frac{\partial}{\partial\mu_2}\right)^{1-l-a-p}\left(\frac{\partial}{\partial\mu_1}-\frac{\partial}{\partial\mu_2}\right)^p\frac{\partial^{2a}}{\partial\mu_1^a\partial\mu_2^a}$$

$$\times\oint dt_1\int_0^\infty d\xi\exp\left[\xi\left(t_1+\frac{i\Delta k}{2}-\frac{\alpha}{4}\frac{1+t}{1-t}+\mu_1\right)\right]\left(t_1+\frac{ik}{2}\right)^{(a-1)/2+i(\beta+m)}\left(t_1-\frac{ik}{2}\right)^{(a-1)/2-i(\beta+m)}$$

$$\times\oint dt_2\int_0^\infty d\eta\exp\left[\eta\left(t_2-\frac{i\Delta k}{2}-\frac{\alpha}{4}\frac{1+t}{1-t}+\mu_2\right)\right]\left(t_2+\frac{ik}{2}\right)^{(a-1)/2+i(\beta-m)}\left(t_2-\frac{ik}{2}\right)^{(a-1)/2-i(\beta-m)}. \quad (25)$$

After having performed the integrations over ξ and η, the remaining integrand in the integrals over t_1 and t_2 have simple poles for

$$t_1'=-\frac{\alpha}{4}\frac{1+t}{1-t}-\mu_1-\frac{i\Delta k}{2} \quad \text{and} \quad t_2'=-\frac{\alpha}{4}\frac{1+t}{1-t}-\mu_2+\frac{i\Delta k}{2}, \text{ respectively.}$$

The application of the theorem of residues gives[13]

$$q_{la}(k, m, \Delta k, t) = (ik)^{-2a}\frac{\alpha^l}{2^{l-a}}C_{kma}\frac{(-1)^{2l+1}}{(1-t)^{2l+2}}\sum_{p=0}^{l-a}c_p\left(\frac{\partial}{\partial\mu_1}+\frac{\partial}{\partial\mu_2}\right)^{1+l-a-p}\left(\frac{\partial}{\partial\mu_1}-\frac{\partial}{\partial\mu_2}\right)^p\frac{\partial^{2a}}{\partial\mu_1^a\partial\mu_2^a}$$

$$\times\left(\frac{\alpha}{4}\frac{1+t}{1-t}-\mu_1-i\frac{\Delta k-k}{2}\right)^{(a-1)/2+i(\beta+m)}\left(\frac{\alpha}{4}\frac{1+t}{1-t}-\mu_1-\frac{i(\Delta k+k)}{2}\right)^{(a-1)/2-i(\beta+m)}$$

$$\times\left(\frac{\alpha}{4}\frac{1+t}{1-t}-\mu_2+i\frac{\Delta k+k}{2}\right)^{(a-1)/2+i(\beta-m)}\left(\frac{\alpha}{4}\frac{1+t}{1-t}-\mu_2+i\frac{\Delta k-k}{2}\right)^{(a-1)/2-i(\beta-m)}. \quad (26)$$

This expression can be simplified, if we restrict ourselves to the zero and first power terms in an expansion with respect to β, which according to (15), (5) and (6) is of the order of magnitude of $(E/W)^{\frac{1}{2}}$ and, accepting (8), can be considered as small compared with unity. Since we have to expect a considerable contribution to the scattered intensity only, if $\Delta k-k$ is of the order of magnitude of α, i.e. if the momentum transferred to the nucleus is of the order of magnitude of the momentum which the electron has in its initial orbit, we can write $\gamma=\alpha/2(\Delta k+k)\cong\alpha/2k$ or, according to (15) and (20)

$$\gamma=2\beta/n. \quad (27)$$

In the expansion of (26) we can then neglect all terms which are quadratic or of higher order in β

[13] Cf. the analogous considerations, which lead to formula (28) of G.

and γ. With

$$v=(2/\alpha)(\Delta k-k);\quad \tau_1=-4\mu_1/\alpha;\quad \tau_2=-4\mu_2/\alpha, \tag{28}$$

and using (14a), we find in our approximation:

$$q_{la}(k,m,\Delta k,t)=8\pi^{-1}(-2)^l\left(\frac{\alpha}{2}\right)^{-2+2mi}\frac{1}{(1-t)^{2l+2}}\frac{k^{1-a}}{(\Delta k+k)^{1-a+2mi}}\left|\Gamma\left[\frac{1-a}{2}+i(\beta+m)\right]\right|$$

$$\times\left|\Gamma\left[\frac{1-a}{2}+i(\beta-m)\right]\right|\lim_{\tau_1,\,\tau_2\to 0}\sum_{p=0}^{l-a}c_p\left(\frac{\partial}{\partial\tau_1}+\frac{\partial}{\partial\tau_2}\right)^{1+l-a-p}\left(\frac{\partial}{\partial\tau_1}-\frac{\partial}{\partial\tau_2}\right)^{p}\frac{\partial^{2a}}{\partial\tau_1^{a}\partial\tau_2^{a}}$$

$$\times\left(\frac{1+t}{1-t}+\tau_1-iv\right)^{(a-1)/2+im}\left(\frac{1+t}{1-t}+\tau_2+iv\right)^{(a-1)/2+im}\cdot$$

$$\times\left\{1+i\beta\lg\frac{1+t+(1-t)(\tau_1-iv)}{1+t+(1-t)(\tau_2+iv)}+i\gamma\left(\frac{a-1}{2}-im\right)(\tau_1-\tau_2)\right\}. \tag{29}$$

Once the expression (29) has been determined for given numbers l and a, we obtain readily the quantity $\epsilon_{nla,\,km}(\Delta k)$ by differentiation with respect to t. Indeed, according to (21) we find

$$\epsilon_{nla,\,km}(\Delta k)=\pi^{\frac{1}{2}}(-1)^l2^{-3-l}(A_{nla})^{\frac{1}{2}}\left.\frac{\partial^{n-l-1}q_{la}(k,m,\Delta k,t)}{\partial t^{n-l-1}}\right|_{t=0}. \tag{30}$$

The constant $(A_{nla})^{\frac{1}{2}}$ of (30) stands in a simple relation to the constant of normalization C_{nla} appearing in (21). Instead of determining C_{nla} from the Eq. (16), we can determine A_{nla} by the equivalent Eq. (17) after having calculated $\epsilon_{nla,\,km}(\Delta k)$ from (30). The fact, that relation (17) remains valid when all quadratic and higher terms in β and γ are neglected can be seen from (29). Indeed, by the substitutions $\tau_1\to\tau_2$, $\tau_2\to\tau_1$, $v\to -v$ all the terms in (29) not containing β or γ do not change, while the terms with β or γ change their sign and *vice versa*. Those terms in $|\epsilon|^2$ which are linear in β or γ are therefore uneven functions of v and therefore their integral over v, or over k as in (17), vanishes, thus giving no contribution to the total scattered intensity.

3. Scattering of Electrons in the K- and L-Shell

We proceed now to calculate the contribution to the Compton scattering of electrons in the different orbits of the K- and L-shells. Assuming hydrogenic orbits, we can express the constants β and γ entering in (29) and (30) in terms of the observed binding energy E, using (5) and (15) and (27). These constants are, of course, different for different orbits and elements.

(a) *s*-electrons

Here, we have $l=a=0$; in the sum $\sum_{p=0}^{l-a}$ of (29), there appears only the term with $p=0$ and it is, according to (24), $c_0=1$ since $P_0^0(\cos\theta)=1$.

A straightforward differentiation with respect to τ_1 and τ_2 and taking the limit $\tau_1,\ \tau_2\to 0$ gives:

$$q_{00}(k,m,\Delta k,t)=8\pi^{-1}\left(\frac{\alpha}{2}\right)^{-2+2mi}\frac{k}{(\Delta k+k)^{1+2mi}}\left|\Gamma\left[\tfrac{1}{2}+i(\beta+m)\right]\right|\left|\Gamma\left[\tfrac{1}{2}+i(\beta-m)\right]\right|$$

$$\times\frac{1}{(1-t)^2}\left[\left(\frac{1+t}{1-t}\right)^2+v^2\right]^{-\frac{1}{2}+im}\left\{\left(\frac{1+t}{1-t}\right)(-1+2im)\left(1+i\beta\lg\frac{1+t-(1-t)iv}{1+t+(1-t)iv}\right)-2\beta v\right\}. \tag{31}$$

In order to obtain explicit expressions for the scattered intensity of the s-electrons in the K- and L-shells, we have to treat the two cases separately.

(α) *K-shell.* Since $n=1$, $l=0$, we obtain from (30), taking simply the expression (31) for $t=0$ and noticing

$$i\beta \lg [(1-iv)/(1+iv)]=2\beta \operatorname{arctg} v$$

$$\epsilon_{100,\,km}(\Delta k)=(A_{100})^{\frac{1}{2}}(\alpha/2)^{-2+2mi}(k/(\Delta k+k)^{1+2mi})\,|\,\Gamma[\tfrac{1}{2}+i(\beta+m)]\,\|\,\Gamma[\tfrac{1}{2}+i(\beta-m)]\,|\,(1+v^2)^{-\frac{1}{2}+im}$$
$$\times\{-1-2\beta \operatorname{arctg} v-2\beta v+2mi(1+2\beta \operatorname{arctg} v)\}. \quad (32)$$

Taking the absolute square of (32), we neglect again all quadratic and higher terms in β. It can be easily seen, that in this approximation the terms containing β in the Γ-functions of (32) can be neglected.

We use the relation[14]

$$|\,\Gamma(\tfrac{1}{2}+im)\,|^2=|\,\Gamma(\tfrac{1}{2}-im)\,|^2=\pi/ch\,\pi m, \qquad \text{and further}$$
$$k=\Delta k-\tfrac{1}{2}\alpha v=\Delta k(1-\alpha/2\Delta k v)\leqq\Delta k(1-\gamma v)$$
$$\Delta k+k=2\Delta k-\tfrac{1}{2}\alpha v=2\Delta k(1-\alpha v/4\Delta k)\leqq 2\Delta k(1-\tfrac{1}{2}\gamma v). \quad (33)$$

Eqs. (33) follow from (28) and (27) which, for $n=1$ gives $\gamma=2\beta$. Hence we obtain

$$|\,\epsilon_{100,\,km}(\Delta k)\,|^2\leqq A_{100}(\alpha/2)^{-4}(\pi^2/4)[(1+v^2)^{-3}/ch^2\pi m]\{(1+4m^2)(1+4\beta \operatorname{arctg} v)+2\beta v\}. \quad (34)$$

For the following integrations over m, we make use of the formula[15]

$$\int_{-\infty}^{+\infty}\frac{m^g dm}{ch^2\pi m}-\int_{-\infty}^{+\infty}\frac{(m+i)^g dm}{ch^2\pi m}=-\frac{4}{\pi}g\left(\frac{i}{2}\right)^g,$$

which, applied for $g=1, 3, 5$ gives

$$\int_{-\infty}^{+\infty}\frac{dm}{ch^2\pi m}=\frac{2}{\pi}, \qquad \int_{-\infty}^{+\infty}\frac{m^2dm}{ch^2\pi m}=\frac{1}{6\pi}, \qquad \int_{-\infty}^{+\infty}\frac{m^4dm}{ch^2\pi m}=\frac{7}{120\pi}. \quad (35)$$

With the help of (35) we find

$$|\,\epsilon_{100}(k,\,\Delta k)\,|^2=\int_{-\infty}^{+\infty}|\,\epsilon_{100,\,km}(\Delta k)\,|^2dm=A_{100}(\alpha/2)^{-4}(\pi/(1+v^2)^3)\{(5/6)(1+4\beta \operatorname{arctg} v)+\beta v\}. \quad (36)$$

In order to satisfy (17) we have to choose the constant A_{100} such, that according to (28)

$$\int_0^{\infty}|\,\epsilon_{100}(k,\,\Delta k)\,|^2dk\leqq(\alpha/2)\int_{-\infty}^{+\infty}|\,\epsilon_{100}(k,\,\Delta k)\,|^2dv=1. \quad (37)$$

Since $1+v^2$ is an even function of v, while arctg v and v are uneven, the terms of (36) containing β give no contribution to the integral (37).

Applying the first of the following formulae

$$\int_{-\infty}^{+\infty}\frac{dv}{(1+v^2)^3}=\frac{3\pi}{8}, \qquad \int_{-\infty}^{+\infty}\frac{dv}{(1+v^2)^4}=\frac{5\pi}{16}, \qquad \int_{-\infty}^{+\infty}\frac{dv}{(1+v^2)^5}=\frac{35\pi}{128} \quad (38)$$

we find

$$(\alpha/2)\int_{-\infty}^{+\infty}|\,\epsilon_{100}(k,\,\Delta k)\,|^2dv=A_{100}(\alpha/2)^{-3}(5\pi^2/16)=1, \quad (39)$$

---

[14] G, page 359.

[15] This equation, is a slightly different form of the equation, given in G in the footnote page 366.

therefore

$$A_{100}=(\alpha/2)^3(16/5\pi^2) \tag{39a}$$

and from (36)

$$|\epsilon_{100}(k,\Delta k)|^2=(16/3\pi\alpha)[1/(1+v^2)^3]\{1+4\beta\,\mathrm{arctg}\,v+(6/5)\beta v\} \tag{40}$$

with $v=(2/\alpha)(\Delta k-k)$. Formula (40) becomes identical with formula (32) of G, if the terms with β are neglected.

(β) *L-shell.* Here we have $n=2, l=0$; in order to obtain $\epsilon_{200,\,km}(\Delta k)$ from (30), we have to derive the expression (31) once with respect to t and take the limit $t=0$. Instead of (32) we find thus

$$\epsilon_{200,\,km}(\Delta k)=(A_{200})^{\frac{1}{2}}(\alpha/2)^{-2+2mi}(k/(\Delta k+k)^{1+2mi})\,|\,\Gamma[\tfrac{1}{2}+i(\beta+m)]\,|\,|\,\Gamma[\tfrac{1}{2}+i(\beta-m)]\,|\,2(1+v^2)^{-1+im}$$

$$\times\left\{-(1+2\beta\,\mathrm{arctg}\,v)\left(2-\frac{3}{1+v^2}+\frac{4m^2}{(1+v^2)^2}\right)-2\beta v\left(1-\frac{5}{1+v^2}\right)\right.$$

$$\left.+2mi\left[(1+2\beta\,\mathrm{arctg}\,v)\left(2-\frac{4}{1+v^2}\right)-\frac{4\beta v}{1+v^2}\right]\right\}, \tag{41}$$

Keeping only the linear terms in β it follows that, instead of (34):

$$|\epsilon_{200,\,km}(\Delta k)|^2=4A_{200}(\alpha/2)^{-4}\pi^2[(1+v^2)^{-3}/ch^2\pi m][k^2/(\Delta k+k)^2]$$

$$\times\left\{[1+4\beta\,\mathrm{arctg}\,v]\left[4-\frac{12}{1+v^2}+\frac{9}{(1+v^2)^2}+4m^2\left(4-\frac{12}{1+v^2}+\frac{10}{(1+v^2)^2}\right)+\frac{16m^4}{(1+v^2)^2}\right]\right.$$

$$\left.+4\beta v\left[2-\frac{13}{1+v^2}+\frac{15}{(1+v^2)^2}-\frac{12m^2}{1+v^2}+\frac{12m^2}{(1+v^2)^2}\right]\right\}.$$

Integrating over m with the help of formulae (35) and using (33) with $\gamma=\beta$ according to (27) for $n=2$, we get

$$|\epsilon_{200}(k,\Delta k)|^2=\int_{-\infty}^{+\infty}|\epsilon_{200,\,km}(\Delta k)|^2dm=A_{200}\left(\frac{\alpha}{2}\right)^{-4}\frac{\pi}{(1+v^2)^3}\times$$

$$\left\{\frac{32}{3}[1+4\beta\,\mathrm{arctg}\,v]\left[1-\frac{3}{1+v^2}+\frac{12}{5}\frac{1}{(1+v^2)^2}\right]+16\beta v\left[\frac{4}{3}-\frac{5}{1+v^2}+\frac{32}{5}\frac{1}{(1+v^2)^2}\right]\right\}. \tag{42}$$

Applying (17) we obtain with the help of formulae (38) in a way, similar to (39) and (39a) the result:

$$(\alpha/2)\int_{-\infty}^{+\infty}|\epsilon_{200}(k,\Delta k)|^2dv=A_{200}(\alpha/2)^{-3}\pi^2=1;\qquad A_{200}=(1/\pi^2)(\alpha/2)^3$$

and therefore

$$|\epsilon_{200}(k,\Delta k)|^2=\frac{64}{3\pi\alpha}\frac{1}{(1+v^2)^3}\left\{[1+4\beta\,\mathrm{arctg}\,v]\left[1-\frac{3}{1+v^2}+\frac{12}{5}\frac{1}{(1+v^2)^2}\right]\right.$$

$$\left.+\beta v\left[2-\frac{15}{2}\frac{1}{1+v^2}+\frac{48}{5}\frac{1}{(1+v^2)^2}\right]\right\}. \tag{43}$$

(b) *p*-electrons in the *L*-shell

Since in this case $n-l-1=0$, it is not necessary to carry out any differentiation with respect to t. It is sufficient therefore to consider the quantity q_{1a}, given by (29) only for $t=0$. Yet we have to

consider separately the two cases $a=0$ and $a=1$, which correspond to the orientations of the angular momentum in the initial state perpendicular and parallel, respectively, to the axis, given by the direction of the vector Δk, defined by (10).

(α) $a=0$. Since $P_1^0(\cos\vartheta)=\cos\vartheta$, we have, according to (24) $c_0=0$; $c_1=1$. This means in (29) a differentiation with respect to τ_1 and τ_2 of the form $\partial^2/\partial\tau_1^2-\partial^2/\partial\tau_2^2$ and leads to the result

$$\epsilon_{210,\,km}(\Delta k)=-\pi^{\frac{1}{2}}2^{-2}(A_{210})^{\frac{1}{2}}q_{10}(k,\,m,\,\Delta k,\,0)=(A_{210})^{\frac{1}{2}}(\alpha/2)^{-2+2mi}(k/(\Delta k+k)^{1+2mi})$$

$$\times|\Gamma[\tfrac{1}{2}+i(\beta+m)]||\Gamma[\tfrac{1}{2}+i(\beta-m)]|\,2(-1+2mi)(1+v^2)^{-\frac{1}{2}+im}\Big\{-mv(1+2\beta\,\mathrm{arctg}\,v)$$

$$+m\gamma(1+v^2)-\frac{2m\beta}{1+4m^2}(1-v^2)+i\Big[-\tfrac{3}{2}v(1+2\beta\,\mathrm{arctg}\,v)-\tfrac{1}{2}\gamma(1+v^2)+\beta\frac{2+4m^2}{1+4m^2}(1-v^2)\Big]\Big\}. \quad (44)$$

Taking the absolute square of (44) and keeping only terms linear in β we find

$$|\epsilon_{210,\,km}(\Delta k)|^2\leqq A_{210}\left(\frac{\alpha}{2}\right)^{-4}\pi^2\frac{(1+v^2)^{-5}}{ch^2\pi m}\frac{k^2}{(\Delta k+k)^2}\{v^2(9+40m^2+16m^4)(1+4\beta\,\mathrm{arctg}\,v)$$

$$+\gamma v(1+v^2)(6+12m^2-32m^4)-8\beta v(1-v^2)(3+4m^2)\}.$$

The integration over m and the use of (33) and (35) leads, in a manner similar to that employed for obtaining (42) to the expression

$$|\epsilon_{210}(k,\,\Delta k)|^2=\int_{-\infty}^{+\infty}|\epsilon_{210,\,km}(\Delta k)|^2dm$$

$$=A_{210}\left(\frac{\alpha}{2}\right)^{-4}\frac{\pi}{60(1+v^2)^4}\left\{384[1+4\beta\,\mathrm{arctg}\,v]\left[1-\frac{1}{1+v^2}\right]+\beta v\left[598-\frac{1216}{1+v^2}\right]\right\}.$$

The determination of A_{210} with the help of (17) gives

$$\frac{\alpha}{2}\int_{-\infty}^{+\infty}|\epsilon_{210}(k,\,\Delta k)|^2dv=A_{210}(\alpha/2)^{-3}\,\pi^2/4=1,$$

$A_{210}=(4/\pi^2)(\alpha/2)^3$ and therefore

$$|\epsilon_{210}(k,\,\Delta k)|^2=\frac{256}{5\pi\alpha}\frac{1}{(1+v^2)^4}\left\{[1+4\beta\,\mathrm{arctg}\,v]\left[1-\frac{1}{1+v^2}\right]+\beta v\left[\frac{299}{192}-\frac{19}{6}\frac{1}{1+v^2}\right]\right\}. \quad (45)$$

(β) $a=1$. Here again the summation over p in (29) contains only the term with $p=0$ and from (24) it follows that $c_0=1$. The differentiation with respect to τ_1, τ_2 in (29) here takes the form

$$(\partial/\partial\tau_1+\partial/\partial\tau_2)(\partial^2/\partial\tau_1\partial\tau_2).$$

One finds

$$\epsilon_{211,\,km}(\Delta k)=-\pi^{\frac{1}{2}}2^{-2}(A_{211})^{\frac{1}{2}}q_{11}(k,\,m,\,\Delta k,\,0)=(A_{211})^{\frac{1}{2}}(\alpha/2)^{-2+2mi}(1/(\Delta k+k)^{2mi})\,|\Gamma[i(\beta+m)]|$$

$$\times|\Gamma[i(\beta-m)]|\,2im(1+v^2)^{-2+im}\{-m^2(1+2\beta\,\mathrm{arctg}\,v)+m^2\gamma v-im[1+2\beta\,\mathrm{arctg}\,v+\beta v-\gamma v]\}. \quad (46)$$

By taking the absolute square of this expression and keeping only the terms linear in β and $\gamma=\beta$, it is again permissible to neglect the term with β in the Γ-functions of (46). From the formulae

$$\Gamma(1+z)=z\Gamma(z) \quad \text{and} \quad \Gamma(z)\Gamma(1-z)=\pi/\sin\pi z$$

it follows $|\Gamma(im)|^2=|\Gamma(-im)|^2=\pi/msh\pi m$ and we obtain from (46)

$$|\epsilon_{211,\,km}(\Delta k)|^2 \leqq A_{211}(\alpha/2)^{-4}4\pi^2[(1+v^2)^{-4}/sh^2\pi m]\{(m^2+m^4)[1+4\beta \operatorname{arctg} v]-2m^4\beta v\}.$$

For the integration over m, we make use of the formula

$$\int_{-\infty}^{+\infty}(m^g dm/sh^2\pi m) = 2^{g-1}/2^{g-1}-1\int(m^g dm/ch^2\pi m),$$

which for $g=2$ and $g=4$, with the help of (35) gives

$$\int_{-\infty}^{+\infty} m^2 dm/sh^2\pi m = 1/3\pi, \qquad \int_{-\infty}^{+\infty} m^4 dm/sh^2\pi m = 1/15\pi. \tag{47}$$

We find thus

$$|\epsilon_{211}(k,\,\Delta k)|^2 = \int_{-\infty}^{+\infty}|\epsilon_{211,\,km}(\Delta k)|^2 dm = A_{211}(\alpha/2)^{-4}(8\pi/15)[1/(1+v^2)^4]\{3(1+4\beta \operatorname{arctg} v)-\beta v\}$$

and with the help of (38)

$$(\alpha/2)\int_{-\infty}^{+\infty}|\epsilon_{211}(k,\,\Delta k)|^2 dv = A_{211}(\alpha/2)^{-2}\pi^2/2 = 1,$$

$A_{211}=(2/\pi^2)(\alpha/2)^3$ and therefore

$$|\epsilon_{211}(k,\,\Delta k)|^2 = (32/5\pi\alpha)(1/(1+v^2)^4)\{1+4\beta \operatorname{arctg} v-\tfrac{1}{3}\beta v\}. \tag{48}$$

4. Total Intensity and Defect of the Compton-Shift for Elements with K- and L-Electrons

With the expressions (40), (43), (45) and (48) we are now able, according to (9) to give the intensity-distribution on the Compton line of any element with given numbers N_{nla} of electrons in an orbit (nla) of the K- or L-shell. Indeed, assuming the electrons as independent, as has been done in the previous paragraphs, we can write for the total intensity of the frequency range $d\nu'$:

$$dI = \sum_{nla} N_{nla} dI_{nla}. \tag{49}$$

It has to be noticed, that for p-electrons in the L-shell all the three orientations of the angular momentum with respect to our chosen axis appear with the same weight. Calling N_3 the number of electrons in any one of the p-orbits, we have therefore in (49) to take:

$$N_{210} = N_3/3; \quad N_{211} = 2N_3/3. \tag{50}$$

Furthermore, we have to remember that the constants α and β as well as the variables v, according to their definition (28) have different significance for different orbits, changing with the binding energy of the corresponding electron. In order to distinguish them, we write instead of α, β and v

for s-electrons in the K-shell: α_1, β_1, v_1,
" " " " L-shell: α_2, β_2, v_2,
" p-electrons " " " " : α_3, β_3, v_3,
and further for abbreviation: $N_{100}=N_1$, $N_{200}=N_2$.

Remembering that according to (28)

$$k = \Delta k - \tfrac{1}{2}v \leqq \Delta k(1-\alpha v/\Delta 2k) \leqq \Delta k(1-2\beta v/n)$$

and using (9), (40), (43), (45), (48) and (50), we find for the total intensity of the range $d\nu'$ the following expression, which is correct, if all terms with second and higher powers in β are neglected:

$$dI=I_P\frac{2\pi^2e^4}{m_0c^4\nu^2}\frac{1+\cos^2\theta}{h\Delta k}d\nu'\frac{16}{3\pi}\left\{\frac{N_1}{\alpha_1}\frac{1}{(1+v_1^2)^3}\left[1+4\beta_1\operatorname{arctg}v_1+\frac{16}{5}\beta_1v_1\right]\right.$$
$$+\frac{4N_2}{\alpha_2}\frac{1}{(1+v_2^2)^3}\left[(1+4\beta_2\operatorname{arctg}v_2+\beta_2v_2)\left(1-\frac{3}{1+v_2^2}+\frac{12}{5}\frac{1}{(1+v_2^2)^2}\right)\right.$$
$$\left.+\beta_2v_2\left(2-\frac{15}{2}\frac{1}{1+v_2^2}+\frac{48}{5}\frac{1}{(1+v_2^2)^2}\right)\right]+\frac{4N_3}{5\alpha_3}\frac{1}{(1+v_3^2)^4}$$
$$\left.\times\left[(1+4\beta_3\operatorname{arctg}v_3+\beta_3v_3)\left(5-\frac{4}{1+v_3^2}\right)+\beta_3v_3\left(\frac{283}{48}-\frac{38}{3}\frac{1}{1+v_3^2}\right)\right]\right\}. \quad (51)$$

In order to obtain the relation between v and the wave-length of the scattered radiation λ', we notice that according to (28) and (6) it is

$$v=\frac{2}{\alpha}(\Delta k-k)=\frac{2}{\alpha}\left\{\left[\frac{8\pi^2\nu^2}{c^2}(1-\cos\theta)\right]^{\frac{1}{2}}-\left[\frac{8\pi^2m_0}{h}\left(\nu-\nu'-\frac{E}{h}\right)\right]^{\frac{1}{2}}\right\} \quad (52)$$

since for $h\nu\ll mc^2$, i.e., $\nu\leqq\nu'$ it follows from (10)

$$(\Delta k)^2=(8\pi^2\nu^2/c^2)(1-\cos\theta). \quad (53)$$

From (5) and (19) we get

$$(8\pi^2m_0/h^2)E=\alpha^2/4. \quad (54)$$

With the notation $\gamma=\alpha/2k\leqq\alpha/2\Delta k$ used before, and

$$\lambda'-\lambda\leqq c(\nu-\nu')/\nu^2=x(h/m_0c)(1-\cos\theta) \quad (55)$$

we can therefore write (52) in the form

$$v=(1/\gamma)\{1-(x-\gamma^2)^{\frac{1}{2}}\}. \quad (56)$$

Since we expect a considerable intensity only in the neighborhood of Compton's value (1), i.e., for $\Delta\lambda=\lambda'-\lambda=(h/m_0c)(1-\cos\theta)$, we write

$$x=1-\delta \quad (57)$$

and, expanding the square-root in (56), keeping only the terms with δ and γ^2, we get

$$v=(1/2\gamma)(\delta+\gamma^2). \quad (58)$$

As long as one neglects all terms with β_1, β_2 and β_3 in (51) and consequently with γ^2 in (56), one sees that the intensity is symmetrically distributed around Compton's value (1), namely, symmetrical around $v=0$ or $\delta=0$. Fig. 1 shows this symmetrical distribution for Be($N_1=N_2=2$, $N_3=0$) assuming for the binding energies the values: $E_1=122$ volts. $E_2=9.5$ volts. Fig. 2 is drawn for $C(N_1=N_2=N_3=2)$ with $E_1=285$ volts; $E_2=24.9$ volts; $E_3=11$ volts.

The appearance of uneven functions of $v_{1,2,3}$ in (51), however, makes the Compton line slightly asymmetrical. Furthermore, it changes the position of the maximum intensity and we are particularly interested in this maximum position, in order to compare it with the empirical results.[5]

Since this maximum will occur for very small values of the variables $v_{1,2,3}$ in (51) it is sufficient to consider in the bracket $\{\}$ in (51) only the terms, linear and quadratic in $v_{1,2,3}$. Near the maximum the bracket becomes

$$Y=\frac{N_1}{\alpha_1}\left[1-3v_1^2+\frac{36}{5}\beta_1v_1\right]+\frac{4N_2}{\alpha_2}\left[\frac{2}{5}-3v_2^2+\frac{61}{10}\beta_2v_2\right]+\frac{4N_3}{5\alpha_3}\left[1-\frac{85}{48}\beta_3v_3\right]. \quad (59)$$

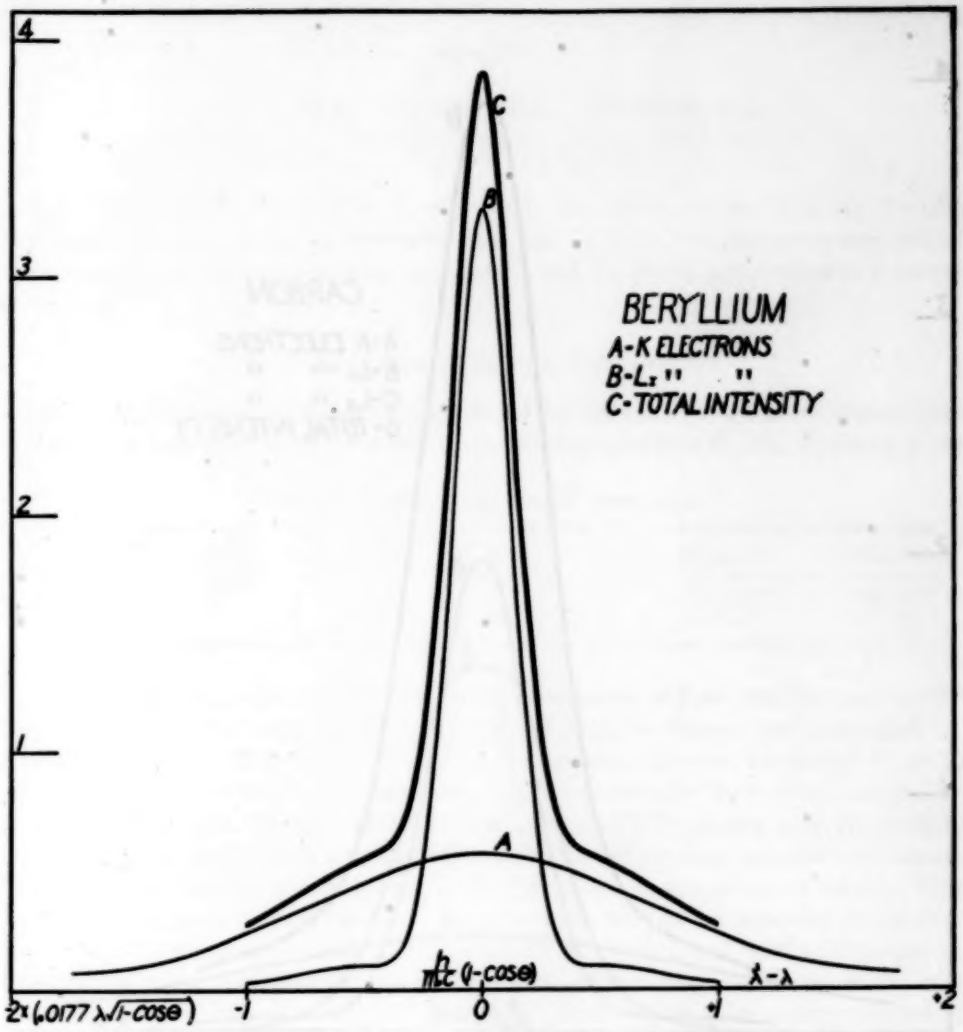

FIG. 1. Intensity-distribution in the Compton-line of beryllium, neglecting all higher order effects, causing asymmetry and defect of the shift. The ordinates are plotted in arbitrary units, the abscissae measure the difference of the wave-length λ' and λ of the scattered and incident radiation, respectively, in units $0.0177\,\lambda(1-\cos\theta)^{\frac{1}{2}}$, θ being the angle between the direction of the incident and scattered radiation. The scale of the abscissae is chosen such that at the origin $\lambda'=\lambda+(h/mc_0)\times(1-\cos\theta)$. The binding energies are assumed to be for the K-electrons, 122 v; for the L_1 electron, 9.5 v.

It is interesting to notice that the third term in (59) does *not* contain v_3^2, the intensity curve for p-electrons near the maximum following a fourth power law.

In order to determine the maximum of Y and therefore of the intensity in the λ-scale, we calculate

$$\frac{\partial Y}{\partial\delta}=\frac{\partial Y}{\partial v_1}\frac{\partial v_1}{\partial\delta}+\frac{\partial Y}{\partial v_2}\frac{\partial v_2}{\partial\delta}+\frac{\partial Y}{\partial v_3}\frac{\partial v_3}{\partial\delta}$$

or, according to (54), (58) and (59)

$$4\Delta k\frac{\partial Y}{\partial\delta}=\frac{N_1}{\gamma_1^2}\left[-\frac{3}{\gamma_1}(\delta+\gamma_1^2)+\frac{18}{5}\gamma_1\right]+\frac{4N_2}{\gamma_2^2}\left[-\frac{3}{\gamma_2}(\delta+\gamma_2^2)+\frac{61}{10}\gamma_2\right]-\frac{17}{12}\frac{N_3}{\gamma_3}.$$

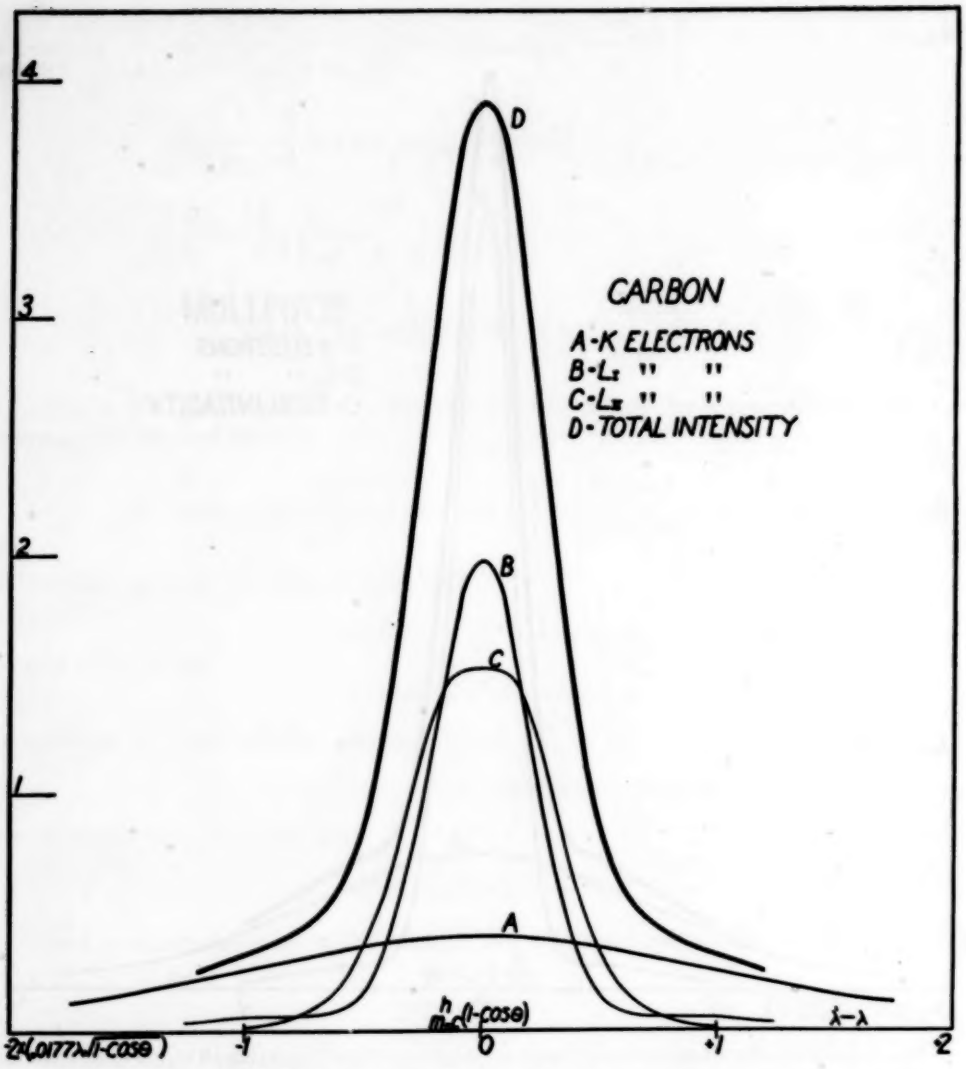

FIG. 2. Intensity distribution in the Compton-line of carbon under the same approximations and in the same scale as in Fig. 1. The binding-energies are assumed to be for the K-electrons, 285 v; for the L_{I}-electrons, 24.9 v; for the L_{II}-electrons, 11 v.

This expression vanishes for

$$\delta=\frac{1}{15}\frac{3N_1/\gamma_1+62N_2/\gamma_2-(85/12)N_3/\gamma_3}{N_1/\gamma_1^3+4N_2/\gamma_2^3}. \tag{60}$$

Using finally (53), (54), (55), (27) and (57), we find for the position of the maximum intensity in the λ scale:

$$\lambda'=\lambda+\frac{h}{m_0c}(1-\cos\theta)-\frac{\lambda^2}{hc}\frac{1}{15}\frac{3N_1/\sqrt{E_1}+62N_2/\sqrt{E_2}-(85/12)N_3/\sqrt{E_3}}{N_1/\sqrt{E_1^3}+4N_2/\sqrt{E_2^3}}. \tag{61}$$

We see that the defect of the Compton shift

$$\delta\lambda=\lambda-\lambda'+(h/m_0c)(1-\cos\theta),$$

as expected from formula (2) has indeed the form

$$\delta\lambda = D\lambda^2 \tag{62}$$

with

$$D = \frac{1}{15hc}\,\frac{3N_1/\sqrt{E_1}+62N_2/\sqrt{E_2}-(85/12)N_3/\sqrt{E_3}}{N_1/\sqrt{E_1^3}+4N_2/\sqrt{E_2^3}}. \tag{63}$$

For the case of H and He, where $N_2=N_3=0$, D can be written in the form (4) $D=\kappa E_1/hc$ with $\kappa=3/5$. For higher atomic numbers, however, one has to treat the complete expression (63), D depending essentially on both the binding energies E_2 and E_3 of the L-electrons in a rather complicated way.

5. Comparison with the Experiment

Table I shows the numerical values of $\delta\lambda$, calculated for Be and C and the corresponding observed values for a primary radiation with $\lambda=0.631$A, the binding energies E_1, E_2, E_3 being given in elec-

Table I. *Theoretical and observed values of* $\delta\lambda$.

	N_1	N_2	N_3	E_1	E_2	E_3	$\delta\lambda_{\text{theor.}}$(A)	$\delta\lambda_{\text{obs.}}$(A)
Be	2	2	0	122	9.5	—	2.8×10^{-4}	2.3×10^{-4}
C	2	2	2	285	24.9	11	6.5×10^{-4}	5.9×10^{-4}

tron-volts. The values $\delta\lambda_{\text{obs.}}$ are taken from the preceding paper of Ross and Kirkpatrick. The dotted lines in their Fig. 4 show the Compton shift as expected from the theory here presented.

One will notice that in both cases of Be and C, the theoretical value lies about 10 to 20 percent higher than the measured value. It does not seem surprising that the theory here proposed will tend to give too high values of $\delta\lambda$. Indeed, with formulae (60) and (61), $\delta\lambda$ has been computed by using the binding energies, as given from spectroscopic data. These binding energies are meant as being the energies needed for removing a specified electron from its atomic orbit to infinity. However, in the solid state, the electrons ejected by the Compton-recoil will not be removed to infinity but into the neighborhood of other atoms in the crystal lattice, a fact which will tend to decrease the "effective binding energy" and therefore $\delta\lambda$. An approximate way of correcting our result might be to subtract from the binding-energies the electronic work function, i.e., the energy needed to bring a conduction electron from the interior of the crystal to infinity, which would account for the sign and the order of magnitude of the correction. We need not say, however, that a more accurate consideration of the forces, due to the interaction of different atoms in the lattice, would require much more elaborate calculations than we intended to give here.

Structure and Width of the L_{III} Absorption Limits of Tantalum, Tungsten and Gold

HENRY SEMAT, *Physics Laboratory, Columbia University*

(Received June 13, 1934)

The double crystal spectrometer was used to investigate the structure and widths of the L_{III} absorption limits of the elements Ta, W and Au, in the free metal and in compounds. Curves of these absorption limits are presented. Tables are given of the measured values of the wave-lengths and of the widths of these limits, and also the relative displacement of these limits in compounds. The widths, in volts, of the L_{III} absorption limits increase with atomic number. There is a decrease in absorption on the short wave-length side of the main edge for these elements corresponding to an absorption line on the short wave-length side of the main edge. Evidence is given to support the hypothesis that x-ray energy levels have definite energy widths.

THE double x-ray spectrometer has been used recently by Barnes,[1] Ross,[2] and Richtmyer and Barnes,[3] for investigating the structure and width of the K absorption limits, and by Hull,[4] for the L_{II} and L_{III} absorption limits of mercury. The single crystal spectrograph has been used for studying the secondary structure on the short wave-length side of the main K and L edges. In particular, Hanawalt[5] has examined the secondary structure of the L_{III} absorption limits of xenon and mercury, and Coster and Veldkamp[6] have examined the secondary structure of the L_{III} limits of gold and platinum.

In the present work, the double x-ray spectrometer was used to investigate the structure and widths of the L_{III} absorption limits of the elements tantalum (73), tungsten (74), and gold (79), and also the structure and relative positions of these limits in chemical compounds containing these elements. The compounds used were Ta_2O_5, K_2TaF_7, H_2WO_4, Au_2O_3 and $KAu(CN)_2$.

Apparatus and Experimental Procedure

The double x-ray spectrometer used in this investigation is identical with that used by Hull[4] and described by Davis and Purks.[7] The ionization current was amplified by an FP–54 pliotron, and read on a Leeds and Northrup Type R galvanometer. Methyl bromide at atmospheric pressure was used in the ionization chamber.

The x-ray tube used in the investigation of the L_{III} limits of tantalum and gold had a standard tungsten target; the filament was made of 10 mil tungsten wire wound in the form of a helix about 7 mm long and 1 mm in diameter. The filament was mounted in a cylindrical cathode made of molybdenum. This type of filament construction gives a large focal spot approximately rectangular in shape, and is well adapted for work with the double x-ray spectrometer. A tungsten x-ray tube could not be used in the study of the L_{III} absorption limit of tungsten because the strong $WL\beta_5$ line is present at about the position of the main edge. Instead, a tube with a gold target and a tantalum filament was used in the investigation of this tungsten absorption limit. The x-ray tubes were generally operated at 40–50 m.a. and 30 kv.

All the substances used in this investigation were in powder form except the free metal gold. Thin absorbing screens of each substance were made by dusting the powder through heavy silk or cotton cloth on to thin paper moistened with castor oil. The gold absorbing screen was made of sheets of gold leaf. Screens of various thicknesses were tried, and the ones finally used were those which gave maximum contrast in transmitted energy on the short and long wave-length sides of the absorption limit. The screens were placed before the first crystal, and were oscillated several times per second in horizontal guides perpendicular to the x-ray beam to smooth out any effects due to the non-uniformities in the screens.

[1] A. H. Barnes, Phys. Rev. **44**, 141 (1933).
[2] P. A. Ross, Phys. Rev. **44**, 977 (1933).
[3] F. K. Richtmyer and S. W. Barnes, Science **77**, 459 (1933).
[4] H. L. Hull, Phys. Rev. **40**, 676 (1932).
[5] J. D. Hanawalt, Phys. Rev. **37**, 715 (1931).
[6] D. Coster and J. Veldkamp, Zeits. f. Physik **74**, 191 (1932).
[7] Bergen Davis and H. Purks, Proc. Nat. Acad. Sci. **13**, 419 (1927).

The procedure in obtaining the curves was as follows: for any given wave-length, as determined by the position of the second crystal, three readings of the ionization current were taken without an absorbing screen, then three readings were taken with an absorbing screen in place. Corrections could then be made for any variations in the background energy. Each point on a curve represents the average of three such readings. Several curves were obtained for each substance investigated.

The positions of the L_{III} limits were determined with reference to neighboring lines in the L series of tungsten. The Ta limit was determined with reference to the β_1, β_2 and β_3 lines, the W limit with reference to the β_5, β_7 and β_{10} lines, and the Au limit with reference to the γ_2, γ_3 and γ_4 lines. The relative displacement of the L_{III} edge in a compound with respect to the edge in the free metal was determined by taking readings, at each setting of the second crystal, of the background energy, the energy transmitted through the free metal, and the energy transmitted through the compound.

Experimental Results

The structures and widths of the absorption limits of the substances investigated are shown in Figs. 1, 2 and 3. While these curves are the results of individual runs, they are typical of several curves obtained for each substance. The curves are plotted with transmitted energy as ordinates, and wave-lengths in X.U. as abscissae. The values of the abscissae in volts and in seconds of arc are also indicated on the graphs.

The width of the main absorption edge was measured by drawing a straight line tangent to the curve, and determining its intersections with the ordinates of maximum and minimum energy. (See Fig. 1.) Corrections to these observed widths due to the crystals, as calculated by means of the formula developed by Schwarzschild,[8] are negligible. The width of the rocking curve for the crystals in the (1, −1) position is 12 seconds of arc. The wave-length of the absorption limit is taken as that of the midpoint of the main edge. Table I gives the values of the wave-lengths of the absorption limits, and also their widths, in volts and in X-units. The values for Ta and Au are averaged from ten curves, the values for W from five curves. It will be noticed that the widths, in volts, of the L_{III} absorption limits of these elements increase with the atomic number. Fig. 4 shows that in the region of atomic numbers 74–80, these widths lie on a straight line. The width of the L_{III} edge of Hg (80) is that obtained by Hull.[4]

Table I. L_{III} *absorption limits.*

Atomic number	Element	Wave-length (X-units)	Width of absorption edge (volts)	(X-units)
73	Ta	1252.9±0.2	10.8±1.0	1.36±0.13
74	W	1213.4±0.1	11.6±0.5	1.41±0.06
79	Au	1037.8±0.2	14.6±0.7	1.21±0.06

The curves for tantalum and tungsten show certain similarities. In particular there is a slight decrease in absorption for the free metals on the short wave-length side of the main edge. This corresponds to an absorption line on the short wave-length side of the absorption edge. Sandstrom[9] using the single crystal photographic method, shows a microphotometer curve of the tungsten L_{III} edge which exhibits this same effect. This decrease in absorption on the short wave-length side becomes much more pronounced in the compounds containing these elements. Furthermore, the main edges of these elements in the compounds investigated are all displaced towards the short wave-length side with respect to the main edge of the free metal. It is interesting to note that both of these elements belong to the group in which an inner level, the $O_{IV, V}$ or $5d$ level is not filled.

Fig. 3 shows that the shape of the L_{III} edge of gold is different from that of Ta and W. While the curve for gold also shows an absorption line on the short wave-length side of the absorption limit, it differs from the curves for Ta and W in that the absorption begins to increase at about 17 volts from the center of the main edge and reaches a maximum value about 26 volts from the main edge. Furthermore, the displacement of the edge in a compound is very small; in the case of AuO_3 it is negative, that is, towards longer wave-lengths, and in the case of $KAu(CN)_2$ it is practically zero within the limits of

[8] M. Schwarzschild, Phys. Rev. **32**, 162 (1928).

[9] A. Sandstrom, Zeits. f. Physik **66**, 784 (1930).

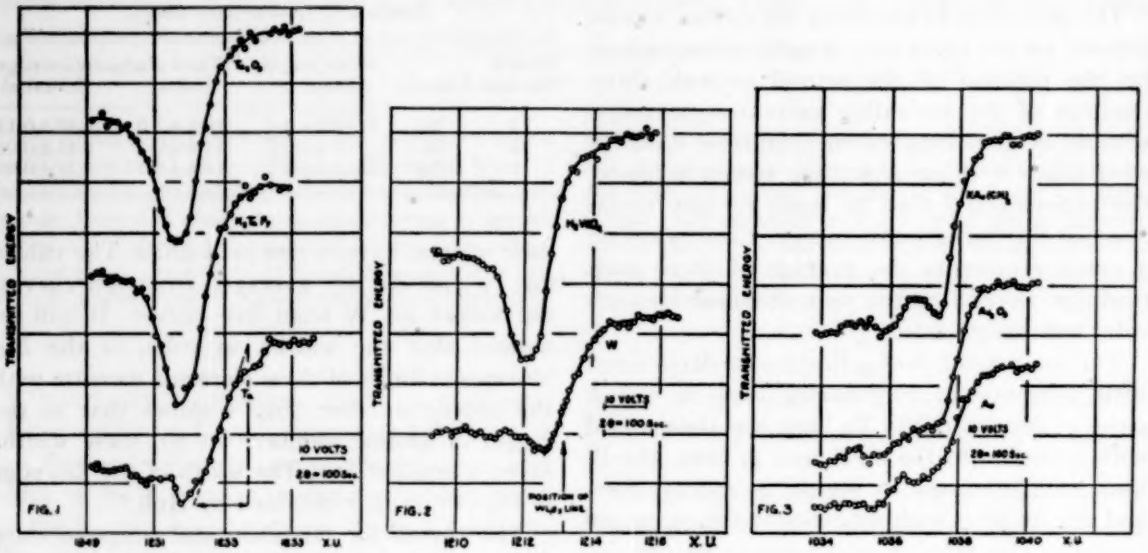

FIG. 1. FIG. 2. FIG. 3.

FIG. 1. Tantalum L_{III} absorption limit in the free metal and in compounds.
FIG. 2. Tungsten L_{III} absorption limit in the free metal and in a compound.
FIG. 3. Gold L_{III} absorption limit in the free metal and in compounds.

experimental error. It is interesting to note that gold is the first element in which the 5*d* level is complete as shown by Allison[10] in his investigation of the intensity ratio of the $L\beta_5$ line to the $L\beta_1$ line for the elements from atomic number 74 to 83. (See Table II.)

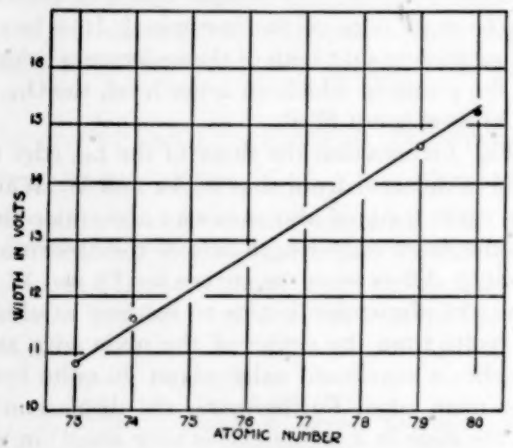

FIG. 4. Width of L_{III} absorption limit plotted against atomic number.

TABLE II. *Displacement of the L_{III} edges in compounds relative to the edges in the free metal.*

Element	Compound	Relative displacement in volts
Ta	Ta_2O_5	3.8 ± 0.2
	K_2TaF_7	3.6 ± 0.3
W	H_2WO_4	4.8 ± 0.4
Au	Au_2O_3	-1.4 ± 0.7
	$KAu(CN)_2$	0

DISCUSSION

Tables of wave-lengths of absorption limits usually give several different values for the same limit for a single element. Frequently this is due to the fact that compounds were used in determining the wave-length of the absorption limit. Nishina[11] measured the wave-lengths of the L_{III} absorption limits of Ta and W using Ta_2O_5 and WO_3, respectively, and obtained values smaller than those given in Table I. This is in agreement with the result that the edges of these compounds are displaced towards shorter wave-lengths.

[10] S. K. Allison, Phys. Rev. **34**, 7 (1929).

[11] Y. Nishina, Phil. Mag. **49**, 521 (1925).

A comparison of the data on the widths of the K and L absorption limits of the same element leads to the conclusion that x-ray energy levels are of finite energy width. For example, Richtmyer and Barnes[3] found the width of the K limit of tungsten to be 133 volts, and that of gold to be 160 volts. These values are more than ten times the widths of the L_{III} limits of the corresponding elements. Since the process of absorption consists essentially in the removal of an electron from an inner x-ray level to one of the optical levels or completely outside the atom, the difference between the widths of the K and L_{III} absorption limits must be due to the difference in the widths of the K and L_{III} energy levels themselves.

Let us assume that the width of the main absorption limit is due to two terms, (1) the energy width of the x-ray level from which the electron is removed, and (2) the energy width of the combined optical levels to which the electron may be raised. Thus, if A represents the width of the K level, and B the width of the L_{III} level, and C the width of the combined optical levels, then the width of the main K absorption limit is $A+C$, and the width of the L_{III} absorption limit is $B+C$. The magnitude of C for an element of atomic number Z may be taken as the ionization potential of the element of atomic number $Z+1$. In accordance with the conclusions of Weisskopf[12] and Weisskopf and Wigner,[13] an x-ray spectral line should be the sum of the widths of the energy levels involved in the transition. Thus the width of the K line should be $A+B$, since this line is due to a transition from the L_{III} level to the K level. The magnitude of B is of the order of a few volts, of the same order of magnitude as C. Hence the width of the $K\alpha_1$ line should be approximately equal to the width of the K limit for any one element. Furthermore, the width of the $K\alpha_1$ line and the width of the K absorption limit should vary in a similar manner with atomic number.

It must be emphasized that the method used in measuring the width of an absorption limit is entirely arbitrary. It might also be noted that the width of an absorption limit is not necessarily the width of an atomic energy level. For a comparison of the widths of absorption limits and of lines, the recent data of Ross[2] on the K absorption limits and Allison's[14] data on the widths of the $K\alpha_1$ lines for the same elements may be used. We get good quantitative agreement if we compare twice the width at half maximum of a $K\alpha_1$ line with the measured width of the K absorption limit of the same element. Zinn [15] presents a curve giving the width of the K absorption limit as a function of atomic number and shows that above atomic number 32, the width of the K absorption limit increases as the fourth power of the atomic number, while for elements of lower atomic number the widths are practically constant. The curve given by Allison[14] for the width of the $K\alpha_1$ line as a function of atomic number is very similar to that given by Zinn,[15] and follows a fourth power law for atomic numbers greater than 32. The fact that the widths of the K absorption limits all have practically the same value for elements below atomic number 32 is to be expected on the basis of the above assumption since the width of an absorption edge cannot be less than C. In a similar manner the widths of the L_{III} absorption limits should reach a limiting value for elements below atomic number 73.

The writer is indebted to Professor Bergen Davis for having suggested this investigation, and for his continued interest and encouragement throughout the progress of this work.

[12] V. Weisskopf, Ann. d. Physik **9**, 23 (1931).
[13] V. Weisskopf and E. Wigner, Zeits. f. Physik **63**, 54 (1930).
[14] S. K. Allison, Phys. Rev. **44**, 63 (1933).
[15] W. H. Zinn, Phys. Rev. **46**, 659 (1934).

The Dispersion of the Electro-Optical Kerr Effect in Carbon Dioxide

GILFORD G. QUARLES, *University of Virginia*

(Received August 16, 1934)

The dispersion of the electro-optical Kerr effect in CO_2 has been studied from 4000A to 7500A. The results are in better agreement with the Langevin-Born theory than with that of Havelock. An absolute value of the Kerr constant B for CO_2 has been determined. This is $(0.249 \pm 0.003) \times 10^{-10}$ for a temperature of 17.5°C, a wave-length of 5890A and a pressure of one atmosphere.

THE dispersion of the electro-optical Kerr effect in liquids has been studied by a number of investigators,[1] but data on gases are very meager. Yet the conditions upon which the theoretical discussions are based can be realized more nearly in gases and vapors. The variation of the Kerr effect with wave-length from 4000A to 7500A has been studied in CO_2. The method and results are given in this paper, together with a comparison with theory. An absolute value of the Kerr constant for CO_2 also has been determined.

There are three theoretical formulas which may be used in a study of the dispersion of the electro-optical Kerr effect. The first of these is the Havelock[2] equation

$$B = C_1(n^2-1)^2/n\lambda \qquad (1)$$

in which B is the Kerr constant, n the index of refraction, λ the wave-length of the light, and C_1 a constant. According to the Langevin-Born[3] theory of the Kerr effect, B is given by

$$B = C_2(n^2-1)(n^2+2)/n\lambda, \qquad (2)$$

C_2 being a constant. Quantum-mechanical treatment by Serber[4] merely adds to this expression a correction term.

Szivessy[5] has compared experiment with the first of these equations and finds agreement within the limits of the precision of his data.

Experimental Method

The experiments were performed by using a modification of the method developed by Beams and Stevenson,[6] and improved by Bruce.[7] The Kerr cell containing the gas being studied was the same as that used by Bruce[7] in his later experiments. The optical arrangement was the same except for the use of a monochromator. A caesium oxide photoelectric tube was used for measuring the intensity of the light beams. This tube is a Westinghouse type SR-50 vacuum tube (obtained through the courtesy of Drs. E. D. Wilson and D. D. Knowles) having the base removed and the cavity in the bottom of the tube filled with special insulating wax, with a grounded guard ring around one terminal. The current from this cell was passed through a high resistance (10^{11} ohms) and the resultant voltage drop impressed on the control grid of an FP-54 pliotron operating in a circuit similar to that of DuBridge and Brown.[8]

The high potential was obtained by rectifying the output of an x-ray transformer and measured with a Wulf[9] electrometer reading to 50,000 ± 0.5 percent volts. Any existing ripple in the voltage was too small to be detected. The gas pressures were measured by a Bourdon goose neck spring gauge, calibrated against a dead weight piston gauge, the zero of the goose neck gauge being checked for each set of measurements. The temperature of the Kerr cell was held at 35.0°C in a thermostat.

The gas was from a commercial cylinder. It gave a negative test for sulfides and sulfites, and

[1] For general references see Beams, Rev. Mod. Phys. **4**, 133 (1932); Szivessy, Handb. d. Physik **21**, 724–884, J. Springer (1929); see also Ingersoll and Winch, Phys. Rev. **44**, 399 (1933).

[2] Havelock, Proc. Roy. Soc. **A80**, 28 (1907); **A84**, 492 (1911); Phys. Rev. **28**, 136 (1909).

[3] Langevin, Le radium **7**, 249 (1910); Born, Ann. d. Physik **55**, 177 (1918).

[4] Serber, Phys. Rev. **43**, 1011 (1933).

[5] Szivessy, Zeits. f. Physik **26**, 326 (1924).

[6] Beams and Stevenson, Phys. Rev. **38**, 133 (1931).

[7] Bruce, Phys. Rev. **44**, 689 (1933).

[8] DuBridge and Brown, R. S. I. **4**, 532 (1933).

[9] Wulf, Phys. Zeits. **31**, 315, 1030 (1930).

showed 0.22 percent gaseous impurities. A correction was made to the pressure for this. The gas was passed over P_2O_5 and through a cotton wool filter.

The wave-length bands were checked with a constant deviation spectroscope, observing the beams as they emerged from the Kerr cell. The bands were between 175A and 250A wide.

Results

The results of a typical run at a density of 0.1335 g/cc are shown graphically in Fig. 1, the reciprocal of the Kerr constant B being plotted to an arbitrary scale against the wave-length in Angstrom units. Two theoretical curves are shown, the dotted one being from the Langevin-Born equation, and the dashed one from the Havelock equation. The experimental points are shown by circles. The scales of the ordinates are adjusted so that the curves agree at one point. It seems that the experimental points agree slightly better with the Langevin-Born equation than with the other. This is shown more clearly in Table I in which are listed the data plotted in the figure, together with the squares of the differences between the theoretical and experimental values. The sum of these squares is seen to be much larger for the Havelock equation than for that of Langevin-Born, indicating better agreement with the latter. The precision of the data is hardly high enough to justify an attempt to compute the correction term in Serber's equation. Values of n used in these calculations were obtained from Phillips'[10] data.

TABLE I. *Values of reciprocal of the Kerr constant.*

Wave-length	1/B Exp.	1/B Havelock	1/B Langevin-Born	Square of residuals Havelock, Exp.	Square of residuals Langevin-Born, Exp.
4000A	221	213	214	64	49
5000	268	269	269	1	1
5000	270	269	269	1	1
6500	352	356	354	16	4
6500	349	356	354	49	25
7000	381	385	381	16	0
7000	385	385	381	0	16
7500	410	415	409	25	1
Sum of squares of residuals				172	97

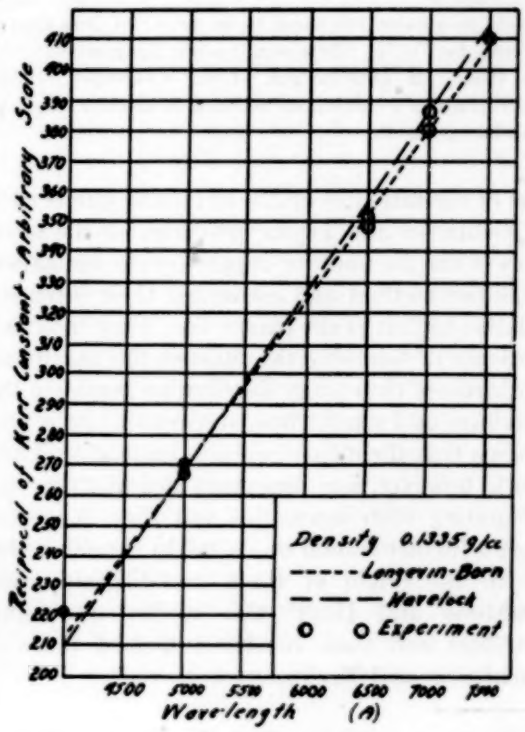

FIG. 1.

Many such sets of data have been taken at densities ranging from 0.1 g/cc to 0.2 g/cc with different groups of wave-lengths, and the value of C_2 in Eq. (2) has been computed for each measurement. The deviation of the mean of this quantity for the individual runs is about ½ percent.

In order to compare the data obtained for different pressures, it is necessary to re-write Eq. (2) to involve the dielectric constant ϵ which depends on the density, giving

$$B = C_2 \frac{(n^2-1)(n^2+2)(\epsilon+2)^2}{n\lambda}. \qquad (3)$$

The values of ϵ used were obtained from Keyes and Kirkwood.[11] The quantity C_2 was computed from this equation for each of the measurements. Each set is consistent to within about ½ percent, but the values of C_2 differ among them by much larger percentages than over any one set. This is probably due to some undiscovered systematic error which affects absolute but not relative

[10] Phillips, Proc. Roy. Soc. **A97**, 225 (1920).
[11] Keyes and Kirkwood, Phys. Rev. **36**, 754 (1930).

values. However, the mean of all the values of C_3 is $(5.70\pm0.06)\times10^{-14}$.

This value of C_3 can be used in Eq. (3) to compute an absolute value of the Kerr constant for any experimental conditions desired. The value of B computed for a wave-length of 5890A, a temperature of 17.5°C and a pressure of one atmosphere is $0.249\pm0.003\times10^{-10}$. The experimental value obtained by Szivessy[6] is 0.24×10^{-10}, while Bruce's[7] preliminary measurements yielded 0.28×10^{-10}. The value of B computed from a relation between the Kerr constant and the light scattering coefficient Δ[12] is 0.29×10^{-10} with Parthasarathy's[13] value of Δ. In view of the difference in the value of this quantity as obtained by different observers, the agreement between experimental and theoretical values of B may be said to be fair.

ACKNOWLEDGMENTS

The author wishes to express appreciation to Dr. J. W. Beams under whose direction this work was done, to Dr. L. G. Hoxton for assistance in the preparation of the manuscript and to the other members of the laboratory staff for the interest which they have shown in the work.

[12] See Brigleb and Wolf, Forts. der Ch., Phys. u. Phys. Ch. **21**, 155 (1931).

[13] Parthasarathy, Ind. J. Phys. **7**, 148 (1932).

OCTOBER 15, 1934 PHYSICAL REVIEW VOLUME 46

Intensities of Satellites of $L\beta_2$

ANNA W. PEARSALL, *Cornell University*

(Received August 17, 1934)

By use of the Siegbahn x-ray spectrograph, the intensities, relative to the parent line, of the satellites of the x-ray line $L\beta_2$, have been studied in the atomic number range $40<Z<53$, inclusive. The "integrated intensity" (total area of satellite structure, comprising four lines) is about 4 percent of that of $L\beta_2$ for Cb(41); rises to a maximum of 52 percent for Ag(47); and then drops rapidly to a value too small to be measured (less than 1 percent) for Te(52). These results are in disagreement with the theory of Druyvesteyn (Diss., Groningen, 1928), which predicts a continuous decrease in satellite intensity with increasing Z.

ALTHOUGH numerous experimenters have reported the presence of "satellites"—those fainter lines on the short wave-length side of the diagram lines in the x-ray spectrum—there has been little study of them other than determinations of wave-length. Data on wave-lengths are to be found in Siegbahn's *Spektroskopie der Röntgenstrahlen*. R. D. Richtmyer[1] in studying the satellites of the $L\beta_2$ line observed that they are not found above atomic number 53. He noted qualitatively that there was a rapid variation in their intensity with a change in atomic number. Later Richtmyer and Kaufman[2] found that the satellites of this line appear again at about atomic number 73. Coster[3] reported the reappearance of one of the satellites of $L\beta_2$ at atomic number 68.

Richtmyer and Taylor[4] investigated the satellites of the $L\alpha$ lines for copper by the ionization chamber method and estimated their intensity relative to that of the parent line. They took as a measure of intensity the ratio of the maximum ordinates of the energy distribution curves of the satellites and parent line, respectively; it is now known that the ratio of areas is preferable. Their work, however, was important as a first attempt at getting such intensities and they suggested that a further similar study might furnish a clue as to the origin of these non-diagram lines. DuMond and Hoyt[5] also studied the same satellites and their results confirmed those of Richtmyer and Taylor.

[1] R. D. Richtmyer, Phys. Rev. **38**, 1802 (1931).
[2] Richtmyer and Kaufman, Phys. Rev. **44**, 605 (1933).
[3] Coster, Phil. Mag. **43**, 1070 (1922).
[4] Richtmyer and Taylor, Phys. Rev. **36**, 1044 (1930).
[5] DuMond and Hoyt, Phys. Rev. **36**, 1702 (1930).

A theory was advanced by Wentzel[6] that these lines originate in a single-electron transition between doubly ionized states. Druyvesteyn[7] assumed for the several satellites he studied, the double ionization states according to Wentzel's theory and from this theory, determined satisfactorily the wave-lengths of satellites of $L\beta_1$ and $L\beta_2$. But the theory did not apply well to those of $L\alpha$. He also derived a formula for the probability of such double ionizations. Since his equation for wave-lengths checked roughly with his observations, it might be expected that the second formula, based on the same classical assumptions, would also fit experimental data.

Richtmyer[8] has proposed as an alternative theory, a two-electron transition between doubly ionized states. This hypothesis is sometimes called the "double jump" theory of satellite origin.

It was with the hope that a knowledge of intensities would help to make clear the origin of these lines that the present work was undertaken. A study was made of the $L\beta_2$ line and its satellites for elements in the atomic number range 40 to 53 inclusive and the ratio of the intensities of the satellites to that of the parent line was obtained. Stated briefly, the results are that a marked variation in relative intensity occurs with change in atomic number. Beginning at $Z=40$, there is an increase up to a maximum for atomic number 47 and then a rapid decrease until the satellites disappear entirely at $Z=53$. The results do not even roughly agree with values of relative intensities computed from Druyvesteyn's formula.

A series of thirteen x-ray plates was made with a Siegbahn vacuum spectrograph with a calcite crystal. Elements from zirconium, atomic number 40, to iodine, 53 (except 43) were studied. Wherever possible the element in metallic form was used on the removable anti-cathode. In a few cases, a powdered form of the element was rubbed or pounded into the roughened copper wedge of the target. The tube was run at a voltage approximately five times that necessary for the excitation of the parent line. Tube current and time of exposure were varied so as to produce a plate in which the maximum photographic density was in the range 0.3 to 0.5 since below that density, intensities are proportional to photographic density which is defined by the relation: Density$=\log(1/T)$ where T is the transmission of the plate. Microphotometer records were made from each plate and these

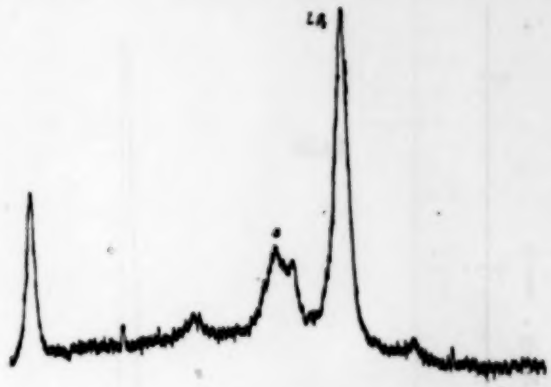

FIG. 1. Microphotometer record of $L\beta_2$ for Ag(47) showing the satellite structure at S.

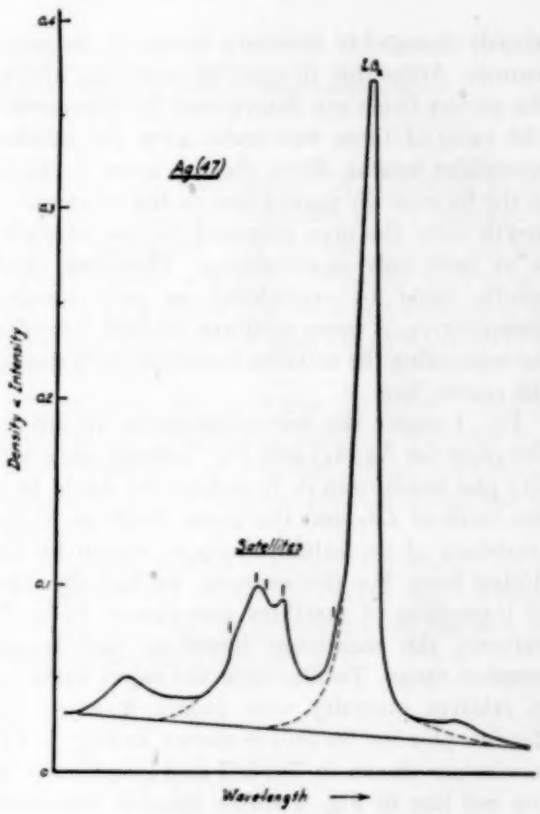

FIG. 2. Density plot for Ag(47).

[6] Wentzel, Ann. d. Physik **66**, 437 (1921).
[7] Druyvesteyn, Dissertation, Groningen, 1928.
[8] Richtmyer, Phil. Mag. **6**, 64 (1928).

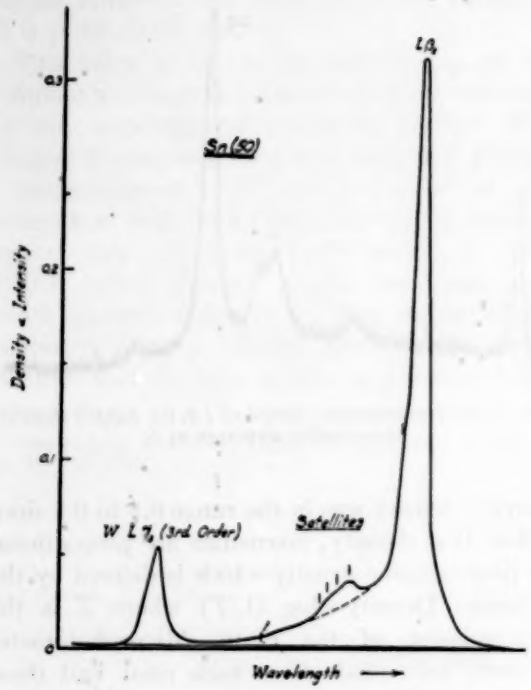

FIG. 3. Density plot for Sn(50).

records changed to intensity curves in the usual manner. Areas due to satellite structure and to the parent line were determined by planimeter. The ratio of these two areas gave the relative intensities sought. Since there is some doubt as to the form of the parent line on the short wavelength side, the area assumed for the satellites is at best only approximate. Therefore these results must be considered as only roughly quantitative. A more accurate method is needed for separating the satellite structure from that of the parent line.

Fig. 1 shows the microphotometer record for the plate for Ag (47) and Fig. 2 shows the intensity plot made from it. Note here the doubt as to the form of $L\beta_2$ and the guess made as to the boundary of the satellite area as shown by the dotted lines. For this element, we find the ratio of intensities of satellites and parent to be 52 percent, the maximum found in this atomic number range. To illustrate the rapid variation in relative intensity with atomic number, the density plot for Sn (50) is shown in Fig. 3. The results are shown in Table I and graphically by the full line in Fig. 4 where relative intensities are plotted against atomic number. The curve begins at about 5 percent for atomic number 40, rises gradually to a maximum in the vicinity of atomic number 47, then drops rapidly toward zero for atomic number 53.

Druyvesteyn's formula for the relative probability N_{LM}' of double (LM) to single (L) ionizations is:

$$N_{LM}' = An_M(Z-\alpha_M)^2/(Z-\gamma_M)^4, \qquad (1)$$

where Z is the atomic number; γ_M is the total screening constant; α_M is the inner screening constant; n_M is the number of electrons in the M shell; A is a constant which depends upon the relative energies of the L and M ionized states and the initial energy of the cathode-ray electron as it strikes the target. To obtain the relative intensity R of satellites to parent line for a given element, the above ionization ratio should be corrected for the ratio P of probabilities of transitions between singly and doubly ionized states respectively. R is given by

$$R = PAn_M(Z-\alpha_M)^2/(Z-\gamma_M)^4. \qquad (2)$$

Assuming that P does not vary rapidly from one element to another and that therefore to a first approximation it may be assumed constant, the value of PA was determined by using the observed value of R for Ag(47). The values of R for the other elements were then determined for the two cases where $\alpha_M = 10$ and $\alpha_M = 20$. Values of γ_M were taken from a curve in Pauling and Goudsmit.[9] The computed values of relative intensities are shown by the dotted lines in Fig. 4. It is readily seen that for no values of α_M do

TABLE I. *Values of ratio of intensities of satellite to parent line.*

Atomic number	Relative Intensities observed	computed for $\alpha_M = 10$	$\alpha_M = 20$
40	7.4%	151.0%	126.0%
41	4.3	126.0	108.5
42	11.2	107.0	94.0
44	26.8	78.0	73.0
45	32.8	67.7	64.5
46	46.9	59.1	57.8
47	52.2	52.2	52.2
48	13.2	45.2	46.1
49	8.9	40.6	42.2
50	3.5	36.6	38.5
51	2.8	32.9	35.1
52	—	29.6	32.5
53	0.0	27.1	29.9

[9] Pauling and Goudsmit, *Structure of Line Spectra*, p. 187.

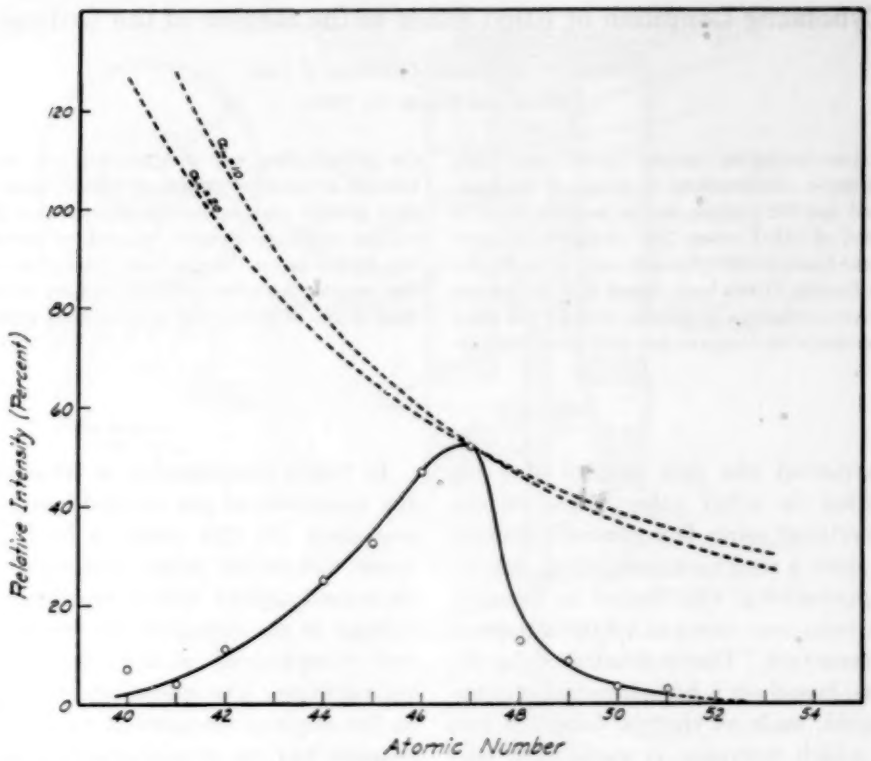

FIG. 4. Variation in intensities of satellites of $L\beta_2$ with atomic number (solid line). The dotted lines show relative intensities computed by Eq. (2). The arbitrary determination of the constant PA by use of the data for Ag(47) yields values of relative intensities many times greater than those predicted by Druyvesteyn's formula.

the theoretical curves even roughly coincide with the form of the observed curve. Obviously Eq. (2) does not even approximately agree with experimental facts.

In further disagreement with Eq. (2) is the work of Richtmyer and Barnes[10] who find the intensity of satellites of $L\beta_2$ for Au(79) to be 6.0 percent relative to that of $L\beta_2$. Eq. (2) predicts only a gradual decrease in relative intensity with increasing atomic number. It does not provide for the reappearance of the satellites and their increasing intensity in the high atomic number range. Similar facts have been observed for the satellites of $L\alpha$. Hirsh and Richtmyer[11] found a curve of intensities for $L\alpha$ similar to that in Fig. 4, with a maximum of 70 percent for $Z=45$. Richtmyer and Barnes[10] report the relative intensities of satellites of $L\alpha$ for Au(79) to be 5.0 percent. In each case the disappearance of the satellites is coincident with the completion of an electron shell.

Seemingly, the addition of outer electrons profoundly influences the production of satellites. At the present time however, there is no theory of satellite origin that can account for all the observed facts.

The writer wishes to express her sincere appreciation for the valuable advice and criticism given by Dr. F. K. Richtmyer during the progress of this research.

[10] Richtmyer and Barnes, Phys. Rev. **46**, 352 (1934).
[11] Hirsh and Richtmyer, Phys. Rev. **44**, 955 (1933).

The Cybotactic Condition of Ethyl Ether in the Region of the Critical Point

ROSS D. SPANGLER, *University of Iowa*

(Received August 22, 1934)

X-ray diffraction-ionization current curves have been taken at thirty-seven combinations of values of pressure, temperature and specific volume in the neighborhood of the critical point of ethyl ether. The results have been interpreted on the basis of the cybotactic view of molecular organization in liquids. It has been found that the groups are very sensitive to changes in specific volume but show much less dependence on temperature and pressure; that the groups disappear at approximately the same specific volume at various values of temperature and pressure; that groups may appear in the gaseous state; and that beyond a certain specific volume no groups appear and the curves are of the gas type. Using the cybotactic view one secures a rather definite picture of what occurs in fluid in the neighborhood of its critical point.

NOLL[1] reported the first results of x-ray diffraction in ethyl ether when in the region of the critical point. It is generally known[2] that liquids show a structure simulating, but by no means approaching, that found in crystals. There are at least two views as to the nature of this "liquid structure." One is illustrated by the computations, based on a homogeneous conception of a liquid, such as that of Gingrich and Warren[3] to which reference is made in a succeeding paper. Another[4] is that the liquid is nonhomogeneous but, at any instant, there are enough molecules in groups, simulating crystalline structure, called cybotactic groups, to indicate this temporary and vacillating structure when investigated by x-rays. These groups do not have definite boundaries but are temporary regions of orderliness shading off into regions of little orderliness. The former view is quantitatively successful in matching the experimental curves. The latter view is not so easily subjected to mathematical treatment and is content to point out the simulation of crystal structure for which the theory is well known. Both views are approximate, the former adjusting the view to the theory then to be applied and the latter using the crystal theory already established as an approximate guide to an understanding as to what occurs within the liquid. It is the latter view which is used in this discussion.

In Noll's investigation of what takes place in the transition of gas to liquid only one pressure was used. At this pressure he found that the x-ray diffraction peaks indicative of structure decreased rapidly with temperature and specific volume in the region of the critical temperature and disappeared a few degrees above that temperature. The questions arising and serving as the origin of the present work were: (1) What relation has the critical temperature or either of the other critical constants to the disappearance of the liquid diffraction peaks? (2) What is the most effective single factor in the formation of cybotactic groups, pressure, specific volume, or temperature? (3) Is there any change in the diffraction effect as one goes from below to above the critical temperature if the specific volume remains the same?

EXPERIMENTAL

The major difficulties encountered were the uncorrected differential absorption by the aluminum container, sufficiently accurate temperature measurements, and uniform conditions in the ether specimen. The first difficulty was overcome by making use of double filters,[5] the second and third by modifications of the Noll apparatus.

The arrangement of the x-ray tube, of the Soller slits, and of the ionization chamber was like that previously used in this laboratory.[6] The detail of the apparatus, used to hold and

[1] W. Noll, Phys. Rev. **42**, 336 (1932).
[2] See papers by Stewart and co-workers, Phys. Rev. (1927–34); for a complete review of the literature see Debye, Ergebnisse der tech. Röntgenkunde **2**, 1 (1931).
[3] Gingrich and Warren, Phys. Rev. **45**, 292 (1933).
[4] See for instance, Stewart, J. Chem. Phys. **2**, 147 (1934).
[5] P. A. Ross, Phys. Rev. **21**, 426 (1926); J. O. S. A. **16**, 433 (1928).
[6] Stewart and Morrow, Phys. Rev. **30**, 232 (1927), and subsequent papers.

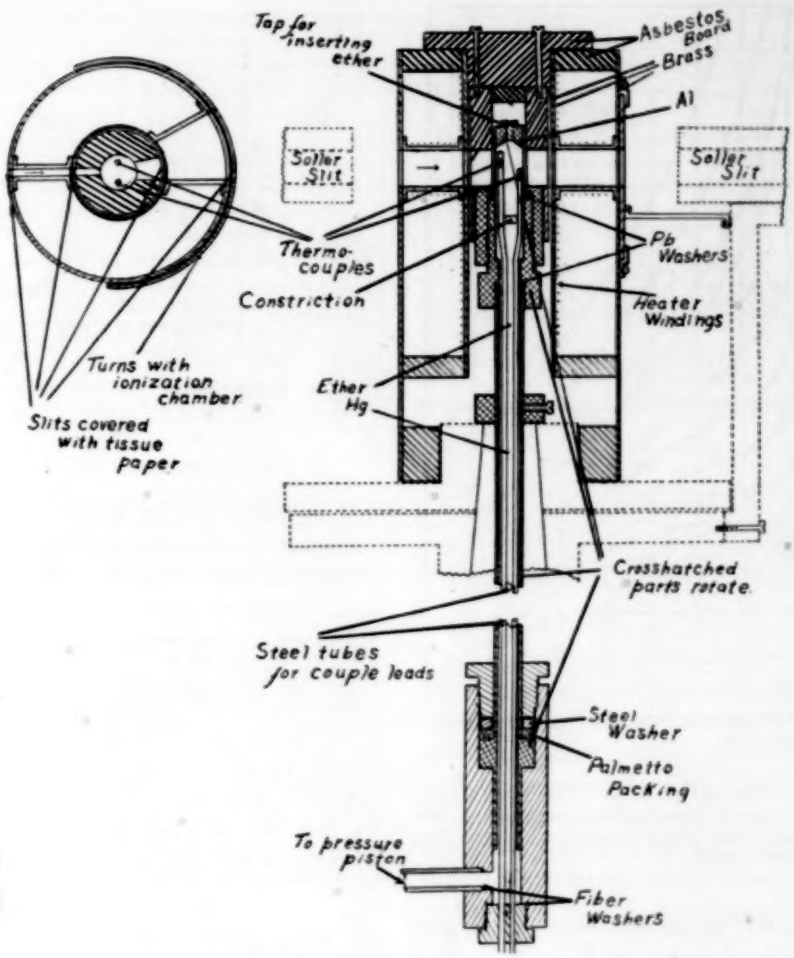

FIG. 1. Horizontal and longitudinal sections of apparatus used to heat and hold ether under pressure.

stir the ether and to permit temperature and pressure measurements, is shown in Fig. 1. The ether was held in an aluminum tube[7] which had an inside diameter of 1.27 cm, and a wall thickness of about 0.027 cm. Two thermocouples were held along the side of the x-ray beam by small steel tubes which remained stationary while the aluminum tube rotated thus stirring the ether. Temperatures were accurate to within 0.5 percent. The pressure was produced and maintained by a dead weight pressure piston of the type used to calibrate pressure gauges and was transmitted to the ether by a column of oil and mercury. Pressures were measured with an estimated accuracy of 0.6 percent. The specific volume was determined by reference to a P–V–T diagram[8] for ether. A reduced copy of the graph used is shown in Fig. 2. The small circles represent points at which diffraction curves were taken. A part of the observations were made with a Compton electrometer using the rate of drift method, and the remainder with a direct current amplifier using an FP-54 tube.[9] A re-

[7] Containers made of magnesium and of Dow metal were tried, but they did not withstand the pressure at the temperatures used here. There seemed to be a decided weakening of each at about 170°C. Containers of a beryllium-aluminum alloy were tried by Noll, but the material was porous so that the ether passed directly through the walls.

[8] Data taken from Schroer, Zeits. f. physik. Chemie **140**, 381 (1929).

[9] L. A. DuBridge, Phys. Rev. **37**, 392 (1931).

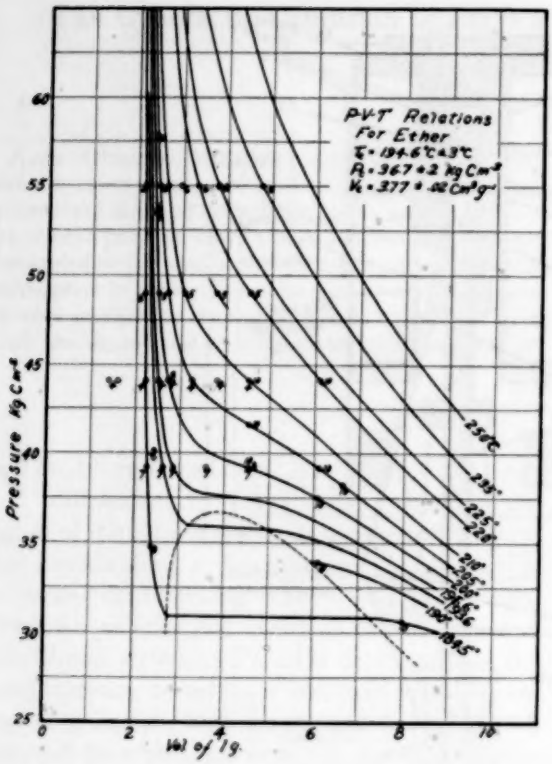

FIG. 2. *P–V–T* relations for ether. The small circles represent points at which observations were made. The numbers at each point refer to the figure in which the data taken at the point are found.

sistance of 8.4×10^{10} ohms was used in the grid circuit. It was found necessary to build a close fitting shield around the tube and the grid connections and dehydrate this with P_2O_5 in order to obtain stability. With the amplifier, observations could be taken with a great saving of time and a large number of tests showed this method as reliable as that of the electrometer.

The filters used were made of $SrCO_3$ and of ZrO_2. They were balanced by taking the diffraction curve of Al and adjusting the relative effective thicknesses by turning one of them about an axis perpendicular to the direction of the x-ray beam, so that the same intensity was obtained through each of them for the $K\beta$ and the general radiation. A curve representing the transmission of the filters when balanced is shown in Fig. 3. The crosses represent the intensity from Al with the $SrCO_3$ and the circles the intensity with the ZrO_2, respectively, in the beam.

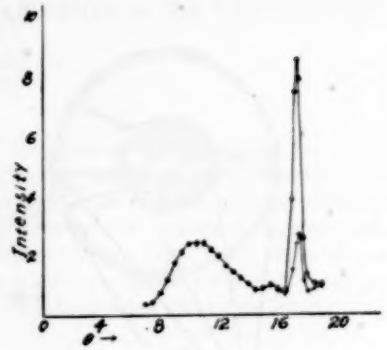

FIG. 3. Transmission through ZrO_2 and $SrCO_3$ filters.

EXPERIMENTAL RESULTS

The results of the experiments are shown in Figs. 4 to 10. θ is the angle between the direction of the incident beam and that of the scattered one. Ionization currents are relative values, yet the comparative values from one curve to another in any figure are as actually measured. The ordinates in the figures are readings with the ZrO_2 filter minus those with the $SrCO_3$ in the beam. To save space, several curves are on each plot, but with zero ordinates shifted as indicated on the left of each graph. Each curve is the average of at least six separate determinations.

CORRECTIONS

All curves were corrected for scattering from air the Soller slits and from the aluminum container. Corrections for natural electrometer drifts were taken care of automatically by the balanced filters. Corrections were made for difference in absorption and for the difference in the number of molecules acting as scattering units at different densities. That is, all the curves in any one figure are corrected so that they represent scattering from the same number of molecules, and thus makes them comparable. A correction for the incoherent scattering was not needed.

DISCUSSION

Several different types of curves appear in Figs. 4 to 10 ranging from those with a very pronounced peak and with little intensity at small angles to those with no peak and increasing

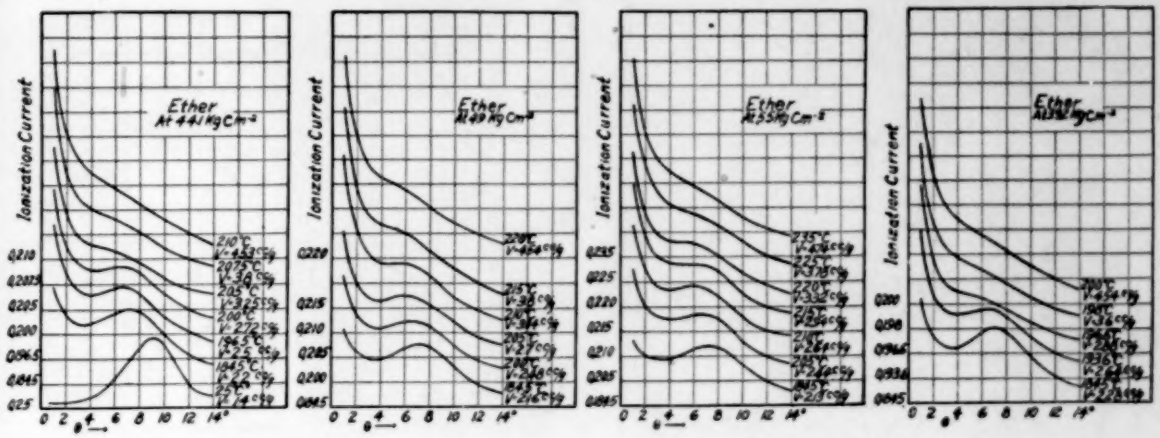

FIG. 4. FIG. 5. FIG. 6. FIG. 7.

FIG. 4. X-ray diffraction of ethyl ether at 44.1 kg/cm². Data taken with amplifier.
FIG. 5. X-ray diffraction of ether at the constant pressure of 49 kg/cm². Data taken with amplifier.
FIG. 6. X-ray diffraction of ether at the constant pressure of 55 kg/cm². Data taken with amplifier.
FIG. 7. X-ray diffraction of ether at the constant pressure of 39.2 kg/cm². Data taken with amplifier.

intensity at small angles. The former are typical liquid diffraction curves, the peaks appearing as a result of the cybotactic molecular grouping of the molecules in the liquid. The latter are typical gas curves signifying a random distribution of molecules. Other curves have a shape which corresponds to neither a liquid nor a gas but appears to be equivalent to a combination of the two types—liquid and gas.

The different groups of curves show the following:

(1) With constant pressure, 44.1 kg/cm², and increasing temperature and specific volume (see Fig. 4) the diffraction curve changes from that typical of a liquid, 25°C curve, Fig. 4, to that typical of a gas, 210°C curve, Fig. 4. Figs. 5, 6 and 7 show the same trend at pressures of 49, 55 and 39.2 kg/cm². Constant x-ray intensities, the same amplifier sensitivity and correction for density make these curves comparable from figure to figure as well as from curve to curve.

(2) With constant temperature the peak decreases and disappears with increasing specific volume. This is shown for 200°C in Fig. 8.

(3) With constant specific volume no significant change is noticed with increasing temperature and pressure. This is shown for a specific volume of 2.4 cc/g in Fig. 9, for 4.54 and 6.12 cc/g in Fig. 10. This non-variability with constant volume is true as one passes from the liquid phase, the two lower curves, Fig. 9, where the ether is below the critical temperature, to the gaseous phase, two upper curves, Fig. 9, where the ether is above the critical temperature. It is to be noted here that the specific volume is unique in its effect, for a variation along an isometric produces no noticeable change in the diffraction effect, while a variation along an isothermal, Fig. 8, an isobar, Fig. 4, or along

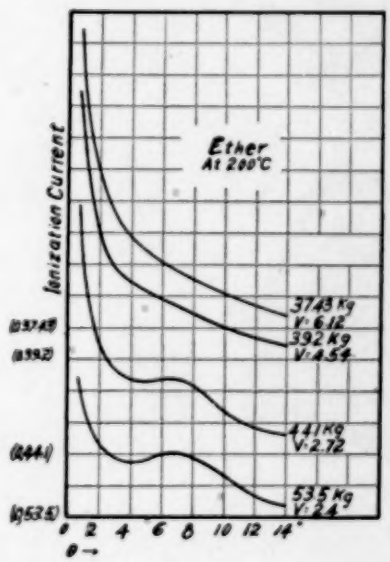

FIG. 8. X-ray diffraction of ether at the constant temperature of 200°C. Data taken with electrometer.

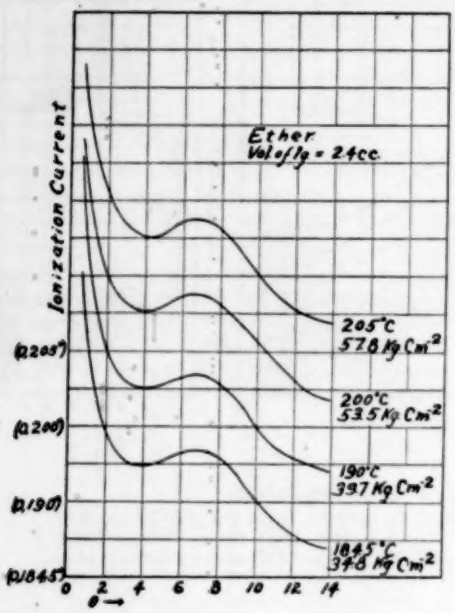

FIG. 9. X-ray diffraction of ethyl ether at the constant specific volume of 2.4 cc/g.

any line except an isometric does produce a change in the diffraction effect. This uniqueness of specific volume arises from the nature of the molecular forces which undoubtedly vary rapidly with the distance of separation of the molecules and thus the effect is not wholly unexpected. The similar curves for like specific volumes may be interpreted as representing the same condition of structure or extent of cybotactic groupings.

(4) Peaks are found with the ether in the gaseous state, i.e., in the region above the critical temperature, provided the pressure is great enough to produce a specific volume of the gas equal to that showing peaks at another pressure.

(5) While the specific volume is the controlling factor in the formation of the liquid structure at volumes less than about 4 cc/g it has no noticeable effect at specific volumes greater than this value, for all of the typical "gas" curves, those corresponding to a specific volume of about 4 cc/g or greater, show the same features independent of temperature, pressure and volume. These curves are shown in Fig. 10. They show that over a wide range of temperature, pressure and specific volume there is no marked alteration in the type of curve

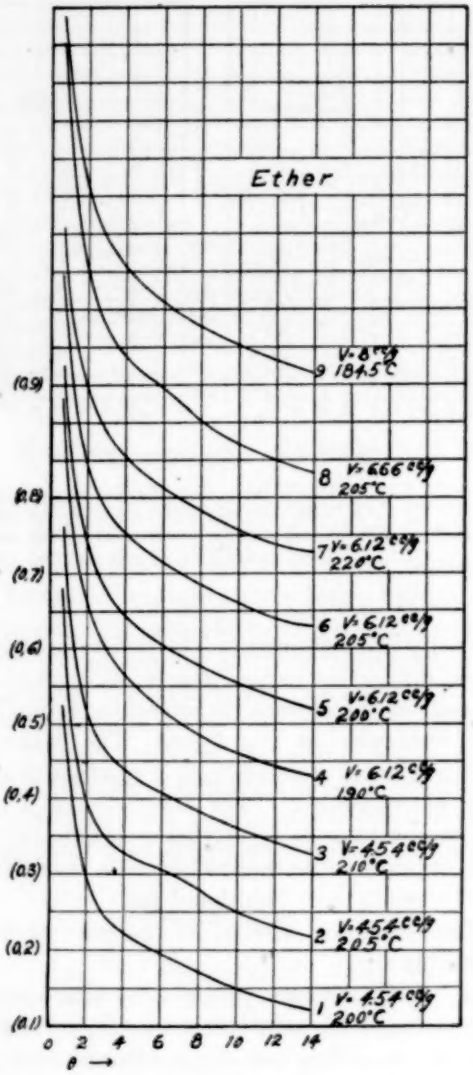

FIG. 10. X-ray diffraction of ether at specific volumes greater than 4 cc/g.

obtained. While one would not expect pressure alone to affect the character of the curve, it is significant that a change in specific volume does not alter it. This corresponds to the view that, after a certain distance of separation of the molecules has been obtained, the molecular forces are no longer effective in producing orderliness among the molecules.

(6) At approximately the specific volume of 3.8 cc/g the liquid structure is yet in evidence but at 4.54 cc/g its presence can no longer be certain. At 6.12 cc/g there is no detectable

indication. These facts are brought out in Figs. 4, 5, 6 and 7. The fact that the critical specific volume is 3.77 cc/g does not lead to a definite connection between the critical specific volume and that corresponding to the disappearance of the peaks. The values of both are dependent upon molecular forces but they arise from different circumstances. The liquid structure is wholly in the interior of the liquid, whereas the critical specific volume is the volume at which two phases in equilibrium become possible at the critical temperature.

In the foregoing the presence of peaks, with or without gaseous diffraction, is assumed to indicate the formation of some cybotactic groups, the incipient ones, of course, not being in size or structure alike throughout the experiments. Thus is shown what transpires in the sample as its pressure, temperature and volume are altered. One may not, however, conclude from the size of the peaks the exact extent to which the cybotactic condition prevails. Nevertheless, what occurs on the interior with change in pressure, temperature and volume is now more easily apprehended through the exhibition of the interior through x-ray diffraction.

In conclusion the writer wishes to express his thanks to Professor G. W. Stewart who suggested this problem and under whose direction the work was done.

OCTOBER 15, 1934 PHYSICAL REVIEW VOLUME 46

The Cybotactic Condition of Isopentane in the Region of the Critical Point

CARL A. BENZ AND G. W. STEWART, *University of Iowa, Iowa City*

(Received August 22, 1934)

X-ray diffraction-ionization curves have been obtained, at various values of pressure, volume and temperature, of isopentane near the critical point. The results are: (1) that, as is the case with ethyl ether, the specific volume is unique in determining the extent of cybotactic groups; (2) that the specific volume at which these groups disappear is ninety percent greater than the critical volume; (3) that the internal description of liquefaction above the critical pressure, as the fluid passes from gas to liquid, is the same for both isopentane and ethyl ether.

THE experimental work of Spangler[1] in the foregoing paper enables one to describe what occurs in a fluid near the critical point. The present paper is supplementary thereto, reporting the results of investigation of a second fluid, isopentane, this being selected[2] because the necessary values of temperature, pressure and specific volume were available and because the demands were within the limitations of the equipment, particularly that of a thin-walled cylinder enclosing the fluid.

The apparatus is essentially similar to that of Spangler[1] except that measurements were made entirely with an electrometer and an improved ionization chamber with an interior wire cage to reduce the α-particle ionization. The two sets of equipment were entirely separate but they gave identical results as was demonstrated by repeating some of the ethyl ether data with the isopentane apparatus. The experimental curves have been corrected as described in the foregoing article of Spangler.

RESULTS

Fig. 1 is the P–V–T diagram[3] for isopentane and was used to obtain the critical volume from the other two measured quantities. Figs. 2 to 8

[1] Spangler, preceding article in this journal.

[2] The isopentane was kindly supplied by the research department of the Phillips Petroleum Company. It was 99.7 percent pure.

[3] S. Young, Proc. Phys. Soc. London **13**, 602 (1899).

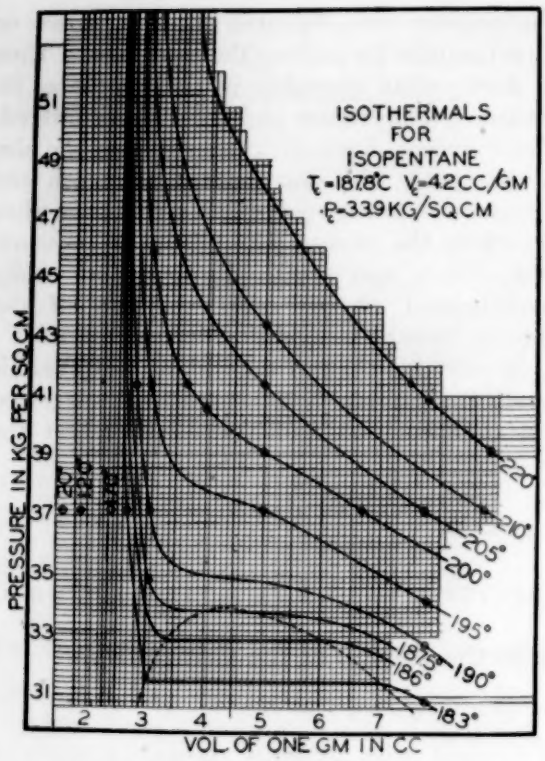

FIG. 1. P–V–T relations for isopentane in the region near the critical point, the observations reported by S. Young in 1899.

give the experimental diffraction curves for isopentane, the pressures, P, being expressed in kg/cm², the specific volume, V, cc/g, and the temperature, T, in degrees centigrade. θ is the angle through which the x-rays are diffracted.

Figs. 2 and 3 show the variation with temperature and specific volume at constant pressures of 37.2 and 41.4 kg/cm², both above the critical pressure of 33.9 kg/cm². There is a gradual change in the character of the diffraction curve with temperature and volume without any peculiarity in the neighborhood of the critical temperature, 187.8°.

In Fig. 4 the great variation in diffraction curves along an isotherm in Fig. 1 is shown by a comparison at 200°C of the curves with four pairs of values of pressures and specific volumes.

Figs. 5, 6, 7 and 8 enable one to compare the diffraction curves for the same specific volume and these show, first, that the curves for the same specific volume are similar and second, that any marked evidence of cybotactic grouping disappears at about 8 g/cc which is 90 percent greater than the critical specific volume.

DISCUSSION

The interpretation of such diffraction curves depends upon the underlying view of the cause of the characteristic diffraction. In the present status of the subject two views are being considered, both of which are alike in requiring a certain regularity of molecular arrangement. One is descriptive, using crystal structure as a point of departure. The other is an attempt to set up models of scattering units that will by calculation give similar curves. Recently Ging-

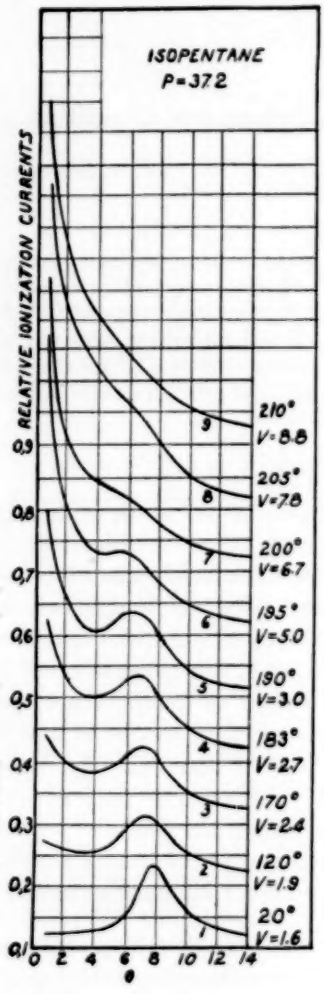

FIG. 2. X-ray diffraction of isopentane at a pressure of 37.2 kg/cm².

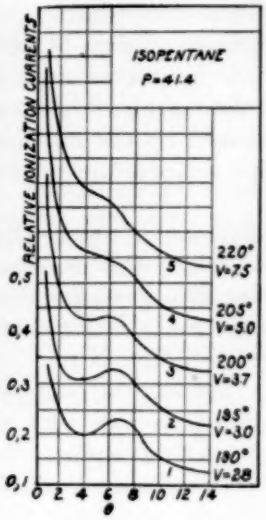

FIG. 3.

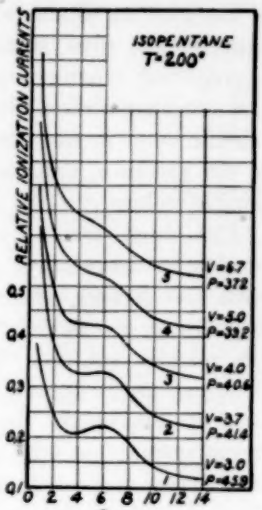

FIG. 4.

FIG. 3. X-ray diffraction of isopentane at a pressure of 41.4 kg/cm².

FIG. 4. X-ray diffraction of isopentane at a temperature of 200°C.

rich and Warren[4] have by the latter method been able to secure diffraction curves closely like those of ethyl ether. As the authors state, they have taken the case of spherical atoms and have made approximations to the density distribution of atoms about any one atom. This treatment for spherical atoms could be rigorous with a complete knowledge of the density distribution. The model of these authors is not the only one possible, nevertheless it is helpful in adding to our confidence in a liquid structure and hence to the descriptive view presently to be mentioned. In this model the molecules are treated as spherical, a smallest distance of approach of molecules is adopted, a concentration of scattering units in a spherical shell is assumed at this distance and then, beginning at a distance eighteen percent greater, the density of the units is regarded as constant throughout the remainder of the fluid. The expression for the scattered intensity is found to be dependent upon the density of the sample. The model is adjusted so that there is fair agreement between the calculated and the observed relative scattering intensities.

The view based upon similarity to crystalline

[4] Gingrich and Warren, Phys. Rev. **45**, 292 (1933).

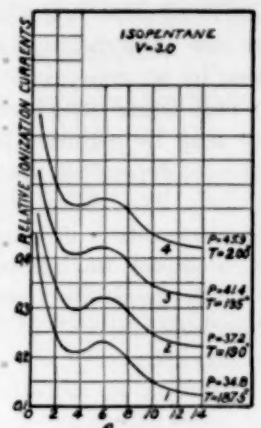

FIG. 5.

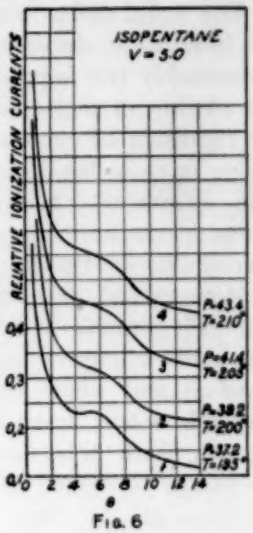

FIG. 6.

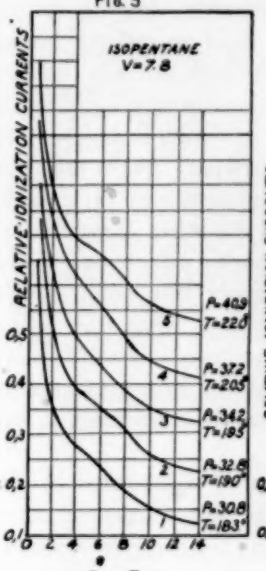

FIG. 7.

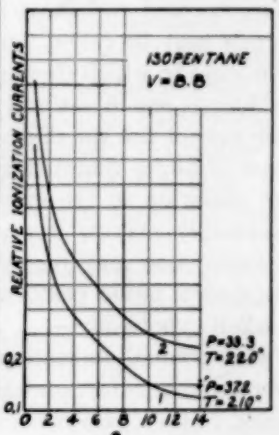

FIG. 8.

FIG. 5. X-ray diffraction of isopentane at a specific volume of 3.0 cc/g.

FIG. 6. X-ray diffraction of isopentane at a specific volume of 5.0 cc/g.

FIG. 7. X-ray diffraction of isopentane at a specific volume of 7.8 cc/g.

FIG. 8. X-ray diffraction of isopentane at a specific volume of 8.8 cc/g.

structure, used by Spangler,[1] gives an excellent picture of what occurs in the fluid in the region of the critical point. In these two liquids, at room conditions, the arrangement of molecules simulates the crystalline structure of the substance but a definite arrangement is not maintained on account of instability, permitting mobility and constant shifting of molecules from one degree of regularity of arrangement to another.

The liquid diffraction curve of ether and also of isopentane shows but one periodicity and presumably this is produced by an approximate parallelism of molecules. This liquid structure[5] or condition of cybotaxis[6] may be regarded as being more or less in evidence, depending upon the volume and temperature. The diffraction curve at the lowest temperature shown in these two fluids is typical of a liquid having an unsymmetrical molecule. The peak in these curves is gradually metamorphosed into a typical gas curve where the molecules are practically at random and where the variation in intensity depends solely upon the molecular scattering factor. With this descriptive view it is not necessary to regard the fluid as strictly homogeneous at any time. Indeed, at any instant there are regions in which a structure is distinctly more marked and those in which it is less. The former may be called "groups." There are then two ways in which these groups may be thought to change, one in size and the other in regularity. One cannot use the diffraction curves to express these changes quantitatively but qualitatively the variation in the curves is what one would reasonably expect. For purposes of discussion, however, one may regard the disappearance of the typical liquid peaks as the vanishing of any marked cybotaxis.

The gradual formation of aggregates in the process of liquefaction has been suggested many times. In these experiments the internal evidence has been secured. There seems to be no adequate reason, however, to suggest the discontinuance of the use of the critical temperature isotherm as an arbitrary boundary between the "liquid" and the "gaseous" states, for neither of these terms can be used to connote a definite character of the interior of a fluid. These x-ray diffraction experiments give some comprehension of the aggregating phenomenon on the interior and at the same time show that the magnitude of this phenomenon is not determined by the relation of the pressure, volume and temperature to the critical values.

The most striking difference between the results for isopentane and ethyl ether is that, with the former, the cybotactic grouping disappears at a specific volume much larger than the critical volume, whereas in the latter the disappearance occurs at almost the critical volume. Obviously the critical volume has no direct connection with cybotactic groupings, for the former has to do with two phases in equilibrium and the latter with the noticeable formation of cybotactic groups. The difference between the two fluids just stated would at once be attributed to differences in molecular forces. The ether is distinctly polar, having a moment of approximately 1.1×10^{-18} c.g.s. units, whereas the isopentane has no measurable moment. It is the non-polar compound that seems to have the more persistent group-forming ability as the separation of the molecules is increased. Thus the forces arising from polarity seem to be of minor importance in the comparison of the two liquids or in a consideration of the molecular forces.

The results with the two liquids are alike in two respects:

(1) In the neighborhood of the critical point and above the critical pressure the formation of cybotactic groups is not dependent upon the critical temperature but most importantly upon the specific volume. An isometric on the P–V–T diagram is the only line designating conditions for diffraction having like typical liquid peaks.

(2) With the pressure above the critical one, the formation of groups increases with decrease in specific volume.

The authors desire to express their thanks to the research laboratory of the Phillips Petroleum Company for the isopentane.

[5] The term "structure" is used with reference to a liquid without any inference that it is crystalline. "Structure" is a common term already applied as "atomic structure" and "crystal structure" and evident value should indicate its general use.

[6] "Cybotaxis" and "cybotactic" refer, in derivation, to space arrangement in liquids and has been found very convenient in referring to the condition of structure in liquids.

Measurement of Nuclear Spin by the Method of Molecular Beams

The Nuclear Spin of Sodium

I. I. RABI AND V. W. COHEN, *Columbia University*

(Received August 24, 1934)

A simple method of velocity selection of arbitrary resolving power for atomic and molecular beams is described. The method consists in spreading the beam into a velocity spectrum, through the action of external fields, and then selecting a portion thereof by means of a movable selector slit. Since all the atoms of the beam of the given velocity interval are utilized, this type of selection has the maximum efficiency. In addition a method of focussing the selected beam to increase intensity and resolution is applied. A ballistic method of using the surface ionization detector was evolved extending its use to beams of exceedingly low intensity. A selected beam of slow Na atoms, obtained and measured in this fashion, was analyzed in a weak and inhomogeneous magnetic field. Four distinct peaks of equal intensity were obtained which represent the $(2i+1)$ nuclear magnetic levels. The spin of the Na nucleus is accordingly equal to 3/2, in units of $h/2\pi$.

INTRODUCTION

THE most direct demonstration of the space quantization of angular momentum was the celebrated Stern-Gerlach experiment. The purpose of the experiments to be described is to demonstrate and measure the angular momentum of the nucleus directly by means of its effect on the space quantization of the angular momentum of the extranuclear configuration in a magnetic field.

The influence of a magnetic field on the different magnetic levels of an atom with nuclear spin "i" situated therein has been described in previous papers.[1,2,3] For the particular case of the alkalis in their normal $^2S_{\frac{1}{2}}$ states, values of the magnetic moments of the various magnetic levels as functions of the magnetic field are shown in Fig. 1 for the nuclear spin 3/2. The total number of magnetic levels is always $2(2i+1)$.

The schematic arrangement of the experiment is shown in Fig. 2. A narrow beam of sodium atoms, defined by slits S_1 and S_2 is allowed to pass through a magnetic velocity selector consisting essentially of an inhomogeneous magnetic field which spreads the beam into the usual velocity spectrum, the field being of sufficient intensity to cause a rather complete decoupling between electronic and nuclear spins. For sodium a field of 2000 gauss is sufficient. In this case the magnetic moments of the $2i+1$ levels arising from a particular value of m_j differ very slightly. By means of a movable selector slit S_3 a portion of the beam is selected for further analysis. After passing through S_3 the beam is homogeneous to an extent to be described below and contains atoms in equal numbers in all the magnetic levels arising from the $2i+1$ values of m_i but associated with only one value of m_j, namely, $+1/2$ or $-1/2$, depending on the direction of the field. The beam is then permitted to pass through a second

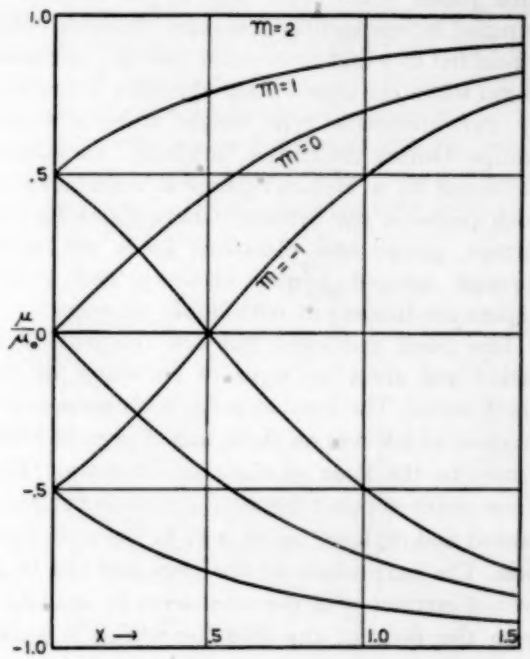

FIG. 1. Variation of the magnetic moments (in Bohr magnetons) of the atoms in the different magnetic levels for $i=3/2$ plotted against $x=(2\mu_0/hc\Delta\nu)H$.

[1] Breit and Rabi, Phys. Rev. **38**, 2082 (1931).
[2] Rabi and Cohen, Phys. Rev. **43**, 582 (1933).
[3] Rabi, Kellogg and Zacharias, Phys. Rev. **46**, 157 (1934).

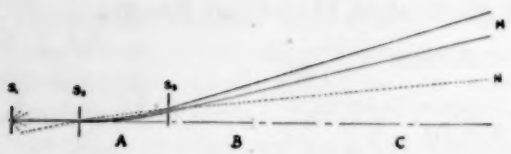

FIG. 2. Schematic arrangement of the slits and field showing the selected and scattered beams.

field of the Stern-Gerlach type. The field is so chosen that there is strong coupling between the nuclear and electronic spins. For sodium this field is of the order of 300 gauss. This brings us into the region of $x=1/2$ in Fig. 1. The atoms are subject to forces which are different for each of the $2i+1$ magnetic levels and the beam is therefore separated into $2i+1$ components, since it is homogeneous in velocity. The spin is evaluated by merely counting the number of peaks in the deflection pattern.

APPARATUS

The apparatus, (Fig. 3) constructed of solder-coated brass tubing, is divided into two sections, an oven chamber and an observation chamber. These are connected by a ground joint cemented with picien wax. Each half of the system is pumped independently, the oven chamber being connected to a fast three stage mercury diffusion pump while the observation chamber is pumped by two umbrella type single stage diffusion pumps. During the runs a "sticking" vacuum as measured by a McLeod gauge is maintained in both parts of the system. Connections for the pumps, gauge and electrical leads are made through ground joints. Mercury and grease vapors are frozen out with liquid air traps.

The oven and oven slit are constructed of nickel and show no signs of corrosion by the alkali metal. The bottom is cut with three radial grooves which rest on three nickel pegs fastened firmly to the floor of the oven chamber. This three point support permits the oven to be removed and replaced accurately to the same position. The narrowness of the pegs and the small area of contact with the oven serve to insulate it from the floor of the chamber which is water-cooled.

The oven is heated by two spirals of 10 mil tungsten wire enclosed in holes drilled in the body of the oven above and below the slit. This arrangement serves to keep the region near the slit at a temperature slightly higher than the rest of the oven. A copper constantan thermocouple is inserted into the body of the oven for temperature measurement. The oven well is covered with a tapered monel metal plug. This plug is hollowed out to permit the alkali vapor to reach the slit through a canal and at the same time to check the creeping of the liquid metal along the nickel surface to the slit. The jaws forming the oven slit are set 0.013 mm apart.

The collimating slit S_2, 0.016 mm wide and 9 cm from the oven slit, is set in a disk which can be rotated by means of a screw about the axis of the beam. If the observation chamber and one-half of the collimating slit be removed, the oven slit is observable from the observation side of the collimating slit. The one edge of the slit remaining is then adjusted parallel to the oven slit with the aid of a telemicroscope and a filar micrometer. The two slits must then be adjusted laterally so that the plane of the beam is aimed parallel to the edges of the pole peices of the magnets. This is determined by sighting at the oven slit through the observation chamber with a telescope and filar micrometer.

THE VELOCITY SELECTOR

A large Dubois magnet (A, Figs. 2 and 3) fitted with pole pieces of the Stern-Gerlach type 6 cm long with a furrow 8 mm wide and a knife edge 4 mm distant furnishes the magnetic field. The selector slit S_3, 0.035 mm wide, was mounted eccentrically on a ground joint and was movable by rotating the joint. The distance from collimator to the selector was 10 cm and the two were adjusted parallel to each other by rotation of the large ground joint which connects the oven chamber to the detecting chamber.

Since the deflection of an atom in a constant field of force perpendicular to its original direction of motion is given by $s=\text{const.}/v^2$ we have $dv/v=ds/2s$. Under the conditions of this experiment dv/v was of the order of 1/10. The velocity selected is varied simply by changing the magnetic field. The resolution can be varied by changing the position of the selector slit.

Where it is undesirable to make the velocity selection with a magnetic field, the same result

can probably be attained by spreading the beam into a velocity spectrum by means of an inhomogeneous electric field. For heavy atoms or molecules even the gravitational field of the earth is not out of the question. The principal technical difficulty which is always involved when a velocity selection is made is to detect the much enfeebled beam.

The Analyzer

The analyzer follows directly after the selector slit and consists of two magnets having pole pieces similar to magnet *A* but the first being 18 cm long and the second 16 cm, with 1.5 cm space between the two. The first magnet *B* supplies the weak analyzing field and is made long in order to obtain sufficient deflection with the small forces available. Magnet *C* has a strong field and serves as a focussing device. The pole pieces of the magnets are so arranged that the furrows of the *B* and *C* magnets are on the same side of the beam as the knife edge of the *A* magnet. This is important for the purpose of resolving the different components. The reason for this can be seen by considering the fact that the selected beam contains a finite velocity range. From any portion of the original beam the faster atoms pass through the selector slit on the side nearer the original beam and the slower atoms on the farther side since the slower atoms suffer the greater deflection. A subsequent deflection in a field similar to the first would therefore broaden the beam still further. Even if the field in the second magnet is reversed this is still the case because an atom with its magnetic moment oriented parallel to the field will be deflected toward the strong field (and *vice versa* for those opposed to the field). If the second field is reversed in direction the magnetic moment will change in direction to follow the direction of the field since the rate of change is small in the period of the Larmor precession. This is to be expected from the theorem of adiabatic transformability applied to the space quantization with respect to the field. However, by changing the pole pieces about, the stronger field is now in the opposite direction and the forces acting, being opposite to those in the first field cause the beam to become narrower instead of broader.

Magnet *C* has a strong field in which all the components are subject to the same force and the effect is to displace the whole deflection pattern toward the center and thus increase the resolution. Magnet *C* has also another very important rôle due to the fact that in addition to the selected beam some atoms scattered in the oven chamber pass through the collimator in the direction of the selector slit and form an additional beam. This is represented by the broken line in Fig. 2. These atoms have the Maxwellian distribution of velocities and are fast compared to the selected beam. This scattered beam comes nearer the center than the selected beam. Although these atoms form about one-five hundredth the total beam intensity, the velocity selection cuts down the intensity to such an extent that the scattered

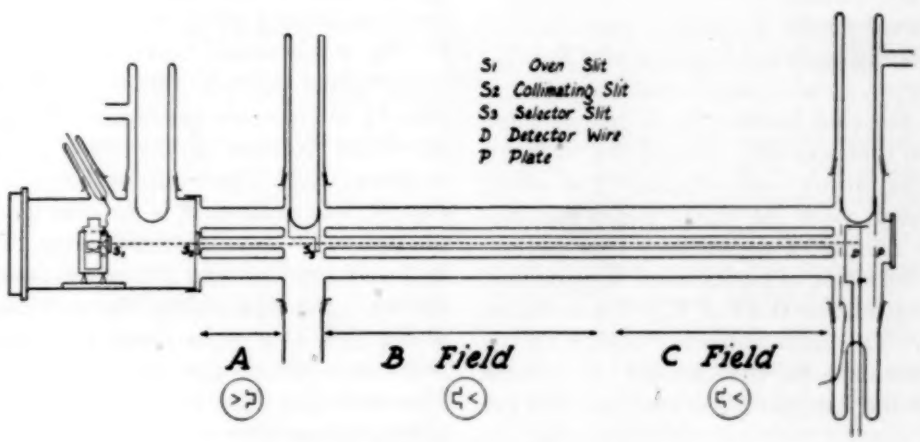

Fig. 3. Diagram of the apparatus.

atoms are as numerous as the selected atoms. The effect of magnet C is to shift the entire deflection pattern away from the region of this scattered peak so as to make the interpretation of the results unambiguous.

The Detector

Detection was effected by means of the surface ionization detector.[4] The 2 mil tungsten filament was mounted eccentrically on a ground joint and was moved laterally by turning the joint. The wire was supported by two adjustable arms so that it could be set parallel to the slit system. For the detection of sodium the wire must be provided with an oxide coat to raise its work function. No special method was used to obtain this coating. When a wire is first used it is carefully heated for a short time at about 1800°K until most of the oxide is driven off. After the beam is detected the wire is heated again until the residual positive ion current when the wire is outside the beam is reduced to about 10^{-13} amp. with the filament at a dull red heat. If too much of the oxide has been removed the wire can usually be activated by admitting a small quantity of air into the apparatus with the filament at about 1400°K. With the beam intensities used in this experiment a well sensitized filament will remain so for the entire run. The filament is maintained at a potential of 45 volts above ground. The positive ion current is measured by means of an FP-54 vacuum tube amplifier with a grid leak of 5×10^{8} ohms. With the galvanometer used the current sensitivity was 10^{-14}A/mm.

The selected beam is usually too weak to measure directly because of background fluctuations. However, by allowing the sodium atoms to deposit on the cold filament from one to three minutes and then suddenly heating the filament, large ballistic throws were obtained. The multiplication factor over the direct beam readings was 20 per minute of deposition. This method eliminates the effect of background fluctuations. All the points except those of Fig. 3 were taken in this way. The galvanometer readings are almost proportional to the amount of sodium deposited if the background is less than the net ballistic reading (ballistic throws minus the background).

Procedure

The sodium used was doubly distilled in vacuum. When the oven is to be loaded the still is cracked and the sodium dropped directly into a dish of petroleum ether and is then transferred to the oven. The lid is then pressed in, the oven set in place and the system is evacuated. During the loading process the sodium is in contact with the air for a fraction of a second and with the petroleum ether for the time taken to evacuate the oven through the slit. The oven is heated slowly to about 200°C to help remove the petroleum ether and occluded gas after which the oven is allowed to cool and stand overnight under vacuum.

In preparation for a run the oven is heated at the rate of 3°C per minute until the beam is first detected at about 300°. The heating rate is then slowed down gradually until 360° is reached, at which temperature the beam intensity is sufficiently high for convenient working conditions. The galvanometer deflection in the center of the beam is about 10^{3} cm, while the vapor pressure in the oven is about 0.2 mm Hg.

When the beam intensity has become stabilized the A field is turned on and the deflection pattern observed. The initial beam and the A field deflection pattern are shown in Fig. 4.

The A field is then thrown off and the selector slit is turned into the center of the beam. This gives a fiduciary position from which slit is turned so that atoms of the required velocity will be selected. The velocities used in this experiment correspond to an energy of about $1/2\ kT$. On Fig. 4 this would correspond to atoms which would arrive at about 80 on the scale. The low velocity is necessary in order to obtain sufficient resolution because of the small forces in the analyzing field. The resulting beam is shown in Fig. 5I. The peak at 78 is the selected beam and the one at 71 is the scattered beam. The C field is then turned on and the selected beam is deflected to the other side of the scattered beam as in Fig. 5II. It is to be noted that the scattered beam does not change its position appreciably. The analyzing field is then turned on and the deflection patterns are observed for the different values of the field.

[4] Taylor, Zeits. f. Physik **57**, 242 (1929).

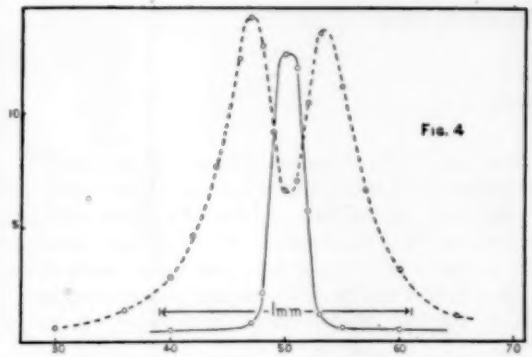

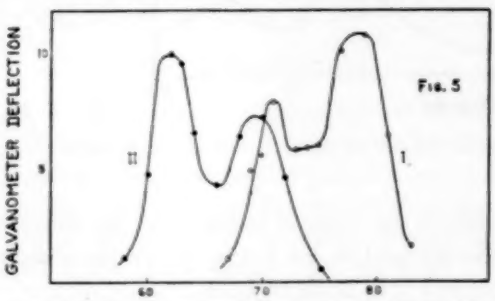

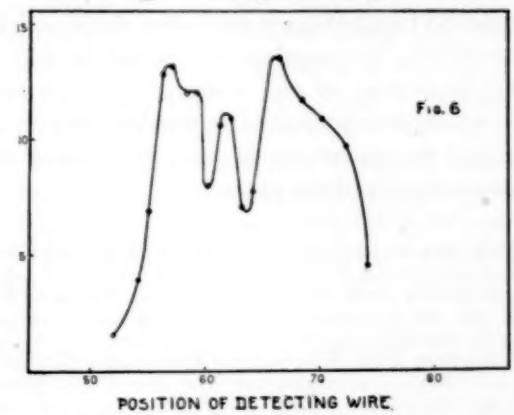

FIG. 4. Experimental curve of the direct beam (full line) and deflection pattern obtained with *A* field alone (dotted line). The ordinate scale of the dotted curve is 5 times that of the full curve.

FIG. 5. Experimental curve of selected and scattered beams; curve I without *C* field and curve II with *C* field. The *B* field was zero in each case.

FIG. 6. Deflection pattern with 55 m.a. through *B* magnet, *A* and *C* fields as in Fig. 5.

RESULTS

The different deflection patterns obtained with the various values of the current through the analyzing magnet *B* are shown in Figs. 6–10. In Fig. 6 the resolution is not yet sufficient to resolve all the peaks. Fig. 7, taken at a somewhat higher field shows the pattern shifted toward the left, that is, toward the position of the original

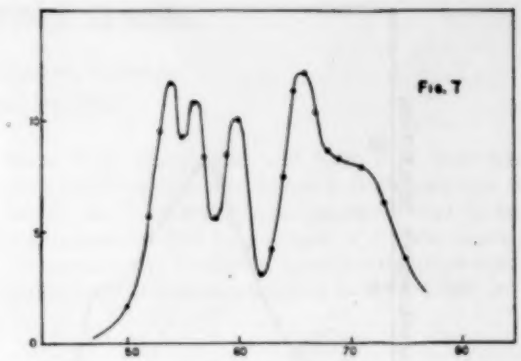

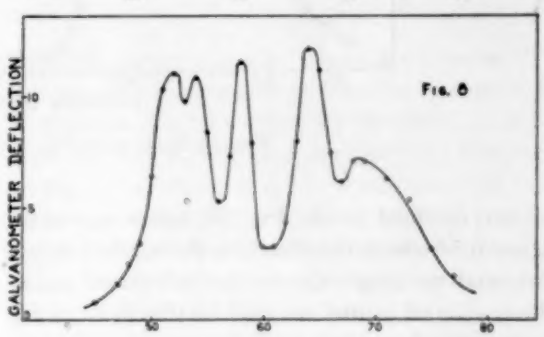

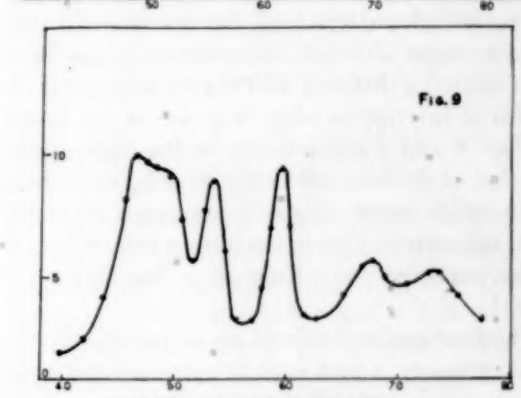

FIG. 7. Same as in Fig. 6 with *B* magnet current 70 m.a.
FIG. 8. Same as in Fig. 6 with *B* magnet current 85 m.a.
FIG. 9. Same as in Fig. 6 with *B* magnet current 110 m.a.

beam and shows four clearly resolved peaks. The shelf on the right is due to the scattered atoms. Fig. 8 shows this still better and the scattered atoms are now almost separated from the pattern of the selected atoms. Fig. 9 shows the scattered atoms in a stronger field being split up into the ordinary Stern-Gerlach pattern, the center of which still remains at the original position of 70 scale divisions, while the deflection pattern of the selected atoms already shows the setting on of the Paschen-Back effect in the failure to resolve

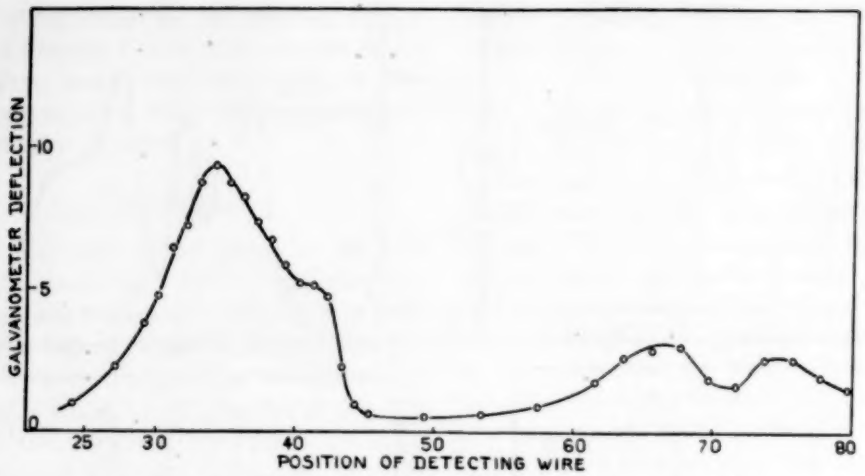

FIG. 10. Same as in Fig. 6 with B magnet current 187 m.a.

the two furthest peaks. Fig. 10, taken at a much higher field where the Paschen-Back effect is well advanced no longer shows the individual peaks. The scattered atoms are still further split in the Stern-Gerlach pattern with the center still at the same position although the selected atoms have been shifted a distance well over a millimeter. It is also of interest to note that one of the peaks in Figs. 6 and 7 are actually to the right of the position of the selected beam showing that these components have magnetic moments in weak fields opposite in sign to the strong field case as is to be expected for values of x less than $1/2$ (Fig. 1).

The four peaks obtained are of practically the same intensity, which is to be expected and have the width of the original beam. Since the number of peaks is equal to $2i+1$, the spin of the sodium nucleus is $3/2$ in units of $h/2\pi$.*

It should be mentioned that since this result is obtained only by counting the number of peaks, it is independent of any assumption as to the Maxwellian distribution of molecular velocities, or of any measurements of field, gradient or of the temperature of the oven.

* This value of the nuclear spin has been confirmed since our first publication (Phys. Rev. **43**, 582 (1933)) by Joffe from intensities in the band spectrum of the Na_2 molecule (Phys. Rev. **45**, 468 (1934)) by Granath and Van Atta from intensity measurements of the hyperfine structure of the resonance lines (Phys. Rev. **44**, 935 (1933)) and by Heydenburg and Ellett from the polarization of resonance radiation of Na in a weak magnetic field. (Phys. Rev. **44**, 326 (1933)).

The Nuclear Spin of Caesium

VICTOR W. COHEN, *Columbia University*

(Received August 24, 1934)

The spin of the caesium nucleus has been measured by the deflection of a beam of atoms in a weak inhomogeneous magnetic field. The method utilizes the fact that the magnetic moment of the atoms in some of the magnetic levels vanishes at certain values of the magnetic field. An examination of the variation of the intensity at the center of the pattern yields distinct maxima at these fields. From the number and position of these maxima, the spin can be uniquely deduced. If the magnetic field is known, the hyperfine structure separation can be deduced with accuracy. The nuclear spin of Cs was found to be 7/2 in units of $h/2\pi$ and the hyperfine structure separation for the normal state was found to be 0.295 ± 0.01 cm^{-1}.

INTRODUCTION

ALTHOUGH the nuclear spin of caesium has been investigated by the hyperfine structure of spectral lines the results have not been decisive. Kopfermann[1] from an investigation of the intervals of the hyperfine structure of some spectral lines of Cs II concluded that the most probable value was 7/2, but was not able to exclude the values 8/2 or 9/2. Jackson[2] found the intensity ratio of the two components of the resonance lines to be 1.27 ± 0.02, consistent with a spin of either 7/2 or 8/2 for which the ratios would be 1.286 and 1.25, respectively. In view of the known difficulties in measurement and interpretation of intensity ratios the possibility of 9/2 is not entirely excluded by this experiment. In view of the importance of having an accurate knowledge of this fundamental nuclear property it was considered worth while to investigate this element with the method of molecular beams.

The method used for sodium[3] was difficult to apply to caesium without a considerable change in the constants of the apparatus. For cases where the spin is large, the deflection pattern must be spread over a wide region in order that the $2i+1$ components be resolved. This was difficult with the apparatus at hand. However, the alternative method[4] to be described is particularly suitable for spins where $i>3/2$ and is almost as direct.

In the present experiment the nuclear spin of caesium is measured by its effect on the Stern-Gerlach pattern of the neutral Cs atom. The theory of this experiment is similar to that of the anomalous Zeeman effect for doublets as developed by Heisenberg and Jordan.[4,5,6] The force acting on an atom in a $^2S_{\frac{1}{2}}$ state, situated in an inhomogeneous magnetic field, of such strength that there is strong interaction both between the nuclear and electronic spins and between each spin and the field, is given by

$$F=\pm\frac{2m/(2i+1)+x}{2(1+[4m/(2i+1)]x+x^2)^{\frac{1}{2}}}g\mu_0\frac{\partial H}{\partial y}, \quad (1)$$

where $$x=\frac{g}{\Delta W}\frac{eh}{4\pi m_0 c}H=\frac{g\mu_0}{\Delta W}H.$$

ΔW is the separation of the hyperfine structure levels in the absence of field, g is the Landé g factor for the electronic configuration, m is the total magnetic quantum number, and i is the nuclear spin quantum number. Eq. (1) shows that the magnetic moment of the entire atom depends upon the nuclear spin and is a multiple-valued function of the field H. The behavior of the function F for a value of 7/2 and 6/2 for i is shown in Fig. 1. Obviously F vanishes for states with negative m when

$$x=-2m/(2i+1), \quad (2)$$

where $-m=i-1/2,\ i-3/2,\ \cdots 0$ for odd spins, and $i-1/2,\ i-3/2,\ \cdots 1/2$ for even spins. For these states the magnetic moment may become positive if the field be increased, and negative if the field be decreased or *vice versa*. The atoms in this state will suffer no deflection in the magnetic

[1] Kopfermann, Zeits. f. Physik **73**, 437 (1932).
[2] Jackson, Proc. Roy. Soc. **A143**, 455 (1933).
[3] The preceding paper in this issue of the Physical Review.
[4] The writer is greatly indebted to Professor I. I. Rabi for the suggestion of this method.
[4] Breit and Rabi, Phys. Rev. **38**, 2082 (1931).
[5] Pauling and Goudsmit, *Structure of Line Spectra*, p. 219, McGraw-Hill, 1930.
[6] Heisenberg and Jordan, Zeits. f. Physik **37**, 263 (1926).

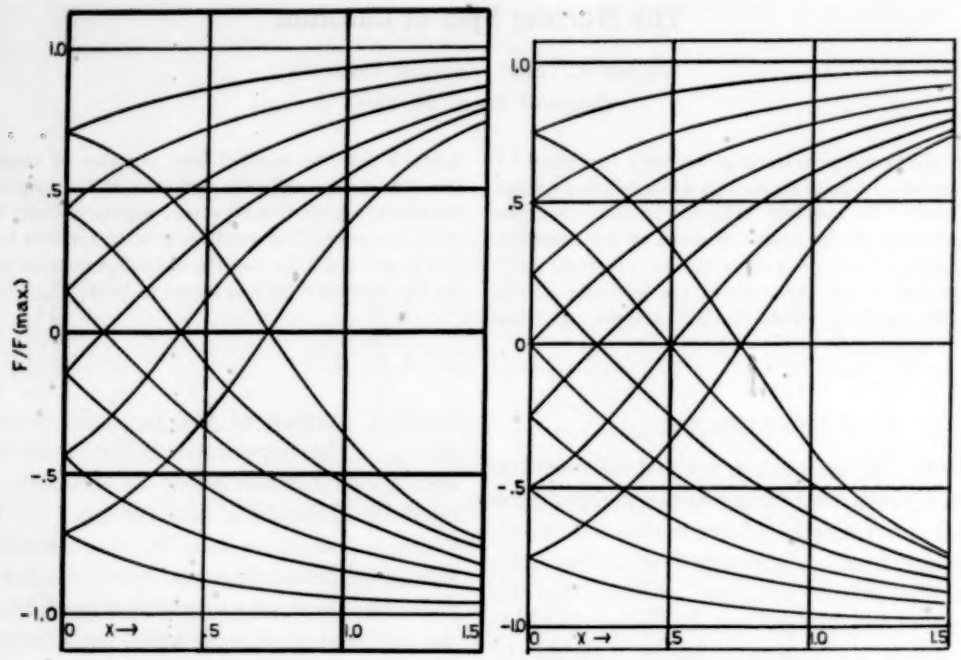

FIG. 1a. FIG. 1b.

FIG. 1. Theoretical curve showing magnetic moment of the atom in Bohr magnetons plotted against x for the different nuclear magnetic levels (a) for $i=6/2$, (b) for $i=7/2$.

field, and the Stern-Gerlach pattern taken at this field will consist of a superposition of the split beam and a beam the same shape as the original beam. (See Fig. 6.) The probability that an atom exist in a state of a given magnetic quantum number $m<i+\frac{1}{2}$ is inversely proportional to twice the statistical weight of that state and is given by $1/(2i+1)$.

The intensity of a beam at its center after passing through an inhomogeneous magnetic field will be the sum of a number of terms each given by the formula:[7]

$$I=2wI_0\left[e^{-y}(y+1)\right]_{\infty}^{s_a/d}, \tag{3}$$

where I_0 is the intensity of the undeflected beam, d is $1/2$ the half-width of the beam, w is the probability of the magnetic state, and s_a takes on a different value for each magnetic moment present at the field, namely,

$$s_a=(F/4kT)(l_1^2+2l_1l_2). \tag{4}$$

s_a represents the deflection of an atom with the most probable velocity, in traversing a magnetic field of length l_1 and distance l_2 from the end of the field to the detector. It is clear from (3) that the contribution to the intensity due to atoms with nonvanishing moments will be small if s_a is large compared to d, and the intensity will be determined mainly by the atoms with zero moment. The gradient $\partial H/\partial y$ is fixed by the construction of the magnet, consequently d must be made small by using narrow slits and s_a large by using a long beam. If now the field be increased or decreased from one of the values given by (2) all the atoms will have nonvanishing magnetic moments and the value of I will decrease. Therefore the measurement of the variation of intensity in the center of the beam with magnetic field should be expected to show maxima at those fields corresponding to zero moment states. The values of x at which these states occur for different values of the nuclear spin are given in Table I.

The relative values of the fields at which the zero moment states occur taking the highest as unity are given in Table IA.

The interpretation of the results of experiments of this type is very simple if sufficient

[7] Stern, Zeits. f. Physik **41**, 563 (1927).

TABLE I. *Values of x of zero moment states for various values of nuclear spin.*

i	1/2	2/2	3/2	4/2	5/2	6/2	7/2	8/2	9/2
x	0	.333	.5	.6	.667	.714	.75	.777	.8
			0	.2	.333	.429	.50	.555	.6
					0	.143	.25	.333	.4
							0	.111	.2
									0

TABLE Ia.

i	1/2	2/2	3/2	4/2	5/2	6/2	7/2	8/2	9/2
H	0	1.0	1.0	1.000	1.000	1.00	1.000	1.000	1.000
$\overline{H(\max)}$			0	.333	.500	.60	.667	.714	.75
					0	.20	.333	.428	.50
							0	.143	.25
									0

resolution is attained. If the number of peaks other than at zero field, which always occurs, be N, then the spin is either $(2N+1)/2$ or $2N/2$. The interval in field between the different peaks is constant in each case. However, the interval between zero and the first peak for even spins is 1/2 of that between successive peaks. The spin is thus uniquely fixed by the number of peaks and their relative positions without recourse to the further evidence of the intensity distribution in the deflection pattern. With spins of 1/2, 2/2 and 3/2, such considerations cannot be avoided by this method. Even if all the maxima are not resolved, the ratios of the fields at the observed maxima may be sufficient to determine the spin, as may be seen from Table Ia.

The value of the field at any one of the peaks is sufficient to determine the hyperfine structure separation between the two terms $f=i+1/2$ and $f=i-1/2$.

APPARATUS

The apparatus used in this experiment is essentially the same as that described in the previous paper[3] except for minor improvements. However, S_3 which was used originally as a selector slit is used here as a collimator, with width 0.019 mm; S_2 which was used originally as a collimator is considered now as a fore slit, with width 0.01 mm and the oven is used as a source with slit width 0.02 mm. This arrangement serves to eliminate the tails of the beam caused by scattering in the oven chamber, and because of the long distance from fore slit to collimator the half-width of the beam is kept down to 0.09 mm. The magnetic field for the deflection is furnished by the magnet previously used as the analyzer (magnet B only).

Apiezon oil pumps were substituted for the mercury pumps, so that, if the system be allowed to stand over night with caesium deposited on the walls of the oven chamber, mercury will not be absorbed. An ionization gauge is connected to the detecting chamber and registers a pressure of 5×10^{-7} mm Hg during the runs.

The height of the beam was shortened from 6 to 4 mm making the field more nearly uniform over its height.

The FP-54 vacuum tube amplifier used in connection with the surface ionization detector has been increased in current sensitivity to 0.8×10^{-14} amp./cm.

PROCEDURE

The caesium is prepared in vacuum by heating CsCl with freshly turned calcium metal shavings. The pure caesium is driven off at about 500°C. After an additional distillation it is driven into a small bulb and sealed off under high vacuum. This bulb is crushed inside the oven by the oven lid under an atmosphere of helium, after which it is placed in the oven chamber and the system evacuated.

The power input to the oven of five watts raises the temperature at the rate of 1.5 degrees per minute at first and gradually brings the oven to equilibrium at the running temperature of 170 to 190°C in about three hours. The full intensity of the original beam gives a galvanometer deflection of 1 to 6×10^3 cm.

When the beam, as collimated by the fore slit has become steady in intensity, the collimator is turned into place. The magnet current is then turned on to 500 m. a., reversed several times, and then brought up from zero in steps of from 5 to 20 m.a. and the intensity in the center of the beam is measured at each value of the current. At certain fields the distribution of intensity in the beam is measured by keeping the current constant and moving the detector wire across the beam. During the course of taking the points of any one curve the total beam intensity does not vary more than three percent.

Magnetic Field

A precise knowledge of the absolute value of the field is unnecessary for the determination of the nuclear spin. The only accurate measurement necessary is the proportional change in field with exciting current. For this purpose a flip coil of two turns, about 140×4 mm situated approximately in the plane of the beam is rotated through an angle of 180 degrees, giving a fluxmeter throw proportional to the field. The magnet is calibrated in this way over the entire range over which it is used. These measurements are not in error by more than one percent. The magnet calibration curve is shown in Fig. 2.

An average value of the field over the height of the beam is obtained by rotating the flip coil in a uniform field which in turn is measured with the aid of a second flip coil whose area is accurately known. The precision in the measurement of ΔW, for which the absolute value of the field enters, is limited chiefly by the difficulty in locating the beam with respect to the flip coil. This, however, does not affect the relative values of the field.

Results and Discussion

A typical curve showing the variation of intensity in the center of the beam with magnetic field is shown in Fig. 3. The peaks at fields B and C are due to atoms having zero moments at these values of the field. The break at A shows up as a slight maximum in some of the runs with a narrower beam width. That there really is a zero moment state at this value of the field, is shown in Fig. 4, the deflection pattern taken at this value of the field. We have here a superposition of a curve having the same form as the direct beam and a curve representing the narrowly split deflection pattern due to the atoms in the other magnetic levels. Fig. 6 is the deflection pattern taken with the much larger value of the field and gradient at C. The high central peak results, again, from the presence of atoms having a zero moment and has the same form as the direct beam. Because of the better resolution with the higher gradient of the field, it now stands quite apart from the rest of the deflection pattern. Since all states have equal statistical weight, the ratio of the intensity at the peak to that of the direct beam should be as $1/(2i+1)$ i.e., 1/8 for a spin of 7/2. The experimental ratios are approximately 1/10. A considerable weakening is to be expected since the field is not constant over the height and width of the beam.

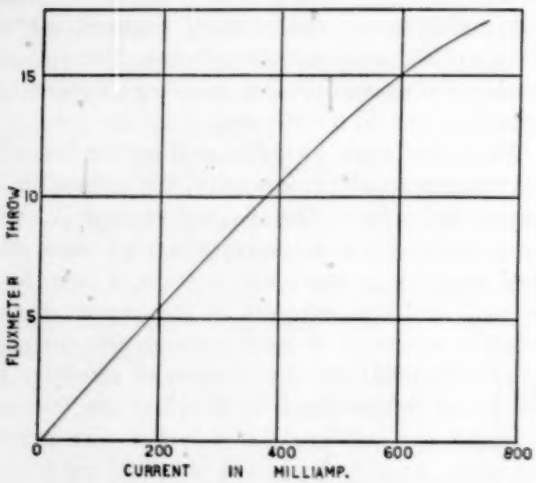

Fig. 2. Magnet calibration curve, fluxmeter throw of 1 cm corresponds to 196 gauss.

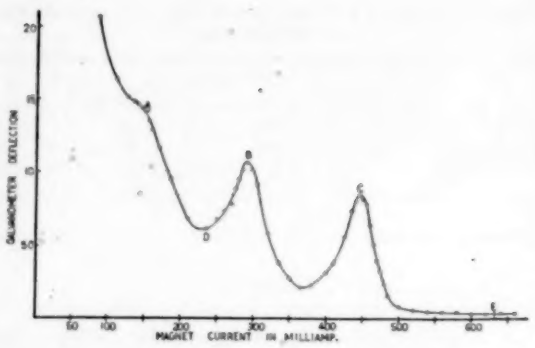

Fig. 3. Experimental curve showing the variation of intensity at the center of the beam with magnet current.

The fact that it is only at particular values of the field that we have components of zero moment is illustrated in Fig. 5, which is a deflection pattern taken at D, where the field and gradient are less than at C. Nevertheless the beam is split in this field with a minimum at the center, proving that all the atoms possess nonvanishing magnetic moments.

The magnet current at which the zero moment state exists is obtained by subtracting the ordinate of an estimated background curve of the intensity due to the atoms of finite moment,

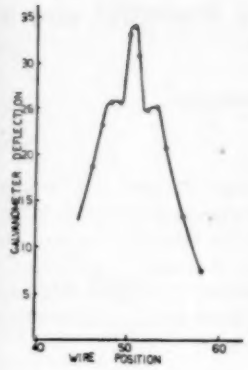

FIG. 4.

FIG. 5.

FIG. 4. Experimental curve showing the distribution of intensity in the beam at *A*.
FIG. 5. Distribution at *D*.

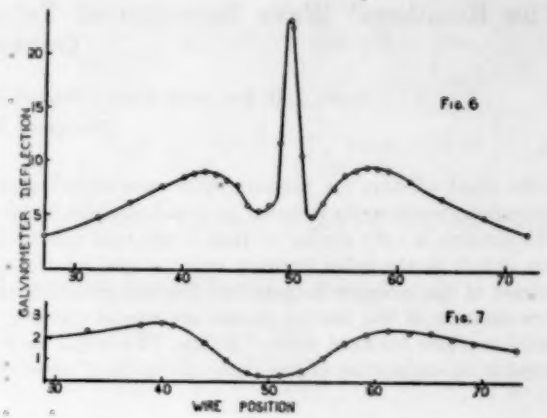

FIG. 6. Distribution at *C*.
FIG. 7. Distribution at *E*.

from the corresponding ordinate of the experimental curve. This shifts the maxima slightly to the right. The fields corresponding to these values of the magnet current are then obtained from the magnet calibration curve.

The relative values of the fields at *A*, *B* and *C*, taking the field at *C* as unity are given in Table II, for five runs.

TABLE II.

Run	I	II	III	IV	V
$H(A)$	.347	.342	.360	.351	not resolved
$H(B)$	.664	.664	.683	.667	.667
$H(C)$	1.000	1.000	1.000	1.000	1.000

The margin of error in locating *A* is about six percent. The ability to resolve this maximum depends largely upon the beam width. The location of *B* and *C* are accurate to one percent. The comparison of the results in Table II with those in IA show that a value of 7/2 for i is the only one consistent with the experimental results. If the spin were 9/2 a fourth maximum should be expected at *E* (Fig. 3). Fig. 7 shows the distribution of intensity found at this field. If there were present any atoms with moments equal to or close to zero, the pattern would be similar to Fig. 6.

The results show an approximate equality of the intervals in the field between the values at the peaks 0, *A*, *B* and *C* which rules out the possibility of any unresolved peaks on the low field side and shows the spin as odd. The fact that there are three peaks again fixes the spin as 7/2.

For the purpose of obtaining a value of ΔW the peak at *C* is most suitable. The position of this peak in the two best runs was at 470 m.a. and at 447 m.a. This difference is due to the fact that the beam traversed a slightly different region of the magnetic field during each run. Since $x=(g/\Delta W)ehH/4\pi m_0 c)=0.75$ at this field, $\Delta\nu=\Delta W/hc=0.295\pm0.01$ cm^{-1}.

In conclusion the author wishes to thank Professor I. I. Rabi for the many helpful suggestions throughout the progress of this work, and his colleagues in the molecular beam laboratory for their generous assistance in the taking of data.

The Rotational Wave Equation of Tetramethylmethane for Zero Potential and a Generalization

LUCIEN J. B. LACOSTE, *Gates Chemical Laboratory, California Institute of Technology*

(Received August 21, 1934)

An exact solution for the rotational wave equation of tetramethylmethane for constant potential has been found. The solution is very similar to that of the rigid spherical top, which is the other limiting case for the rotational motion of the molecule in question. The energy levels for free rotation of the methyl groups are spread out compared to those for fixed methyl groups. This might make possible an estimation of the potential function between the groups. The energy levels might be used to calculate the specific heat. Some selection rules are given for infrared and Raman spectra although the rotational spectra are just beyond the limit of resolution at present. A generalization has been made for a spherical top with attached gyroscopes whose axes are rigidly fixed on the top according to certain symmetry requirements.

I. INTRODUCTION

CONSIDERABLE quantum-mechanical work has been done on the symmetrical top[1] and Nielsen[2] has treated a generalization in which there is a degree of torsional freedom between two principal parts of the rotator about an axis of symmetry. The present paper gives an exact solution for the spherical top with tetrahedrally spaced gyroscopes of equal moments of inertia. This wave equation is of interest because it becomes the rotational wave equation for tetramethylmethane, $C(CH_3)_4$, if a suitable potential function is added.

II. SOLUTION OF THE WAVE EQUATION

The five C atoms of tetramethylmethane, one at the center and four at the corners of a regular tetrahedron, are equivalent to a spherical top. The C atoms at the corners are the C atoms of four methyl groups each of which can rotate about a line through its C atom and the center atom. The methyl groups are equivalent to the tetrahedrally spaced gyroscopes.

The coordinates used are as follows. The angles α_1, α_2, α_3, and α_4 give the positions of the gyroscopes, or methyl groups, with respect to the C_5 tetrahedron. The angles θ, φ and χ are Eulerian angles giving the orientation of the tetrahedron. The axes x_0, y_0, z_0 in Fig. 1 are fixed in space while the axes x, y, z are fixed on the C_5 tetrahedron. θ is the angle between the z_0 and z axes, and φ and χ are, respectively, the angles between the line of nodes and the x and x_0 axes.

The kinetic energy T is given in terms of the angular velocities by the expression

$$2T=I\{\dot{\chi}^2+2\cos\theta\dot{\chi}\dot{\varphi}+\dot{\varphi}^2+\dot{\theta}^2\}+\sum_{k=1}^{4} I_s\{[(Q_{yk}\sin\varphi-Q_{xk}\cos\varphi)\sin\theta+Q_{zk}\cos\theta]2\dot{\chi}\dot{\alpha}_k$$
$$+[Q_{yk}\cos\varphi+Q_{xk}\sin\varphi]2\dot{\theta}\dot{\alpha}_k+2Q_{zk}\dot{\chi}\dot{\alpha}_k+\dot{\alpha}_k^2\}, \quad (1)$$

when I = moment of inertia of the whole molecule with the methyl groups fixed, I_s = moment of inertia of a methyl group about its axis of symmetry, and Q_{xk}, Q_{yk} and Q_{zk} = direction cosines on the previously described x, y and z axes of the axis of rotation of the kth methyl group.

The kinetic energy in terms of the momenta is given by

$$2T=\frac{1}{I_0}\left\{p_\theta^2+\frac{p_\chi^2}{\sin^2\theta}-\frac{2p_\varphi p_\chi\cos\theta}{\sin^2\theta}+\frac{p_\varphi^2}{\sin^2\theta}-\frac{2p_\chi}{\sin\theta}\sum_{k=1}^{4}(Q_{yk}\sin\varphi-Q_{xk}\cos\varphi)p_{\alpha k}\right.$$

[1] D. M. Dennison, Phys. Rev. **28**, 318 (1926); F. Reiche and H. Rademacher, Zeits. f. Physik **39**, 444 (1926); F. Reiche and H. Rademacher, Zeits. f. Physik **41**, 453 (1927); R. de L. Kronig and I. I. Rabi, Phys. Rev. **29**, 262 (1927); C. Manneback, Phys. Zeits. **28**, 72 (1927).

[2] H. H. Nielsen, Phys. Rev. **40**, 445 (1932).

$$-2p_\theta \sum_{k=1}^{4} (Q_{yk}\cos\varphi + Q_{xk}\sin\varphi)p_{\alpha k} - 2p_\varphi\left[\sum_{k=1}^{4} Q_{xk} - \frac{\cos\theta}{\sin\theta}\sum_{k=1}^{4}(Q_{yk}\sin\varphi - Q_{xk}\cos\varphi)\right]p_{\alpha k}$$

$$+ \sum_{k=1}^{4}\frac{I_0}{I_a}p_{\alpha k}^2 + \sum_{k,\,l=1}^{4} p_{\alpha k}p_{\alpha l}\cos kl\Bigg\}, \quad (2)$$

where $I_0 = I - (4/3)I_a$ and $\cos kl$ = the cosine of the angle between the axes of the kth and lth methyl groups.

The wave equation was obtained by the method given by Schrödinger.[3] It is

$$\frac{\partial}{\partial\theta}\left(\sin\theta\frac{\partial\Psi}{\partial\theta}\right) - 2\sin\theta\sum_{k=1}^{4}(Q_{yk}\cos\varphi + Q_{xk}\sin\varphi)\frac{\partial^2\Psi}{\partial\theta\partial\alpha_k} + \frac{1}{\sin\theta}\frac{\partial^2\Psi}{\partial\chi^2} - \frac{2\cos\theta}{\sin\theta}\frac{\partial^2\Psi}{\partial\chi\partial\varphi}$$

$$-2\sum_{k=1}^{4}(Q_{yk}\sin\varphi - Q_{xk}\cos\varphi)\frac{\partial^2\Psi}{\partial\chi\partial\alpha_k} + \frac{1}{\sin\theta}\frac{\partial^2\Psi}{\partial\varphi^2} - 2\sin\theta\sum_{k=1}^{4}Q_{xk}\frac{\partial^2\Psi}{\partial\varphi\partial\alpha_k}$$

$$+2\cos\theta\sum_{k=1}^{4}(Q_{yk}\sin\varphi - Q_{xk}\cos\varphi)\frac{\partial^2\Psi}{\partial\varphi\partial\alpha_k} + \sin\theta\sum_{k=1}^{4}\frac{I_0}{I_a}\frac{\partial^2\Psi}{\partial\alpha_k^2} + \sin\theta\sum_{k,\,l=1}^{4}\cos kl\frac{\partial^2\Psi}{\partial\alpha_k\partial\alpha_l}$$

$$+\frac{8\pi^2 I_0}{h^2}\sin\theta(E-V)\Psi = 0. \quad (3)$$

Only the case in which the potential is zero will be considered. For this case it can be seen from the wave equation that the α_k's are cyclic variables. The wave function can therefore be taken as

$$\Psi(\theta, \varphi, \chi, \alpha_1, \alpha_2, \alpha_3, \alpha_4) = \psi(\theta, \varphi, \chi)\prod_{k=1}^{4} e^{im_k\alpha_k}, \quad (4)$$

where the m_k's are integers because of the single-valuedness of Ψ. Substituting this wave function into the wave equation gives

$$\frac{\partial}{\partial\theta}\left(\sin\theta\frac{\partial\psi}{\partial\theta}\right) - 2i\sin\theta\left[\sum_{k=1}^{4} m_k(Q_{yk}\cos\varphi + Q_{xk}\sin\varphi)\right]\frac{\partial\psi}{\partial\theta} + \frac{1}{\sin\theta}\frac{\partial^2\psi}{\partial\chi^2} - \frac{2\cos\theta}{\sin\theta}\frac{\partial^2\psi}{\partial\chi\partial\varphi}$$

$$-2i\left[\sum_{k=1}^{4} m_k(Q_{yk}\sin\varphi - Q_{xk}\cos\varphi)\right]\frac{\partial\psi}{\partial\chi} + \frac{1}{\sin\theta}\frac{\partial^2\psi}{\partial\varphi^2} - 2i\sin\theta\sum_{k=1}^{4} m_k Q_{xk}\frac{\partial\psi}{\partial\varphi}$$

$$+2i\cos\theta\left[\sum_{k=1}^{4} m_k(Q_{yk}\sin\varphi - Q_{xk}\cos\varphi)\right]\frac{\partial\psi}{\partial\varphi} - \sin\theta\sum_{k=1}^{4}\frac{I_0}{I_a}m_k^2\psi$$

$$-\sin\theta\sum_{k,\,l=1}^{4}\cos klm_k m_l\psi + \frac{8\pi^2 I_0}{h^2}\sin\theta E\psi = 0. \quad (5)$$

It is possible to eliminate the terms in the preceding equation which involve φ explicitly by properly choosing the x, y, z axes with respect to the C_3 tetrahedron. These axes are fixed on the tetrahedron, but their orientation is arbitrary. The proper orientation for the elimination can be found as follows. Along the axes of rotation of the methyl groups consider momentum vectors whose

[3] E. Schrödinger, Ann. d. Physik **79**, 748 (1926); A. Sommerfeld, *Wave Mechanics*, p. 124, E. P. Dutton and Co. Inc.

magnitudes are given by the corresponding quantum numbers m_k. Then the expressions $\sum^4_{k=1} m_k Q_{xk}$, $\sum^4_{k=1} m_k Q_{yk}$, and $\sum^4_{k=1} m_k Q_{zk}$ are components along the x, y and z axes of the resultant momentum of the four methyl groups. For any given values of the m_k's it is always possible to choose the x, y and z axes in such a way that the resultant lies along the z-axis and therefore the x and y components are zero. This can be shown analytically as follows. Take any set of fixed axes x'', y'', z'' on the C_5 tetrahedron. Rotate β degrees about the z''-axis to get the new x', y', z' axes. Next rotate the primed axes δ degrees about the y' axis to get the x, y, z axes. Then the y and x components of the resultant momentum of the methyl groups are, respectively

$$\sum_{k=1}^{4} m_k Q_{yk} = K_2 \sin(\beta - \beta_0) \tag{6}$$

and

$$\sum_{k=1}^{4} m_k Q_{xk} = [K_3^2 + K_2^2 \cos^2(\beta - \beta_0)]^{\frac{1}{2}} \sin(\delta - \delta_0) \tag{7}$$

where K_2, K_3, β_0, and δ_0 depend only on the m_k's and are therefore constant for any particular choice of the m_k's. Taking $\beta = \beta_0$ and $\delta = \delta_0$ gives

$$\sum_{k=1}^{4} m_k Q_{yk} = 0, \tag{8}$$

$$\sum_{k=1}^{4} m_k Q_{xk} = 0, \tag{9}$$

and

$$\sum_{k=1}^{4} m_k Q_{zk} = \left(\sum_{k,\ l=1}^{4} \cos klm_k m_l \right)^{\frac{1}{2}} = \text{the resultant momentum of the four methyl groups.} \tag{10}$$

Define

$$Q = \left(\sum_{k,\ l=1}^{4} \cos klm_k m_l \right)^{\frac{1}{2}}. \tag{11}$$

Then the wave equation becomes

$$\frac{\partial}{\partial\theta}\left(\sin\theta\frac{\partial\psi}{\partial\theta}\right) + \frac{1}{\sin\theta}\frac{\partial^2\psi}{\partial\chi^2} - \frac{2\cos\theta}{\sin\theta}\frac{\partial^2\psi}{\partial\chi\partial\varphi} + \frac{1}{\sin\theta}\frac{\partial^2\psi}{\partial\varphi^2} - 2i\sin\theta Q\frac{\partial\psi}{\partial\varphi} - \sin\theta\sum_{k=1}^{4}\frac{I_0}{I_e}m_k^2\psi$$

$$-\sin\theta Q^2\psi + \frac{8\pi^2 I_0}{h^2}\sin\theta E\psi = 0. \tag{12}$$

Since χ and φ are cyclic, ψ may be taken as

$$\psi(\theta, \varphi, \chi) = \Theta(\theta) e^{im_\varphi \varphi} e^{im_\chi \chi}, \tag{13}$$

where m_χ and m_φ are integers because of the single-valuedness of Ψ. Substituting this value of ψ into the wave equation gives

$$\sin\theta\frac{d}{d\theta}\left(\sin\theta\frac{d\Theta}{d\theta}\right) - \left[m_\chi^2 + m_\varphi^2 - 2m_\chi m_\varphi\cos\theta + \left(\sum_{k=1}^{4}\frac{I_0}{I_e}m_k^2 + Q^2 - 2Qm_\varphi - \frac{8\pi^2 I_0}{h^2}E\right)\sin^2\theta\right]\Theta = 0. \tag{14}$$

Let

$$\lambda = (8\pi^2 I_0/h^2)E - \sum_{k=1}^{4}(I_0/I_e)m_k^2 - Q^2 + 2Qm_\varphi. \tag{15}$$

Then the wave equation becomes identical with the wave equation for the symmetrical top.[4] The

[4] A. Sommerfeld, reference 3, p. 131.

function $\Theta(\theta)$ involves Jacobian polynomials; an expression is given for it later. The energy levels are given by the formula

$$E=(h^2/8\pi^2I_0)\{j(j+1)+\sum_{k=1}^{4}(I_0/I_k)m_k^2+Q^2-2Qm_\varphi\}, \tag{16}$$

where the total quantum number j is an integer equal to or greater than the larger of the two quantities $|m_\varphi|$ and $|m_\chi|$, and Q is the vector sum of the momenta of the methyl groups as given by Eq. (11).

III. Selection Rules

It has been mentioned that the φ-axis was taken in the direction of the resultant momentum of the methyl groups in order to separate the variables. It will now be shown that selection rules for j, m_φ, and m_χ can be obtained for transitions in which it is not necessary to shift the φ-axis, or in other words for transitions in which the direction of the resultant momentum of the methyl groups is not changed with respect to the C_5 tetrahedron. If no interaction between vibration and rotation is assumed, then the wave function can be written as

$$\Psi(\theta, \chi, \varphi, \alpha_1, \cdots\alpha_4, \xi_1, \cdots\xi_n)=\psi(\theta, \chi, \varphi)e^{im_1\alpha_1}\cdots e^{im_4\alpha_4}H_1(\xi_1)\cdots H_n(\xi_n), \tag{17}$$

when the ξ_k's are normal coordinates of vibration, and the $H_k(\xi_k)$'s are the corresponding eigenfunctions.

Let M_i and β_{ik} be, respectively, the electric moment and polarization for axes fixed in space and $M_{i'}$ and $\beta_{i'k'}$ the moment and polarization for axes fixed on the sphere. Then

$$M_i=\sum_{i'}M_{i'}\cos ii' \qquad (18) \qquad \text{and} \qquad \beta_{ik}=\sum_{i',\,k'}\beta_{i'k'}\cos ii'\cos kk', \tag{19}$$

when $\cos ii'$ is the cosine of the angle between the i and i' axes. It can be seen that $M_{i'}$ and $\beta_{i'k'}$ depend on the α_k's and ξ_k's, and the quantum numbers m_1, m_2, m_3 and m_4, which determine the direction of the φ-axis, while the functions $\cos ii'$ depend only on θ, χ, and φ. The matrix elements for the infrared and Raman transition probabilities can therefore be written as

$$(M_i)_{V',\,m_1',\,\cdots m_4',\,j',\,m'_\varphi,\,m'_\chi}^{V,\,m_1,\,\cdots m_4,\,j,\,m_\varphi,\,m_\chi}=\sum_{i'}(M_{i'})_{V',\,m_1',\,\cdots m_4'}^{V,\,m_1,\,\cdots m_4}(\cos ii')_{j',\,m'_\varphi,\,m'_\chi}^{j,\,m_\varphi,\,m_\chi} \tag{20}$$

and

$$(\beta_{ik})_{V',\,m_1',\,\cdots m_4',\,j',\,m'_\varphi,\,m'_\chi}^{V,\,m_1,\,\cdots m_4,\,j,\,m_\varphi,\,m_\chi}=\sum_{i'k'}(\beta_{i'k'})_{V',\,m_1',\,\cdots m_4'}^{V,\,m_1,\,\cdots m_4}(\cos ii'\cos kk')_{j',\,m'_\varphi,\,m'_\chi}^{j,\,m_\varphi,\,m_\chi}, \tag{21}$$

when V and V' represent the totality of vibration quantum numbers. It will be seen that the matrix elements $(\cos ii')_{j',\,m'_\varphi,\,m'_\chi}^{j,\,m_\varphi,\,m_\chi}$ and $(\cos ii'\cos kk')_{j',\,m'_\varphi,\,m'_\chi}^{j,\,m_\varphi,\,m_\chi}$ are the same as those occurring in the corresponding matrices for the symmetrical top. The selection rules for this case are therefore as follows. For infrared transitions Δj, Δm_φ and Δm_χ can have the values 0 or ±1, while for Raman transitions they can have the values 0, ±1, or ±2.

A rough idea of the selection rules for the methyl group quantum numbers can be obtained as follows. Consider classically, first, vibrations of the H atoms of a single methyl group, the C atoms being assumed fixed, and second, vibrations of the C atoms, the H atoms being assumed rigidly fixed to them. The forces and masses involved in these two classes of vibrations show that the frequencies of the two classes differ considerably. It follows that the normal coordinates of vibration of the tetramethylmethane molecule can be divided into two classes with the following properties. Each normal coordinate in the first class depends almost entirely on the coordinates of the H atoms of a single methyl group while the normal coordinates in the second class depend almost entirely on the coordinates of the C atoms. Designate the quantum numbers of the first class by V_1 and V_1' and those of the second class by V_2 and V_2'.

Let the assumption now be made that the electric moment $M_{i'}$ and the polarizability $\beta_{i'k'}$ with respect to the C_5 tetrahedron can be expressed as follows

$$M_{i'}=M_{i'}^{(c)}+\sum_l M_{i'}^{(l)} \quad (22) \qquad \text{and} \qquad \beta_{i'k'}=\beta_{i'k'}^{(c)}+\sum_l \beta_{i'k'}^{(l)}, \quad (23)$$

where the first term on the right in both expressions depends only on the coordinates of the C atoms, and $M_{i'}^{(l)}$ and $\beta_{i'k'}^{(l)}$ depend only on the coordinates of the H atoms in the lth methyl group. The remainder of the argument will be carried out only for the electric moment; it can be applied equally well to the polarizability. Let $M_{i''_l}$ represent the moment of the H atoms of the lth methyl group with respect to axes fixed on this methyl group. Then Eq. (22) becomes

$$M_{i'}=M_{i'}^{(c)}+\sum_{l,\, i''_l} M_{i''_l}\cos i'i''_l, \quad (24)$$

when $\cos i'i''_l$ represents the cosine of the angle between the i' axis and the i''_l axis on the lth methyl group. The matrix element can then be expressed as

$$(M_i)^{j,\, m_\varphi,\, m_\chi,\, \nu_1,\, \nu_2,\, m_1,\, \cdots m_4}_{j',\, m_\varphi',\, m'_\chi,\, \nu_1',\, \nu_2',\, m_1',\, \cdots m_4'}=\sum_{i'}(\cos ii')^{j,\, m_\varphi,\, m_\chi}_{j',\, m_\varphi',\, m'_\chi}\left((M_{i'})^{\nu_1,\, m_1,\, \cdots m_4}_{\nu_1',\, m_1',\, \cdots m_4'}\right)^{\nu_2}_{\nu_2'} \quad (25)$$

when

$$(M_{i'})^{\nu_1,\, m_1,\, \cdots m_4}_{\nu_1',\, m_1',\, \cdots m_4'}=(M_{i'^{(c)}})^{\nu_1}_{\nu_1'}\int e^{i(m_1-m_1')\alpha_1}\cdots e^{i(m_4-m_4')\alpha_4}d\alpha_1\cdots d\alpha_4$$

$$+\sum_{l,\, i''_l}(M_{i''_l})^{\nu_1}_{\nu_1'}\int \cos i'i''_l\, e^{i(m_1-m_1')\alpha_1}\cdots e^{i(m_4-m_4')\alpha_4}d\alpha_1\cdots d\alpha_4. \quad (26)$$

The first integral is zero unless all the m_k's do not change, while the parts of the other integrals involving α_l are the same as those occurring in the case of the rotator. The selection rules therefore become $\Delta m_k=0,\ \pm1$ for infrared transitions. A similar treatment gives $\Delta m_k=0,\ \pm1,\ \pm2$ for Raman transitions. It also follows from Eq. (26) that two m_k's cannot change simultaneously; this is a result of the assumed independence of the electric moment and polarization of the methyl groups. Since this assumption is not strictly true, the selection rules obtained for the m_k's are only approximate.

IV. Discussion of Wave Functions, Energy Levels, and Selection Rules

In summing up it may be said that the Eulerian angle χ and the four angles α_k giving the positions of the methyl groups were cyclic. The Eulerian angle φ was made cyclic by taking the φ-axis in the direction of the resultant momentum of the methyl groups. This gave the following wave function

$$\Psi(\theta,\, \chi,\, \varphi,\, \alpha_1,\, \alpha_2,\, \alpha_3,\, \alpha_4)=\Theta(\theta)e^{im_\chi\chi}e^{im_\varphi\varphi}e^{im_1\alpha_1}e^{im_2\alpha_2}e^{im_3\alpha_3}e^{im_4\alpha_4}, \quad (27)$$

where the quantum numbers are all integers because of the single-valuedness of Ψ. The differential equation obtained for $\Theta(\theta)$ is the well-known one obtained in the case of the symmetrical top. The function $\Theta(\theta)$ is a polynomial of the lth degree in $\cos\theta$ and has the form

$$\Theta_l^{(m_\varphi)(m_\chi)}(\theta)=(1-x)^{|m_\varphi-m_\chi|/2}(1+x)^{|m_\varphi+m_\chi|/2}G_{l-m^*}(p,\, q,\, x), \quad (28)$$

when

$$m^*=(|m_\varphi-m_\chi|+|m_\varphi+m_\chi|)/2, \quad (29)$$

$$G_{l-m^*}(p,\, q,\, x)=\frac{x^{1-q}(1-x)^{q-p}}{q(q+1)\cdots(q+l-m^*-1)}\frac{d^{l-m^*}}{dx^{l-m^*}}\left[x^{q+l-m^*-1}(1-x)^{p+l-m^*-q}\right], \quad (30)$$

$$q=1+|m_\varphi+m_\chi|, \quad (31) \qquad p=2m^*+1 \quad (32) \qquad \text{and} \qquad x=(1+\cos\theta)/2. \quad (33)$$

The function $G_{l-m^*}(p,\, q,\, x)$ is the $l-m$th Jacobian polynomial in x.

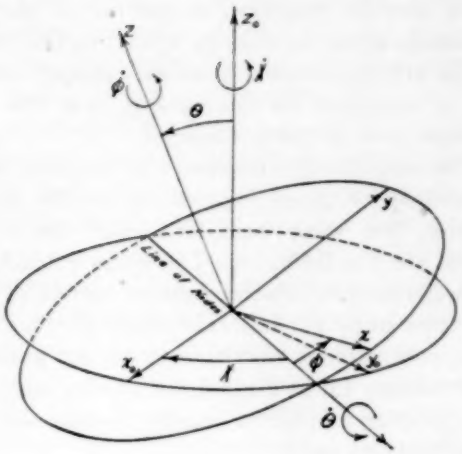

FIG. 1. Eulerian angles.

The energy levels are given by Eq. (16). A diagram of the lower levels is given in Fig. 2 where the lower levels are also given for a molecule of tetramethylmethane with the methyl groups assumed fixed, which is the limiting case of the rotational motion for low temperatures. It can be seen from Fig. 2 that the six lowest energy levels for the two cases nearly coincide. They do not coincide exactly because the moment of inertia of a molecule with free methyl groups is slightly less than it would be if the methyl groups were fixed. This can be seen from the following classical consideration. Consider a torque applied to the molecule about one of its methyl group axes. This methyl group will not have to be accelerated, and therefore a greater acceleration will be given to the rest of the molecule than would be the case if the methyl groups were fixed.

The energy levels above the sixth are spread out compared to those for the rigid spherical top. This is caused by removal of the degeneracy in m_φ in levels above the sixth. The energy levels might be used in calculating the specific heat, and the spreading out of the levels for the case of free rotation might make possible an estimation of the potential function between the methyl groups.

Although the rotational spectra of tetramethylmethane are at present just beyond the limit of resolution, the selection rules may be of value later. For transitions in which the direction of the resultant momentum of the methyl groups remains the same with respect to the C_3 tetrahedron, the selection rules are the same as for a symmetrical top, namely, Δj, Δm_φ and Δm_χ can have the values 0 or ± 1 for infrared transitions and the values 0, ± 1, or ± 2 for Raman transitions. In transitions of the methyl group quantum numbers which involve a shift in the φ-axis, the selection rules for j, m_φ, and m_χ are probably much less sharp because the φ-axis is shifted in a rather arbitrary manner. Approximate selection rules were obtained for the methyl group quantum numbers by assuming that the interaction of H atoms in different methyl groups did not affect the electric moment or polarization. These approximate selection rules indicate that the stronger lines probably occur for infrared transitions in which $\Delta m_k = 0$ or ± 1 and for Raman transitions in which $\Delta m_k = 0$, ± 1, or ± 2.

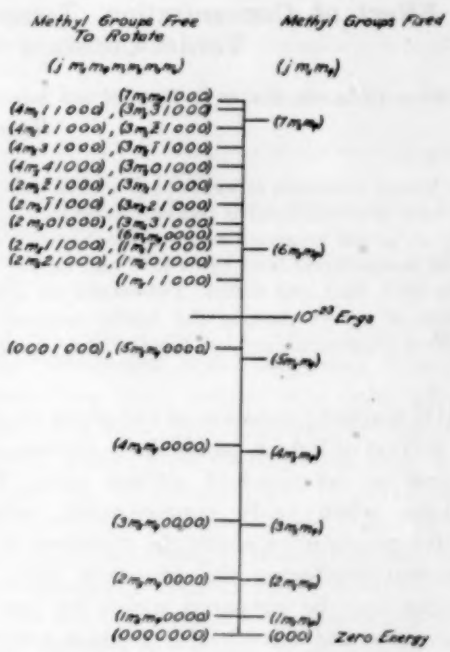

FIG. 2. Energy levels.

V. GENERALIZATION

It has been found possible to generalize the conditions for which a wave equation analogous to Eq. (3) applies. Consider a rigid body with gyroscopes attached to it in such a way that the axes of the gyroscopes pass through the center

of gravity of the combination, the axes being fixed on the rigid frame. Assume the following three conditions to be fulfilled.

(I) The combination of the rigid frame and gyroscopes is a spherical top for all values of the coordinates giving the positions of the gyroscopes.

(II) Each of the gyroscopes is a symmetrical top which rotates about its unique axis through its center of gravity.

(III) The axes of the gyroscopes are placed in such a way that

$$\sum_{k=1}^{n} I_k Q_k^2 = K_1,$$

when I_k = the moment of inertia of the kth gyroscope about its axis, Q_k = the direction cosine of the kth gyroscope axis on an arbitrary axis q, K_1 = a constant for all axes q, and the sum extends over all the gyroscopes.

The only changes necessary to be made in the previously obtained expressions for the kinetic energy, the wave equations, and the energy levels are the following. The sums extend over all n gyroscopes; the moment of inertia I_s must be replaced by I_k; and I_0 becomes $I - K_1$.

In conclusion I wish to express my gratitude to Professor Linus Pauling for having suggested this problem and for having made many valuable contributions to it.

OCTOBER 15, 1934 PHYSICAL REVIEW VOLUME 46

The Effect of Concentration, Temperature and Wave-Length of Light upon the Verdet Constant of Cerous Chloride Solutions

FRANCIS G. SLACK, RALPH L. REEVES AND JAMES A. PEOPLES, JR., *Department of Physics, Vanderbilt University*

(Received June 20, 1934)

The Verdet constants of solutions of cerous chloride in water have been measured at concentrations varying from zero to an almost saturated solution. Measurements were made at temperatures from 10 to 45°C and for the wave-lengths 5893, 5461 and 4481A. The results are given in the form of curves showing the Verdet constant as a function of temperature and as a function of concentration. Tabulated values of the concentration, density, index of refraction and Verdet constant of the solutions are also given. Attention is called to the point that the effect attributed by Allison and Condon to a time lag in the Faraday effect may have been due to a temperature change during the course of their observations.

THE magnetic rotation of the plane of polarization of light is particularly interesting in the case of solutions of cerium salts. These solutions, when fairly concentrated, cause a negative rotation (opposite the direction of flow of current producing the magnetic field) and solutions may be prepared which for any one temperature and wave-length produce zero rotation. Data on the Verdet constant of these materials are not found in any standard tables nor in the literature.

The Verdet constants of solutions of cerous chloride in water from zero concentration to an almost saturated solution have been measured at temperatures from 10°C to 45°C. for three wave-lengths of light. The rotations were measured by means of a Schmidt and Haensch "Lippich" half-shade polarimeter, which could be read to hundredths of a degree. The three light sources used were: (1) the mercury "Lab-arc" with Corning Didymium and G34-Y filters to transmit λ5460.7A; (2) a sodium arc with Jena filters OG-1 and VG-1 (each 2 mm) to transmit the D lines at λ5893; (3) a spark between magnesium electrodes with Jena filters BG-4 plus GG-3 (each 2 mm) to transmit the spark line at λ4481. The spark was operated from a Thordarson spark transformer with a condenser across the secondary.

The liquid whose rotation was being measured was placed in a water jacketed cell[1] 26.15 cm

[1] Thanks are due to Professor H. W. Farwell of Columbia University for the use of these cells.

long with cover glass ends waxed on. The temperature of this cell and contents was controlled by a constant pressure water flow through the jacket which surrounded the cell. The temperature of the water was varied at will by appropriate heaters. Thermometers at the entrance and exit of the water jacket were read frequently during observations and their average taken as the temperature of the liquid during the measurement. These temperatures were held steady for some time prior to starting measurements and the two thermometer readings rarely differed by as much as a degree in spite of the heating, due to the coil used to produce the magnetic field. Thermocouple measurements taken inside the cell agreed within a few tenths of a degree with the average thermometer readings.

The magnetic field was produced by a coil of fifteen layers of No. 20 B. & S. cotton and enamel covered copper wire. The average length of these layers was 18.0 cm and the average number of turns 178.3. The radius of the innermost coil was 1.33 cm, and that of the outermost 1.83 cm. From these data the field strength H at any point along the axis of the cell is easily calculated. By integration the product of the effective field strength times the length of path of the light in the cell is determined. The value of this integral $\int Hdl$ was found to be 3202.2 gauss-cm per ampere of current through the coil. The Verdet constant is then $V=\theta/\int Hdl$, where θ is the measured rotation in minutes per ampere of current. Normally a current of four amperes was used. This current was supplied from a generator and controlled by a fine adjustment rheostat. In order that this adjustment might be accurately made a Leeds and Northrup Type K potentiometer was used to measure the potential drop across a standard 0.10 ohm resistance in series with the coil. The control rheostat was operated by one person so that the galvanometer connected to the potentiometer showed no deflection when observations were made. Since the current through the coil caused considerable heating effect, it was allowed to flow only while observations were being made and was readjusted for each observation. Several observations were made for each point with the light both parallel and anti-parallel to the magnetic field.

As a check on the absolute value of the field strength and on the general set-up the Verdet constant of carbon bisulphide was measured for the mercury and sodium lights and found to check within 0.10 percent of the values given in the *International Critical Tables*.

The cerous chloride salt was obtained from Eimer and Amend. It was C. P. quality with seven molecules of water of crystallization ($CeCl_3$–$7H_2O$). The manufacturer's analysis showed this material to be better than 99.9 percent pure, the impurities being traces of didymium and lanthanum. Specimens Nos. 1–5 inclusive were mixed from one sample and specimens 10, 11 and 12 from a second sample. The solutions were mixed as follows:

Solution No. 1. 50 grams of $CeCl_3$–$7H_2O$ were dissolved in 50 cc of Pyrex distilled water;

Solution No. 2. 15 cc of water were added to 50 cc of solution No. 1;

Solution No. 3. 25 cc of water were added to 50 cc of solution No. 2;

Solution No. 4. 35 cc of water were added to 50 cc of solution No. 3;

Solution No. 5. 60 cc of water were added to 50 cc of solution No. 4;

Solution No. 10. 68.924 grams of $CeCl_3$–$7H_2O$ were dissolved in 45.75 cc of water;

Solution No. 11. 15 cc of water were added to 50 cc of solution No. 10;

Solution No. 12. 35 cc of water were added to 40 cc of solution No. 11.

Solutions Nos. 1 and 10 when mixed were a murky brown color, non-transparent. After being filtered twice these cleared to a pale yellow or amber color and were sufficiently transparent for good observation through the cell. It was necessary to refilter solution No. 11, due to formation of the brown precipitate but the filtration did not change the rotation noticeably. The concentrations given in Table I are calculated by the above data from chemical analyses run on samples Nos. 3, 4, 5, 10 and 12. These analyses[2] were made by the precipitation of cerous oxalate from weakly acidic cerous salt solutions upon the addition of a slight excess of oxalic acid. The precipitations were allowed to stand until distinctly crystalline (24 hrs.), then the cerous oxalate was filtered off, washed, and

[2] Thanks are due Mr. W. R. Myers and Mr. Julian Little of the Chemistry Department for these analyses.

TABLE I.

Solution number	Concentration (g of $CeCl_3$ per cc of sol)	Density (g/cc at 20°)	Index of refraction (26–30°) 5893	Verdet constant $\times 10^3$ minutes per gauss-centimeter 15°	20°	30°	40°	45°
				Mercury line λ5460.7A				
10	0.6415	1.5872	1.4476	−31.35	−30.4	−28.8	−27.6	−26.95
11	0.4935	1.4575	1.4257	−18.60	−17.7	−16.9	−16.15	−15.8
1	0.4670	1.4393	1.4211	−16.9	−16.3	−15.25	−14.2	−13.7
2	0.3592	1.3417	1.4015	− 8.85	− 8.35	− 7.42	− 6.43	− 5.95
12	0.2631	1.2449	1.3820	− 1.75	− 1.45	− 0.85	− 0.35	− 0.10
3	0.2395	1.2270	1.3782	− 0.35	0.00	+ 0.60	+ 1.25	+ 1.60
4	0.1409	1.1335	1.3594	+ 6.42	+ 6.60	+ 6.90	+ 7.25	+ 7.40
5	0.0641	1.0619	1.3449	+11.45	+11.5	+11.7	+11.8	+11.9
Water	0.00	1.000	1.3324	+15.65	+15.6	+15.46	+15.35	+15.3
				Sodium *D* lines λ5893A				
10	0.6415	1.5872	1.4476	−25.6	−24.7	−23.3	−22.1	−21.5
11	0.4935	1.4575	1.4257	−14.85	−14.40	−13.60	−12.7	−12.28
12	0.2631	1.2449	1.3820	− 1.10	− 0.80	− 0.35	+ 0.20	+ 0.45
Water	0.00	1.000	1.3324	+13.20	+13.19	+13.20	+13.18	+13.17
				Magnesium spark line λ4481A				
10	0.6415	1.5872	1.4476	−42.75	−41.55	−39.20	−36.80	−35.60
11	0.4935	1.4575	1.4257	−28.0	−26.75	−25.1	−23.4	−22.75
12	0.2631	1.2449	1.3820	− 5.85	− 5.40	− 4.45	− 3.45	− 3.00

ignited to ceric oxide. The weight of the CeO_2 obtained from a measured sample was thus found and this value converted to the amount of $CeCl_3$ in the original sample. The values obtained for the different samples checked well among themselves and also with concentrations calculated from the known quantities of the ingredients.

The density of each solution was measured at 20°C. The index of refraction at room temperature (26–30°C) for the sodium *D* lines was also measured. These values are given in Table I.

The results of the measurements are given in Figs. 1 and 2 and in Table I. Fig. 1 shows the variation of the Verdet constant with temperature for each of the solutions and for pure water. Only the data for the mercury green light are plotted. Since it was difficult to make observations on the different solutions at the same temperature, the data for Fig. 2 and that given in Table I are taken from large scale graphs similar to Fig. 1. Fig. 2 shows the variation of the Verdet constant with concentration, all points being taken at 20°C. A curve is shown for each wave-length used. Table I gives the solution number, concentration, density, index of refraction, and Verdet constant at several temperatures. From these data curves similar to those shown may be plotted for all cases.

The curves of Fig. 1 indicate, for the more concentrated solutions, a slight departure from the straight line relation between temperature and Verdet constant. This occurs at the lower temperatures. The slope of the curve for pure water is reversed from that for the solutions. This indicates that it would be possible to mix a very dilute solution having no temperature effect over this range of temperatures. The effect of temperature is much greater for the more concentrated solutions. It is also greater for the shorter wave-lengths.

The curves of Fig. 2, showing the variation of the Verdet constant with concentration at one temperature for the three wave-lengths, indicate a departure from the straight line relation at high concentrations. The Schönrock rule of mixtures holds only for the more dilute solutions. The curves cross the axis of zero rotation at concentrations of 0.250 g/cc, 0.240 g/cc and 0.215 g/cc, respectively, for the wave-lengths λ5893, λ5461 and λ4481A. The point shown for λ4481 and pure water was taken from the *Smithsonian Physical Tables* since no data were taken for this point.

Recently Mlle. J. Pernet[3] has measured the magnetic rotatory power of cerous chloride solutions in an attempt to establish a law for the Verdet constant of paramagnetic substances

[3] Mlle. J. Pernet, Comptes Rendus **195**, 376 (1932).

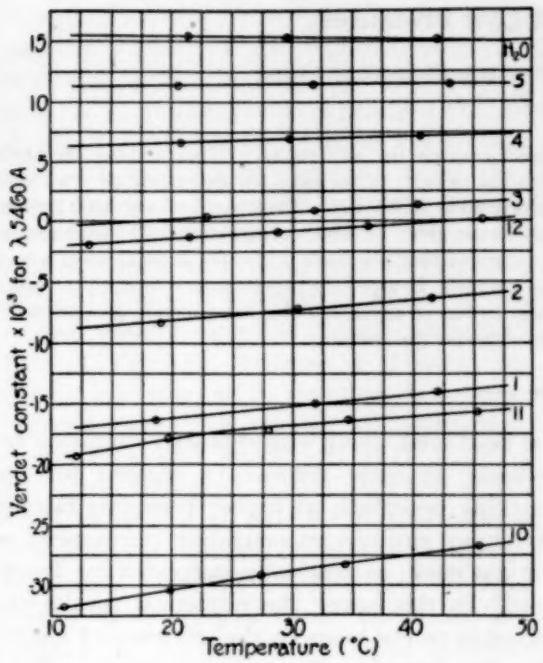

FIG. 1. The Verdet constant for solutions of cerous chloride in water at various concentrations as a function of temperature. All measurements for the mercury green line —λ5460.7A.

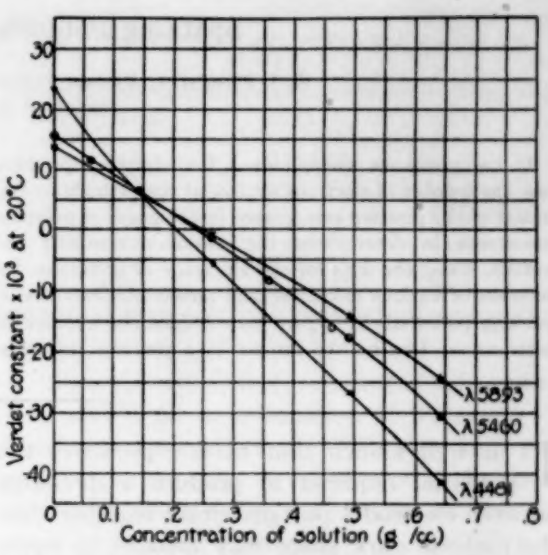

FIG. 2. The Verdet constant for solutions of cerous chloride in water at various wave-lengths of light as a function of concentration. Temperature 20°C.

analogous to that of Weiss for Magnetic Susceptibilities. Pernet's paper is devoted to a discussion of the shape of the curves obtained. She does not show the curves nor give sufficient data to construct them. She does, however, state that for the mercury green line zero rotation was obtained at 22.6°C for a solution of 0.196 g of $CeCl_3$ per g of solution. This is in good agreement with the value here found of $0.240/1.227 = 0.196$ g of $CeCl_3$ per g of solution for zero rotation at 20°C, and with the value 0.198 g of $CeCl_3$ per g of solution at 22.6°C obtained by interpolation from our data.

It is apparent from the curves and from the data of Table I that a solution which gives zero rotation at one temperature will show a noticeable rotation for a temperature differing by only two or three degrees from the temperature of zero rotation. This effect is offered as a possible explanation of the observations of Allison and Condon.[4] Allison and Condon found that a solution which gave zero rotation for a steady magnetic field showed a definite rotation when a high frequency field was applied. They interpreted these data in terms of a time lag in the Faraday effect. It would require very careful temperature control to establish definitely that the data are dependent on frequency and not on temperature. Allison and Condon made their measurements with the magnesium spark line. Data from Table I show the slope of the Verdet constant-temperature curves to be somewhat greater for the magnesium spark line than for the longer wave-lengths.

In conclusion the authors wish to express their appreciation to Mr. T. Lynn for his assistance in making many of the measurements.

[4] Fred Allison and John L. Condon, Phys. Rev. 40, 1021 (1932).

Sparking Potentials at Low Pressures

A. J. DEMPSTER, *Ryerson Physical Laboratory, University of Chicago*
(Received August 29, 1934)

At low pressures where only a few electrons produce ions, the number of electrons set free at the cathode by the impact of the positive ions formed in the gas is of primary importance in determining the minimum sparking potentials. Using the data for the efficiency of ionization by electrons of various velocities, and recent observations of sparking potentials in air, we may deduce the number of electrons set free by the impact of a positive ion on a nickel cathode for any velocity. This number increases with the velocity of the ion from approximately 4 at 3000 volts to 85 at 30,000 volts. These numbers are much greater than those given by direct observations. The explanation is suggested that the spark originates at small spots where the emission is especially abundant, whereas the direct observations of secondary electron emission give an average value for the surface.

IT is well known that at low pressures the potential required to produce a discharge between electrodes that are closer together than the cathode dark space may amount to many thousand volts. The theories of the sparking potential that are based on the occurrence of repeated ionization by collisions of the electrons, or of the positive ions, with the gas molecules, are not applicable to this case of low pressure and high voltage. For example, in air at a pressure of 0.06 mm a potential difference of 20,000 volts is required to produce a discharge between nickel electrodes 1 cm apart. Now from experiments on the number of ions made by an electron in going 1 cm we find that only one-tenth of the electrons leaving the cathode would produce even one positive particle. These positives at low speeds are much less efficient ionizers than the electrons, and at high velocities possibly do not produce any free electrons at all, but merely neutralize themselves by detaching an electron from a neutral molecule. Photoelectrons would also become relatively unimportant as the pressure is reduced and in general the probability of excitation by fast electrons is small compared with the probability of ionization.[1] Photoelectric emission due to radiation excited by the impact of the electrons on the anode must be small as it is negligible in high voltage kenotrons and x-ray tubes.

We are thus led to consider the possibility of interpreting the electrical break down at low pressures and high potentials as due primarily to the release of electrons from the cathode under the impact of the positive ions. This phenomenon has been used, along with repeated ionization by collision, in some theories to account for the sparking potentials at higher pressures instead of relying entirely on ionization phenomena in the gas itself, as originally suggested by Townsend.[2] In this paper the numerical results obtained in recent years on the efficiency of ionization by electrons of various velocities, will be made use of in calculating the number of positives produced in the gas. If the efficiency of the production of secondary electrons at the cathode by positive ion bombardment were known for all ion and metal combinations, we could then deduce the sparking potentials. Our knowledge of this subject is still, however, very incomplete, especially at high velocities.[3] More precise experimental observations can be made of the sparking potentials with various gases and metal electrodes, and the connection between the two phenomena discussed below allows us to deduce the number of electrons emitted under the bombardment of positive ions of any velocity from the minimum sparking potential.

MINIMUM SPARKING POTENTIAL AND PROBABILITY OF IONIZATION

The number of secondary electrons s produced by an electron in going 1 cm through a gas at a pressure of 1 mm of mercury has been determined by several observers. Buchmann[4] gives a sum-

[1] K. K. Darrow, *Electrical Phenomena in Gases*, p. 98.

[2] G. Holst and E. Oosterhuis, Phil. Mag. **46**, 1117 (1923). For a discussion of these theories and observations see: K. K. Darrow, *Electrical Phenomena in Gases*, p. 280.

[3] For references and some experiments with alkali ions see W. S. Stein, Phys. Rev. **40**, 425 (1932).

[4] E. Buchmann, Ann. d. Physik **87**, 524 (1928).

mary in which $s(V)$ is recorded for air for various electron voltages V up to 29,000 volts. If the potential applied between two electrodes 1 cm apart is V_0, and the potential gradient is uniform, an electron leaving the cathode will produce in 1 cm at 1 mm pressure, a number of positive ions given by $(1/V_0)\int_0^{V_0} s(V)dV$. If the distance is d cm this number is multiplied by d. The positive ions will reach the cathode with various energies depending on the position at which they were formed, and on impact will set free various numbers of electrons. Suppose a positive ion of energy V releases $m(V)$ electrons on striking the cathode. Since the number of positives with energy between V and $V+\Delta V$ is $(1/V_0)s(V)\Delta V$, and these release $(1/V_0)s(V)m(V)\Delta V$ electrons from the cathode, we have for the total number of new electrons, released by all the positives, the expression $(1/V_0)\int_0^{V_0} s(V)m(V)dV$. If this is greater than unity a spark will occur, as the number of electrons is multiplied indefinitely. If the pressure is p mm of Hg and the distance is d cm the minimum potential V for a spark is given by $(pd/V)\int_0^V s(V)m(V)dV=1$. This relation connects the minimum sparking potential V with the efficiency of production of electrons $m(V)$ by positive ion impact, when $s(V)$ is sufficiently well known.

We shall use some as yet unpublished observations by S. S. Cerwin on the minimum sparking potentials in air at low pressures with carefully outgassed nickel electrodes, to illustrate how the function $m(V)$ may be deduced. Cerwin's observations for low pressures (p, mm) and short distances (d, cm) such that $p.d.<0.095$ may be shown to agree with the formula, $pde^{V/43,500}=0.10$. If we equate this expression involving V to the above integral expression for the same value of $p.d.$, and differentiate we find,

$$10e^{V/43,500}\left(1+\frac{V}{43,500}\right)=s(V)m(V).$$

Using Buchmann's values for $s(V)$ we deduce the values of $m(V)$ given in Table I. It is of interest that for voltages above 10,000, the number $m(V)$ increases approximately linearly with the voltage. It is quite unnecessary for the observations of V to be expressed in a formula. The experiments give V directly in terms of $p.d.$, and we may plot $1/pd$ as a function of V, say $f(V)$. From this a second curve $Vf(V)$ may be drawn which gives the value of the integral in the above expression for sparking potentials, so that the slope of this curve at any V is the value of $s(V)m(V)$.

TABLE I. *$s(V)$ ionizing collisions in 1 cm at 1 mm pressure; $m(V)$ secondary electrons set free by a positive ion of energy V.*

V (volts)	$s(V)$	$m(V)$
3000	2.70	4.0
5800	2.03	6.35
10600	1.27	12.7
14200	0.90	21.2
18000	0.625	34.7
26000	0.425	71.2
30000	0.40	84.5

When we compare the values of $m(V)$ deduced in this manner, with the direct observations of secondary electron emission we are struck by the fact that Fuchtbauer,[5] Campbell,[6] Baerwald,[7] Stein,[3] and Schneider[8] all found much smaller values. Schneider, for example, found between 4 and 4.6 electrons set free by a hydrogen ion impinging on various metals with energies between 23 and 46 kilovolts.

The most reasonable explanation for the larger numbers in Table I, is that the electron emission in sparking potential observations occurs under very special conditions. A strong field acts at the surface and would be expected to reduce the work function as in thermionic emission. Furthermore a spark will begin at the most favorable spot on the cathode if a sensitive point should exist. On the other hand, the direct observations of secondary electron emission under positive ion bombardment have hitherto been made with very weak fields at the surface of the metal, and the observations give only the average electron emission over the surface.

It is known that in thermionic emission of electrons, sensitive spots on the cathode exist, from which the emission is very much stronger than from other areas at the same tempera-

[5] C. Fuchtbauer, Phys. Zeits. **7**, 153 (1906).
[6] N. Campbell, Phil. Mag. **29**, 783 (1915).
[7] H. Baerwald, Handb. d. Physik, **24**, p. 106.
[8] G. Schneider, Ann. d. Physik **11**, 382 (1931).

ture,[9,10] and it is quite reasonable to suppose that the electron emission under positive ion bombardment is also much greater from some spots on the cathode than from others. There is thus no disagreement with the above theory of the sparking potential, and the values in Table I can be taken as applying to the emission from these sensitive areas.

[9] H. Seemann, Zeits. f. Physik **79**, 742–752 (1932).
[10] A. J. Dempster, Phys. Rev. **46**, 165 (1934).

OCTOBER 15, 1934 PHYSICAL REVIEW VOLUME 46

Vibrations of Tetrahedral Pentatomic Molecules
Part III. Comparison with Experimental Data. Part IV. Isotopic Shifts

JENNY E. ROSENTHAL, *Physics Department, University of Michigan*
(Received August 20, 1934)

Part III. Various specific assumptions as to intramolecular forces are discussed from the point of view of the general theory and are compared with experimental data. CH_4 is found to be the only molecule even approximately to obey valence forces. For some other molecules satisfactory results are obtained by postulating an additional repulsive force inversely proportional to some power of the distance between the corner atoms.

Part IV. Certain relations between the frequencies of the isotopic molecules are found to be independent of the values of the force constants. For YX_4* definite upper and lower limits may be predicted for the values of the active frequencies.

PART III

THE expressions for the normal frequencies of the molecule YX_4 derived in Part II of this paper,[1] may be applied to experimental data with a view of determining the actual values of the constants in the potential energy function V. It has been shown that in the most general case V involves five arbitrary constants, while only four frequencies are observed in the absence of isotopic shifts. From these four frequencies we may evaluate four of the constants as functions of the fifth one, considered as a variable parameter. The notation will in general be the same as used previously, but, in conformity with general usage, the normal vibrations will be designated by ω_1, ω_2, ω_3 and ω_4; $(\omega_3>\omega_4)$. The notational connection between these and the $\omega_{(\rho)}$, $\omega_{(\sigma)}$, $\omega_{(\tau)}$, etc., introduced in Part II is as follows:

$$\omega_1\rightarrow\omega_{(\tau)};\qquad \omega_2\rightarrow\omega_{(\rho),\,(\sigma)};\qquad \omega_3,\ \omega_4\rightarrow\omega_{(\xi\alpha),\,(\eta\beta),\,(\zeta\gamma)}.$$

Of the five constants A, B, C, D and E used in the potential energy expression, two are directly given by the frequencies:

$$C/4\pi^2=m\omega_2^2/4;\qquad E/4\pi^2=m\omega_1^2/16. \tag{32}$$

Choosing D as the variable parameter, we obtain from Eqs. (31) the following expressions for A and B:

$$\begin{aligned} A/4\pi^2&=2m\mu\{\omega_3^2+\omega_4^2\pm[(\omega_3^2-\omega_4^2)^2-(8/\mu m^2)(D/4\pi^2)^2]^{\frac{1}{2}}\};\\ B/4\pi^2&=\tfrac{1}{16}m\{\omega_3^2+\omega_4^2\mp[(\omega_3^2-\omega_4^2)^2-(8/\mu m^2)(D/4\pi^2)^2]^{\frac{1}{2}}\}, \end{aligned} \tag{33}$$

where

$$\mu=M/(4m+M).$$

The sign of the square root is undetermined but, however, is different, for A and B. Since all constants are essentially real, it follows from Eqs. (33) that A, B and D have to lie within certain definite

[1] Jenny Rosenthal, Phys. Rev. **45**, 538 (1934).

TABLE I. *Values of frequencies taken from reference 3.* $\varphi(\omega_1, \omega_2)=[\omega_1^2(1+4m/3M)+\frac{1}{3}\omega_2^2(1+8m/3M)]\times 10^{-4}$.

Molecule	ω_1	ω_2	ω_3	ω_4	$(3\mu/2)^{\frac{1}{2}}$	$\omega_1\omega_2/\omega_3\omega_4$	% diff.	$\varphi(\omega_1, \omega_2)$	$(\omega_3^2+\omega_4^2)\cdot 10^{-4}$	% diff.
CCl_4	460	214	760	311	0.344	0.417	−21	130.25	67.43	48
			790			.401	−16		72.08	45
$SiCl_4$	422	149	608	220	.500	.470	+ 6	53.91	41.81	22
$TiCl_4$	386	119	491	139	.619	.673	− 9	32.17	26.04	19
$SnCl_4$	367	104	401	136	.830	.700	+16	20.04	17.93	10
CBr_4	265	125	667	183	.233	.271	−16	88.95	47.84	46
$SnBr_4$	220	64	279	88	.638	.574	+10	9.94	8.55	14
CH_4	2914	1520	3014	1304	1.061	1.127	− 6	1131.73	1078.46	5
SO_4^{--}	980	451	1113	620	0.707	0.641	+ 9	191.71	162.32	15
ClO_4^-	935	467	1121	634	.728	.614	+16	172.97	165.86	4

limits. The conditions imposed on them are:

$$(D/4\pi^2)^2 \leqslant \tfrac{1}{8}\mu m^2(\omega_3^2-\omega_4^2)^2; \qquad 4\mu m\omega_4^2 \leqslant A/4\pi^2 \leqslant 4\mu m\omega_3^2;$$
$$\tfrac{1}{8}m\omega_3^2 \geqslant B/4\pi^2 \geqslant \tfrac{1}{8}m\omega_4^2. \tag{34}$$

Instead of obtaining A and B as functions of a variable parameter, we may make some more specific assumptions as to intramolecular forces which would involve a smaller number of arbitrary constants. This amounts to postulating a certain definite value for the variable parameter D.

Consider first the valence force case.[2] The potential energy expression contains only two arbitrary constants: the constant of the force along the bond and that of the force perpendicular to it. In terms of the general constants, this is equivalent to setting

$$D'''/4\pi^2=\tfrac{1}{8}m(\omega_1^2-\tfrac{2}{3}\omega_2^2) \qquad \text{and} \qquad A'''/16>B. \tag{35}$$

These results are obtained from Eqs. (19) by letting $f_3=0$, and $f_4=0$ and substituting for C and E their values given by Eqs. (32). The inequality relation between A and B removes the ambiguity in sign in Eqs. (33) as it will be always satisfied if $(1/4)A/\mu>8B$, i.e., if the positive sign is taken for A. If the valence force assumption is valid, the four observed frequencies cannot be independent of each other and should satisfy two definite relations. These are:

$$\omega_1\omega_2/\omega_3\omega_4=(3\mu/2)^{\frac{1}{2}}; \qquad \omega_3^2+\omega_4^2=\tfrac{1}{3}[\omega_1^2(2+1/\mu)+\tfrac{2}{3}\omega_2^2(1+2/\mu)]. \tag{36}$$

A numerical comparison of the right- and left-hand sides of these two equations gives the easiest and quickest way of determining whether any given molecule obeys valence forces. The results of such a comparison are given in Table I. It should be noted that the observed frequencies ν do not coincide exactly with the theoretically predicted ω's, which are normal frequencies of vibration of a harmonic oscillator. Since the anharmonic terms, however, may be expected to be fairly small, to a first approximation $\nu \leqq \omega$; but an agreement in the calculation of better than, say, 5 percent would be purely accidental. The results in Table I show that CH_4 is the only molecule whose vibrations may be explained on the basis of valence forces. Different assumptions will have to be made for the other molecules.

Urey and Bradley[3] suggested: (a) that the potential energy is due to central forces plus forces perpendicular to the bond lines; (b) that the forces along the lines joining the corner atoms are repulsive and inversely proportional to a high power n of the interatomic distance. In terms of the general constants (a) is equivalent to setting:

$$D'/4\pi^2=[\tfrac{5}{8}m(\omega_3^2+\omega_4^2)-\tfrac{1}{2}m(\omega_1^2+\omega_2^2)](1+25/8\mu)^{-1}$$
$$\mp\tfrac{5}{8}m(1+25/8\mu)^{-1}\{(1+25/8\mu)(\omega_3^2-\omega_4^2)^2-(2/\mu)[(5/4)(\omega_3^2+\omega_4^2)-(\omega_1^2+\omega_2^2)]^2\}^{\frac{1}{2}}. \tag{37}$$

[2] We shall, as before mark with a triple prime the constants A, B, C, D and E referring to this case. Similarly, primes will be used in the four-constant case.

[3] H. C. Urey and C. A. Bradley, Jr., Phys. Rev. **38**, 1969 (1931).

TABLE II. *Values of the force constants times $10^{-5}/4\pi^2$ for various molecules.* The values of the f's in parenthesis represent the alternate solutions. Two values are given for CCl_4 corresponding to the two values observed for the frequency ω_3 (probably a perturbation phenomenon).

	CCl_4		$SiCl_4$	$TiCl_4$	$SnCl_4$	CBr_4	$SnBr_4$	CH_4	$SO_4^=$	ClO_4^-
f_1	2.91	3.17	4.35	4.11	3.88	2.35	3.13	7.95	10.26	10.58
f_2	0.43	0.51	0.28	0.29	0.14	0.40	0.14	2.96	1.89	2.56
f_3	1.12	1.06	0.47	0.28	0.21	0.82	0.19	0.13	1.28	0.85
f_4	−0.158	−0.163	−0.098	−0.003	−0.064	−0.132	−0.038	0.046	−0.560	−0.722
(f_1)	1.22	1.32	0.66	0.15	0.58	1.14	0.29	2.47	4.40	5.98
(f_2)	−0.62	−0.64	−2.09	−2.36	−2.28	−0.34	−1.77	−1.74	−2.17	−0.67
(f_3)	1.55	1.52	1.39	1.27	1.03	1.12	0.89	1.51	2.74	2.00
(f_4)	−0.52	−0.56	−0.95	−1.00	−1.06	−0.38	−0.76	−2.11	−2.14	−1.99

Eq. (37) is obtained from Eqs. (20), (31) and (32). It implies that only those four frequencies for which the quantity in { } is positive may be accounted for by a potential energy involving four real constants. Corresponding to D' given by Eq. (37) there are two possible values for A' and B' as the uncertainty in sign in Eqs. (33) is not removed in this case. To discuss these assumptions further, we make use of the constants f_1, f_2, f_3 and f_4 first introduced in Eq. (18). Assumption (b) means that $f_3 = -(n+1)f_4$, where n is a positive number. We calculate directly f_1, f_2, f_3 and f_4. The numerical results are given in Table II. To reduce the very convenient units in which the various f's are given to dynes, it is necessary to multiply them by the square of the velocity of light and the mass (in grams) of the hydrogen atom.

As mentioned before the uncertainty in sign in Eqs. (33) gives rise to two possible sets of constants. In all the cases investigated so far, one of the two sets always consists of a small value for f_1, a large one for f_3, and a negative one for f_2. While this second group of values is usually not consistent with the chemical ideas, there is no a priori reason why, for some molecules, we should not obtain reasonable values for both sets. In any case, the ambiguity can be completely removed only by the presence of isotopic shifts, and we are really not justified in discarding one of the groups as not being consistent with physical ideas. If we consider only the "physically acceptable" set of values we see that the constant of the force between the corner atoms is larger in most instances than the constant of the force perpendicular to the line of bond; this point may be stressed since on the basis of the usual chemical model one would expect $f_1 > f_2 \gg f_3$. We also find that for a number of molecules $f_3/(-f_4) > 2$. It thus appears that the force field proposed by Urey and Bradley will serve to correlate the frequencies of at least some of these molecules. This, however, cannot be regarded as a proof of the correctness of the field since there are four arbitrary constants with which to determine the four frequencies.

PART IV

TABLE III. *Summary of numbering of frequencies.*

Molecule	Frequencies			
YX_4	ω_1	ω_2	ω_3	ω_4
YX_3X^*	ω_1	ω_2	ω_{3a} ω_{3c}	ω_{4a} ω_{4c}
$YX_2X_2^*$	ω_1	ω_{2a} ω_{2b}	ω_{3a} ω_{3b} ω_{3c}	ω_{4a} ω_{4b} ω_{4c}
YXX_3^*	ω_1	ω_2	ω_{3ab} ω_{3c}	ω_{4ab} ω_{4c}
YX_4^*	ω_1	ω_2	ω_3	ω_4

The isotopic shifts for most frequencies are functions of the parameter D and therefore cannot be predicted without knowing or assuming a definite value for this parameter. There are, however, certain relations between the frequencies of the various isotopic molecules, valid under all conditions and possibly of help in analyzing experimental data. The following notation is used in writing these relations: The subscript 0 outside a bracket will indicate that the quantity within refers to YX_4; in general the subscripts I, II, etc., will show the number of X^* atoms in $YX_{4-n}X_n^*$. The numbering of the frequencies is summarized in Table III. For YX_3X^* the connection between the numbered frequencies and the frequencies with Greek letter subscripts

of Eqs. (29) is as follows:

$$\omega_2,\ \omega_{3ab},\ \omega_{4ab}\rightarrow\omega_{(\xi\alpha\rho)},\ (\eta\beta\sigma);\qquad \omega_1,\ \omega_{3c},\ \omega_{4c}\rightarrow\omega_{(\zeta\gamma\tau)}.$$

The following relations are then true ($\kappa=\frac{1}{4}\Delta m/(m+\Delta m)$):

$$\begin{aligned}
&(\omega_2\omega_{3ab}\omega_{4ab})_{\mathrm{I}}=(1-3\kappa/2-\mu\kappa)^{\frac{1}{2}}(\omega_2\omega_3\omega_4)_0;\\
&\left[\omega_2^2(\omega_{3ab}^2+\omega_{4ab}^2)+\omega_{3ab}^2\omega_{4ab}^2\right]_{\mathrm{I}}-(\omega_2^2)_0\left[\omega_2^2+\omega_{3ab}^2+\omega_{4ab}^2\right]_{\mathrm{I}}\\
&\qquad=\left[(1-\tfrac{1}{2}\kappa-\mu\kappa)\omega_3^2\omega_4^2-(1-\kappa)\omega_2^4-\kappa\omega_2^2(\omega_3^2+\omega_4^2)\right]_0;\\
&(\omega_1\omega_{3c}\omega_{4c})_{\mathrm{I}}=(1-3\kappa-\mu\kappa)^{\frac{1}{2}}(\omega_1\omega_3\omega_4)_0;\\
&\left[\omega_1^2(\omega_{3c}^2+\omega_{4c}^2)+\omega_{3c}^2\omega_{4c}^2\right]_{\mathrm{I}}-(\omega_1^2)_0\left[\omega_1^2+\omega_{3c}^2+\omega_{4c}^2\right]_{\mathrm{I}}\\
&\qquad=\left[(1-2\kappa-\mu\kappa)\omega_3^2\omega_4^2-(1-\kappa)\omega_1^4-\kappa\omega_1^2(\omega_3^2+\omega_4^2)\right]_0.
\end{aligned}\tag{38}$$

Similarly for $YX_2X_2^*$ where

$$\omega_{2a}\rightarrow\omega_{(\rho)};\qquad \omega_{3a},\ \omega_{4a}\rightarrow\omega_{(\xi\alpha)};\qquad \omega_{3c},\ \omega_{4c}\rightarrow\omega_{(\xi'\gamma')};\qquad \omega_1,\ \omega_{2b},\ \omega_{3b},\ \omega_{4b}\rightarrow\omega_{(\eta'\beta'\sigma\tau)}$$

the following relations exist:

$$\begin{aligned}
&(\omega_{2a})_{\mathrm{II}}=(1-2\kappa)^{\frac{1}{2}}(\omega_2)_0;\qquad (\omega_{3a}\omega_{4a})_{\mathrm{II}}=(1-3\kappa-2\mu\kappa+4\mu\kappa^2)^{\frac{1}{2}}(\omega_3\omega_4)_0;\\
&(\omega_{3c}\omega_{4c})_{\mathrm{II}}=(1-\kappa-2\mu\kappa)^{\frac{1}{2}}(\omega_3\omega_4)_0;\qquad (\omega_1\omega_{2b}\omega_{3b}\omega_{4b})_{\mathrm{II}}=(1-4\kappa)^{\frac{1}{2}}(1-2\kappa-2\mu\kappa)^{\frac{1}{2}}(\omega_1\omega_2\omega_3\omega_4)_0;\\
&\left[\omega_1^2+\omega_{2b}^2+\omega_{3b}^2+\omega_{4b}^2-\tfrac{1}{2}(\omega_{3a}^2+\omega_{4a}^2+\omega_{3c}^2+\omega_{4c}^2)\right]_{\mathrm{II}}=(1-2\kappa)(\omega_1^2+\omega_2^2)_0;\\
&\left[\omega_1^2\omega_{2b}^2(\omega_{3b}^2+\omega_{4b}^2)+\omega_{3b}^2\omega_{4b}^2(\omega_1^2+\omega_{2b}^2)\right]_{\mathrm{II}}-\tfrac{1}{2}(1-2\kappa)(\omega_1^2\omega_2^2)_0(\omega_{3a}^2+\omega_{4a}^2+\omega_{3c}^2+\omega_{4c}^2)_{\mathrm{II}}\\
&\qquad=\{\omega_3^2\omega_4^2\left[\omega_2^2(1-4\kappa-2\mu\kappa+8\kappa^2/3+16\mu\kappa^2/3)+\omega_1^2(1-4\kappa-2\mu\kappa+4\kappa^2/3+20\mu\kappa^2/3)\right]\\
&\qquad\qquad-2\kappa(1-2\kappa)\omega_1^2\omega_2^2(\omega_3^2+\omega_4^2)\}_0.
\end{aligned}\tag{39}$$

The expressions for the frequencies of YXX_3^* and YX_4^* may be obtained from Eq. (29′) and (31) by substituting $m+\Delta m$ for m and $-\frac{1}{4}\Delta m/m$ for κ. Also, using the same substitution and changing the subscripts I and 0 to III and IV, respectively, we obtain from Eqs. (38) relations connecting the frequencies of YXX_3^* and YX_4^*. The active frequencies of YX_4^* may be written as:

$$m^2\lambda_{\mathrm{IV}}^2-m\lambda_{\mathrm{IV}}\left[\tfrac{1}{4}A(1-4\mu\kappa)/\mu+8B(1-4\kappa)\right]+2(1-4\mu\kappa)(1-4\kappa)(AB-D^2)/\mu=0.\tag{40}$$

While both $(\omega_3)_{\mathrm{IV}}$ and $(\omega_4)_{\mathrm{IV}}$ depend on D, it is possible to obtain their maximum and minimum values from the maximum and minimum values of A and B. In this way we find that:

$$\begin{aligned}
&(1-4\kappa)^{\frac{1}{2}}(\omega_3)_0<(\omega_3)_{\mathrm{IV}}<(1-4\mu\kappa)^{\frac{1}{2}}(\omega_3)_0;\qquad (1-4\mu\kappa)^{\frac{1}{2}}(\omega_4)_0>(\omega_4)_{\mathrm{IV}}>(1-4\kappa)^{\frac{1}{2}}(\omega_4)_0;\\
&\qquad(\omega_3\omega_4)_{\mathrm{IV}}=(1-4\kappa)^{\frac{1}{2}}(1-4\mu\kappa)^{\frac{1}{2}}(\omega_3\omega_4)_0.
\end{aligned}\tag{41}$$

In conclusion I wish to thank Professor D. M. Dennison for his suggestions and interest in this work.

An Interpretation of e^2/mc^2 and h/mc

BORIS PODOLSKY, *Institute for Advanced Study, Princeton, New Jersey*

(Received September 4, 1934)

In this paper a point of view is presented according to which the quantities m and e, the mass and the charge of elementary particles, need not enter into the electrodynamics and the quantum mechanics of electrons, positrons and photons. The only constants entering into the equations, rewritten in this way, are the velocity of light and two independent lengths, namely: $a=e^2/mc^2$, and $b=h/mc$. The first of these lengths determines the scale of electrodynamic phenomena, and has no especial relation to electronic radius. The second determines the scale of quantum-mechanical phenomena. In the absence of particles electromagnetic phenomena have no definite scale. This fact, together with the possibility of creation of electron-positron pairs, leads to the belief that a theory of interactions of electrons, positrons, and photons, giving as a by-product a derivation of the ratio $a/b=\alpha=e^2/hc$, could be formulated without introducing the two other pure numbers $\beta=m/M$ and $\gamma=Gm^2/e^2$. This theory is envisaged as a limiting theory, obtainable from the future general theory by putting $\beta=\gamma=0$. It is then considered from the point of view of the necessity of giving up space-time framework for the description of physical phenomena. It is concluded that the first limiting theory should not necessitate abolition of space and time.

(1)

TO the founders of electrodynamics the problem of interaction of charged bodies was, from a certain point of view, a much more complex problem than it should appear today. Faraday and Maxwell had to deal with interactions of bodies of arbitrary mass and arbitrary charge, and this arbitrariness had to appear explicitly in their equations. Accordingly, the concepts of mass and electric charge were necessary. Today, however, we believe that if we had understood and properly formulated interactions between elementary particles, interactions between bodies of any dimensions could be calculated without any, except mathematical, difficulty. Thus, from this point of view, our problem is considerably simplified.

Let us assume that the elementary particles are the electron, the positron, and the neutron (we do not regard the photon as a particle at all, for it has none of the attributes of a classical particle). Let us further suppose that the interaction between a neutron and other particles is not strictly of electromagnetic nature—leaving open, for the present, the question as to the nature of this interaction. Then we are led to the conclusion that the first problem of electrodynamics is to account for the interaction of electrons and positrons; that is, of particles all having the same mass and numerically the same charge.

If the problem, historically, had occurred in this form, it is likely that the concepts of mass and charge would not have been introduced. For mass, as we now know, arises out of comparison of accelerations of interacting bodies, and would not have occurred at all if all the bodies acquired numerically the same accelerations under the same forces. Similarly, the concept of charge became necessary only because different bodies experienced numerically different forces in the same field, or produced numerically different fields under geometrically similar conditions.

We shall now review briefly some classical formulas, and shall try to see how such formulas may be altered, when account is taken of the simplification introduced by the fact that all particles are of the same mass and of numerically the same charge. We shall find that by so doing we achieve a new interpretation of the constants e^2/mc^2 and h/mc. We shall use h to designate Planck's constant divided by 2π.

(2)

We choose, for the sake of brevity, the representation of classical formulas in the form

$$\delta\int L\,dt=0. \tag{1}$$

We disregard, as presenting no particular interest, the non-relativistic classical treatment. For a free particle in the relativistic theory $L\,dt=dW$ must be invariant. Elementary considerations

lead to

$$dW = -mc\,ds = -mc^2(1-v^2/c^2)^{\frac{1}{2}}dt, \quad (2)$$

where m is an arbitrary constant. For a number of free non-interacting particles this becomes

$$dW = -\sum_k m_k c^2(1-v_k^2/c^2)^{\frac{1}{2}}dt. \quad (3)$$

From the new point of view the constants m_k, which are put in to make Lagrangians of the individual particles additive in the presence of interactions, are unnecessary because the masses are all equal. In fact, presented with this problem without a previous acquaintance with the concept of mass, we would probably write something like this:

$$dW^* = -\sum_k (1-v_k^2/c^2)^{\frac{1}{2}}d\tau, \quad (3^*)$$

where $\tau = ct$. We shall uniformly star all quantities, definitions of which differ from the old definitions.

Corresponding to this W^* the momentum of a free particle may be defined as

$$\mathbf{p}^* = \partial L^*/\partial(\mathbf{v}/c) = (\mathbf{v}/c)/(1-v^2/c^2)^{\frac{1}{2}}, \quad (4^*)$$

instead of the classical

$$\mathbf{p} = m\mathbf{v}/(1-v^2/c^2)^{\frac{1}{2}}. \quad (4)$$

For a particle moving in a given field the classical Lagrangian is:

$$L = -mc^2(1-v^2/c^2)^{\frac{1}{2}} - e\varphi + e\mathbf{A}\cdot\mathbf{v}/c, \quad (5)$$

where φ and $\mathbf{A}$ are the scalar and the vector potentials, respectively. From the new point of view there is no need of introducing a new quantity e. We can write instead

$$L^* = -(1-v^2/c^2)^{\frac{1}{2}} \pm (-\varphi^* + \mathbf{A}^*\cdot\mathbf{v}/c), \quad (5^*)$$

the sign being chosen according to the sign of the particle.[1]

Eq. (5*) leads to the equation of motion

$$\frac{d}{d\tau}\mathbf{p}^* = \frac{d}{dt}\frac{\partial L^*}{\partial \mathbf{v}} = \pm\left(\boldsymbol{E}^* + \frac{\mathbf{v}}{c}\times\boldsymbol{H}^*\right), \quad (6^*)$$

where

$$\boldsymbol{E}^* = -\nabla\varphi^* - \frac{1}{c}\frac{\partial \mathbf{A}^*}{\partial t} \quad \text{and} \quad \boldsymbol{H}^* = \nabla\times\mathbf{A}^*. \quad (7^*)$$

These are to be compared with the usual equations:

$$\frac{d}{dt}\mathbf{p} = e\boldsymbol{E} + e\frac{\mathbf{v}}{c}\times\boldsymbol{H}, \quad (6)$$

where

$$\boldsymbol{E} = -\nabla\varphi - \frac{1}{c}\frac{\partial \mathbf{A}}{\partial t} \quad \text{and} \quad \boldsymbol{H} = \nabla\times\mathbf{A}. \quad (7)$$

Eqs. (7*) lead immediately to the first pair of Maxwell-Lorentz equations, namely:

$$\nabla\times\boldsymbol{E}^* = -\frac{1}{c}\frac{\partial \boldsymbol{H}^*}{\partial t} \quad \text{and} \quad \nabla\cdot\boldsymbol{H}^* = 0, \quad (8^*)$$

which are exactly like the corresponding classical equations. To obtain the other pair of Maxwell-Lorentz equations, it is usual to put $\delta W = 0$, with

$$W = \int\int\{-\rho\varphi + \rho\mathbf{A}\cdot\mathbf{v}/c + (1/8\pi)(E^2 - H^2)\}dV d\tau \quad (9)$$

where ρ is the charge density. This charge density is introduced in order to represent the last two terms of Eq. (5) as a volume integral. Actually, however,

$$\rho = \sum_k e_k\delta(\mathbf{r}-\mathbf{r}_k), \quad (10)$$

where $\delta(\mathbf{r}-\mathbf{r}_k) = \delta(x-x_k)\delta(y-y_k)\delta(z-z_k)$. In the new formulation we can introduce

$$\rho^* = \sum_k \pm\delta(\mathbf{r}-\mathbf{r}_k), \quad (10^*)$$

where the sign of the delta-function for each particle is chosen positive when the particle is positive, and *vice versa*. Instead of Eq. (9) we will then have:

$$W^* = \int\int\{-\rho^*\varphi^* + \rho^*\mathbf{A}^*\cdot\mathbf{v}/c + (1/8\pi a)(E^{*2} - H^{*2})\}dV d\tau. \quad (9^*)$$

As is easily seen, for example from Eq. (5*), φ^* and $\mathbf{A}^*$ are dimensionless; ρ^* is, dimensionally, the number of particles per unit volume; while $\boldsymbol{E}^*$ and $\boldsymbol{H}^*$ are of the dimension $(length)^{-1}$. Thus, the constant a in Eq. (9*) must be dimensionally

[1] We could, of course, introduce e^* which has the value $+1$ or -1, but this would still be different from introducing the constant e, the value of which must be determined experimentally.

a length. We note that it is the first and only constant that we have to introduce into our electrodynamics. This constant must, of course, be determined experimentally; but by comparison with the classical theory we know that

$$a=e^2/mc^2. \tag{11}$$

The constant c, occurring in our equations either as v/c or ct, is properly not an electrodynamic constant at all, but the limiting speed of the relativistic dynamics. Electrodynamics, of course, shows that this must also be the speed of propagation of electromagnetic waves in a vacuum.

The field equations obtained from Eq. (9*) by varying φ^* and $\mathbf{A}^*$, and putting $\delta W^*=0$, are

$$\frac{1}{c}\frac{\partial \boldsymbol{E}^*}{\partial t}-\nabla\times\boldsymbol{H}^*=4\pi a\rho^*(\mathbf{v}/c)$$

$$\text{and}\quad \nabla\cdot\boldsymbol{E}^*=4\pi a\rho^*. \tag{12*}$$

The length a occurs here quite naturally and, obviously, without any direct connection with the electron radius. To be sure, it is here the natural unit of length with which the scale of phenomena is determined. The radius of the electron, if it could be derived on this theory, would naturally be expressed as a numerical multiple of a; but all other phenomena are also expressed in terms of a. Thus, for example, the field of a positive particle at rest would be expressed by the potential

$$\varphi^*=a/r=1/(r/a). \tag{13*}$$

(3)

Turning now to quantum mechanics, we first have the commutation formula

$$p_jq_k-q_kp_j=(h/i)\delta_{jk}I. \tag{14}$$

This we would now write as

$$p^*{}_jq_k-q_kp^*{}_j=(b/i)\delta_{jk}I, \tag{14*}$$

where b is a new constant, to be determined experimentally. Comparison of Eqs. (4) and (4*) shows, however, that

$$\mathbf{p}^*=\mathbf{p}/mc, \tag{15}$$

so that Eqs. (14) and (14*) will be in agreement if

$$b=h/mc. \tag{16}$$

To obtain Schroedinger's equation in the new form, we first obtain the energy of a particle. This is

$$E^*=(1+p^{*2})^{\frac{1}{2}}\pm\varphi^*=\pm\varphi^*+1+\tfrac{1}{2}p^{*2}+\cdots, \tag{17*}$$

where the vector potential was dropped. Taking the first approximation, and dropping the unit, which corresponds classically to dropping mc^2 from the expression for the energy, we finally have

$$E^*=\pm\varphi^*+\tfrac{1}{2}p^{*2}.$$

Corresponding to this the Schroedinger equation is

$$\nabla^2\psi+(2/b^2)(E^*\mp\varphi^*)\psi=0. \tag{18*}$$

Comparison of Eq. (17*) with the usual expression for the energy shows that

$$E^*=E/mc^2. \tag{19}$$

Therefore the relation between the energy and the frequency of a photon,

$$E=2\pi h\nu, \tag{20}$$

will become

$$E^*=2\pi h\nu/mc^2=2\pi b/\lambda, \tag{20*}$$

where λ is the wave-length of light.

Eqs. (14*), (18*) and (20*) show that the scale of quantum phenomena is given by the fundamental length b, the only constant of the dimension of length occurring in the equations. Here we see a confirmation of the surmise of L. L. Whyte[2] that the primary purpose of the quantity h in quantum mechanics is the introduction of a new standard of length. In fact, Whyte writes down an equation (reference 2, p. 22) equivalent to our Eq. (20*).

(4)

The fine structure constant $\alpha=a/b$ first makes its appearance when we combine electromagnetic and quantum-mechanical equations. Thus, if we substitute the potential from Eq. (13*) into Eq. (18*), choosing the lower sign in the latter, we obtain the Schroedinger equation for a

[2] L. L. Whyte, *Critique of Physics*, Norton and Co., New York (1931).

hydrogen atom,

$$\nabla^2\psi+(2/b^2)(E^*+a/r)\psi=0. \qquad (21^*)$$

The eigen values of this equation are

$$E^*=-(1/2n^2)(a/b)^2=-\alpha^2/2n^2, \qquad (22^*)$$

where n is the quantum number. The scale of the distribution of the probability of position of the electron turns out to depend upon

$$r_0=b^2/a=b/\alpha, \qquad (23)$$

where r_0 is the radius of the first Bohr's orbit for the hydrogen atom. Finally, Rydberg's constant, expressed as a wave-length, is here expressed as

$$R_\lambda=4\pi b^2/a^2=4\pi b/\alpha^2. \qquad (24)$$

If we should now decide to use either a or b as the fundamental unit of length, expressing the space coordinates and ct in terms of this unit, there would be no dimensional constants in our theory at all; while the only dimensionless constant occurring in the theory would be α. Such a description of physical phenomena seems to be what was intended in the *item 4* of Whyte's program for research (reference 2, p. 144).

It is, of course, not suggested that the above discussion is in any sense a part of the structure of the future theory. The whole of this paper is rather in the nature of an attempt at a preliminary clearing of the ground for the future edifice.

(5)

The duality of electromagnetic phenomena expresses itself through the appearance of *two* independent standards of length. Is it too much to hope for that the next step in the development of electrodynamics, as it is here defined, should give us a theory explaining their ratio? I think not.

It may be urged that we don't know that α is *not* a function of the other two independent pure numbers appearing in our theories, namely: $\beta=m/M$ and $\gamma=Gm^2/e^2$, where M is the mass of the neutron and G the gravitational constant. My belief that these other numbers are irrelevant to the kind of a theory I have in mind is based on the following considerations: As can be seen from Eq. (9*), in the absence of particles the constant a is unnecessary, and in fact does not occur in the field equations. Thus, the only scale of length relevant to a correct description of pure radiation would seem to be the constant b occurring in Eq. (20*). Consider, now, creation of a pair electron+positron by a collision of two photons, a process now generally admitted to be possible. Such a pair immediately re-introduces the constant a. It seems to me that this is a strong evidence for supposing that this constant, and therefore α, had pre-existed in the original radiation. In other words, it seems that there must be something existing in the structure of radiation which determines the charge of the electron that may be created.

It is, of course, not categorically asserted that gravitation, for instance, can have nothing to do with the phenomenon of a pair creation. But it seems to me that, if it has any effect at all, it will be to introduce a small correction to the value of α; possibly a correction proportional to some power of the small constant γ. I believe, therefore, that a theoretical derivation of at least a good first approximation to α should be one of the by-products of the next important step in the development of quantum electrodynamics.

The theory, a possibility of which is here discussed, must naturally be something vastly different from numerous attempts, recently in vogue, at so manipulating known material as to make a combination approximately equal to the experimental value of a physical constant. The three fundamental aspects of this theory should be: first, an explanation of the way in which electrons and positrons interact, one that would make it clear that all the requirements of the theory can be satisfied only if the interaction corresponds to $e^2=hc\alpha$; second, an explanation of the phenomenon of quantization, making clear that the theory demands that $h=e^2/\alpha c$; and, finally, an explanation of the nature of radiation, explaining why the limiting velocity of relativistic dynamics should be $c=e^2/\alpha h$. As was pointed out by Bohr, at the theoretical conference in Copenhagen last year, it is obviously impossible, starting with a theory valid for all possible values of the constants occurring in it, to derive any relation between such constants. It is for this reason that the relation $a/b=\alpha$, with a particular numerical value of α, must be a *necessary condition* for the validity of the theory.

(6)

We may hope that, ultimately, a theory will be formulated in which all the three independent pure numbers, α, β and γ will find their proper explanation. I hold it unlikely, however, that such a theory could be conceived at once. It seems to me much more likely that the progress will be through two intermediate limiting theories. The first such theory, the theory discussed above, would correspond to the limiting case $\beta=\gamma=0$; or $M=\infty$ and $G=0$. The second limiting theory, it seems likely, will be the theory with β finite, but $\gamma=0$. And finally would come the general theory.

Now, it has been often pointed out that without a possibility of constructing a measuring means, with which a coordinate system can be mapped out with any desired degree of accuracy, space and time, and therefore geometry, lose their significance; that, becoming vague, they had best be given up.[3] While entirely in agreement with such general conclusions, I wish to call attention to the fact that, on the basis of the point of view here presented, the necessity of giving up a space-time framework may not be as imminent as it may seem.

Thus, in constructing our first limiting theory, we put $M=\infty$. But this means that all the quantities, $h/M\Delta v$, h/Mc, and e^2/Mc^2, which control the accuracy of locating nuclei within crystal lattices, become zeros in this theory. This means that within the first limiting theory there is no inherent need for giving up space-time description. So far, at least, the various uncertainties connected with the electron may be ascribed to the electron, and not to the space-time framework.

[3] As the latest, and one of the best, examples of this kind see E. Schroedinger, Naturwiss. **22**, 518 (1934).

OCTOBER 15, 1934 PHYSICAL REVIEW VOLUME 46

Approximate Wave Functions and Atomic Field for Mercury

D. R. HARTREE, *University of Manchester, England*

(Received August 9, 1934)

Approximate wave functions and atomic field for mercury have been calculated by the method of the self-consistent field, and tables of preliminary results are given. A considerable amount of the calculations was carried out on the differential analyzer, and a short account of the application of the differential analyzer to this work is given.

§1. INTRODUCTION

THE heaviest atom for which calculations of the approximate atomic field and wave functions by the method of the "self-consistent field"[1] has so far been completed is Cs. During the past year, calculations have been in progress for Hg, and though the approximation to the self-consistent field has not yet been carried far enough for the results to be considered as final, it seems desirable to publish the results so far obtained, as they may provide a good enough approximation for some purposes, and it may be some time before better results are available.

The amount of work involved in the determination of the self-consistent field of Hg is very considerable, not only on account of the number of one-electron wave functions to be determined, but also because of the sensitiveness of the $(5d)^{10}$ group, and to a less extent of the $(4f)^{14}$ group, to a change in the estimate of the atomic field. The $(5d)^{10}$ group shows in rather a pronounced way the phenomenon of "overstability" already noted[2] for the $(3d)^{10}$ group of Cu^+, and the $(4f)^{14}$ group, though not overstable, is inconveniently sensitive.

[1] D. R. Hartree, Proc. Camb. Phil. Soc. **24**, 89, 111 (1928); Proc. Roy. Soc. **A141**, 282 (1933); **143**, 506 (1934). The Proc. Camb. Phil. Soc. papers will be referred to as I, and the Proc. Roy. Soc. papers as II and III, respectively.

[2] See II, pp. 287, 295.

So far, nine stages of approximation to the self-consistent field have been carried out. The main portion of the numerical integration involved in the first five stages was carried out on the differential analyzer of Dr. Bush,[3] at the Massachusetts Institute of Technology, in the course of a visit to Boston, Massachusetts, last summer, and the further stages have been carried out numerically. Some mechanical assistance such as that provided by the differential analyzer is almost necessary for an undertaking of this magnitude, and the work of carrying through the subsequent approximations numerically has emphasized its value for such calculations. I wish to express my great indebtedness to Dr. Bush for giving me the opportunity to use the differential analyzer for this work, and to Dr. Caldwell and others of the staff of the differential analyzer for instruction in the use of the machine, and for valuable help in operating it. In the later numerical stages of the work, I have had most valuable assistance from Mr. W. Hartree.

§2. Theory

If the wave function ψ for an electron in a central field is written

$$\psi=[P(r)/r]S_l(\theta, \phi),$$

then $P(r)$ satisfies the equation[4]

$$d^2P/dr^2+[2(E-V)-l(l+1)/r^2]P=0, \quad (1)$$

where $V=V(r)$ is the potential of the central field and E is the energy of the electron in that field, and r, E, V are in atomic units. In the "self-consistent field" approximation to a many-electron atom, each electron is considered to move in the field of the nucleus and of the Schrödinger charge distribution of the other electrons, so that V for any one radial wave function P depends on the solutions of the equations for the others; the "self-consistent" set of radial wave functions is generally determined by trial and error.

The solution of (1) is an oscillating function of r over the classical range of possible motion of a particle with energy E and angular momentum $[l(l+1)]^{\frac{1}{2}}$. The "wave-length" of the oscillations increases considerably with increasing r, and so, to a less extent, does the amplitude, and it seemed likely that for the solution of the equation by the differential analyzer, it would be most convenient to transform it by using as independent variable an increasing function of r, in terms of which the "wave-length" of an oscillation would remain approximately constant. Such a transformation was also suggested by the fact that in numerical integration of Eq. (1), the interval of integration has to be changed several times in the course of an integration; it seemed probable that corresponding scale changes for the independent variable would have to be made when using the differential analyzer, and these it seemed desirable to avoid.

Of the core wave functions previously calculated, the (5s) of Cs was the one with the most radial nodes, and was used to examine what would be the most suitable change of independent variable for this purpose. The approximate radii of the nodes, and maxima and minima, of P for this wave function are given in Table I; the

Table I. *Cs (5s) radial wave function.*

Nodes r	Ratio of r for successive nodes	Maxima of $\lvert P\rvert$ r	Ratio of r for successive maxima of $\lvert P\rvert$	P
0.035		0.013		0.06
	4		6	
.14		.08		−.10
	2½		3	
.37		.24		.14
	2½		2½	
.89		.58		−.22
			3	
		1.7		.41

magnitudes of the maxima and minima of P are also given. The second and fourth columns show that the ratios of the radii of successive nodes or maxima of $|P|$ are roughly uniform, and this suggests the use of log r as independent variable.

Putting $$\rho=\log r, \quad (2)$$

(1) becomes

$$\frac{d^2P}{d\rho^2}-\frac{dP}{d\rho}+[2Er^2+2rZ_\rho-l(l+1)]P=0, \quad (3)$$

where $$Z_\rho=-rV. \quad (4)$$

[3] V. Bush, J. Frank. Inst., Oct. 1931.
[4] See I, Eq. (2.3).

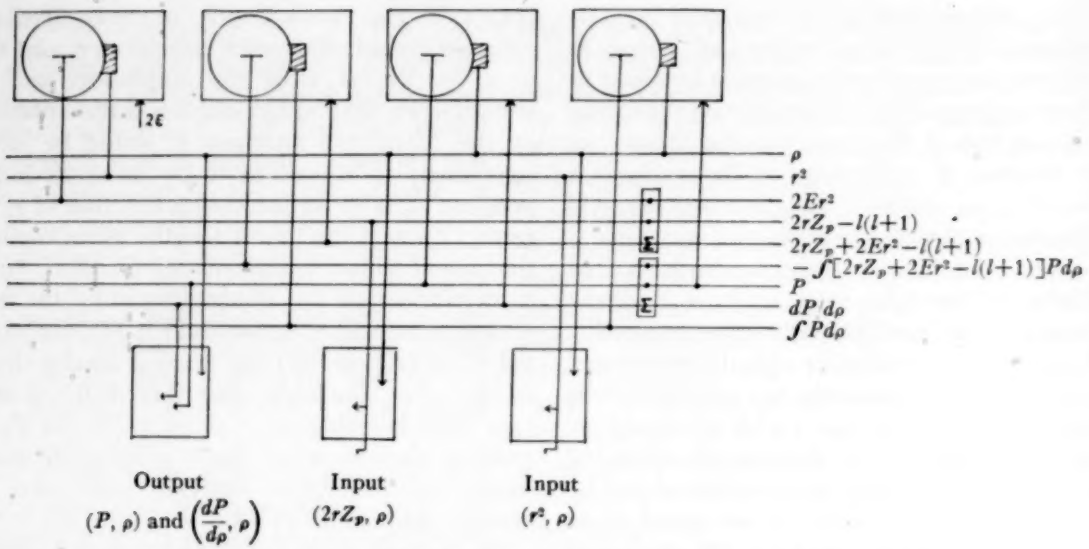

FIG. 1. Schematic set-up of differential analyzer for solution of the radial wave equation in the form $\frac{d^2P}{d\rho^2}+\frac{dP}{d\rho}+[2Er^2+2rZ_p-l(l+1)]P=0$. ($\rho=\log r$.)

Integrating (3) formally with respect to ρ gives

$$dP/d\rho=P-\int[2Er^2+2rZ_p-l(l+1)]Pd\rho, \qquad (5)$$

which suggests the differential analyzer set-up shown diagrammatically in Fig. 1.

Since the determination of the energy parameter E for each radial wave function has to be made by trial and error, and also since the same potential Z_p/r can be used, to an adequate approximation in the earlier stages of the work, for different wave functions of the same n and different l, it follows that a number of solutions of (5), with different values of E and l, but with the same function rZ_p, are required. The $l(l+1)$ term can be taken into account by the initial setting of the appropriate integrator, and to avoid drawing a large number of input curves of $2Er^2+2rZ_p$ with different trial values of E, it is most convenient to construct this sum mechanically, by the addition of the two terms, fed from different input tables, one table carrying a curve of $2rZ_p$ against ρ and the other a curve of $r^2(=e^{2\rho})$ against ρ. The input from the latter rotates an integrator whose setting during any one run is constant; small changes of E are made by altering the integrator setting, large changes are made by altering the zero of ρ on the (r^2,ρ) input table. Apart from this point, the machine set-up is straightforward.

For the numerical work in the later stages of approximation to the self-consistent field, Eq. (3), in which the first derivative appears explicitly, is not convenient, but this term can be removed by a change of dependent variable which gives

$$(d^2/d\rho^2)(Pr^{-\frac{1}{2}})+[2Er^2+2rZ_p-(l+\tfrac{1}{2})^2](Pr^{-\frac{1}{2}})=0. \qquad (6)$$

This equation is quite convenient for numerical work, and has the advantage over Eq. (1) that the changes in integration interval required are much fewer; it might also prove slightly better than (3) for work with the differential analyzer.

It has also the advantage that successive maxima of $Pr^{-\frac{1}{2}}$ are roughly equal, so that the same number of decimal places in $Pr^{-\frac{1}{2}}$ give about the same relative accuracy over the whole range where P is important. This is not unconnected with the fact that the "wave-length" of the oscillations of P is approximately uniform in $\log r$. This can be seen by considering the transformation of the equation

$$d^2y/dx^2+f(x)y=0 \qquad (7)$$

by a simultaneous change of independent variable from x to $X=X(x)$, and of dependent variable from y to $Y=g(x)y$. It is easily verified that in order that the term in dY/dX in the transformed equation should vanish, the transformations of dependent and independent variable must be related by

$$g^{\frac{1}{2}}dX/dx=\text{constant}. \tag{8}$$

If the equation then transforms to

$$d^2Y/dX^2+F(X)Y=0 \tag{9}$$

and $F(X)$ is positive and nearly constant, both the "amplitude" and "wave-length" of the oscillations of Y will be nearly uniform. Thus if the independent variable is transformed so that the "wave-length" of the oscillations of the solution is nearly uniform, and the dependent variable is transformed by $Y=g(x)y$ where $g(x)$ is given by (8), the amplitude of the oscillations of Y is also nearly uniform. In particular if $X=\log x$, (8) gives $g=x^{-\frac{1}{2}}$, which corresponds to the transformation used to give (6).

For large r, the solution of (3) which tends to 0 as $r\to\infty$ can be written

$$P=e^{-\int\zeta d\rho}, \tag{10}$$

where ζ satisfies the equation

$$d\zeta/d\rho=(\zeta+\tfrac{1}{2})^2+2Er^2+2rZ_p-(l+\tfrac{1}{2})^2. \tag{11}$$

The solution of this equation can also be obtained on the differential analyzer; the integration is carried inwards (i.e., in the direction of ρ decreasing) from an initial value of ζ obtained by approximation. The result of this integration is very insensitive to the exact initial value of ζ, hence if the start of the integration is taken well outside the range in which P is appreciable, quite a rough approximation for the initial value of ζ is adequate.

Two methods were used for the determination of characteristic values of the energy parameter E, using the differential analyzer. One method was to take solutions of (3), with different trial values of E, until one was found which tended asymptotically to 0 as $\rho\to\infty$; this was not altogether satisfactory as for large ρ the solution is very sensitive and may be seriously affected by small instrumental errors, and since these errors are cumulative, and may be random rather than systematic, interpolation between solutions with different values of E may not be reliable. The other method, which seemed preferable in practice, was to take solutions of (3) with ρ increasing, and of (11) with ρ decreasing, with different values of E, the solutions being taken to the outermost node of $dP/d\rho$ (which is also a zero of ζ), and E chosen so that the two values for the radius of this node, obtained from the outward and inward integrations, agreed. Values of P outside the node were then determined by integration of (10). The capacity of the differential analyzer was enough to accommodate the set-up for Eq. (11) as well as that for (3), and the change from one to the other could be made very simply and quickly.

§3. Procedure

The following is an outline of the procedure adopted. For the first seven stages of approximation to the self-consistent field, the calculations were done for the Hg^{++} ion, as it seemed likely to be easiest to deal first with this ion and then later to add the $(6s)^2$ group.

Contributions to $Z(=r^2\times$field intensity at radius r) from the electron groups $(1s)^2$ to $(4d)^{10}$ were first estimated by extrapolation from the results for other atoms for which calculations of the self-consistent field have been made (or rather by interpolation between these results and the results for an infinite nuclear charge, when the one-electron wave functions of the non-relativistic self-consistent field approximation to the many-electron atom are hydrogen-like). The estimates for these groups were made over the whole range for which these contributions are appreciable; for the other groups $(4f)^{14}$ to $(5d)^{10}$ similar estimates were made for $r\leq 0.2$ only. For $r>0.2$, the Thomas-Fermi field was taken and modified so as to join smoothly, at $r=0.2$, to the aggregate of the estimated contributions to the field from the different groups.

Wave functions for the groups $(4f)^{14}$ to $(5d)^{10}$ were calculated in this modified Thomas-Fermi field, and contributions to Z calculated from these wave functions. Subsequently, calculations were based on estimates of contributions to Z from all groups.

TABLE II. $Pr^{-\frac{1}{2}}$ *as a function of* $\log r$, *for the one-electron wave functions (unnormalized) for normal states of neutral Hg and* Hg^{++} ($\rho = \log_e (1000\, r)$ (r *in atomic units*)).

ρ	r	(1s)	(2s)	(3s)	(4s)	(5s)	(6s)	(2p)	(3p)	(4p)	(5p)	(3d)	(4d)	(5d)	(4f)	Hg^{++} (5d)
0	.001	11.68	11.67	11.67	11.67	11.67	11.67	0.12	0.12	0.12	0.12	0.001	0.001	0.001	0.0000	0.001
4/12	.00140	13.37	13.35	13.34	13.34	13.34	13.34	0.20	0.20	0.20	0.20	0.003	0.003	0.003	0.0000	0.003
8/12	.00195	15.11	15.06	15.05	15.05	15.05	15.05	0.32	0.32	0.32	0.32	0.006	0.006	0.006	0.0000	0.006
1	.00272	16.78	16.68	16.66	16.66	16.66	16.66	0.51	0.51	0.51	0.51	0.014	0.014	0.014	0.0000	0.014
4/12	.00379	18.19	17.97	17.94	17.93	17.93	17.93	0.80	0.80	0.80	0.80	0.032	0.032	0.032	0.0001	0.032
8/12	.00529	19.06	18.60	18.53	18.51	18.51	18.51	1.25	1.25	1.25	1.25	0.071	0.070	0.070	0.0004	0.070
2	.00739	19.05	18.09	17.96	17.92	17.92	17.92	1.89	1.89	1.89	1.89	0.155	0.151	0.151	0.0012	0.151
4/12	.01031	17.83	15.94	15.67	15.60	15.59	15.59	2.78	2.76	2.75	2.75	0.329	0.320	0.320	0.0036	0.320
8/12	.01439	15.22	11.69	11.20	11.08	11.06	11.06	3.91	3.85	3.82	3.82	0.682	0.66	0.66	0.011	0.661
3	.02009	11.43	5.36	4.57	4.38	4.35	4.35	5.16	5.00	4.92	4.91	1.357	1.31	1.31	0.031	1.312
2/12	.0237	9.31	1.63	0.70	0.48	0.45	0.45	5.76	5.49	5.36	5.34	1.88	1.81	1.81	0.052	1.81
4/12	.0280	7.19	−2.20	−3.21	−3.45	−3.48	−3.48	6.26	5.84	5.63	5.60	2.56	2.46	2.46	0.086	2.46
6/12	.0331	5.23	−5.86	−6.81	−7.03	−7.06	−7.06	6.61	5.96	5.67	5.62	3.42	3.26	3.26	0.141	3.26
8/12	.0391	3.53	−9.00	−9.68	−9.81	−9.83	−9.83	6.75	5.76	5.41	5.35	4.47	4.24	4.24	0.228	4.24
10/12	.0462	2.19	−11.31	−11.36	−11.32	−11.31	−11.31	6.62	5.18	4.75	4.68	5.71	5.37	5.37	0.360	5.37
4	.0560	1.23	−12.51	−11.46	−11.16	−11.09	−11.08	6.19	4.16	3.64	3.56	7.08	6.58	6.57	0.560	6.57
2/12	.0645	0.61	−12.50	−9.81	−9.13	−8.99	−8.97	5.48	2.72	2.13	2.03	8.50	7.75	7.73	0.85	7.73
4/12	.0762	0.27	−11.34	−6.49	−5.40	−5.17	−5.14	4.55	0.97	0.33	0.21	9.81	8.71	8.66	1.25	8.66
6/12	.0900	0.10	−9.34	−1.98	−0.54	−0.25	−0.21	3.51	−0.91	−1.51	−1.63	10.84	9.22	9.10	1.80	9.10
8/12	.1063	0.03	−6.93	+2.90	+4.42	+4.71	+4.74	2.48	−2.65	−3.07	−3.15	11.37	9.03	8.83	2.50	8.83
10/12	.1256	0.01	−4.58	7.19	8.24	8.39	8.41	1.57	−3.98	−4.00	−4.01	11.24	7.93	7.61	3.34	7.61
5	.1484		−2.66	10.00	9.77	9.62	9.60	0.89	−4.66	−4.02	−3.89	10.41	5.86	5.39	4.30	5.39
1/12	.1613		−1.92	10.68	9.46	9.10	9.04	0.64	−4.74	−3.66	−3.44	9.74	4.49	3.93	4.80	3.93
2/12	.1753		−1.33	10.86	8.42	7.81	7.71	0.44	−4.64	−3.06	−2.75	8.93	2.94	2.31	5.29	2.31
3/12	.1906		−0.89	10.56	6.72	5.85	5.74	0.29	−4.39	−2.26	−1.86	8.00	1.27	0.59	5.76	0.59
4/12	.2071		−0.56	9.86	4.49	3.37	3.23	0.19	−4.01	−1.30	−0.83	7.00	−0.45	−1.17	6.20	−1.17
5/12	.2251		−0.34	8.84	1.89	0.58	0.42	0.11	−3.54	−0.26	+0.26	5.98	−2.15	−2.86	6.57	−2.86
6/12	.2447		−0.19	7.62	−0.86	−2.26	−2.42	0.07	−3.02	+0.81	1.34	4.97	−3.75	−4.40	6.86	−4.40
7/12	.2660		−0.10	6.31	−3.55	−4.88	−5.03	0.04	−2.48	1.81	2.30	4.01	−5.18	−5.68	7.07	−5.68
8/12	.2891		−0.05	5.02	−5.95	−7.03	−7.14	0.02	−1.97	2.70	3.07	3.14	−6.35	−6.63	7.17	−6.63
9/12	.3142		−0.02	3.83	−7.90	−8.49	−8.52	0.01	−1.50	3.40	3.57	2.38	−7.22	−7.19	7.15	−7.19
10/12	.3415		−0.01	2.79	−9.27	−9.12	−9.04		−1.10	3.88	3.77	1.74	−7.76	−7.30	7.01	−7.30
11/12	.3712			1.94	−10.00	−8.85	−8.64		−0.77	4.13	3.64	1.22	−7.97	−6.97	6.76	−6.97
6	.4034			1.29	−10.12	−7.72	−7.36		−0.51	4.15	3.21	.83	−7.85	−6.23	6.42	−6.23
1/12	.4385			0.81	−9.69	−5.86	−5.35		−0.34	3.97	2.50	.53	−7.46	−5.09	6.00	−5.09
2/12	.4766			0.49	−8.84	−3.45	−2.80		−0.20	3.64	1.59	.33	−6.85	−3.66	5.51	−3.66
3/12	.5180			0.27	−7.70	−0.74	+0.03		−0.11	3.19	0.56	.20	−6.10	−2.02	4.97	−2.02
4/12	.5630			0.15	−6.42	+2.05	2.86		−0.06	2.69	−0.52	.11	−5.25	−0.27	4.41	−0.27
5/12	.6120			0.07	−5.13	4.57	5.41		−0.03	2.18	−1.56	.06	−4.38	+1.50	3.84	+1.50
6/12	.6651			0.03	−3.92	6.90	7.45		−0.01	1.70	−2.49	.03	−3.53	3.19	3.28	3.19
7/12	.723			0.01	−2.86	8.61	8.81			1.27	−3.25	.01	−2.75	4.72	2.74	4.72
8/12	.786				−1.99	9.70	9.37			0.91	−3.79		−2.07	6.01	2.24	6.01
9/12	.854				−1.32	10.16	9.12			0.62	−4.10		−1.50	7.01	1.80	7.01
10/12	.928				−0.84	10.04	8.11			0.40	−4.18		−1.04	7.71	1.41	7.71
11/12	1.009				−0.50	9.43	6.45			0.25	−4.06		−0.70	8.10	1.08	8.10
7	1.097				−0.28	8.45	4.31			0.15	−3.78		−0.45	8.20	0.80	8.20
1/12	1.192				−0.15	7.28	1.86			0.08	−3.39		−0.27	8.07	0.58	8.06
2/12	1.296				−0.08	6.02	−0.70			0.04	−2.93		−0.16	7.70	0.41	7.69
3/12	1.408				−0.04	4.79	−3.23			0.02	−2.44		−0.09	7.19	0.28	7.18
4/12	1.530				−0.02	3.66	−5.58			0.01	−1.97		−0.05	6.57	0.18	6.56
5/12	1.663				−0.01	2.69	−7.56				−1.54		−0.03	5.89	0.11	5.88
6/12	1.808					1.90	−9.38				−1.16		−0.01	5.17	0.07	5.16
7/12	1.965					1.29	−10.72				−0.84			4.47	0.04	4.45
8/12	2.136					0.84	−11.65				−0.58			3.79	0.02	3.77
9/12	2.322					0.52	−12.19				−0.40			3.16	0.01	3.12
10/12	2.538					0.31	−12.35				−0.26			2.59		2.53
11/12	2.743					0.18	−12.16				−0.16			2.08		2.01
8	2.981					0.10	−11.69				−0.10			1.64		1.56
1/12	3.240					0.05	−10.97				−0.06			1.26		1.18
2/12	3.522					0.02	−10.06				−0.03			0.95		0.86
3/12	3.828					0.01	−9.02				−0.01			0.70		0.61
4/12	4.160						−7.91							0.51		0.42
5/12	4.522						−6.76							0.36		0.27
6/12	4.915						−5.65							0.24		0.17
7/12	5.342						−4.60							0.16		0.10
8/12	5.81						−3.63							0.10		0.06
9/12	6.31						−2.78							0.06		0.03
10/12	6.86						−2.07							0.03		0.02
11/12	7.46						−1.49							0.02		0.01
9	8.10						−1.03							0.01		
1/12	8.81						−0.69									
2/12	9.57						−0.44									
3/12	10.40						−0.26									
4/12	11.31						−0.15									
5/12	12.29						−0.08									
6/12	13.36						−0.04									
7/12	14.52						−0.02									
8/12	15.78						−0.01									

	(1s)	(2s)	(3s)	(4s)	(5s)	(6s)	(2p)	(3p)	(4p)	(5p)	(3d)	(4d)	(5d)	4f)
$Pr^{-(l+1)}$ $r=0$	400	400	400	400	400	400			4000			40,000		40,000
$r=.001$	369.2	369.0	368.9	368.9	368.9	368.9			3843			38,950		39,210
ϵ (Hg^{++})	5548	925	218	47.2	8.06	—	892	201.5	40.2	5.70	171	27.8	2.07	9.56
ϵ (Hg neutral)						0.47							0.93	
$24\int_0^\infty Pdr$	1.898	17.25	77.9	313.8	1580	28650	3.503	14.14	55.1	320	61.15	217.7	2481	
												(Hg^{++})	2442	185.9

It was hoped that the aggregate contribution to Z from the groups $(1s)^2$ to $(3d)^{10}$ would not differ from that given by the self-consistent field by more than about 0.3, and as any error in these contributions would be in the region of small r, for which Z is large, it would be a small proportion of the total Z, and would not affect the wave functions seriously. The first nine approximations were concerned entirely with making the outer groups ($n \geq 4$) approximately self-consistent, first for Hg^{++} and then for Hg; it was only after this that the wave functions $(1s)$ to $(3d)$ were calculated, and it was then found that the errors in the estimates of the contributions of these groups to Z were well within the limit hoped for.

In the numerical stages of the work, the integration of (6) was not carried all the way from the immediate neighborhood of the origin, but for small r (where the solution is insensitive to the exact field) the differential analyzer solution was taken, and the numerical solution was only worked for the outer part of the range of integration, the starting values for the numerical integration being taken from the machine solution for an earlier trial field. For example, the machine solution was taken from $\rho = \log_e (1000\, r) = 0$ in all cases, but for the wave functions with $n = 5$, the numerical integration was only started at $\rho = 4$.

The approximation to the self-consistent field has so far been carried to such a stage that the difference between the estimated and calculated total Z for the whole atom is nowhere greater than 0.15. Calculations are now in progress with revised estimates of contributions from all groups, and the numerical integration is being taken from $\rho = 0$ in all cases.

§4. Results

The main results so far obtained are given in Tables II and III. Table II gives $Pr^{-\frac{1}{2}}$ for the one-electron wave functions of the various groups; the $(5d)$ wave function is appreciably perturbed when the $(6s)^2$ group is added to Hg^{++} to make neutral Hg, so is given for both states of ionization; $(5s)$ and $(5p)$ have as yet only been calculated for Hg^{++}, but will be much less affected by the presence or absence of the $(6s)^2$ group. This perturbation of the $(5d)$ wave function makes the contribution of the $(5d)^{10}$ group to Z for Hg^{++} and for neutral Hg differ by as much as 0.1 over a small range of r.

TABLE III. *$2Z_p$ for normal state of neutral Hg.*
(Potential energy of electron at radius $r = Z_p/r$ atomic units.)

ρ	$2Z_p$	ρ	$2Z_p$	ρ	$2Z_p$	ρ	$2Z_p$
0	158.92	4	118.74	6	36.75	8	0.87
2/12	158.72	1/12	116.16	1/12	33.46	1/12	0.67
4/12	158.49	2/12	113.49	2/12	30.41	2/12	0.50
6/12	158.22	3/12	110.71	3/12	27.60	3/12	0.37
8/12	157.90	4/12	107.82	4/12	25.02	4/12	0.26
10/12	157.52	5/12	104.85	5/12	22.64	5/12	0.18
1	157.07	6/12	101.76	6/12	20.42	6/12	0.12
2/12	156.55	7/12	98.56	7/12	18.31	7/12	0.08
4/12	155.94	8/12	95.24	8/12	16.29	8/12	0.05
6/12	155.23	9/12	91.82	9/12	14.37	9/12	0.03
8/12	154.40	10/12	88.31	10/12	12.56	10/12	0.01$_8$
10/12	153.44	11/12	84.74	11/12	10.87	11/12	0.00$_8$
2	152.32	5	81.10	7	9.30	9	0.00$_4$
2/12	151.04	1/12	77.43	1/12	7.91	1/12	0.00$_2$
4/12	149.58	2/12	73.75	2/12	6.68		
6/12	147.91	3/12	70.08	3/12	5.60		
8/12	146.01	4/12	66.41	4/12	4.67		
10/12	143.85	5/12	62.72	5/12	3.88		
3	141.40	6/12	59.00	6/12	3.21		
2/12	138.63	7/12	55.25	7/12	2.64		
4/12	135.50	8/12	51.48	8/12	2.15		
6/12	131.97	9/12	47.68	9/12	1.74		
8/12	127.99	10/12	43.93	10/12	1.40		
10/12	123.58	11/12	40.26	11/12	1.11		
4	118.74	6	36.75	8	0.87		

Table III gives the total $2Z_p$ for the neutral Hg atom; this is given as it is required, for example, for the calculation of the elastic scattering of electrons by Hg. The $2Z_p$ given in this table refers not to the field for which the wave functions given in Table II were calculated, but to the field, based on the *revised* estimates of contributions to Z, which is being used as a start for the calculation of a better approximation to the self-consistent field. Thus the values of $2Z_p$ tabulated in Table III, multiplied by $1/r$, give the best approximation yet available to the potential of the self-consistent field of Hg.

It should perhaps be emphasized that since the work is all based on Schrödinger's Eq. (1), it does not take account of any relativity or spin effects, which will be considerable in an atom as heavy as this.

LETTERS TO THE EDITOR

Prompt publication of brief reports of important discoveries in physics may be secured by addressing them to this department. Closing dates for this department are, for the first issue of the month, the twentieth of the preceding month; for the second issue, the fifth of the month. The Board of Editors does not hold itself responsible for the opinions expressed by the correspondents.

Heights of Nuclear Potential Barriers

Pollard[1] concludes from estimates based on penetration and scattering experiments that in light nuclei the barrier height, U_M, is a linear function of atomic number, Z, and shows that an approximate relation of this kind might be anticipated from Heisenberg's[2] theory. Heisenberg's approximations, however, lead directly to a proportionality between U_M and $Z/M^{\frac{1}{3}}$, where M is the mass number. Over limited ranges of atomic number there is no necessary conflict of these two approximate relations, but over wider ranges the second more nearly represents the claims of the theory. As the theory has been shown[3] to be in harmony with a wide variety of experimental data, it is of interest to compare barrier heights calculated by it with other indications as to their magnitude. This is done in the accompanying figure.

Curve I is the smoothed curve through points obtained by using chemical atomic weights (for the sake of averages), in place of M in the equation $U_M = 2Ze^2/r_0M^{\frac{1}{3}}$. U_M is here the barrier height for alpha-particles and $r_0M^{\frac{1}{3}}$ the "radius" of the nucleus as discussed and evaluated in the previous paper.[3] The curve is dotted below $Z=10$ to indicate its tentative character in this region.[3] The circles represent Pollard's estimates for Li, Be, B, C, N, F and Al, while the three dots are Chadwick's[4] values for Li, Be and Al. The cross at $Z=13$ is the value given by Rutherford, Chadwick and Ellis[5] as deduced from the early scattering experiments on aluminum. Curve II is the line adopted by Pollard to represent his results (here extrapolated, solely for comparison of general trends, far beyond the data to which it applies).

The calculated curve is in general somewhat higher than the experimental points. This may result from real inaccuracy of the equation in this range. Since, however, penetration may become appreciable some distance below the top of the barrier (especially if broad resonance levels near the peak are present), the experimental values should be regarded as minimum estimates, and the agreement therefore fairly good.

The only other data that may be compared with curve I are the Coulombic potentials calculated from the "effective radii" of the radio-elements (in their "normal" states) obtained by Gamow[6] from their decay periods. These are represented by the triangles in the figure. From the nature of Gamow's approximation to the form of the actual barrier, these calculated potentials vary with the degree of excitation, and all must be higher than U_M. With one exception these points do fall above the curve calculated here. This is equivalent to the conclusion previously discussed[3] that the radius of the Heisenberg theory must always be greater than in Gamow's. In a general way

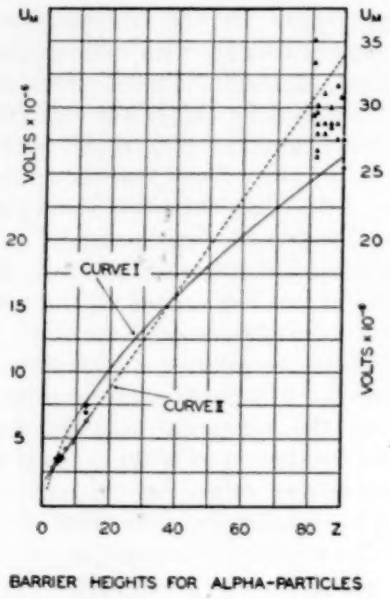

FIG. 1.

therefore the values here obtained are consistent with the quantum-mechanical results. It is thought that they may be regarded as fairly reasonable approximations to the true barrier heights.

Assuming this to be the case, it is interesting to compare the energies of emitted alpha-particles with the barrier heights. The fastest natural alpha-particles have energies of the order of 10 or 12 m.e.v. They are, therefore, escaping, with very short life periods, from their parent nuclei at levels some 12 or 14 m.e.v. below the top of the barrier. It would appear that the energy of an incoming particle need be only a few million volts higher than this, and still very considerably below the barrier crest, to have an appreciable probability of penetration, even without resonance.

E. D. EASTMAN

Department of Chemistry,
University of California,
Berkeley, California,
September 27, 1934.

[1] Pollard, Phil. Mag. **16**, 1131 (1933).
[2] Heisenberg, Zeits. f. Physik **77**, 1 (1932).
[3] Eastman, Phys. Rev. **46**, 1 (1934).
[4] Chadwick, Proc. Roy. Soc. Bakerian Lecture (1933).
[5] Rutherford, Chadwick and Ellis, *Radiations from Radioactive Substances*, The Macmillan Co., New York, 1930, p. 278.
[6] Gamow, *Der Bau des Atomkerns und die Radioaktivität*, Leipzig, 1932, p. 63.

Absence of Low Energy Radiations from Potassium and Rubidium

The work of Sargent[1] on the upper energy limit of the continuous β-ray spectra revealing linear relations between the log of the decay constants and the upper energy limits for β-ray emitters has placed the radioactive potassium and rubidium nuclei in somewhat anomalous positions due to their abnormally high upper energy limits. The relations would predict an upper limit of between 500 and 12,000 electron volts for K instead of the 700,000 e.v. value found by Anderson and Neddermeyer[2] in their cloud-chamber measurement of the curvatures in a magnetic field. For rubidium the upper limit energy should lie between 1000 and 18,000 e.v. The actual rubidium upper limit, though not well established, is definitely outside this range.

This application of the Sargent relations to elements of atomic number so widely different from those for which they were experimentally derived seems to have been justified by Anderson and Neddermeyer[2] in their measurement of the upper energy limits for the positron spectra of radioactive B, C, and Al. An additional confirmatory datum is the 11,000 e.v. upper limit for the β-ray from neodymium reported previously by the author.[3] The point on the Sargent plot representing this value is subject to some uncertainty due to lack of knowledge of the identity of the particular neodymium isotope responsible. This is still small enough however to allow substantiation of the relation if it be assumed that the emitting isotope is not less than 0.1 percent of the nuclei.

Gamow[4] has suggested that the β-radiations that are observed in these two cases are not emitted by potassium and rubidium themselves but by short-lived secondaries formed by the slow emission of low-energy α-particles of ranges 0.24 cm and 0.63 cm, respectively.

The present communication is a report of a search for such low energy radiations by means of the screen-walled Geiger-Müller counter apparatus used in work on neodymium and samarium and previously described in detail in this journal.[5] The samples were placed on the inner surface of a cylinder concentric with the counter and at about 7 mm distance from the counter walls. Throughout the work about 1 cm pressure of argon gas was used in the chamber.

Fig. 1 presents the results of potassium obtained by measuring the specific activity of KCl layers as a function of their thickness. The solid line represents the data for relatively thick layers which were comparatively easily obtained and subject to small uncertainty; and the circled point, the activity of the thinnest layer used. The horizontal lines above and below indicate the probable error of the result computed by the standard method.[6] Two of the broken lines represent the effects which should have been observed if 0.5 or 0.05 cm α's were emitted. They were computed by means of the Bragg-Kleeman rule which will certainly at least give a lower limit for the effect to be expected because it is known to give values for the atomic stopping powers too high for short range α-particles. It was also assumed that radioactive equilibrium should exist so that one α should be emitted for

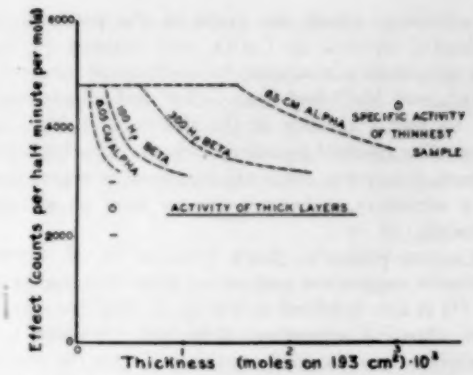

FIG. 1. Specific activity of KCl samples plotted as a function of their thicknesses.

each β-particle. The other two broken lines represent the effects to be expected if 300 or 100 $H\rho$ (8000 or 870 e.v.) β-rays were emitted. These were calculated on the assumption that the effect of scattering by the sample itself was negligible because the number of particles scattered into the counter should approximately equal the number scattered out due to the geometry of the apparatus. The $H\rho$ range data used were those of Schonland[7] extrapolated slightly. This procedure is more or less justified by the agreement found in the case of the neodymium β-radiation between the measured range and the value calculated on the basis of the assumption using Schonland's data.[8] It seems fairly clear that no α-particle of range much greater than 0.05 cm or β-particle with energy much greater than 50 $H\rho$ (500 e.v.) is emitted by K. Since the predicted values for both processes lie above these values it seems improbable that any sort of preliminary radiation is emitted.

Fig. 2 presents the results of a similar study of $RbClO_4$. It is clear that here the limits of energy can be set even lower than in the potassium case, while the expected energies are higher, as previously mentioned. It is therefore even more improbable than in the potassium case that rubidium emits a low energy α- or β-particle initially.

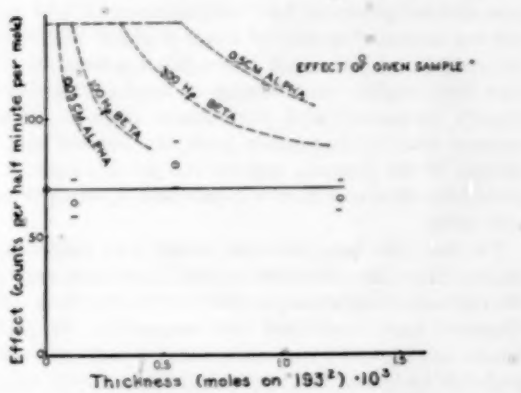

FIG. 2. Specific activity of $RbClO_4$ samples plotted as a function of their thicknesses.

An additional check was made on the potassium by precipitating calcium as $CaCO_3$ and chlorine as AgCl from a potassium salt solution to which small amounts of $Ca(NO_3)_2$ and NaCl had been added and attempting to detect an initial activity of the $CaCO_3$ and AgCl precipitates. The residual potassium salt was also checked for a decrease in activity. All of the results were negative and make a secondary of half-life greater than 30 sec. very improbable.

The author wishes to thank Professor W. M. Latimer for valuable suggestions and advice given him during this work. He is also indebted to Mr. D. E. Hull for carrying out the chemical separations described. Professor J. R. Oppenheimer was also kind enough to discuss the problem of the effect of scattering of low energy β-particles on their being absorbed by the sample.

W. F. LIBBY

Department of Chemistry,
University of California,
Berkeley, California,
September 24, 1934.

[1] Sargent, Proc. Roy. Soc. **A139**, 659 (1933).
[2] Anderson and Neddermeyer, Phys. Rev. **45**, 653 (1934)..
[3] Libby, Phys. Rev. **45**, 845 (1934).
[4] Gamow, Nature **133**, 744 (1934).
[5] Libby, Phys. Rev. **46**, 196 (1934).
[6] Cf. reference 5, page 200.
[7] Schonland, Proc. Roy. Soc. **A104**, 235 (1923); **A108**, 187 (1925).
[8] Cf. reference 5, page 202 or Libby, Phys. Rev. **45**, 845 (1934).

Radioactive Sodium Produced by Deuton Bombardment

In the course of a general experimental investigation of artificial radioactivity in our laboratory, I have discovered an unusually interesting case of radioactivity induced in sodium by deutons. The radioactive substance has a half-life of 15 ± 0.5 hours and gives off beta- and gamma-rays in equal numbers. The beta-rays are reduced to one-half by 0.1 g/cm^2 Al. The absorption of the gamma-rays in Pb is, within experimental uncertainty, exponential, indicating monochromatic radiation. The absorption per electron of the radiation in Al, Cu and Pb is approximately 0.84×10^{-25}, 1.2×10^{-25} and 1.7×10^{-25}, respectively, indicating[1, 2] about 5.5 m.e.v. radiation. The estimated saturation activity produced by 1 microampere of 1.75 m.e.v. deutons bombarding sodium metal is about 3×10^7 disintegrating atoms per second. The yield of radioactive atoms rises very rapidly with voltage of bombarding deutons, roughly in accord with the Gamow formula. Thus it appears that by increasing both the current and the voltage of the deutons, sodium can be activated in the laboratory with an intensity expressible in terms of many millicuries.

The fact that beta-particles, rather than positrons, are emitted from the activated sodium suggests at once that the radioactive substance is $_{11}Na^{24}$ which decays to $_{12}Mg^{24}$. Chemical tests confirmed this supposition. It perhaps should be mentioned that many uses for radio-sodium will probably be found. In the physical laboratory it provides a presumably monochromatic source of high energy gamma-radiation of great intensity. In the biological field radio-sodium has interesting possibilities that hardly need be emphasized here.

Dr. Edwin McMillan and I have also been studying the radioactivity induced in aluminum by deuton bombardment. Here also electrons, rather than positrons, are given off from a radioactive isotope, $_{13}Al^{28}$, which decays with a half-life of 2′ 33″.

Radio-sodium and radio-aluminum have been produced also by neutron bombardment first by Fermi[3] in his pioneer experiments and later by Curie, Joliot and Preiswerk[4] and in our laboratory.[5]

The details of these experiments will shortly be submitted for publication in the *Physical Review*.

I am much indebted to Dr. Edwin McMillan and Dr. Malcolm C. Henderson for their assistance in some of the experiments. I wish to acknowledge with thanks also the financial support of the Research Corporation, the Chemical Foundation and the Josiah Macy, Jr. Foundation.

ERNEST O. LAWRENCE

Radiation Laboratory, Department of Physics,
University of California,
Berkeley, California,
September 29, 1934.

[1] E. McMillan, Phys. Rev. **46**, 325 (1934).
[2] Bethe and Heitler, Proc. Roy. Soc. **A146**, 83 (1934).
[3] Collected results of Fermi and his collaborators: E. Fermi, E. Amaldi, O. D'Agostino, F. Rasetti and E. Segrè, Proc. Roy. Soc. **A146**, 483 (1934).
[4] I. Curie, F. Joliot and I. Preiswerk, C. R. Ac. Sc. Paris **198**, 2089 (1934).
[5] M. S. Livingston, M. C. Henderson and E. O. Lawrence, Proc. Nat. Acad. Sci. **20**, 470 (1934).

Band Spectrum of LiH and LiD

The observations previously reported by us[1] on the $^1\Sigma \rightarrow {}^1\Sigma$ bands of Li^7H have been greatly extended by absorption photographs at temperatures up to 900°C. On these plates some 2300 lines have been assigned including 45 bands of Li^7H and 13 of Li^6H.

Photographs taken under the same conditions with an atmosphere of deuterium of high purity have resulted in excellent plates of the corresponding heavy hydride bands. The new spectrum extends from about 3175A to the absorption limit of the Li_2 molecule in the red and though similar to that of the light hydride is considerably richer in lines. Some 34 bands including, however, only a fraction of the new lines present, have been identified as belonging to Li^7D. Plates taken at the highest temperatures show many faint lines which do not correspond with any lines of Li^7H or Li^6H and are undoubtedly due to LiD, though quantum assignments have not yet been made.

The isotope shifts for Li^7H and Li^7D are the largest to be expected for any hydride molecule other than HD itself. In the case of the (17, 0) band this amounts to about 147A. Although the ultimate values of the molecular constants for LiH have not been determined our results indicate that the observed isotope bands (LiD) lie slightly to the *high* frequency side of those calculated from the ordinary isotope theory. The (14–0) band for which the best data are at hand gives a discrepancy in this direction which is

several times the experimental uncertainty and suggests strongly that the upper $^1\Sigma$ state is showing evidence of the non-identity of the potential energy curves for hydrides and deuterides found by Hulthén and Holst[2] and interpreted by Kronig.[3] According to Kronig's interpretation the deuteride molecule should have a slightly *smaller* equilibrium distance and slightly *greater* vibrational frequency than the usual theory assumes. The magnitude of the effect depends on the L-value of the state formed by allowing the nuclei to coalesce and on the stability of the atomic state thus obtained. In our case the atomic state in point is the first excited $^1S_0$ state of Be for which $L=0$ and which is presumably somewhat less stable than the ^1S state of argon (the coalesced nuclear state for HCl which does not show this effect to a measurable extent). Hence a small effect in the indicated direction should be present in the LiD bands.

In this connection it should be noted that Jevon's tabulations of the vibrational constants of the upper $^1\Sigma$ state of LiH are erroneous.

Similar experiments on the light and heavy hydrides of sodium are in progress and results will be reported in the near future.

F. H. CRAWFORD
T. JORGENSEN

Jefferson Physical Laboratory,
Harvard University,
September 29, 1934.

[1] F. H. Crawford and T. Jorgensen, Phys. Rev. **45**, 737 (1934).
[2] Hulthén and Holst, Nature **133**, 496 (1934).
[3] Kronig, Physica **1**, 617 (1934).